24th Electromagnetic Induction Workshop

13-20 August 2018, Helsingør Denmark

www.emiw2018.org

Abstracts Session 3

SESSIONS DESCRIPTION

Session 3. Exploration, Monitoring and Hazards

EM methods are widely used for obtaining electrical properties of the underground (the resistivity, magnetic permeability, dielectric constant, or IP parameters) ranging from the near surface to the upper mantle. Different techniques and their combinations are applied for different tasks in exploration, monitoring and hazard assessment. We are pleased to invite researchers to submit abstracts of their works related to recent developments and case studies that highlight the role of EM induction in mineral exploration, oil and gas, groundwater and geothermal, environmental and engineering, and natural hazards assessment. We will appreciate contributions on different aspects of EM methods application to exploring, tracking, fluid injections and sequestration studies. We warmly solicit contributions that emphasize and evaluate the role of EM methods to natural resources exploitation, hazard assessment through EM monitoring both in seismic and volcanic environments. Finally, we also encourage contributions addressing the data processing and interpretation of EM exploration techniques aimed at lithological characterization as well as at determination of petrophysical and hydrophysicall properties of rocks.

Sub-sessions: S3.1 Exploration; S3.2 Monitoring, 3.3 Hazards

Conveners: Shimeles Fisseha , Jared Peacock ,Ted Bertrand, Yin Changchun

3-D Joint inversion of MT+AMT data over Proterozoic Dalma Volcanics, Eastern India

Roshan K. Singh[1], Shalivahan[1*] and Ved P Maurya[2]
[1] IIT(ISM), Dhanbad, India, roshanmanjitsingh@gmail.com, *shalivahan@iitism.ac.in
[2] Observatório Nacional, Rio de Janeiro –Brazil, vedankur@gmail.com

SUMMARY

The Proterozoic Dalma volcanics (DV) and its northern fringe within the North Singhbhum Mobile Belt (NSMB) has been established as a metallogenic province by geological and geophysical studies. Regional 2-D Magenetotelluric studies in the area crossing the Singhbhum Group of Metapelites (SGM), DV and Singhbhum GroUp of Quartzite and Pelite (SGQP) reported three prominent conducting features, one within DV and other two at northern and southern margins of DV. Further, it has been shown that the conducting feature in the northern margin of DV (i.e., between DV and SGM) is more robust as compared to the others. Due to limited MT resolution the shallow conducting 3-D features could not be mapped. These tempted us to acquire Audio Magnetotelluric (AMT) data sets in the northern fringe of DV. The data was acquired at an interval of ~ 500m for a profile length of ~7.5 km. 3D MT+AMT joint inversion for impedance data was performed to obtain resistivity cross-section of the area. Resistivity cross-sections from the 3D joint MT+AMT inversion for the impedance data is in broad agreement with previous 2-D results but with modified dimension and location. Shallow conducting feature lies at the northern end of SGM whereas a conducting feature with a maximum depth of 500 m is present at the boundary of SGM and DV. A distinct and well developed conducting feature lies within DV is observed upto a depth of ~ 2.5 km. SGQP is marked by a well-developed resistive feature upto a depth of ~ 1 km.

Keywords: Joint inversion, 3D inversion

INTRODUCTION

The Eastern Indian Craton (EIC) comprises of Chottanagpur Gneissic Complex (CGC) at the northern end, a mobile belt known as North Singhbhum Mobile Belt (NSMB) in central part and a craton, Singhbhum Craton (SC) at the southern end. Geological (Deb, 2014) and geophysical studies (Shalivahan et al., 2014) studies establishes EIC as a Proterozoic metallogenic province. Deb (2014) showed that most of the gold occurrences of the NSMB are present in the meta-sedimentary belt lying north of the DVs. There are four gold deposits reported in northern fringe of DV in meta sediments-meta basics, meta sediments-meta volcanics with percentage of sulfides varying from 0.5% to 1.5 % and chlorite schist, quartzites are Lawa (23° 01'N, 86° 05'E), Maysera (23° 03' N, 86° 01'E), Pahardiha (22° 30', 85° 16') and Parasi (22° 57' N, 85° 40' E) (Figure 1). Evolution of the Proterozoic DVs has been linked with the metallogenic belts lying at the northern fringes of the DVs. The Inductively Coupled Plasma Atomic Emission Spectroscopy (ICP-AES) studies of rock samples show the presence of gold, silver, copper, lead, zinc and uranium. The conductor in the northern fringe of DVs was linked with VMS or Au-VMS deposits (Maurya et al., 2015). Tectonism related to such type plume activity might be a probable cause for volcanogenic massive sulfide (VMS) setting in this area (Sarkar and Deb, 1974; Sarkar, 1984). Maurya et al. (2015) carried 2-D modelling for regional investigation of Dalma and its adjoining Singhbhum Group of Metapelites (SGM) and Singhbhum Group of Quartzite and Pelites (SGQP) formations. They reported three prominent conducting features, one within DV and other two at northern and southern margins of DV. Further, they concluded that the conducting feature in the northern margin of DV is more robust as compared to the other two conductors.

However, they were unable to model MT frequencies less than 0.1 Hz, due to presence of strong 3-D effects and hinted towards the presence of shallow conducing heterogeneities producing 3D influence on MT short periods. Taking into account of these observations, we further acquired 16 AMT sites with better spatial cover over Dalma and SGM regions. In this paper we try to map the shallow conducting features and the deep conducting features and establish any link between them using joint 3D MT + AMT inversion for impedance data with the help of ModEM code (Egbert and Kelbert, 2012; Kelbert et al., 2014).

Geological Background

Dalma volcanic is ~200 km long and 3-7 km wide, an arcuate belt and comprises mainly of green schist facies rocks of Singhbhum group and meta-

volcanics. It is a part of NSMB which lies to the north of Singhbhum Shear Zone (SSZ) between Singhbhum nucleus in the south and Chottanagpur Gneissic Complex (CGC) in the north (Figure 1). The northern fringe of DV is mostly covered by magnetite-quartz-biotite-sericite schist. Phyllites and quartzites form the host rock. The northern fringe of DV is also characterized by intrusives such as ultramafic, quartz veins and amphibolites. The presence of volcanic tuffs, quartzites, metapelites, felsic volcanics, carbon phyllites and graphitic rocks in the study area is indicated by the Petrographic studies (Chatterjee et al., 2013).

AMT data Acquisition

AMT sounding for 16 sites were acquired with an average spacing of ~ 500 m over both DV and SGM domain. Time series were collected for **2E** (North and East) and **3H** (North, East and vertical) components at each site. At each site the time series were collected for all five components using MTU-5A equipment from Phoenix Geophysics Ltd. To measure the electric field Pb-PbCl2 electrodes were used whereas for the magnetic field induction coils have been used. The length of the electrical dipole was ~100m. AMT data have been processed using the extra-hybrid approach by Shalivahan et al. (2006). In total these 16 AMT soundings and 7 MT soundings acquired earlier (Maurya *et al.* 2015) have been used for interpretation. The average station spacing of MT soundings is of ~ 1.5 km covering a profile length of ~10 km. MT data covers frequencies between 320 - 0.00055 Hz whereas AMT data has been acquired in the frequency range of 10 kHz - 10 Hz.

Setting up 3-D Inversion

Joint 3-D MT+AMT inversion for impedance (Z) have been performed data using ModEM code (Egbert and Kelbert, 2012; Kelbert et al., 2014). To perform the inversion the model domain have been discretized into 20 X 85 X 50 cells with horizontal cell dimension of 0.15 km x 0.15 km. Along the vertical direction the initial cell size was 0.015 km and it increases by a factor of 1.2 towards the edge of last five cells. Near-surface heterogeneities are included in the inversion by providing fine model discretization (Meqbel et al. 2014). This also helps to recover a better data fits. To obtain optimum value of initial half-space resistivity inversion has been performed for various values of resistivity namely 10, 50, 200 and 500 ohm-m which converged to RMS of 2.44, 2.27, 2.40 and 2.50 respectively. Error floor was computed based on the % of square root of product of off-diagonal components. Error floor of 20% and 10 % for diagonal and off-diagonal components of full impedance was used. Despite having not the minimum RMS with 10 ohm-m uniform resistivity, the final interpretation has been performed with this as the features are well developed and consistent with 2D results.

Results and Discussions

Joint MT+AMT 3D inversion model of impedance data is shown in Figure 2. It shows the regional resistivity cross section of the area for a maximum depth of 4 km (Fig. 2a) and 1 km (Fig. 2b) respectively. It is observed that two shallow conducting features C1 at the northern end of SGM and C2 at the northern boundary between SGM and DV. These conductors extend upto a maximum depth of ~500 m and are well-developed laterally as well. Dalma volcanics is marked by distinct conducting feature C3. This feature can be seen along the DV upto a depth of ~ 2.5 km. At the southern end of DV another conducting feature C4 is seen. Within SGQP we find a resistive feature R1 which appears upto a depth of ~ 1 km. To the south of this resistor a conductor C5 at a depth of 500 m is developed which extends beneath R1. Thus, all the prominent geological domain in the study area are delineated. Figure 2b shows the model upto 1 km only. It is observed that the shallow resistors and conductors are mapped which were not delineated in previous MT studies. Further, conducting feature all along the boundary of SGM and DV and within DV are observed and establishes the link between shallow and deep conducting features.

Conclusion

2D MT studies (Maurya et al. 2015) showed the presence of three conductors (i) at the northern boundary of Singhbhum Group of Metapelite and Dalma Volcanics, (ii) within Dalma Volcanics (iii) at the southern boundary of Dalma Volcanics and Singhbhum Group of Quartzite and Metapelites. Further, they indicated that the presence of shallow conducting heterogeneities which was not mapped due to the limited resolution of MT data. Therefore, 16 AMT soundings were acquired in the northern fringe of Dalma Volcanics. These along with earlier acquired MT data of Maurya et al. (2015) has been used to map the various geological domains, delineate the shallow 3D features and establish link between these shallow features to the earlier mapped deep conducting features. Joint MT+AMT 3D inversion of impedance data was performed to obtain the resistivity cross-section. The model establishes the boundaries of the geological domain within the study area. Further, it also delineates the shallow and deep conducting feature and establishes the link between them which was not observed in earlier MT studies.

Acknowledgement

The authors are thankful to N. Meqbel for providing 3D grid software.

References

Chatterjee, P., De, S., Ranaivoson, M., Mazumder, R. and Arima, M., 2013. A review of the ~1600 Ma sedimentation, volcanism, and tectono-thermal events in the Singhbhum craton, Eastern India. Geoscience Frontiers. **4**, 277–287.

Deb, M., 2014. Precambrian geodynamics and metallogeny of the Indian shield. Ore Geol. Rev. **57**, 1–28.

Egbert, G. D. and Kelbert, A. 2012. Computational Recipes for Electromagnetic Inverse Problems. Geophys. J. Int. **189**, 251–267.doi: 10.1111/j.1365-246X.2011.05347.x

Kelbert, A., Meqbel, N., Egbert, G.D. and Tandon, K. 2014. ModEM: a modular system for inversion of electromagnetic geophysical data. Comput. Geosci. **66**, 40–53.

Maurya, V. P., Shalivahan, Bhattacharya, B.B. and Das, L.K., 2015. Preliminary magnetotelluric results across Dalma Volcanics, Eastern India: Inferences on metallogeny. Journal of Applied Geophysics. **115**, 71–182.

MECL,2010.Geological report on Detailed Exploration for Gold ore in Parasi (Central Block) gold Gold deposit –Phase-I & Phase-II, north of Sonapet anticline, dist:Ranchi, Jharkhand.

Meqbel, N.M., Egbert, G.D., Wannamaker, P. E., Kelbert, A. and Schultz, A. 2014. Deep electrical resistivity structure of the northwestern U.S. derived from 3-D inversion of US Array magnetotelluric data. Earth and Planetary Science Letters. **402, 290**–304

Shalivahan, Bhattacharya, B.B., Rao, C., N.V. and Maurya V.P. 2014. Thin lithosphere–asthenosphere boundary beneath Eastern Indian craton. Tectonophysics. **612–613**, 128–133.

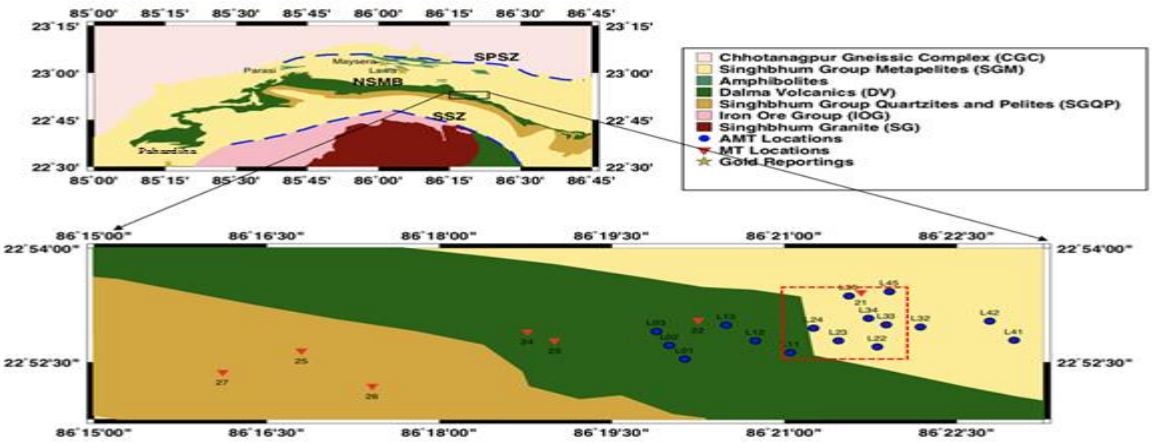

Figure 1: Geological map (modified after Saha, 1994) showing major lithologies of North Singhbhum Mobile Belt and its adjoining area with MT locations (top left), zoomed MT/AMT locations in the northern fringes of Dalma Volcanics (bottom). Star symbol shows the gold reporting in neighboring locations. The red rectangle broadly shows the location of conductor (C1) in the northern fringe of Dalma Volcanics from previous 2-D MT studies (adapted from Maurya et al. 2015).SPSZ corresponds to South Purulia Shear Zone; SSZ corresponds to Singhbhum Shear Zone.

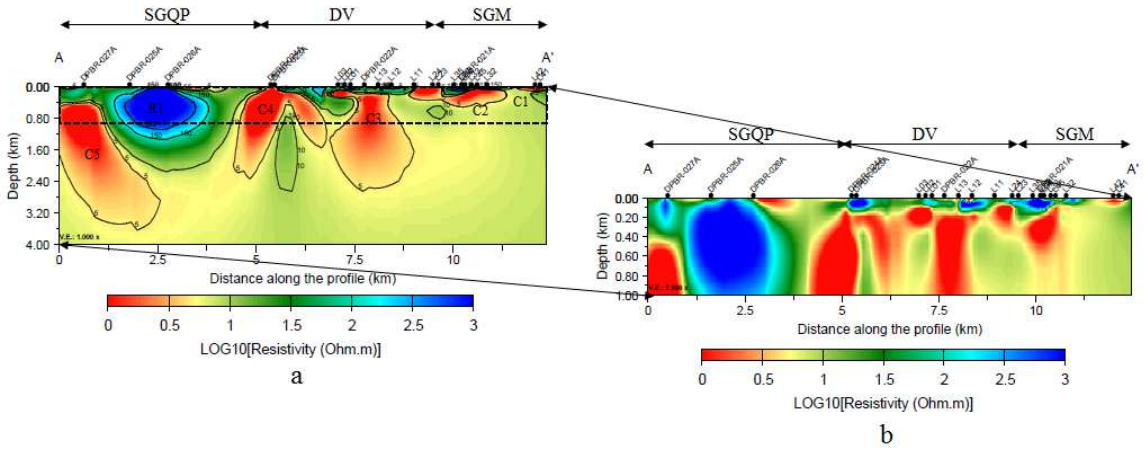

Figure 2: (a) Joint MT+ AMT inversion for impedance data upto a maximum depth of 4 km. The dashed rectangle shows the area upto a depth of 1 km and the extracted portion is shown in (b).

3-D magnetotelluric inversion for geothermal exploration in Socompa volcanic zone, NW Argentina

L. Guevara[1], A. Favetto[2] and C. Pomposiello [2]
[1]Universidad Nacional de La Plata (UNLP) - Comisión Nacional de Investigaciones Científicas (CONICET), liliguevara@ingeis.uba.ar
[2]Universidad de Buenos Aires (UBA) - Comisión Nacional de Investigaciones Científicas (CONICET), favetto@ingeis.uba.ar - cpomposi@ingeis.uba.ar

SUMMARY

The Socompa volcano lies in the arid core of the Puna region. It is a stratovolcano whose summit reaches 6,051 m high and it is located between the limit of the Antofagasta region, Chile and the Province of Salta, Argentina. The volcano is located in a sterile environment, and the diversity and abundance of life that has been documented in the region is explained through a geothermal system revealed in the form of fumaroles and hot springs of stable temperatures. These manifestations suggest the importance of a magnetotelluric (MT) research to study a potential geothermal field that has not been explored. The MT method has been widely used in geothermal exploration.
In December 2017, we carried out the first survey in the region. The present work is oriented to determine the top of the layer that could be the reservoir of the geothermal system. According to the literature, thermal manifestations are located in the Socompa Lagoon and in Quebrada del Agua fault. The survey consisted in 34 MT stations that covered the area. A 3D inversion was performed employing the ModEM code using a frequency range from 1 to 1000 Hz. The results showed a highly conductive layer at approximately 450 m depth.

Keywords: Magnetotelluric, Socompa volcano, Geothermal field

INTRODUCTION

Socompa volcano is the most voluminuos stratovolcano of the Central Volcanic Zone in western South America, where volcanism is due to the Nazca plate subduction below the South American plate. The volcano presents on its northwest flank an extensive scar caused by the collapse of a portion of the building that produced a large avalanche of debris (25 Km^2) (see Figure 1). The age of a deposit related to the collapse was estimated about 7200 years ago. There was evident post-avalanche activity, including lava flows and dacitic domes within the scar of the avalanche that has not been dated (Grosse et al, 2017). The southeast flanks present a steep slope towards a basin that is 3400 m above sea level, and that contains the Socompa lagoon (Argentina) where a small stream and a number of seeps bring hydrothermal water from the volcanic system into the lagoon (Farias et al, 2013). The main structural features are Quebrada del Agua fault and to a system faults from the circular lineament of dacitic domes that delimit the low of the lagoon and the low that surrounds the volcano (Seggiaro and Apaza, 2018).

Quebrada del Agua Volcano-sedimentary Complex at 200 m depth is the formation that is expected be acting as seal and reservoir of the geothermal field. It is composed by piroclastites, conglomerates, andesites and dacitic and riodacitic domes and it is assigned to the upper Oligocene-Lower Miocene period (Zapppettini and Blasco, 2001). Three members were identified, lower, middle and upper, with estimated thicknesses of 110 m, 200 m and 230 m, respectively. Above Quebrada del Agua Complex there are andesitic and dacitic lavas (Seggiaro and Apaza, 2018). In the region the formations are mainly resistive and if there is a hydrothermal pro-

cess the alteration of the clays would lead to a significant decrease in resistivity (Muñoz, 2014).

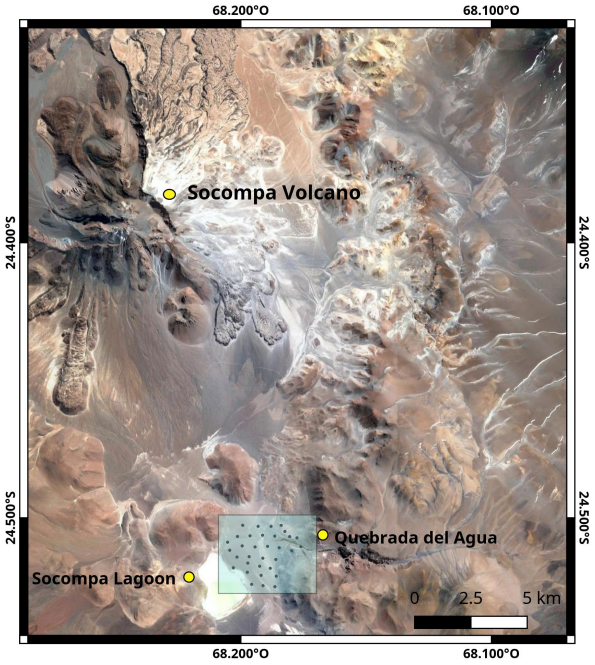

Figure 1: Socompa volcano and main regional features. The light blue area shows the MT sites distribution.

3-D INVERSION

For 3-D inversion we used ModEM code developed by Egbert and Kelbert (2012). The 34 MT sites are separated around 500 m. In total the model has 45x50x105 cells in the X, Y and Z directions, respectively, where the X axis point towards geographic north, the Y axis towards east and the Z axis down. The horizontal cell size is 170 m in X and 150 m in Y direction, consider at list a cell between sites, and out of the area cells increment by a linear factor of 1.2. In vertical, the thickness of the first cell was 5 m and the increment applied was lineal in a factor of 1.05.

To determine the best half-space value for the prior model multiple inversions were carried out, and the value chosen was 30 Ωm since it has the best nrms fit. The inversion was performed using 32 periods from 0.001-1 s, and in this first step we inverted off-diagonal impedance tensor elements. Error floor was set at 5 $\%$ of $|Z_{xy} * Z_{yx}|^{1/2}$ and the covariance in 0.3 in all directions.

RESULTS

After 80 iterations, the final nrms achieved was 1.81.

Previous inversion, 1-D analysis of each site was carried out using the Winlink code. From this analysis it was observed that the resistivity drops drastically from hundreds of Ωm to values close to 1 Ωm for an average depth of 500 m. In order to validate the results a half-space of 30 Ωm with a layer thickness of 200 m of 1 Ωm at 500 m depth covering the region where it is expected was considered as prior model. The parameter that was modified until the discrepancy between the models was negligible was the increase in Z. For a linear increase of 1.15, the greatest difference between the half-space model and the half-space model with the layer is the resolution of the thickness of the conductive layer, being much greater for the first case. As the increase considered decreases, this discrepancy becomes smaller. Finally, for an increment of 1.05 the final nrms of the half-space with the layer was 1.85 and the models do not show considerable differences. For all the increments considered, the depth of the conductive layer did not vary significantly.

Figure 2 and Figure 3 shows the principal structures observed. The model presents:

- A resistive layer (> 500 Ωm) on the surface
- Conductive bodies (< 5 Ωm) near lagoon
- A layer of low resistivity (< 5 Ωm) at a depth about 400-500 m with a thickness of 150 m covering the study area

Under the conductive layer the model can not resolve structures.

The surface layer that covers the area is resistive as expected for volcanic rocks. The conductive bodies observed near surface in the vicinity of the lagoon are associated with seeps which bring hydrothermal water into the lagoon. Finally, the conductive layer is associated with hydrothermal alteration, and since the depth of the Quebrada del Agua Complex is around 200 m is estimated that it is associated with the upper and/or middle member.

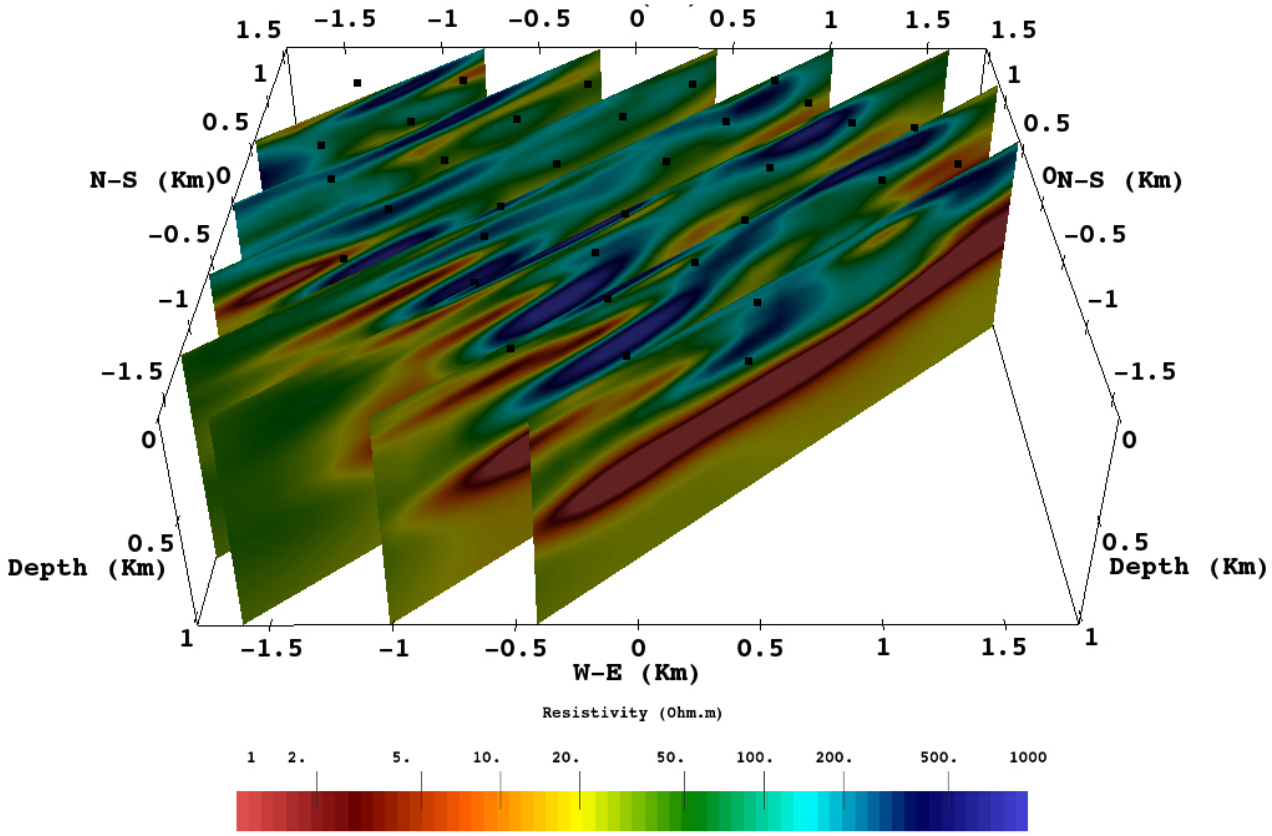

Figure 2: Vertical slices in the direction of Quebrada del Agua-Socompa Lagoon (NE-SW).

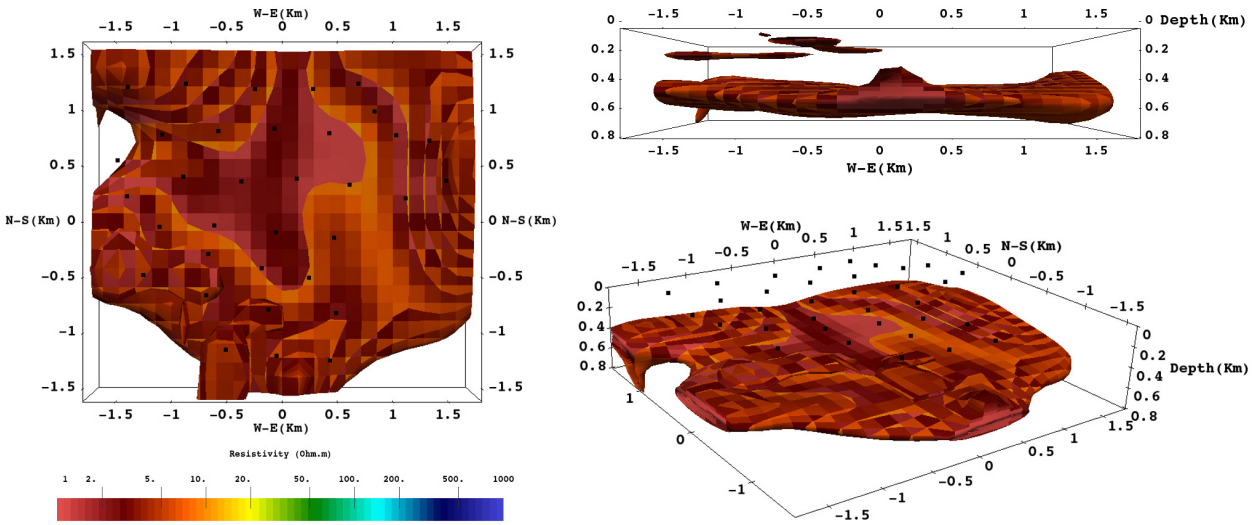

Figure 3: Conductive structures (< 5 Ωm).

CONCLUSION

From 3-D inversion a surface resistive layer (> 500Ωm) associated with volcanic deposits was observed. At 400-500 m depth, a conductive layer (<5 Ωm) of 150 m thickness was detected associated with hydrothermal process that would take place in the upper and / or middle member of Quebrada del Agua Complex. Under the conductive layer a resistive layer associated with the geothermal reservoir is expected but the model can not determine structures below it.

In order to delineate the boundary of the resource field, in October/November 2018 another survey will be carried out to cover the southern region of Socompa lagoon. It will also MT data be registered with other equipment that covers longer periods in order to study the structures below the conductive layer and to try to delimit the heat source of Socompa geothermal field.

ACKNOWLEDGMENTS

We thank SEGEMAR, in particular to geothermal department, for allowing us to use the data, to Gabriel Giordanengo (Instituto de Geocronología y Geología Isotópica, INGEIS) for his invaluable technical assistance during the surveys. We also thanks to A. Kelbert, and G. Egbert for providing their inversion algorithm and to Naser Meqbel for providing his Grid3D software.

REFERENCES

Egbert G, Kelbert A (2012) Computational recipes for electromagnetic inverse problems. Geophysical Journal International 189(1):251–267

Farias ME, Rascovan N, Toneatti DM, Albarracin VH, Flores MR, Poire DG, Collavino MM, Aguilar OM, Vazquez MP, Polerecky L (2013) The discovery of stromatolites developing at 3570 m above sea level in a high-altitude volcanic lake Socompa, Argentinean Andes. PloS one 8(1):e53497

Grosse P, Guzman S, Petrinovik I (2017) Volcanes compuestos cenozoicos del noroeste argentino. In: Ciencias de la Tierra y Recursos Naturales del NOA. Relatorio del XX Congreso Geológico Argentino, San Miguel de Tucumán, pp 484–517

Muñoz P (2014) Exploring for geothermal resources with electromagnetic methods. Surveys in geophysics 35(1):101–122

Seggiaro R, Apaza F (2018) Geologia y estructuras relacionadas al proyecto geotermico Socompa. Tech. rep., Servicio Geologico Minero Argentino

Zapppettini EO, Blasco G (2001) Hoja Geologica 2569-11, Socompa, Provincia de Salta, Republica Argentina. Tech. rep., Servicio Geologico Minero Argentino. Buletin 26:65

3-D modelling of storm time ground geoelectric field spatio-temporal evolution for the Northeastern United States

E. Ivannikova[1], M. Kruglyakov[1,2], A. Kuvshinov[1], L. Rastätter[3], A. Pulkkinen[3], C. Ngwira[3] and B. Murphy[4]
[1]Institute of Geophysics, ETH Zurich, Zurich, Switzerland, elena.ivannikova@erdw.ethz.ch
[2]GEMRC IPE RAS, Troitsk, Moscow, Russian Federation
[3]NASA Goddard Space Flight Center, Greenbelt, Maryland, USA
[4]Oregon State University, Corvallis, Oregon, USA

SUMMARY

During geomagnetic storms a strong electric field is induced in the conducting Earth. This field drives electric currents (so-called, geomagnetically induced currents) in ground-based technological systems, affecting their operation. Understanding (via modelling) the spatio-temporal evolution of the ground geoelectric field is a key to predicting, assessing, and, potentially, forecasting the space weather impact on critical infrastructure.

We present the results of the ground geoelectric field three-dimensional (3-D) modelling for the Northeastern United States due to St. Patrick geomagnetic storm in March 2015. Varying in both time and space inducing source model is constructed using a 3-D magnetohydrodynamic physics-based simulation of near-Earth space. We explore the effects, arising from conductivity contrasts, for various conductivity models of the region, including a realistic 3-D model, obtained using the EarthScope project magnetotelluric data inversion. We conclude, that the ground geoelectric field in the region is subject to substantial perturbation due to coastal and galvanic effects.

Keywords: electromagnetic modelling, magnetohydrodynamic modelling, 3-D conductivity models

3D TEM Forward Modelling of Volcanic Environments

Carolin Ader, Klaus Spitzer, Matthias Hort

May 25, 2018

Investigation and monitoring of volcanoes is important because understanding volcanic processes is crucial in estimating volcanic risk. Among these processes, those inside volcanic conduits are of prime interest as they control the final rise of magma prior to an eruption, but cannot be observed directly. For example, Strombolian eruptions are assumed to be driven by gas slugs which rise inside the conduit and burst at the magma air interface. Unfortunately, the final rise of these gas slugs has not been quantified in the field well yet.
The transient electromagnetic method (TEM) is a promising geophysical method for imaging fast changes in conductivity distribution as expected by gas slugs ($<$10s). Due to its multiple time gates TEM covers a variety of penetration depths. The time range with a maximum of 10 ms allows for numerous subsequent measurements during the final rise of the gas slug.
In order to reveal the possibilities and limitations of TEM applied to a volcanic environment we present 3D forward calculations using models guided by the shape of Stromboli volcano, including volcanic features such as topography and axisymmetric conduits. Thus, we consider challenging geometries both in computational memory and numerical stability.
The modelling process includes the use of a digital elevation model of Stromboli volcano. Our simulation code uses finite elements on an unstructured tetrahedral mesh for spatial discretization and either an implicit Euler or rational Arnoldi method for temporal resolution. As virtual measurands (i.e. simulation quantities) we consider both the electrical field and the time derivative of the vertical component of the magnetic flux density.
The results of our virtual experiments are used to determine an ideal configuration for a field experiment at Stromboli volcano.

The preliminary observation of CSELF earthquake monitoring network

Tang Ji, Zhao Guoze，Chen Xiaobin, Han Bin, Wang Lifeng, Zhan Yan, Xiao Qibin, Dong Zeyi
State Key Laboratory of Earthquake Dynamics, Institute of Geology, China Earthquake Administration,
Beijing, China, 100029
email to tangji@ies.ac.cn

SUMMARY

A Control source of extremely low frequency (CSELF) electromagnetics network for earthquake monitoring has been setup since 2015 in China. The 5 components layout of MT measurement used in all stations and GMS-07 system made by Metronix is equipped in the station. Observation mixed CSELF and nature source. Data record configuration is that natural field will be observed by using 3 sample bands with sampling rate 4096Hz，256Hz and 16Hz and that Control source record by using 4 sampling rates with 2048Hz, 512 Hz, 128Hz and 32Hz. For nature source observation, the 16Hz records continuously in all-day and the high and medium frequency band use a slices record with recycling acquisition in every 10 minutes with length of about 4 to 8 seconds and 64 to 128 seconds, respectively. All the data is automatically processed by server installed in the observatory. The EDI files including EM field spectrums and MT responses and time series files sent the data center in geology institute, China Earthquake Administration by internet.

There shows preliminary observation for nature source since the network set up. Some variation characteristics of EM field spectrum and the apparent resistivity with time has been observed. They show some regular and irregular changes as following:

1) The EM spectrum shows Annual change characteristics that maximum amplitude appears in the summer and minimum value in winter.
2) The apparent resistivity changes of different frequencies depend on the station. Some stations are very stable and some stations change with time. The apparent resistivity changes maybe related to deformation.
3) Schumann resonance shows Annual change characteristics that maximum amplitude appears in the summer and minimum value in winter. But the resonance frequencies change with the season.
4) There are some earthquakes events happened. The Electromagnetic precursors were observed. The apparent resistivity increased about 2 month before the earthquake and the EM field changes enhanced also.

This study is supported by The ELF Engineering Project for Underground exploration of China (15212Z0000001), National Natural Science Foundation of China (41674081) and China Earthquake Administration etc.

Keywords: Electromagnetic field, CSELF, Earthquake, Apparent resistivity.

A Detailed Model of the Irish High Voltage Power Network for Simulating GICs

S. Blake[1], P. Gallagher[1], J. Campanyà[1], C. Hogg[2], C. Beggan[3], A. Thomson[3], G. Richardson[3], D. Bell[4]

[1]Trinity College Dublin, Ireland, email contact: blakese@tcd.ie
[2]Dublin Institute for Advanced Studies, Ireland
[3]British Geological Survey, UK
[4]EirGrid plc, Ireland

SUMMARY

Constructing a power network model for geomagnetically induced current (GIC) calculations requires information on the DC resistances of elements within a network. This information is often not known, and power network models are simplified as a result, with assumptions used for network element resistances. Ireland's relatively small, isolated network presents an opportunity to model a complete power network in detail, using as much real-world information as possible. A complete model of the Irish 400, 275, 220 and 110 kV network was made for GIC calculations, with detailed information on the number, type and DC resistances of transformers. The measured grounding resistances at a number of substations were also included in the model, which represents a considerable improvement on previous models of the Irish power network for GIC calculations. Sensitivity tests were performed to show how calculated GIC amplitudes are affected by different aspects of the model. These tests investigated: (1) How the orientation of a uniform electric field affects GICs. (2) The effect of including/omitting lower-voltage elements of the power network. (3) How the substation grounding resistances assumptions affected GIC values. It was found that changing the grounding resistance value had a considerable effect on calculated GICs at some substations, and no discernible effect at others.

Keywords: Geomagnetically Induced Currents, Ireland, electric power network

A floating transient electromagnetic system to acquire dense data on volcanic lakes - Investigation of the Furnas hydrothermal system (São Miguel Island, Azores)

P. Yogeshwar[1], M. Küpper[1], B. Tezkan[1], V. Rath[2], D. Kiyan[2], C. Hogg[2], S. Byrdina[3], J. V. Cruz[4,5], C. Andrade[5] and F. Viveiros[5]

[1]Institute of Geophysics and Meteorology, University of Cologne, Germany, yogeshwar@geo.uni-koeln.de

[2]Dublin Institute for Advanced Studies, School of Cosmic Physics - Geophysics Section, Ireland

[3]Université de Savoie Mont Blanc, Institut des Sciences de la Terre (ISTerre), France

[4]Department of Geosciences, University of the Azores, Ponta Delgada, Portugal

[5]Research Institute for Volcanology and Risk Assessment, University of the Azores, Ponta Delgada, Portugal

Often geophysical surveys leave out water covered areas due to inaccessibility, leading to a lack of resolution in derived subsurface images and consequently leading to interpretation uncertainty. For measurements on volcanic lakes we used a floating transient electromagnetic system (FloatTEM) composing an in-loop TEM configuration. The current FloatTEM system allows for earth exploration down to approximately 200 m depth but can be modified to a semi-FloatTEM system for deep exploration down to 500 m depth using large sources and mobile receivers. The existing FloatTEM system was successfully applied to image sedimentary deposits of a volcanic maar lake in the Eifel/Germany. Recently, the FloatTEM system was successfully used to image the hydrothermal system and CO_2 outgassing areas of the Furnas intracaldera volcanic lake. The Furnas Volcano is located in the eastern part of São Miguel island. Volcanic activity is mostly prominent in the northern part of the caldera, where fumarolic fields, thermal springs and intense CO_2 outgassing are the main hydrothermal manifestations. The Furnas lake is roundly shaped and has a diameter of around 1.5 - 2 km. As there were no previous geophysical measurements conducted on the lake, the structures below the lake as well as the extent of the hydrothermal system were unknown.

The floating 18 m x 18 m square measurement system is built of a frame of conventional plastic drain pipes. While on water, the TEM construction is pulled by a boat also containing the measurement equipment. The pipes are tight together using several tow ropes with adjustable tension belts to ensure stability on water. Additional fenders and floats are used to ensure sufficient buoyancy. To allow for enhanced survey speed and dense data acquisition the FloatTEM system was continuously pulled with a maximum speed of 0.2 m/s. During the field survey 52 stations were measured while the boat and the pipe construction were anchored on the lake. In order to provide a dense data coverage in the northern lake area where intense CO_2 outgassing was detected, measurements were conducted continuously while the boat was slowly pulling the FloatTEM system. The continuous driven measurements resulted in around 500 soundings near the fumarolic fields. The exploration depth of the continuous measurements is around 80 m, whereas the anchored soundings provide depth information down to approximately 180 m. We achieved to collect a large and very dense data set, consisting of more than 650 TEM soundings in total on the lake and six land-based reference stations. The data is inverted using conventional 1D inversion schemes. In addition, a 2D modeling study is performed to analyze 2D effects in the TEM data and rule out miss-interpretations. The results show a well conducting anomaly in approximately 50 m depth below the water level in the northern part of the lake, that correlates well to the already known CO_2 outgassing anomalies and the hydrothermal system. Towards the main lake in the southern part, the good conductor dips downwards to approximately 120 m depth. This well conducting structure is currently interpreted as the shallow aquifer that feeds the surface hydrothermal manifestations, although other interpretations cannot be excluded. This mobile measurements are a rather new approach for TEM surveys on volcanic lakes, that proved to be a success with respect to survey speed and data coverage.

Keywords: transient electromagnetics (TEM), volcanic lakes, Furnas hydrothermal system, Azores

A study of an ore deposit in northern Sweden using surface and borehole magnetotelluric data

Thomas Kalscheuer[1], Lisa Dossow[1], Niklas Juhojuntti[2] and Lars Dynesius[1]
[1]Uppsala University, Department of Earth Sciences, Uppsala, Sweden,
e-mail: thomas.kalscheuer@geo.uu.se.
[2]LKAB, Kiruna, Sweden.

SUMMARY

During the last 30 years, standard magnetotelluric (MT) measurements at the surface have been routinely used to delineate ore deposits at depth. However, mineral prospecting is often accompanied by intensive drilling programs. At its best, these drilling programs have been utilised in inversion of MT data by including borehole logs as prior constraints. Nevertheless, previous synthetic studies have investigated to what extent combinations of MT surface and borehole measurements can improve models of electrical resistivity as compared to models computed from surface data alone. Possible types of MT borehole data include vertical gradient magnetometry data, vertical magnetic transfer functions and vertical electric transfer functions relying upon borehole measurements of horizontal magnetic fields, vertical magnetic fields and vertical electric fields, respectively. Since suitable magnetic field sensors are not presently available, we recorded combinations of MT surface impedances and axial voltages (i.e. electric fields integrated along boreholes) at a mineral exploration site in northern Sweden close to Kiruna. Our contribution covers the following theoretical and interpretational aspects. First, we introduce axial voltage transfer functions for borehole measurements of the telluric field and describe system response effects of the electric field cable and excess cable on the winch. Second, we present a preliminary 2D inversion model of the surface MT impedance data. Third, we discuss the compatibility of the axial voltage transfer function derived from our borehole field data with the 2D inversion model. In the near future, we will include the axial voltage transfer functions in the inversion of the field data. The required functionality for the 2D inversion scheme has already been developed.

Keywords: Magnetotellurics, borehole measurements, ore deposits, 2D inversion

An approach to coupling geospace and regional 3-D electromagnetic induction modellings

E. Ivannikova[1], M. Kruglyakov[1,2], A. Kuvshinov[1], L. Rastätter[3], A. Pulkkinen[3]
[1]Institute of Geophysics, ETH Zurich, Zurich, Switzerland, elena.ivannikova@erdw.ethz.ch
[2]GEMRC IPE RAS, Troitsk, Moscow, Russian Federation
[3]NASA Goddard Space Flight Center, Greenbelt, Maryland, USA

SUMMARY

In order to assess hazards from Space Weather we developed an approach to coupled regional 3-D electromagnetic forward modelling from far geospace down to the surface of the Earth. The approach involves four main steps. First, we run a global magnetohydrodynamic model of the near-Earth space for geomagnetic disturbance of interest. Then, using the results of magnetohydrodynamic modelling, we compute the spatio-temporal distribution of the external magnetic field for this event on a regular grid at the surface of the Earth. Third, the external field is converted into equivalent current (source), and, finally, for a given source and a given 3-D conductivity model of the Earth the spatio-temporal distribution of the ground electromagnetic field is computed in the region of interest. Using this approach and the British Isles as a test region, we perform 3-D modelling of ground electromagnetic field for the Halloween geomagnetic storm in November 2003 and discuss the results.

Keywords: electromagnetic modelling, magnetohydrodynamic modelling, 3-D conductivity models

Analysis of the applicability of electromagnetic geophysical data to processing of seismic reflection data for recognition of near-surface geology

Adam Cygal[1], Michal Stefaniuk[1], Jolanta Pilch[1], Krzysztof Dzwinel[2] and Marek Sada [3]

[1] AGH University of Science and Technology, cygal@agh.edu.pl
[2]ORLEN Upstream, Krzysztof.Dzwinel@orlen.pl
[3] PBG Geophysical Exploration Ltd., m.sada@pbg.com.pl

SUMMARY

Multivariate non – seismic geophysical surveys was made in a framework of “Blue Gas I” program. Research area was located in the region of Lublin Basin. The near-surface geology of the study area is consisted of horizontal, undisturbed Jurassic and Cretaceous sediments overlaid by Pleistocene unconsolidated cover. The works was performed to obtain shallow distribution of P-wave velocity for static correction computation. Joint inversion methods was applied to obtain detailed velocity, density and resistivity fields. Along 6 km seismic test line, the 2D seismic reflection, magnetotelluric (AMT/MT), gravity, transient electromagnetic (MulTEM – Multi Transient Electromagnetic Method, LoTEM – Long Offset Transient Electromagnetic Method) and resistivity (ERT - Electrical Resistivity Tomography , VES - Vertical electrical sounding) data was collected.

The first stage of work was related to joint inversion of gravity and seismic data. During this stage, the problem of high sensitivity of the inversion results to methodology of initial models construction was encountered. Integrated analysis of well logs, available geological datasets and hydrogeological data indicate that for the proper calculation of seismic static correction and appropriate imaging of the characteristic of geological conditions the use of independent data is necessary (for example resistivity or electromagnetic data).

Obtained results of integrated interpretation of independent geophysical and geological data allowed for validation of near surface velocity models for static correction computation. As a consequence, a better results of reflection seismic data processing which influenced on proper imaging of deep structures in the seismic sections were received.

This paper was prepared based on results of investigations carried out in the framework of the project entitled: Blue Gas I – GASLUPSEISM. We appreciate the support from Halliburton/Landmark (SeisSpace) and GeoTomo LLC (TomoPlus 2D/3D) to perform this study.

Keywords: Magnetotellurics, Transient Electromagnetic Method, seismic data processing, simultaneous joint inversion, static correction.

Application of multi-offset arrays in TEM studies on the Siberian platform

Sofia Kompaniets[1], Nikolay Kozhevnikov[2]
[1]CJSC Irkutsk Electroprospecting Company, Irkutsk, Russia, ksv@ierp.ru
[2]Institute of petroleum geology and geophysics SB RAS, Novosibirsk, Russia,
KozhevnikovNO@ipgg.sbras.ru

SUMMARY

Yearly, about ten thousand TEM soundings are carried out in the search for and exploration of oil and gas fields on the Siberian platform. In this region, induced electrical polarization and magnetic viscosity of the near-surface rocks have a significant effect on the TEM response. The use of multi-offset arrays makes it possible to recognize and evaluate induced polarization and magnetic viscosity effects in the TEM data.

Keywords: TEM, induced polarization, magnetic viscosity, Siberian platform

INTRODUCTION

When studying the sedimentary cover of the Siberian Platform, the TEM sounding method is one of the main tools, in combination with seismic prospecting, for oil and gas exploration. The geoelectrical model of the sedimentary cover is favorable for using TEM soundings: the conductance of reservoirs is 10 – 20 S which is sufficient to be seen against the background of the total sedimentary cover conductance of 50-300 S (Mandelbaum et al. 1984). Along with oil and gas prospection, the TEM method is used in search for and exploration of ore deposits, in hydrogeology, and engineering geology (Stognii and Korotkov 2010).

In recent years, multi-offset TEM arrays have found wide application in the study of the Siberian platform. These arrays allow simultaneous recording of several TEM responses from one transmitter loop.

An even more important advantage of using such arrays is the ability to recognize the manifestations of induced polarization (IP) and magnetic viscosity (MV) phenomena affecting TEM responses measured in studies of the Siberian platform (Kozhevnikov and Antonov 2009, Kompaniets et al. 2013, Kozhevnikov et al. 2016).

MULTI-OFFSET ARRAYS AND TECHNOLOGY

A geoelectrical model, targets and stage of the survey, and network of seismic profiles determine parameters of the TEM array.

Usually, at the exploratory stage, the number of measurement points per square kilometer is 8 – 12, and during monitoring about 20 – 25.

TEM surveys are carried out using the SGS-TEM telemetric measuring system (Sharlov et al. 2010). In the case of profile works, a five-offset array is used with 18m by 18 m receiving loops located in the transmitter loop center (coaxial receiving loop), and at offsets of 500 m and 1000 m (offset receiving loops). The current in the transmitter loop is 40 to 200 A. At each measuring point, from 15 to 30 transients are recorded each of which results from stacking of 100 to 200 voltage time series. Usually, this ensures the latest measuring time of 500 – 2000 ms.

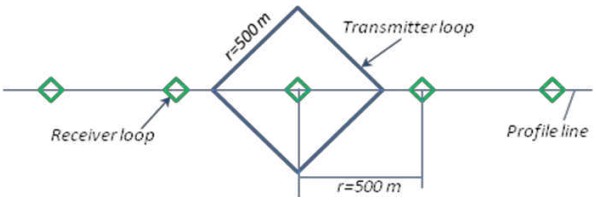

Figure 1. Multi-offset TEM array.

To control the quality of the TEM data, R. Guseinov (2015) has developed a special technique for recognizing and estimating systematic measurement errors.

IINDUCED POLARIZATION AND MAGNETIC VISCOSITY EFFECTS

As mentioned above, important feature of multi-offset arrays is that they allow one to recognize magnetic viscosity and induced polarization effects in the TEM data.

Figure 2 illustrates the induced polarization effect. At late times, the apparent resistivities for coaxial receiver loop are higher than those for the offset loops. Usually, the difference between apparent

resistivity curves becomes noticeable starting from about of 20 to 60 ms (Figure 2).

On the south of the Siberian platform, about 60% of the available (more than 70,000 transients) TEM data are affected by the IP phenomenon.

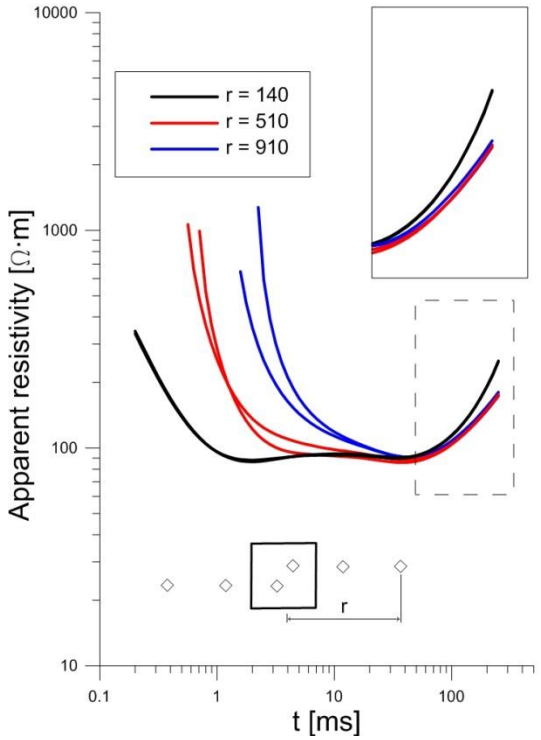

Figure 2. TEM apparent resistivity curves exhibiting the induced polarization effect: (A) general view, (B) late time response.

Rocks of the trap formation, which exhibit strong magnetic viscosity, cover a significant part of the Siberian platform. Recall that Magnetic viscosity is a property of materials containing ferro- and ferrimagnetic particles. It manifests itself as a time lag of the magnetization change from the change in the applied magnetic field.

Until recently, magnetic viscosity effect in TEM data was observed predominantly when working with small size arrays. However, with the today's TEM measuring systems and processing techniques, magnetic viscosity effects have become noticeable when using large TEM arrays. Modeling TEM responses for multi-offset arrays with allowance made for magnetic viscosity effect has proved that this effect is associated with traps and tuffs of the Triassic effusive formations (Kozhevnikov 2016)

Unlike induced polarization response, TEM voltage response to magnetically viscous ground decays more slowly than that due to the EM induction. For central loop arrays, magnetic viscosity response is added to and for offset arrays subtracted from the EM response. Figure 3 shows that at late times central loop apparent resistivities are smaller than those for the offset loops. For receiver loops located outside the transmitter loop, the contribution of the magnetic viscosity response to the total one decreases with the offset.

Inversion of TEM data affected by magnetic viscosity is still an unsolved problem. As for the IP-affected TEM response, after it is recognized it can be interpreted in terms of conductive and polarizable ground model.

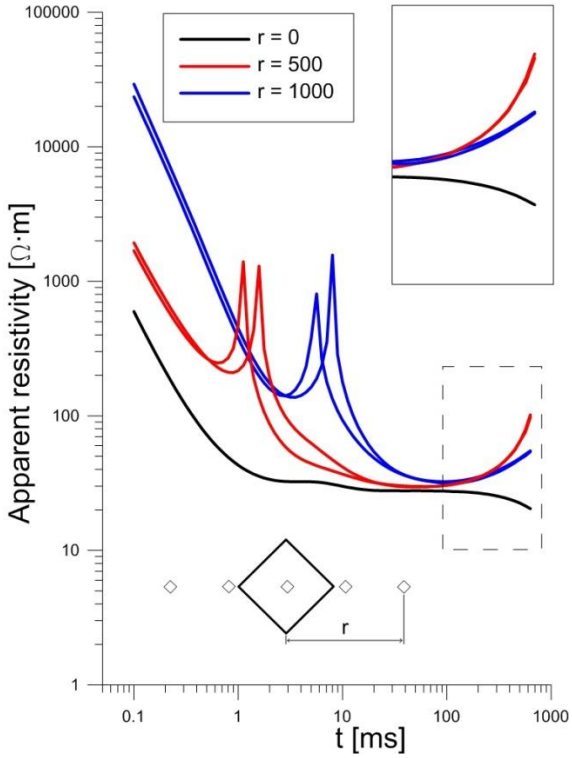

Figure 3. TEM apparent resistivity curves exhibiting the magnetic viscosity effect: (A) general view, (B) late time response.

Usually, polarization is accounted for by using, in calculation of a TEM response, complex frequency-dependent Cole-Cole resistivity $\rho^*(\omega)$:

$$\rho*(\omega) = \rho_0\left\{1-\eta\left[1-\frac{1}{1+(j\omega\tau)^c}\right]\right\},$$

where $j=\sqrt{-1}$; ω is the angular frequency; ρ_0 is the dc resistivity; η is the chargeability (from 0 to 1); c is the exponent; τ is the relaxation time.

Figure 4 shows an example of interpretation of IP affected TEM sounding data obtained during TEM survey over an area located in the south of the Siberian platform.

Inversion of the TEM data shows that polarizable are near-surface rocks with chargeability of 0.01 to

0.2 (Figure 4). The areas of increased chargeability correlate spatially with those where the Jurassic rocks are mapped on the surface.

According to the description of the core samples, pyrite aggregates are present at depth from 0 to 150 m in Jurassic and Cambrian sedimentary rocks. There are also thin layers of coal and carbonaceous argillites which are supposed to contribute to the IP response.

Inversion without taking into account the IP response results in appearing deep resistive 'features' which, as it is known, actually do not exist. On geoelectric section such 'features' are manifested as vertical resistive zones and do not lend themselves to reasonable geological interpretation.

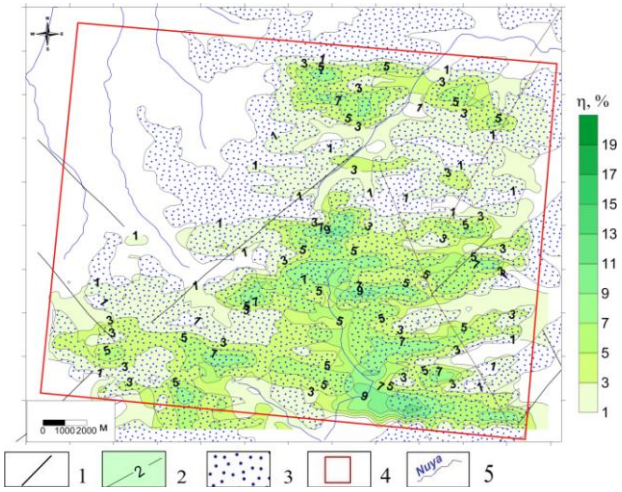

Figure 4. Map of chargeability and location of Jurassic rocks**:** (1) tectonic faults according to the geological map of scale 1: 200000; (2) chargeability contour lines; (3) Jurassic sediments; (4) TEM survey area; (5) – river network.

CONCLUSIONS

The use of multi-offset arrays makes it possible to recognize and evaluate induced polarization and magnetic viscosity effects in the TEM data.

REFERENCES

Guseynov RG (2015) System for assessing the quality of signals of TEM. Author's abstract of the PhD thesis. Irkutsk.

Kompaniets SV, Kozhevnikov NO, Antonov EYu (2013) The manifestation of and account for inductively induced polarization in the TEM data from the south of the Siberian platform. Geofizica 2: 35 – 40.

Kozhevnikov NO, Antonov EYu (2009) TEM studies of polarizable ground. Geophysical Journal 31: 104 – 118.

Kozhevnikov NO, Agafonov YuA, Buddo IV, Kompaniets SV (2016) The effect of the Siberian flood basalts magnetic viscosity on a TEM sounding response, 23rd EMIW, Chiang Mai, Thailand.

Mandelbaum MM, Rabinovich BI, Surkov VS (1984) Geophysical methods in the search for oil and gas deposits on the Siberian platform. Novosibirsk.

Stognii VV, Korotkov UV (2010) Search for kimberlite bodies by the TEM prospecting method. Novosibirsk.

Sharlov MV, Agafonov YuA, Stefanenko SM (2010) Telemetric TEM systems SGS-TEM and FastSnap. Efficiency and experience of use. Instruments and systems of exploration geophysics 01(31): 20 – 24.

Application of spectral induced polarization method (SIP) at complex studying of low-contrast magnetic anomalies

Anastasia Solovieva[1], Victor Kulikov[1,2]

[1] Nord-West Ltd., Moscow, Russia, solovieva@nw-geophysics.ru
[2] Lomonosov Moscow State University, Moscow, Russia

SUMMARY

The purpose of this study is to identify various geophysical and geological section parameters by integrating electrical and magnetic exploration. The objects of research are the paleovalleys filled with deposits of clay, loam and sand. The complex geophysical work presented a detailed ground magnetic prospecting, electric profiling and spectral induced polarization method (SIP), which is based on the IP measurements at several frequencies in frequency domain. SIP method was carried out using a symmetrical four-electrode Schlumberger array with special spacing (AB/2) and step between points. This array allows getting data as a result of electric tomography and to carry out two-dimensional inversion.

Particular attention was paid to section elements, which are characterized by high values of magnetic susceptibility and chargeability. For all the collected materials complex interpretation was performed, we received two-dimensional model of resistivity and chargeability and held lithological core analysis.

The main conclusion of the research is that the anomalies in the magnetic field and the high values of the induced polarization are due to the presence of finely dispersed iron compounds and the iron in amorphous form.

Keywords: spectral induced polarization, magnetic prospecting, paleovalley, complex interpretation

Aquifer delineation using the Tempest AEM system

A.Smiarowski[1], S. Ryan[2], D. Schafer[2], F. Miorelli[1] and W. Soyer[1]
[1]CGG Multi-Physics, adam.smiarowski@cgg.com, federico.miorelli@cgg.com, wolfgang.soyer@cgg.com
[2]DWER, sheryl.ryan@dwer.wa.gov.au, david.schafer@dwer.wa.gov.au

SUMMARY

The Western Australia Department of Water and Environmental Regulation (DWER) utilized the Tempest system in a survey over the North Gnangara Mound, Perth Basin in 2013, to image hydrogeology relevant to groundwater resources important to Perth's public water supply. In 2017, DWER extended the survey to target the Leederville-Parmelia aquifer, by flying an adjacent area covering the Dandaragan Plateau approximately from Gingin to Eneabba to the north, using an updated Tempest system.

In total over 10 000 line kilometres have been flown covering a combined area of over 6000km2. Borehole resistivity, lithological logs and groundwater chemistry from over 300 bores was used to help interpret and constrain the inversion of the acquired AEM data. Recharge zones, regional throughflow directions, faults that act as flow barriers, groundwater discharge zones, and the extent of regionally important aquitards have been able to be inferred and mapped. Estimates of the minimum thicknesses of fresh groundwater (<500mg/L and <1000 mg/L TDS) have been made for the Superficial and Leederville-Parmelia aquifers. The surveys have helped clarify hypotheses about faults that act as flow barriers and regional flow directions that are important for groundwater allocation planning.

In this paper we present the results of both surveys, and key hydrogeological outcomes. We also compare the data from the two AEM surveys highlighting system developments, how these have led to improved data quality, and improved interpreted geological and hydrogeological outcomes.

Keywords: groundwater, aquifer, Tempest, time domain electromagnetics, salinity

INTRODUCTION

The northern Perth Basin supplies water for residential consumption, agriculture and mining operations in the area. The Perth Basin is a north to north-northwest trending, onshore and offshore sedimentary basin extending about 1300km along the south-western coast of Australia. Sediment thickness extends to about 12km onshore. There are four primary aquifers in the basin: the Superficial, Leederville, Leederville-Parmelia and Yarragadee aquifers. Using a network of more than 700 monitoring bores, it has been found that in some places the depth to water table has risen due to extensive clearing of native vegetation, while elsewhere it has declined due to extraction and a drying climate.

The area has been extensively studied with hydrogeological investigations in order to provide a secure supply of water. The Tempest fixed-wing electromagnetic system has contributed to the understanding of the hydrogeological conditions of the area with a survey flown over the North Gnangara Mound in 2013 and a recent extension of that survey over the Dandaragan Plateau to target the Leederville-Parmelia aquifer.

The Tempest system has been used extensively for hydrogeological mapping and groundwater exploration. The fixed-wing Tempest platform is able to economically survey extensive areas, important for regional surveying. Tempest has been extremely successful in hydrogeological applications due to its calibration providing data ideal for inversion modelling. A study by Sorensen et al (2015) compared calibration of ground and airborne EM data, finding that conductivity models from ground EM and Tempest provided consistent results. The authors concluded that Tempest could be used to standardize ground-based or other airborne-based survey data.

The calibrated nature of Tempest ensures that data is repeatable. This is very important for large regional scales which may be surveyed over multiple years and where consistency and repeatability of the system data is necessary for correct interpretation of data. Fitzpatrick (2013) used 36 Tempest surveys collected over a decade to build a basin-wide conductivity model for uranium exploration. Fitzpatrick showed that Tempest conductivity depth slices from different surveys (and flown with different aircraft) could be

merged together without any levelling, speaking to the calibration of the system. This is important for merging the northern Perth Basin survey here (flown with a Cessna 208) with the North Gnangara Mound survey flown in 2013 (using the Shorts Skyvan).

Method and Results

Tempest electromagnetic and magnetic data were collected in June of 2017, covering 6350 line-km. The survey area is shown in Figure 1 along with the sub-cropping geology. Tempest was operated at a 25Hz base frequency (the system is able to operate from 12.5 to 225Hz). Tempest transmits a 50% duty cycle square wave which is deconvolved to a 100% step response, providing 20ms of measurement time with a 13 microsecond sample interval. The system receiver measures all 3 components of the electromagnetic field. Data is stacked to provide a measurement station approximately every 12m. The receiver is nominally 115m behind and 45m below the transmitter; this is monitored with a GPS on the receiver to ensure accuracy when inverting Tempest data. Inclinometers provide transmitter and receiver attitude. Data are currently being modelled with the 1D inversion algorithm GALEI (Brodie, 2016).

An example of borehole resistivity data with lithology from drilling compared with AEM 1D inversion from the 2013 North Gnangara survey is shown in Figure 2. Note that the 2013 survey utilized a 75Hz base frequency so will not have the same investigation depth as a 25Hz dataset. The inversion model from the Tempest data shows excellent agreement with the borehole resistivity log in the near-surface, speaking to the calibrated nature of Tempest. Tempest correctly shows increased conductivity at the conductive Upper Parmelia and Kardinya Shale units. At depths greater than 100m, the Tempest-derived model shows correlation with the borehole resistivity trend but as the unit is beneath the conductive shale (resistor under conductor) it is more difficult to image precisely.

Figure 3 shows profile data from the Tempest system along with Layered Earth Inversion (LEI) and a Conductivity Depth Image (CDI) created from EMFlow (Macnae and Lamontagne, 1991). The borehole lithology (colours show lithology change, not conductivity) is superimposed over the LEI and CDI models. The LEI section of the Tempest data maps the thickness of the surficial sediments well and correctly maps depth extent of the relatively conductive silty sandstone and shale units. The section then slowly transitions to show the resistive sandstones at depth.

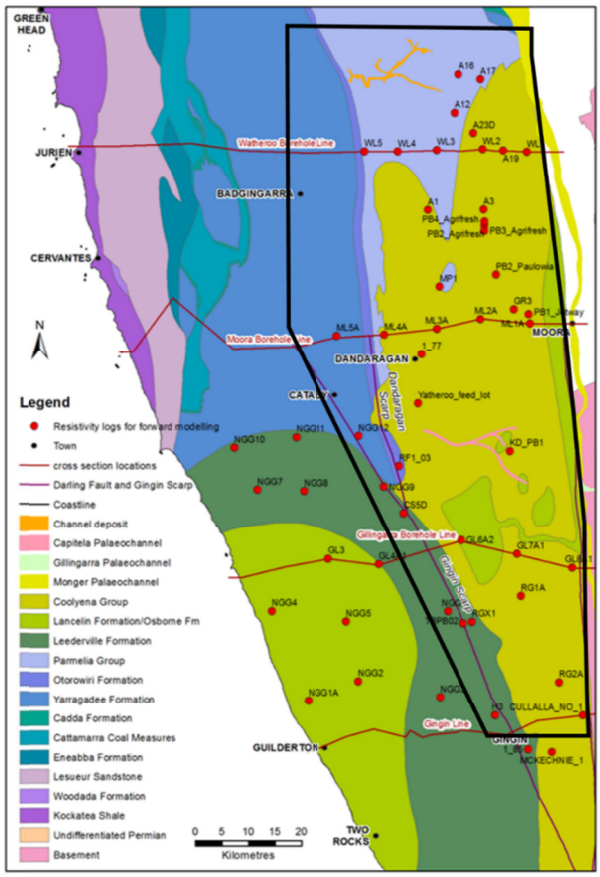

Figure 1. Sub-cropping geology of the northern Perth Basin. Boreholes are denoted by red circles while the black outlines show the current AEM survey area.

Figure 4 shows an example CDI section from the current survey. In an effort to map the water quality in the region, a previously determined power relationship between formation resistivity and groundwater salinity from borehole data for sediments in the Perth Basin has been applied to determine conductivity zones representing groundwater with different amounts of total dissolved solids (TDS). The colour palette reflects this conversion of total dissolved solids to conductivity for the region; starting from resistive, the colours indicate groundwater with salinity of less than 500, 1000, 1500, 2000, 3000 and more than 5000 mg/L TDS. The thick red layer at the left side of the section is thought to relate to evaporation concentration of salt near the coast while the thin red layers inland are likely clay layers.

Conclusions

Inversion of the newly acquired data acquired at 25Hz in the northern Perth Basin by GALEI algorithm is ongoing. Preliminary results have shown excellent correlation with outcropping clayey formations such as the Otorowiri Formation that is consistent with existing 3-D geological modelling.

This has allowed the geological model to be refined. While the power relationship between formation resistivity and groundwater salinity from borehole measurements is strictly representative of groundwater salinity from sandy beds a broad approximation of the general 3-D salinity distribution to moderate depths in the aquifer consistent with borehole data has been delineated. When the derived salinity zones are viewed in conjunction with the modelled location of clayey formations a clear picture of the distribution of groundwater salinity can be inferred at a regional scale. Important results to date include to detection of fresh groundwater under clayey formations which is consistent with field observations. The confidence depth of the data is however, a very important consideration when inferring deep fresh groundwater as resistive artefacts under shallow conductive zones can occur. Overall the surveys have provided an excellent regional scale delineation of major aquifers, aquitards and the 3-D distribution of salinity in the northern Perth Basin. Ongoing constrained inversion of the acquired data will continue to improve the 3-D conceptualization of groundwater flow in the northern Perth Basin.

REFERENCES

Brodie R (2016) User Manual for Geoscience Australia's Airborne Electromagnetic Inversion Software. Geoscience Australia.

Fitzpatrick A (2013) Maximising the benefit of historic airborne EM through new modelling – 36 surveys over a decade for building a basin-wide conductivity model for uranium exploration. SAGA Biennial Conference and Exhibition, South Africa.

Macnae J and Lamontagne Y (1987) Imaging quasi-layered conductive structures by simple processing of transient electromagnetic data. Geophysics, 52, 4.

Sørensen C, Munday T, Heinson G (2015) Integrated interpretation of overlapping AEM datasets achieved through standardisation. Exploration Geophysics 46: 309-319.

Baba K, Tarits P, Chave AD, Evans RL, Hirth G, Mackie RL (2006) Electrical structure beneath the northern MELT line on the East Pacific Rise at 15 degrees 45'S. Geophys Res Lett 33(22): L22,301

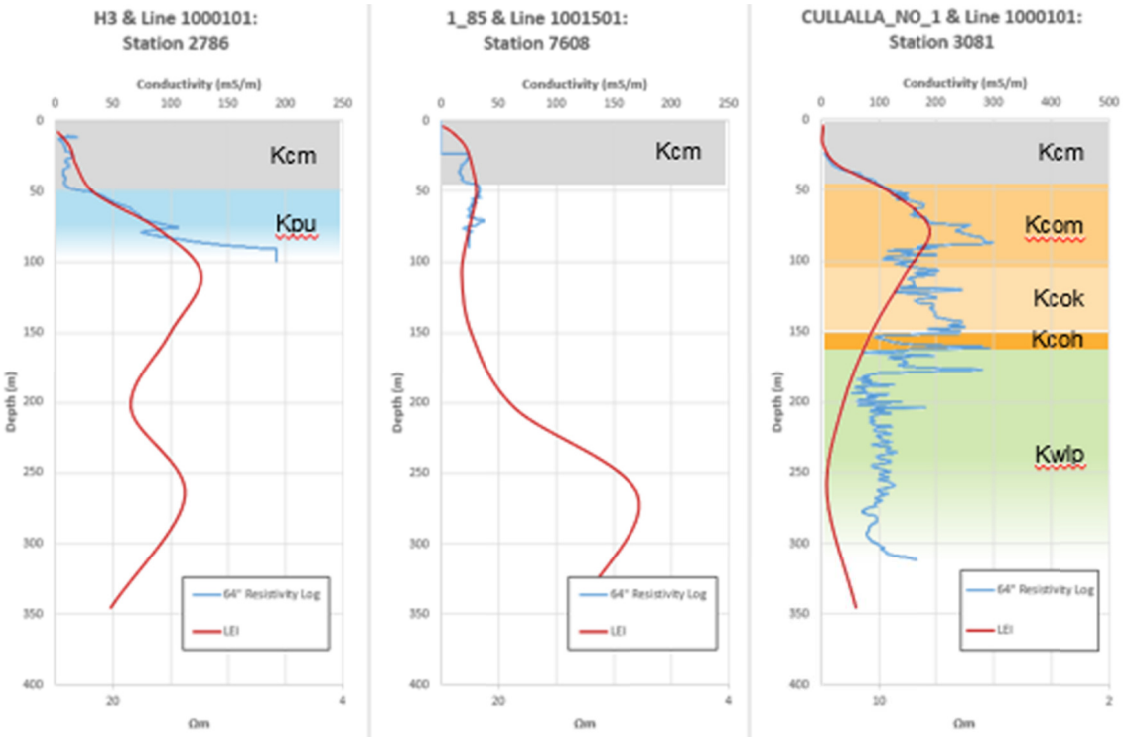

Figure 2: Wireline borehole conductivity (blue line) with drilled lithology information (coloured box). AEM LEI data is superimposed in red. Kpu – Upper Parmelia (sandstone with basal siltstone which acts as aquitard); Kcm – Molecap Greensand surficial sediment; Kcok Mirrabooka Member silty, poorly-sorted sandstone; Kcok Kardinya Shale; Kcoh- Henley Sandstone; Kwlp – Pinjar Member of the Leederville Formation. The right-most image is the Cullalla_NO_1 borehole shown in Figure 3.

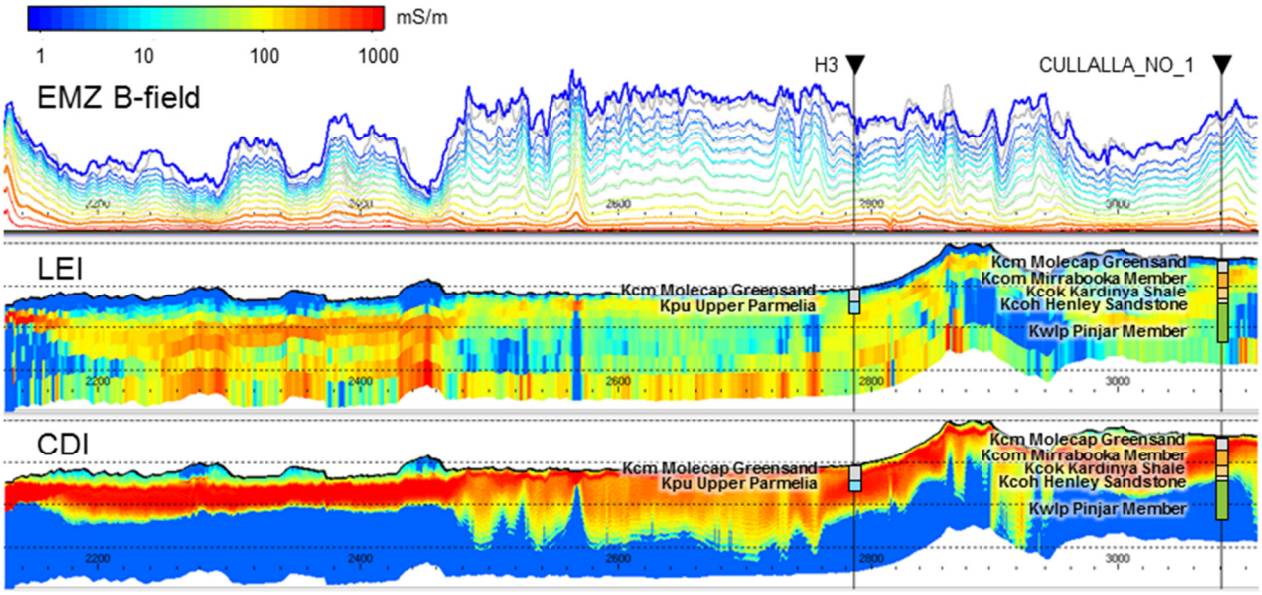

Figure 3: Tempest 75Hz data (top) along with layered earth inversion model (middle) and EMFlow conductivity depth image (bottom). The borehole lithology log has been superimposed with colour denoting a different lithology, not conductivity.

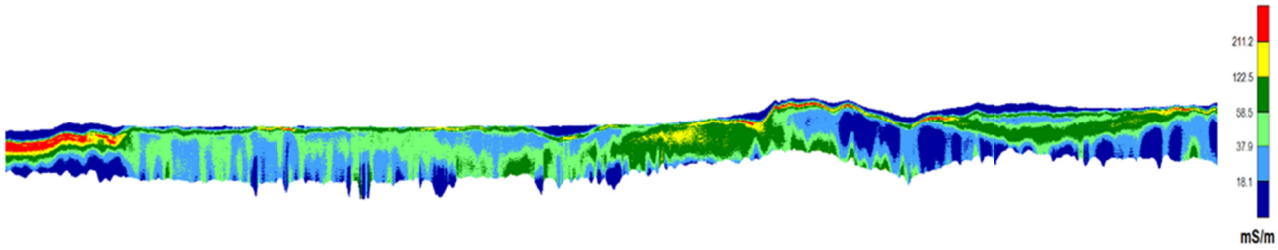

Figure 4: Conductivity depth section (EMFlow) with the colour intervals corresponding with amount of total dissolved solids in a sandy formation (providing an indication of water quality), ranging from brackish (red) to fresh (blue).

Characterising thermal water circulation in fractured bedrock using a multi-disciplinary approach: a case study of St. Gorman's Well, Ireland

S. Blake[1], T. Henry[1], J.P. Moore[1], J. Murray[1], J. Campanyà[2], M.R. Muller[2], A.G. Jones[2], V. Rath[2], J. Walsh[1]

[1]Irish Centre for Research in Applied Geosciences (iCRAG), email contact: sarah.blake@icrag-centre.org
[2]Dublin Institute for Advanced Studies, Ireland

SUMMARY

A hydrogeological conceptual model of the source, circulation pathways and temporal variation of a low-enthalpy thermal spring in a fractured limestone setting is derived from a multi-disciplinary approach. St. Gorman's Well is a thermal spring in east-central Ireland with a complex and variable temperature profile (maximum of 21.8 °C). Geophysical data from a three-dimensional (3-D) audio-magnetotelluric (AMT) survey are combined with time-lapse hydrogeological data, and a previous hydrochemical analysis to investigate the operation of this intriguing hydrothermal system.

Hydrochemical analysis and time-lapse measurements suggest that the thermal waters flow within the fractured limestones of the Carboniferous Dublin Basin at all times but display variability in discharge and temperature. The 3-D electrical resistivity model of the subsurface revealed two prominent structures: 1) a NW-aligned faulted contact between two limestone lithologies; and 2) a dissolutionally-enhanced, N-aligned, fault of probable Cenozoic age. The intersection of these two structures, which has allowed for karstification of the limestone bedrock, has created conduits facilitating the operation of a relatively deep hydrothermal circulation pattern (likely estimated depths between 240 and 1,000 m) within the limestone succession of the Dublin Basin. The results of this study support a hypothesis that the maximum temperature and simultaneous increased discharge observed at St. Gorman's Well each winter is the result of rapid infiltration, heating and re-circulation of meteoric waters within a structurally controlled hydrothermal circulation system.

Keywords: Thermal groundwater, Karst, Low-enthalpy geothermal exploration, Audio-magnetotellurics, Hydrochemistry

Characterization of intermediate depth reservoirs in complex coastal areas with CSEM method

N. COPPO[1], M. DARNET[1], F. BRETAUDEAU[1], P. WAWRZYNIAK[1], J. PORTE[1], F. REMBERT[12], T. JACOB and C. LAMOTTE[1].
[1]BRGM, n.coppo@brgm.fr
[1]BRGM, m.darnet@brgm.fr
[1]BRGM, f.bretaudeau@brgm.fr
[1]BRGM, p.wawrzyniak@brgm.fr
[1]BRGM, j.porte@brgm.fr
[2]METIS-UPMC, flore.rembert@upmc.fr
[1]BRGM, t.jacob@brgm.fr
[1]BRGM, c.lamotte@brgm.fr

SUMMARY

The characterization of water resources at intermediate depths (200-1500 m) in coastal peri-urban environments requires the implementation of specific and complementary geophysical techniques to overcome as much as possible the influence of anthropogenic noise and problems related to human infrastructures. Within the frame of the DEM'EAUX THAU project aiming at understanding and ultimately better manage the interactions between meteoritic, marine and deep thermal water in a karstic carbonate reservoir, we undertook to acquire 3D electromagnetic data around Balaruc-les-Bains (Hérault, France) to complete the hydrogeological and geological investigations. 91 controlled-source electromagnetic (CSEM) stations were collected both on-shore (56) and off-shore (35) on the Etang de Thau over ~25 km^2 in the frequency range 0.125 – 8192 Hz using 2 powerful 22kVA transmitters running simultaneously at opposite side of the survey area.

This paper mainly focuses on the analysis of the CSEM data in obvious coastal 3D context. As a first step, apparent resistivity maps show a good agreement with both gravity data and expected geology of the area. Then, 1-D inversion (based on OCCAM1D, Key (2009)) was tried but failed due to the complexity of the area, mainly caused by the highly conductive Etang de Thau lake (~0.16 Ωm) and its rugged geometry. In a third step, 2.5-D inversions along profiles crossing the Etang de Thau have been tried using MARE2DEM (Key and Ovall, 2011) to deal with the shallow highly conductive layer but only partially reconstructed the resistivity distribution at depth due to the too simplistic 2.5D assumption.

Finally 3-D modelling considering the water layer and its complete bathymetry has been performed using the POLYEM3D software (Bretaudeau et al. 2018 – this workshop). The simulations highlight that even though the depth of the water does not exceed 15m, significant charge accumulations all along the coast are visible and depend on the depth and shape of the water layer. These effects are of the order of magnitude of the anomalies sought and can clearly not be neglected during the inversion. Current work consists in performing 3D inversion using the POLYEM3D inversion code by including all the complexity of the water layer.

Keywords: Controlled-Source Electro-Magnetics, On and Off-shore CSEM acquisition, Groundwater management, 3-D EM modelling and inversion

Combined quantitative interpretation of GCM and DC sounding data from selected area in Cracow, Poland.

W. Klityński[1] and S. Oryński[2]
[1]Faculty of Geology, Geophysics and Environmental Protection, AGH University of Science and Technology, al. Mickiewicza 30, 30-059 Cracow, Poland
[2]Institute of Geophysics, Polish academy of Sciences, ks. Janusza 64, 01-452 Warsaw, Poland

ABSTRACT

Apparent conductivity is a value that is measured with the use of Ground Conductivity Meters (GCM). The apparent conductivity, σ_a [mS/m], is a geoelectric parameter, which characterizes heterogeneous medium that is in the field of view of the measurement array. The apparent conductivity can be treated as some resultant conductivity of a heterogeneous medium, in which the spatial distribution of 'true' conductivity is imposed by the geological built-up. Apparent conductivity is measured using the horizontal (HD) and vertical (VD) magnetic dipole at a several levels of depth (using different spacing). The area around the transmitting coil in which (for given frequency and conductivity) measurement is done is called near zone or induction zone.
Ground conductivity meters: CMD-MiniExplorer and CMD-Explorer, produced by the GF Instruments, s.r.o., are designed for induction profiling. The equipment employs the HD and VD configurations and measures apparent conductivity, and owing a six different options for spacing (s= 0.32, 0.71, 1.18 for MiniExplorer and 1.48, 2.82, 4.49 for Explorer. There are two types of configuration available. It allows to regulate the depth of penetration.
The GCM measurements were made along two profiles with a one meter measurement step in two different areas of Cracow (Poland). For the purposes of the geoelectrical identification of the medium, there were carried out a benchmark DC-resistivity soundings, with a measuring step of 5 meters along the same profiles. Measurement were carried out with the Schlumberger 4-electrode system.
The results of quantitative interpretation of DC-resistivity and GCM soundings were linked to the lithology of the studied medium. There were used two different interpretation algorithms for both methods: Occam and Levenberg-Marquardt (LMA). In the LMA method there is obtained a model with a clear contrast between the successive layers as a result of the interpretation. The result of the Occam interpretation is a model with smoothed resistivity distribution and diffuse boundaries between layers.
The research was carried out in two different areas in Cracow, first one in the Błonia area (right side of the Vistula river) and second one in the Ruczaj district (left side of the Vistula river). The distribution of the interpreted resistivity was compared with the literature data about lithology and resistivity occurring in this area. In the second case, the first interpreted layer is soil with a subsoil (conductivity approx. 20 mS/m) and a volume of several dozen centimetres. Below them, there are clays, (conductivity approx. 55-60 mS/m) and a thickness of about 3 meters. Below the layer of clays there is a gypsum complex with conductivity about 14 mS/m and a thickness of about 12 meters. The conductivity of this complex determined as a result of the interpretation of GCM data is greater - it is about 30 mS/m. This is due to much greater sensitivity of the GCM method to the occurrence of small, dispersed conductive zones in the gypsum (e.g., loams, wet karst voids). These gypsums are part of the evaporative works that have been created as a result of Tortonian sea regression. The Miocene aquifer is associated with the layer of skeletal gypsum. The last recognized layer is the low-resistive loam of the Wieliczka layers. This layer is too deep to be recognized by the GCM method. The resistivity of clays obtained as a result of the interpretation of DC-R soundings is about 3 Ωm (conductivity approx. 300 mS/m).
Carrying out GCM measurements for six different depth ranges (levels) allowed to perform a two-dimensional GCM data inversion using the Res2Dinv software. The inversion results in the form of cross-cut conductivities are smoothed (i.e. the conductivity at the boundaries between different mediums changes gradually) and are a certain averaging of the conductivity distribution in the studied medium.
The GCM method proved to be effective in recognizing shallow geological layers in the Cracow area. Due to the specific geological structure, the range of conductivity of geological layers (from a dozen to several dozen mS / m) allowed to qualify the condition of the near-field zone for the GCM method and the clear geoelectric contrasts allowed to separate the most important layers.

Keywords: Ground Conductivity Meter, DC Resistivity, Occam Inversion

Abstract, 24th EM Induction Workshop, Helsingør, Denmark, August 12-19, 2018

Continuous MT monitoring: Resistivity variations related to the large March 9, 1998 eruption at La Fournaise Volcano.

Pierre Wawrzyniak[1] p.wawrzyniak@brgm.fr
Jacques Zlotnicki[2]
Pascal Sailhac[3]
Guy Marquis[4]
1 Bureau des Recherches Géologiques et Minières, 3 av ; Claude Guillemin, BP 36009, 45060 Orléans 7 Cedex2, France
2 CNRS, UMR6524-OPGC-UPB, avenue des Landais, BP80026, 63177 Aubière Cedex,
3 GEOPS, CNRS-UMR 8148, Université Paris Sud, Orsay, France
4 France IPGS, CNRS-UMR7516, Université de Strasbourg, France

The 2645 m-high La Fournaise volcano, located in the Southwest of Réunion Island (Indian Ocean), is a shield basaltic volcano where effusive eruptions generally occur along long fissures starting from the summit, alongside major fractures that characterize the eruptions' dynamism and effusivity. Between 1992 and 1998, the volcano underwent a quiet period during which few earthquakes were recorded. Minor seismic activity returned after 1997 and picked up in March 1998 during the 35 hours preceding the March 9 eruption. From 1996, two autonomous stations (CSV and BAV) were installed on the volcano. CSV was located inside the Enclos Fouqué caldera while BAV was positioned 8.2 km NW of the volcano summit. Horizontal components of the electric and magnetic fields were sampled every 20seconds. Continuous time-series were available from 1996 to 1999 at CSV, and from 1997 to March 1998 at BAV.

Data have been processed using both single-station and remote-reference processing. Both results show apparent resistivity variations synchronous to the eruption. Time-lapse impedance estimates are computed on overlapping time windows of about two days at both stations. They show that the only time interval between 1996 and 1999 undergoing a decrease of the observed impedance coincides with the March 1998 eruption. At CSV, the resistivity started to drop about five days before the eruption, reached several local minima until April, and then slowly increased as the volcanic crisis reduced in activity. After the end of the crisis in September 1998, the apparent resistivity recovered its pre-crisis value. The time-lapse results also show variability in directionality: sharp and elongated phase tensor ellipse residuals also appear during the eruption with a N105° orientation, suggesting the emergence of an almost NS-striking dyke. A simple 1D reference model built from MT soundings performed during the quiet period (1996 to February 1998) and including a 3D NS-striking dyke shows a good agreement with the spatial distribution of the resistivity variations observed during the eruption.

CSAMT for Natural Gas Hydrate in the Qilian Mountain Permafrost of China

Da Lei[1,2,4], Qingyun Di[1,2,4], Hui Fang[3], Shumin Wang[3], Dawei Yao[3], Haobin Dong[5], Liangyong Yang[4]
[1]Key Laboratory of Shale Gas and Geoengineering, CAS , Institute of Geology and Geophysics, Chinese Academy of Sciences, Beijing 100029, China
[2]Institute of Earth Sciences, Chinese Academy of Sciences, Beijing 100029, China
[3]Institute of Geophysical and Geochemical Exploration CAGS, Langfang 065000, China
[4]University of Chinese Academy of Sciences, Beijing, 100049, China
[5]China University of Geosciences, Wuhan, 430074, China

SUMMARY

Gas hydrate is a newly discovered energy resource in recent decades. It mainly exists in the permafrost of polar region, deep water strata near the continental margin and sediments at the bottom of deep lakes. In this study, we carried out Controlled Source Audio Frequency Magnetotelluric (CSAMT) surveys along three profiles within the vicinity of the DK-1 hole belonging to "Gas hydrate Scientific Drilling Project at Qilian Mountain permafrost region" drilled in 2008 (Zhu Youhai, Zhang Yongqin, et al. 2010). The thickness of shallow permafrost layer, location of fractures and configuration of geological structures within the survey region were all determined based on the 3-D inversion results obtained from CSAMT data, using the regional geological background information as constraint. These deductions are highly consistent with the DK-1 borehole data, meaning our approach is generally reliable. Consequently, the CSAMT method can be applied successfully to delineate fractured structures and determine permafrost cover thickness, which are essential for gas hydrate formation and migration.

Keywords: Gas hydrate, Permafrost, CSAMT, 3-D inversion

INTRODUCTION

Gas hydrates are crystalline minerals composed of water and certain gases, it occurs mainly in huge quantities in the seafloor and in permafrost regions. It is a potential source of combustible energy, with global resources that amount to $2.1\times10^{15}m^3$, which is twice as coal, oil and natural gas resources all together (Kvenvolden 1988, Makogon et al. 2007). Therefore, countries all over the world, especially the developed countries and countries with energy shortages have attached great importance to research gas hydrate. Countries such as the United States, Japan, Germany, India, Canada and other countries have established their own natural gas hydrate research and development plan, which is stepping up its exploration, development and utilization. Based on the investigation of permafrost gas hydrate internationally, there are nine hydrates in permafrost regions have been found, which are mainly distributed in countries such as Russia, the United States and Canada, and other countries of Central Arctic permafrost zone(Collett 1993, Collett and Dallimore 2000; Dallimore and Collett 2005) However, natural gas hydrate has not yet been found in low-latitude mountain regions. China has the third largest permafrost deposit in the world over the Tibetan Plateau and the Greater Xing'an Mountains region in large tracts of permafrost zone. This accounts for about 22.3% of the total land area (Zhou Youwu et al. 2000).

In gas hydrate exploration, marine seismic reflection method has proved to be an effective method (Xu et al. 2006; Liu et al. 2008；Schmitt et al. 2005；Xu Ming cai et al. 2012). EM methods have only recently been applied in the field characterization of hydrate deposits (Weitemeyer et al. 2005; Yuan & Edwards 2000). The use of electromagnetic method in gas hydrate prospecting is seldom in China, so in 2009, we conducted a research on the application of CSAMT method in gas hydrate exploration over the Qilian Mountains of Muli, and made use of the method to identify gas hydrate formation, migration, fault and frozen soil cover and a preliminary understanding of its layer thickness.

ELECTRICAL CHARACTERISTICS

The CSAMT survey carried out in this permafrost region of the Qilian Mountains was based on the resistivity difference between target geological bodies (eg, gas hydrate formation, permafrost, structural faults, etc.) and surrounding rocks. Gas hydrates were found at the Middle Jurassic Jiangcang Formation lying under the permafrost zone. Gas hydrates occur in the fissures of siltstones, mudstones and oil shale, or in the pores of sandstones. The apparent resistivity values of the sandstone, shale and mudstone, which with the gas hydrate are mainly within the range 370–490 Ωm, 75–210 Ωm and 150–250 Ωm respectively. From the comparison of log curves, it can be

concluded that the apparent resistivity values of sandstone and mudstone without gas hydrate are 2-3 times higher than that of sandstone and mudstone with gas hydrate. This means that the resistivity value of both the permafrost layer and gas hydrate are several times higher than that of surrounding rock strata. With increase in the thickness of the gas hydrate formation, the resistivity value of the formation becomes even higher than that of the surrounding rock.

WORKING METHODS AND DATA ACQUISITION

In CSAMT sounding, the length of line 1 is 4000 m, the length of line 2 is 2000 m, and the length of line 3 is 2000 m. line 1 is approximately parallel to line 2 while line 3 is approximately perpendicular to line 1 and line 2. Grounded dipole source with a length of 1.2 km and transmission frequency ranging from 1 to 9600 Hz was used for this survey. The distance between each receiver dipole is 48 m. The source is usually a fixed electric dipole on the ground，in the place far away from source area, the horizontal component of electrical field and orthogonal component of magnetic field are measured. The AB-MN dipole equatorial array is usually adopted in CSAMT sounding.

DATA PROCESSING AND INVERSION

Data editing and near zone frequencies of data selection were performed using a visual human-computer interaction software. We used the ModEM code to invert apparent resistivity and impedance phase of the near area. The 3-D inversion of three profiles CSAMT data was performed in the ModEM frame [Egbert and Kelbert, 2012; Kelbert et al., 2014] by using only ρxy, φxy) as inputs. The same error floors of 8% for all off-diagonal impedances was by set in the 3-D inversion. The model was gridded as 100 × 52× 50 in the computational coordinates with the same scale in the x, y and z directions. The horizontal grid size is 100 m at every depth and increases exponentially at where four presumed transverse boundaries reached. The z direction grid size is 50 to 100 m at every depth and increases exponentially at where four presumed transverse boundaries reached. Hence, we only show three section beneath the profile from 3-D inversion results for an initial model of 100 Ωm homogeneous half-space, which was obtained after 199 iterations with the total normalized RMS = 2.13.

The CSAMT 3-D inversion resistivity sections and interpretation inference results with resistivity loggings and seismic section for line 1, line 2 and line 3, respectively. The resistivity logging data was in good agreement with the obtained CSAMT inversion result, and the high-resistivity anomaly in the shallow part is relatively clear, and first gas hydrate reservoir of DK-3 corresponds to the bottom of the high-resistivity anomaly, another two gas hydrate reservoir of DK-3 near to faults of seismic. CSAMT shows that the electrical structure was more consistent with seismic fracture and resistivity logging. However, it is difficult to distinguish the gas hydrate layers on the CSAMT resistivity inversion sections. There are two reasons for these blind sights: firstly, the gas hydrate layer is small, and current technical level and detection precision makes it difficult to identify the deposit; Secondly, the gas hydrate layer is close to the permafrost layer, or close to the faults.

CONCLUSIONS

CSAMT at the Qilian Mountain Permafrost for gas hydrate was successfully analyzed with the help of ModEM 3-D inversion. CSAMT is clear to the fault structures in the area. CSAMT can distinguish between the fault structures, which are needed for the migration and storage of the natural gas. CSAMT is more consistent with seismic fracture and resistivity logging in the electrical structure, faults and thickness of the shallow high resistivity layer. From the perspective of the gas hydrate accumulation and storage in the permafrost region, the good permafrost cap rock and the developed natural gas migration and storage channel provides a better geological environment for the formation and storage of natural gas hydrate.

Please do include a Conclusions section that summarizes the outcomes in about 300 words or less. Conclusions let people know what was achieved and will be the other part that most people read. Please make it as clear and concise as possible.

ACKNOWLEDGEMENTS

This research was supported by project 863, "Geophysical Prospecting Technology for Natural Gas Hydrate in Permafrost Zone" (Issue No. 2012AA061403) , Special national 127 (No. GZHL20110324), and National Key Research and Development Program of China (Grant No. 2016YFC0600101, No. 2016YFC0601102, 2016YFC0601104 & 2017ZX05008-007).

REFERENCES

COLLETTT S. (1993) Permafrost-associated gas hydrate accumulations [J]. In: SLOAN E D, HAPPER J, HNATOW M (eds.).1993. International Conference on Natural Gas Hydrates [M].Annals of the New York Academy of Science, 715: 247-269

COLLETT T. S., DALLIMORE S. R. (2000) Permafrost-related natural gas hydrate [J]. In: MAX M D (eds.). 2000. Natural Gas Hydrate in Oceanic and Permafrost Environments [M]. TheNetherlands: Kluwer Academic Publishers, 43-60

DALLIMORE S. R., COLLETT T. S. 2005. Summary and implication of the Mallik 2002 gas hydrate production research well program [J]. In: DALLIMORE S. R. and COLLETT T. S. (eds.).2005. Scientific Results from the Mallik (2002) Gas Hydrate Production Research Well Program, Mackenzie Delta, Northwest Territories, Canada [M]. Geological Survey of Canada,Bulletin, 2005, 585: 1-36

deGroot-Hedlin C., Constable S. (1990) Occam's inversion to generate smooth, two-dimensional models from magnetotelluric data. Geophysics, 55:1613-1624

Egbert GD, Kelbert A (2012) Computational recipes for electromagnetic inverse problems. Geophys J Int 189:251–267

Kelbert A, Meqbel N, Egbert GD, Tandonc K (2014) ModEM: a modular system for inversion of electromagnetic geophysical data. Comput Geosci 66: 40–53

KVENVOLDEN K. A. (1988) Methane hydrate-a major reservoir ofcarbon in the shallow geosphere [J]. Chemical Geology, 71:41-51

Liu Yan jun，Liu Xi wu，Liu Da meng (2008) Applications of seismic techniques to gas hydrates prediction[J]. Applier Geophysics，5(1) :67–73

MAKOGON Y. F., HOLDITCH S. A., MAKOGON T. Y. (2007) Natural gas-hydrates — A potential energy source for the 21st Century[J]. Journal of Petroleum Science and Engineering, 56: 14-31

Schmitt D.R., M. Welz, Rokosh C. D. (2005) High-resolution seismic imaging over thick permafrost at the 2002 Mallik drill site[J]. Geological Survey of Canada, Bulletin, 585:1-13

Weitemeyer, K., Constable, S., Key, K. & Behrens, J. (2005) The use of marine EM methods for mapping gas hydrates. Proceedings Offshore Technology Conference (CD-ROM), Houston, TX, 2-5 May 2005, 5pp

Xu Huaning，Li Li qiang，Shu Hu (2006) The seismic reflecting characteristics of gas hydrate bearing strata and its possible distribution in the South China Sea[J]. Applied Geophysics, 3 (1) : 42－47(in Chinese with English abstract)

Xu Ming cai,Liu Jian xun,Chai Ming tao, et al. An experimental study of natural gas hydrates in the Muli region, Qinghai Province by the seismic reflection method[J]. Geology and Exploration, 2012, 48(6):1180-1187

Yuan, J., & Edwards, R.N. (2000) The assessment of marine gas hydrates through electrical remote sounding: Hydrate without a BSR Geophysical Research Letters 27:2397–2400

ZHOU You-wu, GUO Dong-xin, QIU Guo-dong, CHENG Guo-dong, LI Shu-de. (2000) China permafrost[M]. Beijing:Science press (in Chinese with English abstract)

CSAMT investigation for geological structures in a HLRW preselected site

Zhiguo An[1], Qingyun Di[2], Zhongxing Wang[3], Meng Li[4], Changmin Fu[5]
[1]Institute of Geology and Geophysics, CAS, Beijing, China, zgancas@mail.iggcas.ac.cn
[2]Institute of Geology and Geophysics, CAS, Beijing, China, qydi@mail.iggcas.ac.cn
[3]Institute of Geology and Geophysics, CAS, Beijing, China, zxwang@mail.iggcas.ac.cn
[4]Institute of Geology and Geophysics, CAS, Beijing, China, 19870414orochi@163.com
[5]Institute of Geology and Geophysics, CAS, Beijing, China, fcm168@mail.iggcas.ac.cn

SUMMARY

This paper discusses the use of Controlled Source Audio-frequency Magnetotelluric method (CSAMT) in geological structure exploration at an area preselected for high level radioactive waste (HLRW) in northwest China. The survey objective is to find the weak geological structures which will cause damage to the safety and stability of underground repository, and to evaluate the rock mass quality based on electrical resistivity characteristics. In 2014 We conducted a dense CSAMT survey, combined with borehole information to delineate the local weak geological structures. The comparison between the interpreted results and geologic information shows that both are in agreement. The preliminary results offer detailed information about the electrical structures of Nuorigong rock mass from the surface to 1400 m deep, so the interrelationship between the target rock mass and its surroundings were analyzed to show their shapes. In conclusion, CSAMT results are helpful in exploring the subsurface for geological structures and competent rock mass. It can also provide the reliable geophysical evidence and scientific reference for complete and consistent evaluation of the deep geological structures, and aid in comprehensive assessment of preselected sites for HLRW disposal, such as further study in the design and construction of an underground man-made repository.

Keywords: CSAMT, Geological structure, HLRW, Site characteristics

CSEM experiment and MT-CSEM 2D joint inversion for a geothermal study the Vallès Basin (Catalan Costal Range, NE Spain)

Pilar Queralt [1].; Juanjo Ledo[1].; Alex Marcuello, and Gemma Mitjanas[1]

[1]Geomodes, University of Barcelona, pilar.queralt@ub.edu

SUMMARY

Nowadays, low-enthalpy deep geothermal reservoirs are targets as resources to generate heat in urban areas

Different geophysical surveys have determined the presence of geothermal anomalies detected in the La Garriga - Samalús area, in Valles Basin (Catalan Coastal Ranges, NE Spain). However, the setting remains poorly understood and largely untapped, and the fractured nature of the granite bedrock represents a geological challenge.

The Vallès Half-graben could allow the study of a complex and multiphase tectonic/fluid history encompassed by four tectonic events. Every tectonic event has conditioned the characteristics of the fractures system and, therefore, the fluid circulation regime. Since the Neogene, hydrothermal fluids up to 190ºC had ascended through the faults and characterized the Vallès fault by hydrothermal conditions, which remain active until nowadays.

Forced convection seems to be the most plausible model to explain the La Garriga-Samalús geothermal anomaly, having the recharge zone in the Montseny Massif with a water circulation pattern through the Paleozoic on its way down. Two MT/AMT profiles have imaged, the subsurface of the main fault with reasonable good resolution which probably acts as the main conduit for fluids in its way up.

To assess the benefits of land-CSEM measurements, surface-surface CSEM profiles coinciding with the previous AMT/MT profiles were carried out. Moreover, taking advantage of old deep boreholes with metallic casing present in the area, we have tested different CSEM configurations (single-LEMAN, double LEMAN, etc) to explore how the source signal and/or the recorded signal could increase the signal/noise ratio.
We will present the preliminary results of these tests as well as the 2D MT-CSEM joint inversion.

CSEM Signal Frequency Content Due to Geologic Structures, Oilfield Infrastructure, and Subsurface Fluid Movement as Applied to Hydraulic Fracturing

Mark S. Hickey[1], Santiago Treviño [1], Oscar Vasquez [1] and Mark E. Everett[2]
[1]Deep Imaging
[2]Department of Geology and Geophysics, Texas A&M University

SUMMARY

Land-based controlled-source electromagnetics (CSEM) is currently being used to monitor fluid injection during hydraulic fracture operations. The ability of a CSEM system to interrogate a fluid-filled fracture network at depth is aided by the highly conductive metal wellbore casing, as well as the connectivity of the fracture network. However, differences in the amplitude spectrum of the frequency response, as a function of location of surface receivers, due to the injected fluid is a result of a complex combination of the interaction of the fluid-filled fracture network at depth with the oilfield infrastructure and natural geological structures. In this study, these differences, as metal infrastructure and geological structures are added to the system, are investigated.

We start with a simple case of a single wellbore with an analogous synthetic fracture network embedded in a half space and gradually increase the geometrical complexity of the system, ending with a model of layered, anisotropic and isotropic geology with multiple wellbores extending to different depths. We study how the signal strength at the surface varies with frequency. The secondary signal strength depends on the depth, formation type, number of well casings, and also parameters associated with the hydraulic fracturing process.

We apply the modeling capability to field results from the Anadarko basin where electromagnetic data have been generated and recorded using surface transmitters and receivers. A baseline CSEM response is recorded prior to fluid injection and imaging is made possible by applying simple processing workflows. The images identify changes in reservoir conductivity in response to fluid and proppant placement. The case study shows CSEM responses migrating towards an anomalous structure in the formation during different hydraulic fracturing stages. This reveals the effect on hydraulic fracturing of natural geological structures, in this case, a fault.

Both the modeling and field example show that the change in surface CSEM response due to fluid injection is dependent on the subsurface geoelectrical structure. An understanding of how the frequency content of CSEM response amplitudes change with depth and subsurface complexity can aid in isolating and interpreting hydraulic fracture geophysical indicators.

Keywords: CSEM, Hydraulic Fracturing, Modeling, Case Studies

Down to Earth with a hazard from space: Geoelectric hazard maps from MT impedance and magnetic observatory data

P. A. Bedrosian[1], J. J. Love[2], G. Lucas[2], A. Kelbert[2]
[1]U.S. Geological Survey; Geology, Geophysics, and Geochemistry Science Center, pbedrosian@usgs.gov
[2]U.S. Geological Survey; Geomagnetism Program

SUMMARY

Worldwide, electric-power networks are at risk of damage or collapse due to extreme space-weather events. Past failures, including collapse of the Hydro-Quebec power grid during a 1989 magnetic storm, led the United States Federal Energy Regulatory Commission to mandate regional assessments of power-grid vulnerability. Of importance to such assessments are maps conveying the spatial variability of surface electric (geoelectric) fields that drive geomagnetically-induced currents (GICs) in power networks. These fields, together with network topology and grounding resistance data, can be used within power system analysis software to estimate GICs in critical infrastructure.

In constructing hazard maps, we are interested in the likelihood of a damaging event occurring within a given time interval and for a specific geographic area. Within this context, we generate maps of geoelectric field amplitude that will, on average, be exceeded once per century. Several factors conspire to affect field amplitude and polarization, including (a) the intensity, polarization, and spectral content of a specific magnetic storm, (b) geomagnetic latitude, which relates to the intensity and spatial complexity of the inducing geomagnetic fields, and (c) subsurface electrical conductivity structure, a reflection of geology and tectonics. The latter we investigate using magnetotelluric (MT) impedance data as the primary constraint, while the former two factors are accounted for via statistical analysis of long magnetometer time series acquired at observatories. In our approach, the spatial resolution of these maps is controlled by MT station density, which over much of the United States (U.S.) is equal to the 70-km nominal station spacing of the EarthScope MT array.

Hazard maps, in our formulation, are generated in one of two ways, dependent upon proximity to relatively sparse magnetic observatory data. Where close to an observatory (loosely defined as within 3° latitude/longitude), estimated MT impedance tensors are convolved with decades of 1-minute magnetic observatory data to generate time series of geoelectric-field data. The statistics of these time-series are then directly analyzed and extrapolated to determine 100-year geoelectric-field exceedance estimates. Alternatively, a synthetic geomagnetic disturbance (e.g. a 1-nT amplitude, 240-sec period, linearly-polarized geomagnetic field) can be multiplied by an MT impedance to generate a synthetic geoelectric field. These geoelectric fields can then be scaled by 100-year exceedance estimates of the geomagnetic field, obtained from a latitude-dependent statistical analysis and extrapolation of global magnetic observatory data. The latter approach is applicable anywhere impedance data are available but is a gross oversimplification of the spectral content of a magnetic storm. Remarkably, results obtained by the two approaches for the northwestern and eastern U.S. are very similar.

We have, to date, constructed hazard maps showing 100-year geoelectric-field exceedance values for about half of the contiguous U.S. In examining these maps, it is clear that subsurface conductivity within the crust and uppermost mantle is a first-order control on geoelectric-field amplitude. Field amplitude varies by more than two orders of magnitude, sometimes over distances of <100 km; such variations can, in numerous cases, be directly related to the underlying geology. The importance of the Earth filter is further evident in maps of average field polarization, with tectonic-scale features such as the Appalachian Mountains strongly channeling subsurface currents. Ongoing efforts to expand and refine these hazard maps include the incorporation of legacy MT data and the use of synthetic impedances obtained from 3D resistivity models. Large parts of the U.S., however, including major population centers, remain incomplete due to a lack of magnetic-field measurements and publicly-available MT impedance data.

Keywords: geomagnetically-induced currents, magnetotellurics, space weather, hazard maps

Electromagnetic characterization of the Central Tertiary Basin, Svalbard

P. Betlem[1,2], T. Beka[2,3], U. Autio[4], M. Smirnov[5] and K. Senger[2]
[1]Iceland School of Energy, Reykjavik University, peter.betlem@unis.no
[2]Department of Arctic Geology, University Centre in Svalbard, kim.senger@unis.no
[3]Department of Physics and Technology, University of Tromsø, thomas.beka@uit.no
[4]Oulu Mining School, University of Oulu, uula.autio@oulu.fi
[5]Department of Civil, Environmental and Natural Resources Engineering, Luleå University of Technology, maxim.smirnov@ltu.se

SUMMARY

The Arctic archipelago of Svalbard provides suitable conditions for EM data acquisition valuable for near-surface to crustal scale studies. Comprehensive broadband MT acquisition campaigns focussing on the geothermal potential of the region were conducted between 2013 and 2016 targeting readily accessible areas of the archipelago. In this contribution, we present previously unpublished MT data from Reindalen to characterise the electrical conductivity structure of the Central Tertiary Basin (CTB), a Paleogene foreland basin formed during transpression between Greenland and Svalbard. The new resistivity model is integrated and jointly interpreted with available 2D seismic and exploration well data sets.

The presented MT data were collected with 2 km average station spacing in April 2015 along a SW-NE oriented profile of 21 km in Reindalen, the largest post-glacial valley on Spitsbergen. Nine out of the ten measured MT sites provided data of high quality and were included in this analysis. Unable to obtain a stable regional level strike, the determinant of the impedance tensor was inverted to aid analysis in 2D.

Dimensionality analysis pointed out 3D behaviour that warranted further interpretation of the data in 3D. We modelled the data in 3D by including bathymetry and topography of the region using the ModEM 3D inversion code on a high-performance computing facility. To better account for topography, we experimented by adding homogeneous z-layers on top of the model. Inverting this model improved the starting RMS value considerably; however, the model was minima-locked and the data could not be fitted adequately. To overcome this, we prepared a model that had its z-layer thickness increasing logarithmically by a value of 1.2 and buried the MT data sites at their respective elevation levels within the model. This approach led to a reasonable data fit that provided a final data misfit RMS value of 1.37. We also noticed that a cross-section of the final 3D model following the measurement sites strongly correlated with its 2D determinant counterpart.

The final MT model indicates a shallow resistor in the uppermost 1 km, followed by a characteristic south-westerly dipping conductive zone at 1-4 km depth, and a deep, laterally constrained conductor at > 10 km depth. The shallow resistor is strongest on the outer SW edge of the Reindalen profile. A thickening trend is observed from NE to SW that may indicate highly lithified Tertiary sediments. Presence of permafrost in the shallower part of the profile complicates the electrical conductivity structure of the near-surface.

The geometry of the dipping conductor is perfectly aligned with the dipping strata on the eastern flank of the CTB, as identified on 2D seismic line NH9108-07. The conductor diminishes in strength down-dip, perhaps related to porosity loss with depth. While no exploration wells directly intersect the MT profile, we compared the MT model with two deep boreholes, each located within 10 km from the edges of the profile and penetrating down to 2.3 and 2.5 km, respectively. We also compared the MT model with a third 3.3 km deep borehole drilled 15 km south of the profile. These comparisons suggest that the conductive layer may represent Lower-Middle Triassic siliciclastic deposits overlying highly resistive Permian platform carbonates.

In the deeper part, the MT data indicates a deep, laterally constrained, 5 km wide conductor at 10-16 km depth. It is unclear whether the deep and shallow conductors are connected, but seismic data indicates the presence of possible fluid escape structures. Furthermore, we link the observations from Reindalen to previously acquired and presented MT data from Adventdalen and Sassendalen to the north. We conclude that MT represents an effective and important method to characterize the structural features onshore Svalbard, and is highly complementary to regional seismic data and exploratory well data.

Key words: Svalbard, 3D inversion, joint interpretation, magnetotellurics, Tertiary basin

Electromagnetic exploration for unconventional geothermal systems in Mexico: The GEMex Project

Claudia Arango-Galván[1], Gylfi Páll Hersir[2], Ásdís Benediktsdóttir[2], José M. Romo-Jones[3], José Luis Salas-Corrales[1], Thalia Avilés-Esquivel[3], Sebastian Held[4], Adele Manzella[5], Alessandro Santilano[5], Eva Schill[6]

[1]Institute of Geophysics, UNAM (Mexico), claudiar@igeofisica.unam.mx
[2]Iceland GeoSurvey, ÍSOR (Iceland)
[3]Earth Sciences Division, CICESE (México)
[4]Institute of Applied Geosciences, Karlsruhe Institute of Technology (Germany)
[5]Institute of Geosciences and Earth Resources, CNR (Italy)
[6] Institute for Nuclear Waste Disposal, Karlsruhe Institute of Technology (Germany)

SUMMARY

The GEMex Project is a scientific cooperation on the development of superhot and enhanced geothermal systems that is being conducted by a bilateral consortium formed by European and Mexican experts. The objective is to add their long-term expertise to investigate unconventional geothermal fields in detail. For this purpose, two different sites have been selected in the eastern area of the Trans-Mexican Volcanic Belt, having two different goals. The main objective at Acoculco caldera is to develop new methodologies for the characterisation and exploitation of a low-permeability field that shall produce energy by utilisation of an EGS. On the other hand, at the currently producing Los Humeros geothermal field, the idea is to apply new developments for characterising and better understanding superhot conditions (> 350°C) found in some sectors of the reservoir (SHGS) and enhance future exploitation attempts. The project started in October 2016 and it will end in 2020. It has been organised into several work packages (WP), grouped by disciplines. Specifically, the WP5 – Detection of Deep Structures – includes the geoelectrical characterisation using both magnetotellurics and time domain electromagnetics. In addition to the acquisition of electromagnetic data (already performed in both research areas), the activities planned in this project include novel modelling of previous geophysical data, the calculation of synthetic models for the optimisation of the three-dimensional inversion, 1D-, 2D- and 3D-modelling including joint and advanced constrained inversion schemes as well as multi-objective joint optimisation. Finally, a comparison of the results with previously obtained data in similar geothermal fields will be performed.
The ultimate goal is to generate a comprehensive reservoir model by integrating the information of the geoelectrical-imaging with results obtained by other geoscientific disciplines (geophysics, geology and geochemistry) in order to study the variation of the subsurface physical properties and their role in the dynamics of the reservoirs.

Keywords: Magnetotellurics, Time domain electromagnetics, Unconventional geothermal system, Mexico

Electromagnetic Modeling in Unconventional Reservoirs: a 3D Anisotropic Approach

Ana Curcio[1,2]
[1]Instituto de Geodesia y Geofísica Aplicada, Universidad de Buenos Aires, Argentina
[2]Proingeo SA, anitacurcio@gmail.com

SUMMARY

The objective of the present research is to model the three-dimensional anisotropic electromagnetic (EM) response during the hydraulic fracturing in an unconventional reservoir. In this procedure the formation changes from hydrocarbon saturated to water saturated, what in turn induces an electrical conductivity anomaly, because fluid flow occurs and petrophysical parameters change. This anomaly is dynamic and in consequence the coefficients in Maxwell equations become space-time dependent.
Unconventional reservoirs have a considerable degree of anisotropy, which can account for twenty to forty percent of error if taken isotropy in sandstone reservoirs and being higher in shales. The causes of anisotropy are layering, preferred orientation of the small-scale features and alignment of flat shape grains in addition to the presence of natural fractures.
To consider this effect, approximation of anisotropic Maxwell equations was performed under a Leapfrog-FEM method. This technique is based on conforming mixed finite-element spaces and solves the weak form according to the Nédélec scheme, who has demonstrated that under this scheme the Electrical field have continuous tangential component across edges in the mesh. Leapfrog time stepping was used to discretize in time, so that the fully discrete sequence is first solved for the electric field, and then it is solved for the magnetic field.
Numerical examples show EM responses of different hydraulic fracturing geometries immersed in different anisotropic unconventional reservoirs for three receiver-transmitter configurations: surface-surface; surface-borehole; borehole-borehole. This response is sensitive to saturation distribution and the petrohysical relations assumed.

Keywords: 3D Electromagnetics, Anisotropy, Leapfrog-FEM, Nedelec, Unconventional Reservoir

EM-microseismic reservoir monitoring system

Sofia Davydycheva[1], T. Hanstein[1], M. Smirnov[1,2], K. M. Strack[1]
[1] KMS Technologies, USA, info@KMSTechnologies.com
[2] Department of Civil, Environmental and Natural Resources Engineering, Luleå University of Technology, Sweden, maxim.smirnov@ltu.se

SUMMARY

A new technology for reservoir monitoring includes full field controlled-source electromagnetics (CSEM) in addition to microseismics measurements. To mitigate the risk, we have developed full technology cycle: from patents, hardware, acquisition methodology, to data processing and interpreting in 3D. The system can acquire surface-to-surface and surface-to-borehole measurements. EM data are used to track fluids, due to their high sensitivity to the fluid resistivity, while seismic data relate primarily to the reservoir boundaries. Having seismic and EM sensors in the same recording unit allows the addressing of the multi-physics character of the problem early on in the workflow at low cost. While planning a survey, we perform careful 3D modeling feasibility studies, including the noise level measurement on the site. Dense EM field measurement allows for data redundancy for the most accurate interpretation. In addition, we apply a novel method to focus the EM image information directly below the receiver.

Keywords: CSEM, 3D modeling, reservoir monitoring, anisotropy.

INTRODUCTION

In enhanced oil recovery, EM methods provide unique opportunities to track fluid movements due to changes in electrical properties at the flow boundaries. Thus, the EM data and interpretation could yield considerably more value than traditional microseismic interpretation alone. At the same time, technology has progressed such that it is now routine recording virtually an unlimited number of channels at low cost and interpreting data in 3D.

Surface-to-surface CSEM applications using a grounded electric dipole in time domain (Strack, 1992; 2014) are more promising for land applications than frequency domain CSEM (Constable, 2010), since it is advantageous to record once the transmitter is off, after the airwave has passed (Kumar & Hoversten, 2012).

Reservoir monitoring essentially poses a time-lapse exercise, where measurements that link downhole and surface-to-surface data enable critical calibration and increasing sensitivity to fluid variations in the reservoir. Such a wealth of EM information, tied to 3D surface and borehole seismic data also permits to extrapolate fluid movements and seal integrity away from a given well bore. Because of this complexity, it is necessary to carry out 3D modeling feasibility to fully understand the reservoir effects.

To date, EM applications for reservoir monitoring are in an early stage of development. Presently, only limited monitoring applications have been reported (Hoversten et al. 2015, Tietze et al. 2015; Thiel, 2016).

As novel contribution we derived a methodology and additional measurements where the information content can be focused below the receivers using either Focused Source EM (FSEM) (Davydycheva & Rykhlinski, 2011) or vertical electric field measurements in shallow vertical boreholes.

METHODOLOGY

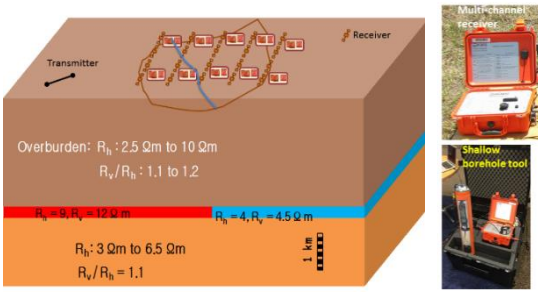

Figure 1: Flooded anisotropic reservoir model and monitoring setup.

We developed a commercial land microseismic-EM system for reservoir monitoring (Figure 1). The system includes high-power transmitter and multi-component microseismic-EM receivers with practically unlimited number of channels. In the present paper we concentrate on EM measurements. Six-component EM sensors (3 electrical & 3 magnetic components) are situated on the Earth surface and in shallow vertical boreholes to enable vertical electric field measurement. For this we use a commercial shallow borehole tool

(SBHT) (on the bottom-left). Shallow observation wells of the depth of 20-40 m can easily be prepared. Deep borehole full field sensors are optional.

Every reservoir monitoring case is carefully studied for feasibility: 3D modeling-based study is performed to determine those of six EM components which exhibit the strongest anomalies. Mandatory on-site noise measurement is performed to establish technical and commercial viability. The field setup is configured based on the 3D feasibility study, and time lapse data are acquired, processed, calibrated using available well logs and linked to microseismic data.

Figure 2 shows vertical cross-section of a heavy oil reservoir (Passalaqua et al. 2016). Its approximate 3D model (left-center) is used for 3D modeling feasibility study. The blue parallelepiped represents the steam/water flood area of 500x500x140 m. A 400-m long transmitter situated at the origin excites the formation with rectangular impulses, and multicomponent EM receivers above the flood area are shown as green triangles.

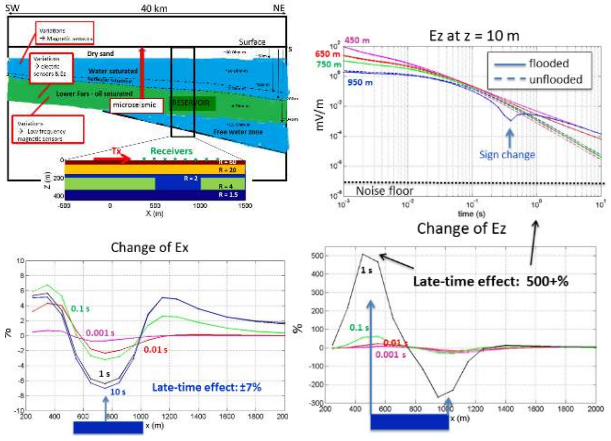

Figure 2: Heavy oil reservoir: steam-injection model (left top), Ex (left-bottom) and Ez (right) responses to the flooded area.

The responses of the vertical electric field before and after the flood are shown in Figure 2 as a function of time after the transmitter turn-off (top-right) and relative responses are shown as a function of the distance to the transmitter (bottom: measurements compared to a fully oil saturated state). They were simulated using a 3D finite-difference (FD) method by Davydycheva & Druskin (1999). Late-time responses are significantly affected, especially above the flood area edges at 500 and 1000 m. Thus, the flooded area contour may be determined with great accuracy through the measurement of Ez component using SBHT in vertical boreholes above the reservoir. Since the reservoir is relatively shallow, the effect is strong enough at relatively early times below 1 s. E*z* is the most sensitive to vertical currents significantly affected by resistive/conductive oil/water saturated (unflooded/flooded) rocks. Effect of traditional inline dipole-dipole measurement Ex is in the range of several per cent. It is smaller, since Ex is sensitive to horizontal currents, much less affected by relatively thin resistor (reservoir).

In the case of deeper reservoirs, the feasibility often reveals the reservoir response at much later times after turn-off, when signal is close to the noise floor. A simplified 2D anisotropic model as depicted in Figure 1 with the reservoir (red) at the depth of 2 km was derived from a vertical resistivity log. As the waterfront (blue) moves, the receiver array on the surface records the multi-component EM response. In Figure 3, the *x*-directed dipole transmitter is co-aligned with the waterfront propagation direction, for simplicity of the analysis. To estimate the sensitivity to the reservoir resistivity the response of all three components of the magnetic and the electric field, including Ez component, were simulated at several times after turn-off, while the responses were well above the noise floor.

Synthetic time lapse response of the vertical component E*z* is shown in Figure 3. It demonstrates sufficient sensitivity to the reservoir properties, while the standard inline component Ex gives only 1.5% anomaly (not shown). The signal level was well above the noise floor measured on the site. Figure 3 also demonstrates importance of the resistivity anisotropy: even though the anisotropy ratio Rv/Rh does not exceed 1.2 in this case, a noticeable difference in Ez response in the presence (top) and absence of the anisotropy (bottom) can be seen.

We also account for the effect of steel casing on the surface EM field: modeling shows that it can mostly be ignored as long as the transmitter's and receivers' groundings are placed at 200+m from cased wells.

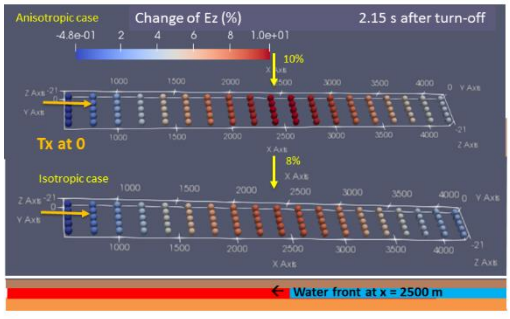

Figure 3: Time lapse E*z* change above the waterfront at 2.15 s. after turn-off: anisotropic (top), & isotropic case when Rh = Rv (bottom).

VERTICAL FOCUSING USING CIRCULAR DIPOLES

Measurement of the vertical electric field requires drilling shallow vertical wells to place the receivers.

If those are unavailable, an alternative FSEM measurement by Davydycheva & Rykhlinski (2011) can help. It utilizes circular electric dipole cancelling ingoing and outgoing horizontal currents and making data sensitive to a narrow column of rocks under the receiver, thus focusing the sensitivity vertically downward, as shown in Figure 4 (left-top), without the need to drill vertical wells.

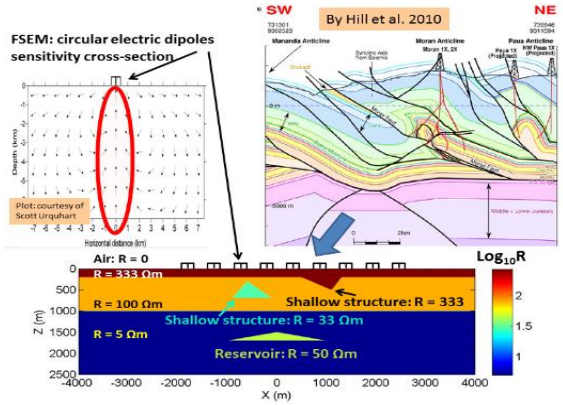

Figure 4: Papua New Guinea feasibility: model setup & derivation.

Figure 4 also illustrates a derivation of 3D model (bottom) for the feasibility study of a complex reservoir in Papua New Guinea. The reservoir is in Jurassic sandstones with overburden of 1000-1500 m of carbonates and 800-1500 m of shales (Hill et al. 2010). The resistivities were taken from magnetotelluric data by Hoversten (1996). We included in the model shallow structures whose effect happens to be very strong: they change the standard CSEM inline dipole-dipole response beyond recognition, as shown in Figure 5. FSEM method (Figure 6) gives stronger reservoir response and allows partial removal of unwanted shallow effects through the subtraction of measurements acquired at different times after turn-off (see for details Davydycheva & Ryhklinski, 2011).

Figure 7 shows an example of data processing, for field data acquired using the circular dipole.

SURFACE-TO-BOREHOLE MEASUREMENT

If the reservoir depth is greater than 3 km, surface monitoring methods may be insufficient due to the lack of sensitivity. Then we utilize surface-to-borehole measurements. Figure 8 shows 3D cross-section of Bakken field reservoir. The formation is excited by a 1-km long grounded dipole transmitter (red). Borehole receivers are situated in a deep horizontal well. Flooded/depleted/hyrdo-fracturing target area is shown in light-blue. Figure 9 shows 3D modeling results and demonstrate good sensitivity of time-domain measurements to a water front moving from negative *y*-direction, from a parallel injector well situated inside the reservoir (not shown since it is situated behind the (*x,z*) plane) at the same depth as the producer. The deep borehole receivers are situated at *x* = 3000 m inside the lower Bakken reservoir in (*x,z*) plane. The water front was modeled as a rectangular block of vertical extend of 31 m, the horizontal extend of 4000 m in *x* and 400 m in *y* (bottom-left). The background 1D (horizontally-layered) anisotropic resistivity model was derived from a vertical log, while the resistivity of the flooded area (8.16 Ωm) was derived using Archie's law taking into account the reservoir porosity (Strack and Aziz, 2013). Since the background model is symmetric w.r.t. (*x,z*) plane, B*y* is the only non-zero component of the magnetic field in the borehole receivers inside the unflooded reservoir; it is why B*x* and B*z* "unflooded" are equal to zero and not shown. As the waterfront approaches the producer well, a non-zero B*x* and B*z* emerge, which can be analyzed to determine the distance to the water front.

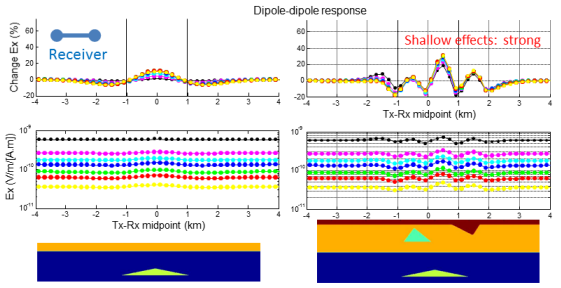

Figure 5: Papua New Guinea case: standard CSEM in the absence (left) and presence (right) of shallow structures. Tx-Rx offset: 1 km.

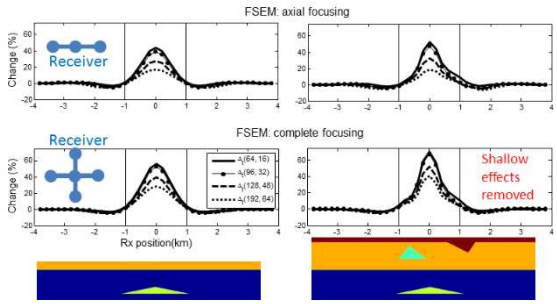

Figure 6: Papua New Guinea case: FSEM feasibility. Offset: 1 km.

CONCLUSION

A multi-channel full field EM-microseismic measurement system has been developed for surface-to-surface and surface-to-borehole applications. Those EM components which exhibit the strongest anomalies, determined by 3D modeling, are combined with on-site noise measurements to establish technical and commercial viability. The system includes high-power transmitter and multi-channel receivers. Promising results are obtained using shallow borehole tool, sensitive to vertical currents affected by thin horizontal resistors - typical reservoirs. In

addition, novel focused measurements on the Earth surface allow focusing the EM imaging information directly below the receiver. The new robust data processing software efficiently de-noise the data. The system stability methodologies were confirmed by actual field measurements.

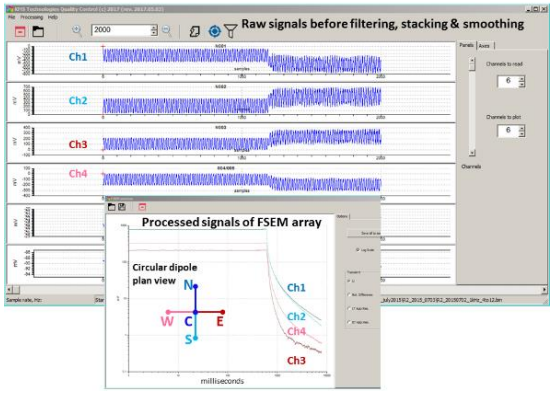

Figure 7: circular electric dipole noisy data example and four-channel data processing: before (top) and after filtering, stacking and smoothing (bottom).

ACKNOWLEDGEMENT

We appreciate valuable help by Xiayu Xu, and KMS Technologies for permission to publish the paper.

REFERENCES

Constable S (2010) Ten years of marine CSEM for hydrocarbon exploration, Geophysics 75, no. 5, A67-A81.

Davydycheva S and Druskin V (1999) Staggered grid for Maxwell's equations in arbitrary 3-D inhomogeneous anisotropic media, in: Oristaglio M, and Spies B, Eds. Three-dimensional electromagnetics: SEG, 119-137.

Davydycheva, S, and Rykhlinski NI (2011) Focused-source electromagnetic survey versus standard CSEM: 3D modeling in complex geometries, Geophysics 76(1), F27-F41.

Hill KS, Lucas K and Bradley K (2010) Structural styles in the Papuan Fold Belt, Papua New Guinea: constrains from analogue modelling, Geological Society, London, Special Publications 2010, v. 348, 353-434.

Hoversten GM (1996) Papua New Guinea MT: looking where seismic is blind, Geophysical Prospecting, 44, 935-963

Hoversten GM, Commer M, Haber E, and Schwarzbach C (2015) Hydro-frac monitoring using ground time-domain electromagnetics, Geophysical Prospecting, 63, no. 6, 1508-1526.

Kumar D, and Hovesten GM (2012) Geophysical model response in shale gas, Geohorizons 17, 32-37.

Passalacqua H, Boonyasaknanoon P, and Strack K (2016) Integrated Geophysical Reservoir Monitoring for Heavy Oil, Soc. Petr. Eng., SPE-184089-MS.

Strack KM, LeBrocq K, Moss DC, Petry H, Vozoff K, and Wolfgram PA (1988) Resolving resistive layers with LOTEM in hydrocarbon exploration: case histories. Paper 4-23, 50th Annual Meeting, EAGE, The Hague.

Strack KM (1992) Exploration with deep transient electromagnetics. Elsevier, 373 p.

Strack KM (2004) Combine surface and borehole integrated electromagnetic apparatus to determine reservoir fluid properties. U. S. Patent 6,739,165.

Strack KM (2014) Future directions of Electromagnetic Methods for Hydrocarbon Applications. Surveys in Geophysics 35, 157-177.

Strack KM, and Aziz AA (2013) Advances in electromagnetics for reservoir monitoring, Geohorizons (Special shale issue), 32-44.

Thiel S (2016) Electromagnetic monitoring of hydraulic fracking: relationship to permeability, seismicity and stress, the 23rd Electromagnetic Induction Workshop, Chiang Mai, Thailand, 14-20 August 2016.

Tietze K, Ritter O, and Veeken P (2015) Controlled source electromagnetic monitoring of reservoir oil Saturation using a novel borehole-to-surface configuration, Geophysical Prospecting 63, no. 6, 1468-1490.

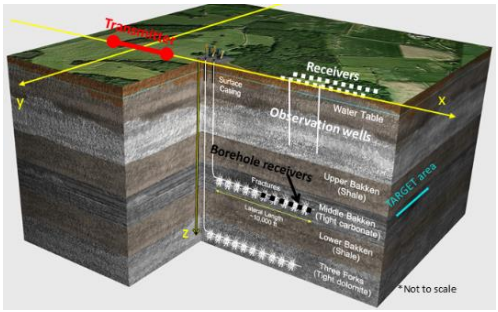

Figure 8: Bakken field 3D cross-section (courtesy of Miscoseismic Inc.) and monitoring setup.

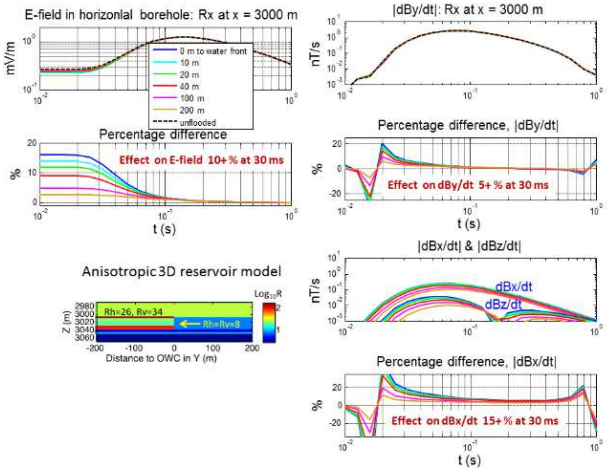

Figure 9: Borehole-to-surface on Bakken: effect of approaching oil-water contact on EM responses.

Exploration for Devonian reef in southern China with 3D MT inversion result

Liangjun Yan[1,2], Xingbing Xie[1,2], Fengjiao Xu[1], Wenbao Hu[1], Lei Zhou[1]

1. Key Laboratory of Exploration Technologies for Oil and Gas Resources (Yangtze University), Ministry of Education, China
2. Key lab of geophysical prospecting, CNPC, Beijing

1. Introduction

The reef oil traps are widely distributed in the areas of carbonate rocks. Among the 45 recognized huge oil reservoirs, 10 are related to the reef trap. The area covered by carbonate rocks in southern China is more than 700000 square kilometers. Reefs in middle Devonian were widely developed, so there is a great potential in the exploration for reef oil reservoir （В.Г.Кузнецов，1983；Jia and, Hao, 1989）. Geological studies have found that the distribution of reefs is closely related to the sedimentary facies. The platform margin or slope of the deep part of the depression is a favorable area for reef growth, the development of reef is closely related to topography and tectonics. Therefore, the study of sedimentary facies and the partition for reef facies are of great significance for the exploration of subtle reefs.

Meng(1994) pointed out to explore the reef trap with electromagnetic methods in the early 90s of last century, and led the electrical reef exploration work in southern China with petroleum electric prospecting teams(Yan et al. 2002). A comprehensive geophysical method, that is the area selection with geology, the partition for reef facies with MT, and the target evaluation with controllable source electromagnetic method, has been put forward. Through more than 5 years of effort, a great deal of good geological results was reached. Limited by the methodology and technology, the instrument performance, the level of processing and interpretation, and the complex surface geological condition in southern China, MT data collection was very difficult. The MT sites can only be irregularly distributed in the study area, which seriously affects the accuracy and geological effect of two-dimensional MT inversion and interpretation. Figure 1 shows a 14 lines of MT site distribution in Huanjiang, Guangxi province. The purpose was to explore the reefs and their spatial distribution in middle Devonian layers. In figure 1 we could see that because of terrain the survey lines were seriously distorted and could not carry out two-dimensional MT inversion effectively. Now the MT 3D inversion has entered the mature application stage (Smith and Booker, 1991; Ledo, 2005; Lin Changhong et al. 2012), the 323 MT sites in the study area were irregularly and uniformly distributed within 3600 square kilometers, by 1 to 3km space interval, which was an ideal data for 3D MT inversion. The middle Devonian of the study area was mainly low resistivity sand and mudstone. The electrical properties of sand and mud layers change in the transverse direction, due to the difference of sedimentary facies, and the middle and high resistance reefs are also distributed.

In this paper, 3D MT inversion was designed to characterize the spatial and electrical characteristics of the top and bottom interfaces of the middle Devonian mudstone layer, and it was very important to study the basement undulation and the sedimentary facies in order to explore subtle reefs. The principle of facies partition was the combination of geology and electrical method. The first is to analyze the sedimentary paleogeography, then divide the facies with the base undulation, shape and depth of the resistivity. The distribution of the subtle reefs was circled by the partition of the platform, platform margin and basin facies.

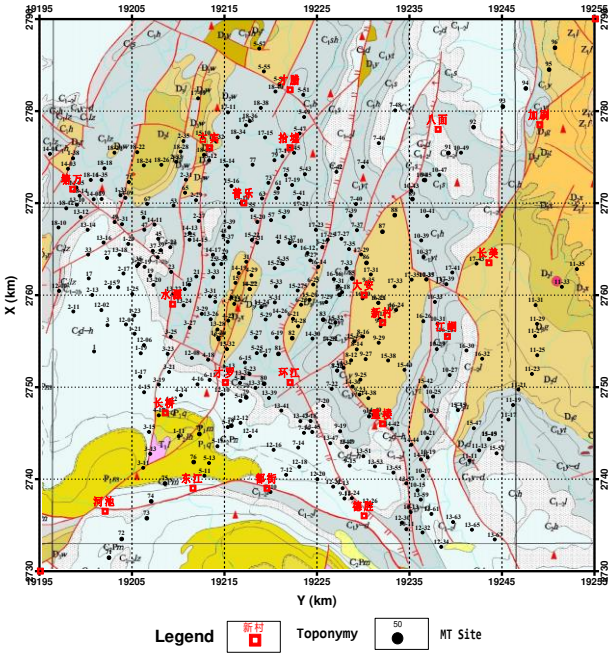

Figure 1 The MT site distribution in Huangjiang, Guangxi

2. Petrophysics of reef and its sedimentary facies

2.1 The physical and electrical properties of reef

Reefs are constructed in the shallow sea environment by bioaccumulation of carbonate rocks. They are a special geological body with unique void space,

composed of core-reef, fore-reef and back-reef. The reef core is rich in reef building organisms, which are characterized by massive and speckled structures. Meanwhile, the core-reef is most vulnerable to secondary effect such as recrystallization and dolomization. The fore-reef has double properties. On the one hand, it was the light colored clastic limestone carried by the reef core after the destruction. On the other hand, the dark particles and muddy limestone and dolomite, which are rising from the depressions, have the characteristics of stratiform structure, the near reef core is coarser and the reef core was obviously thinner. The back-reef is often a light-colored limestone with diversified structures. The combined characteristics of the reef body made the distribution of the maximum porosity and permeability zone in the range of reef body unsymmetrical. Due to the primary cracks and secondary dolomization and recrystallization, the average porosity of reefs is usually about 5-8%. The porosity of reef combinations with cyclic and interstitial growth could reach 20%. For fore-reef basin facies or post-reef lagoon carbonate rocks, their porosity are usually less than 2-3%.

The reef's solid skeleton is composed of non-conductive minerals, and its electrical conductivity mainly depends on the pore water's resistivity and porosity. When the reef is filled with water, especially when it is rich in high salinity brine, it will exhibit obvious low resistivity characteristics. When the reef contains oil and gas, the non-conductive oil and gas replaces the space of the water, so that the resistivity of the rock rises, and its degree is obviously related to the saturation of oil and gas. Therefore, at the top of the oil and gas accumulation, the relatively low resistivity of the reef may be changed. However, in general, the reef body is characterized by high resistance. When the reservoir has good physical properties, it could be seen as high resistance before and after the reef, while the core core is low resistance.

2.2 Reef sedimentary facies and its electrical characteristics

In the Middle Devonian, the area was a set of shallow-sea and coastal facies sediments. The reef-building organisms are extremely prosperous and constituted a combination of reef and beach formations, forming a sea-type carbonate deposit on the edge of the shelf. From shallow to deep, the sedimentary facies were the platform facies, platform marginal facies, slopes facies, and basin facies (figure 2).

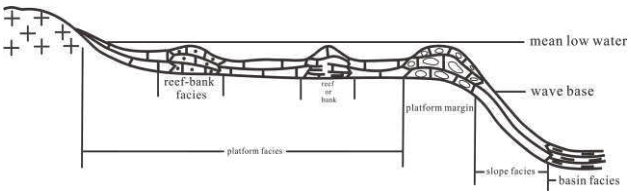

Figure 2 the model of reef sedimentation

The reef geology study (В.Г.Кузнецов, 1983) believes that the edge of the platform gets along with the shallow water and the deep water boundary. In this stripped area the sea water has good brightness and aeration conditions, and the deep water up along the slope carries a large amount of nitrogen, phosphorus and potassium, which are the most beneficial for reef's growth. The area has the characteristics of banded distribution, large thickness of sedimentary and violent lithology. The rock assemblage of platform facies (carbonate rocks) is interspersed with the rock assemblage of the basin facies (mainly clay rock), and the electrical properties were extremely unstable. In contrast, the basin facies is mostly mudstone deposit, showing low resistivity, while platform facies is carbonate rock deposition, showing high and medium resistivity (figure 3).

In summary, the formation of reefs has obvious distribution rules. Starting from the sedimentary model of continental carbonate rocks on the edge of the continental shelf, they often appear as clusters and belts on the marginal facies of the platform. Therefore, in the exploration for reef, it is an important technical route to find and study the high resistance or low resistance groups distributed in the belt of the platform margin facies.

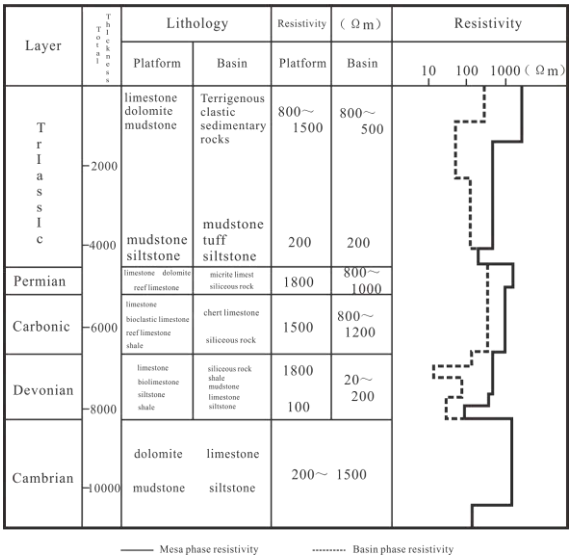

Figure 3 the lateral change of stratum resistivity with the facies

3. Three-Dimensional MT inversion method

Based on the inversion algorithm in data space and the source code of Siripunvaraporn (2005), we have developed 3D MT inversion software with high performance computing workstation based on GPU parallel computation, and which has reached the practical level. The flowchart of inversion simplification is shown in figure 4.

321 sites of MT date with 30 frequency samples from 240-0.0011Hz were used to do 3D inversion. The initial model was gridded by 80×80×88 (NS×WE×DEPTH) dimensions. The surface grid is 850×950 square meters, and the first depth of the surface grid is 10 meters, the equal interval in the depth in logarithm domain was carried. Half space model with 100 Ω . m was set up, the termination criterion was set as 5%. 5 days computation time on 21 cores cluster were consumed, the final error of fitting was 5.14%.

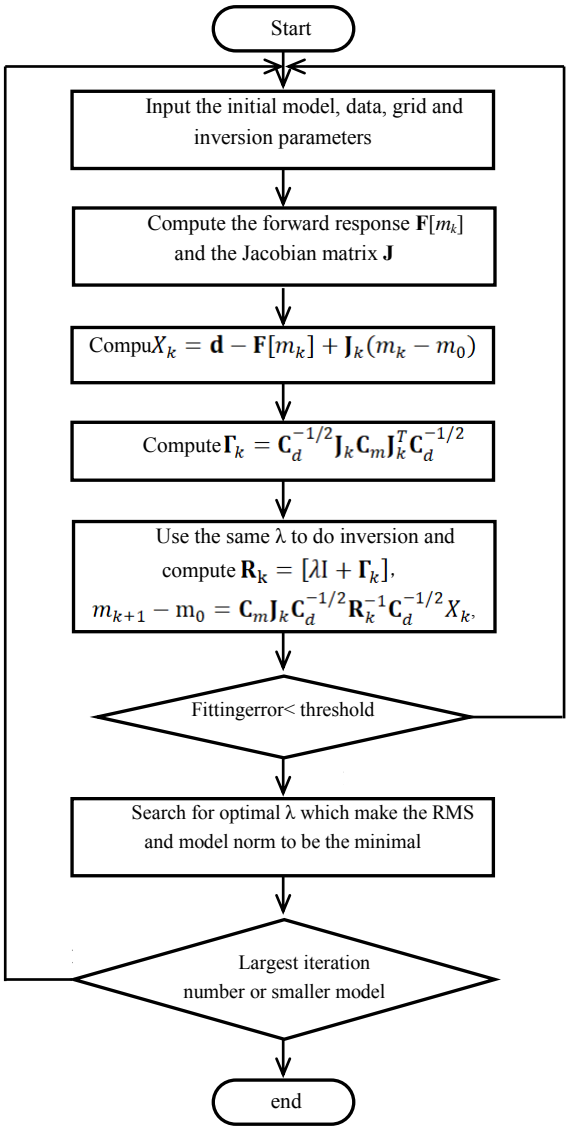

Figure 4 flowchart of 3D MT Inversion

4. Inverted result analysis

Figure 5 is the inverted 3D electrical structure model. It is very clearly that the area could be divided into three zones. The southwest region is low resistivity zone, the central belt from northwest to southeast was middle resistance zone, and the northern and western regions are high resistance zones(Figure 6). Combined with geological and lithological backgrounds, we could partition the basin facies, platform edge facies and platform facies. On the edge of the platform, the high resistance anomalous bodies circled by middle resistivity layer should be interpreted as subtle reefs. In order to find the anomalous zone of reef body, we calculated the average resistivity of the middle devonian stratum and the resistivity contour was shown in figure 7. In the figure, there are two high resistance abnormal body with no root of limited block, and were surrounded by sand mudstone layer or packages, and are located in the middle devonian platform edge facies zone. These two anomalies were interpreted as the reefs.

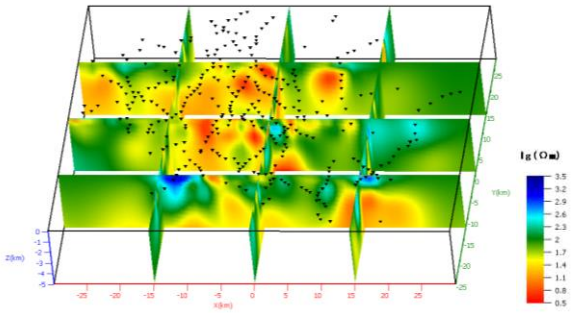

Figure 5 Inverted 3D resitivity model

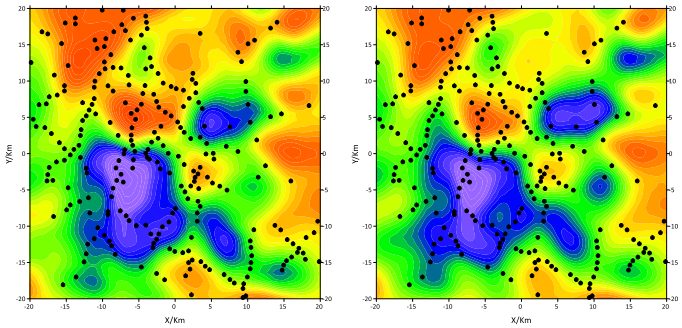

Figure 6 the horizontal slices of resistivity at depth (Left: -2500m Right: -3000m)

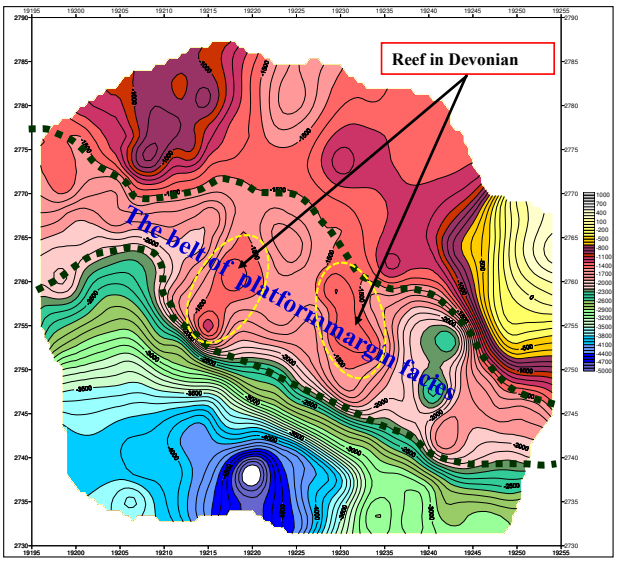

Figure 7 the divided sedimentary facies with 3DMT

5. Conclusion

Based on the irregular MT data distributed in the area of 3600 square kilometers in Huanjiang, Guangxi, 3D resistivity model was gotten with 3D inversion. According to the background of geology and rock-physics, the conductive mudstone layer of middle Devonian was identified. In this layer the lateral change of resistivity can be guided to divide sedimentary facies, so that the platform margin facies in this area was marked. In the belt of platform margin facies two resistance anomalies were circled.

Acknowledgement

The authors thank for the support of Key lab of geophysical prospecting, CNPC, and BGP non-seismic research group. The study supported by NSFC(Grant No.: U1562109; 41774082), the national major research plan(Grant No.: 2016YFC0601104, 2016ZX05004-003).

Reference

[1] В.Г.Кузнецов, reef geology and its characteristic of oil and gas. Petroleum publish house, 1983.

[2] Chen Xiao bin， the study of MT forward, inversion and the development of visual soft. Phd. Thesis, 2003.

[3] Jia Zhenyuan, Hao Shisheng, the formation and distribution of oil and gas in carbonate rocks. Petroleum publish house,1988.

[4] Lin Changhong, Tan Handong, Tong Tuo, 2012. 3D MT inversion with the sparse lines of MT data. Geoscience, Vol. 26(6), P1185-1192.

[5] Ledo J., 2005. 2-D versus 3-D magneteteuric data interpretation. Surveys in Geophysics, 26:511-543.

[6] Men ersheng， 1994， Petroleum geophysical exploration in carbonate rock area. The proceeding of oil and gas exploration in carbonate rock area in southern China, Jiangshu science and technology publish house.

[7] Smith J T, Booker J R, 1991. Rapid inversion of two- and three-dimensional magnetetelluric data. 96:3905-3922.

[8] Siripunvaraporn W. 2005, Three-dimensional magnetetelluric inversion: data-space method. Physics of the Earth and Planetary Interiors, 150(1-2):3-14.

[9] Yan Liangjun，EM methods and application in carbonate rock area in southern China. Petroleum publish house, 2001.

Finding haystacks: A new approach to mineral exploration

G. Heinson[1], Ben Kay[2], Kate Robertson[3], Stephan Thiel[4]

[1]University of Adelaide, Graham.Heinson@adelaide.edu.au
[2]University of Adelaide, Ben.Kay@adelaide.edu.au
[3]Geological Survey of South Australia, Kate.Robertson2@sa.gov.au
[4]Geological Survey of South Australia, Stephan.Thiel@sa.gov.au

SUMMARY

A challenge for the global mineral exploration industry is to identify world-class deposits under thick layers of sedimentary cover. Traditional approaches target the small-scale economic ore deposit, with declining rates of success over past decades. However, an alternative approach is to image deeper parts of the Earth's crust to find a much larger footprint where the metals originated. By finding the deep source we can also map potential pathways through the upper crust to define new prospective areas beneath sedimentary cover. So, rather than looking for the needle, it is better to first identify the haystack.

An MT program across the Curnamona Province, Australia that hosts the world-class Broken Hill mineral deposit has imaged a potential new iron-oxide copper gold uranium (IOCG-U) system. Two- and three-dimensional modelling images a lower-crustal region of resistivity <10 Ω.m aligned along a zone of 1590 Ma magmatism. The least resistive (~1 Ω.m) part terminates at the brittle-ductile transition at ~10 km, directly beneath a rifted sedimentary basin. Above the brittle-ductile transition, a narrow low-resistivity zones (~100 Ω.m) branches to the surface beneath the region of thinnest cover. We argue this whole-of-crust imaging encapsulates the deep mineral system and maps pathways of metalliferous fluids from lower crust and possibly mantle sources to emplacement at discrete locations in the upper crust.

Keywords: Mineral exploration, mineral systems, terrane-scale, camp-scale, deposit-scale.

INTRODUCTION

A significant challenge for the mineral exploration industry is to identify deep signatures of world-class magmatic mineral systems and the conceptual understanding of terrane-scale fertility under cover at which mineral systems operate (Griffin et al. 2013; Groves and Santosh 2015; Tassara et al. 2017). Approaching this challenge from a mineral system viewpoint, with deep sources and fluxes that are magnitudes larger on a spatial scale (McCuaig and Hronsky 2014), and performing scale-reduction techniques that narrow the exploration space from terrane (~100 km scale) to camp (~10 km scale) to deposit (~1 km scale) will improve the predictive ability for mineral exploration (Figure 1).

The MT method yields electrical resistivity images that provides insight into the current thermal and geochemical composition of the crust and upper mantle. As such properties result from tectonic and metamorphic events, the current resistivity profile is a record of the integrated events over deep time and their preservation (Selway, 2014). Depth and lateral resolution of resistivity properties is a combination of bandwidth of measurements, spacing of sites and the distribution of resistivity properties. However, with careful survey planning, the MT technique spans the exploration scale-lengths from the lithosphere-asthenosphere boundary to thickness of sedimentary cover, and thus is well placed to image an entire mineral system (Heinson et al. 2006).

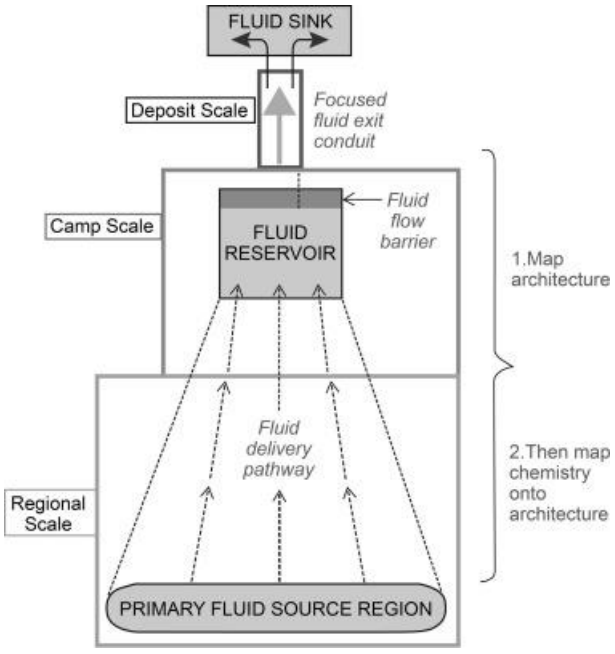

Figure 1 Conceptual framework for a magmatic mineral system generated by deep fluid fluxes in the lower crust or upper mantle (from McCuaig and Hronsky 2014).

TERRANE SCALE

On a continental-scale the Australian Lithospheric Architecture Magnetotelluric Project (AusLAMP) is designed to image resistivity properties of the entire Australian lithosphere to a depth of 200 km or more, with 3000 long-period MT sites spaced 55 km apart (about 0.5° at mid-latitudes). AusLAMP commenced in 2013 and is undertaken and analysed in craton and orogeny-scale programs, typically 50-200 sites over area dimensions of order 10^6 km^2.

An array of 75 AusLAMP sites over the Ikara-Flinders Ranges, Curnamona Province and adjacent sedimentary basins showed significant resistivity heterogeneity in the mid-lower crust, as shown in Figure 2 (Robertson et al. 2016). A north-south low-resistivity region of 1 Ω.m at 10 km depth was observed in the eastern side of the Curnamona Province that had previously been identified as the Flinders Conductivity Anomaly. At depths of 20-40 km, the lower crust is anomalously conductive at about 10 Ω.m in a wide area centred under the central part of the Curnamona Province. At sub-Moho depths, Robertson et al. (2016) showed there to be relatively homogenous and resistive upper mantle to 200 km, suggesting a deep lithosphere-asthenosphere boundary consistent with the presence of diamond-bearing kimberlite pipes in the southern Ikara-Flinders Ranges.

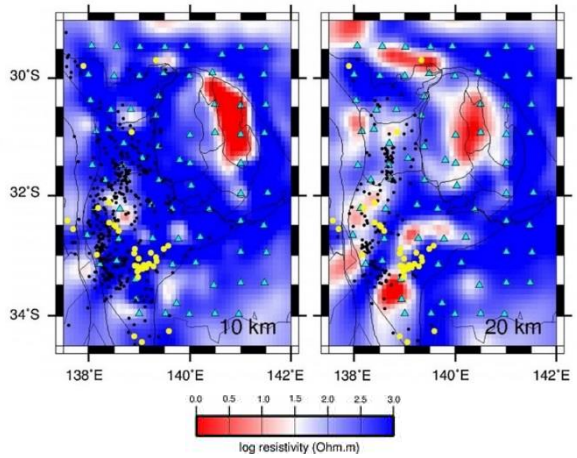

Figure 2 Resistivity depth slices from 3D inversion of AusLAMP MT data at 10 km and 20 km modified from Robertson et al. (2016). Blue triangles are AusLAMP MT stations, yellow circles are discovered diamonds and black circles are earthquake hypocentres between 10 ±1 km and 20 ±2 km respectively.

CAMP SCALE

AusLAMP is designed for terrane-scale investigation but lacks finer-scale resolution of crustal resistivity heterogeneity from the Moho to the sedimentary cover. To provide a link between terrane and camp-scale mineral systems, a 60-site broadband MT (0.001-1000 s) east-west survey was undertaken with a 2 km site spacing. Most of the sites were on Quaternary cover overlying sequences of Mesozoic and Proterozoic sediments that are typically >100 m and can be several kilometres thick. Thus, there is almost no outcrop of basement rocks until the eastern end of the line crosses onto the Barrier Ranges, and hence very little is known of the geology of the basement (Figure 3).

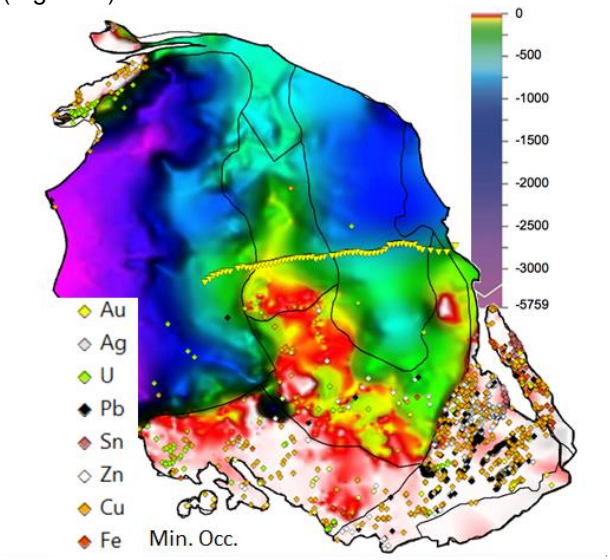

Figure 3. Sedimentary cover thickness of the Curnamona Province and mineral occurrences (Fabris et al. 2010). Yellow triangles show the location of broadband MT sites. Note that almost all the known mineral occurrences have been found in areas of cover < 50 m (red – white areas).

A broadband MT survey was conducted along a 120 km east-west transect across the central Curnamona Province in 2017 in two phases (Figure 4). The first survey consisted of 48 broadband stations at intervals of 2 km in South Australia component with a remote-reference station located 50 km south of the transect. The second survey consisted of 10 broadband stations spaced at intervals from 2 - 4 km in New South Wales, with each site remotely referenced to an adjacent site. Four components (Bx, By, Ex, Ey) were recorded for approximately 45 hours for each station, with a sample rate of 1000 Hz using the GSSA-AuScope LEMI-423 broadband MT instruments. The magnetic induction components, Bx and By (with x north and y east), were recorded using LEMI-120 induction coil magnetometers that were orientated

parallel to the 50 m electrical dipoles. Each station was rotated to geographic coordinates using the geomagnetic declination of the area, which ranged from 7° - 8°.

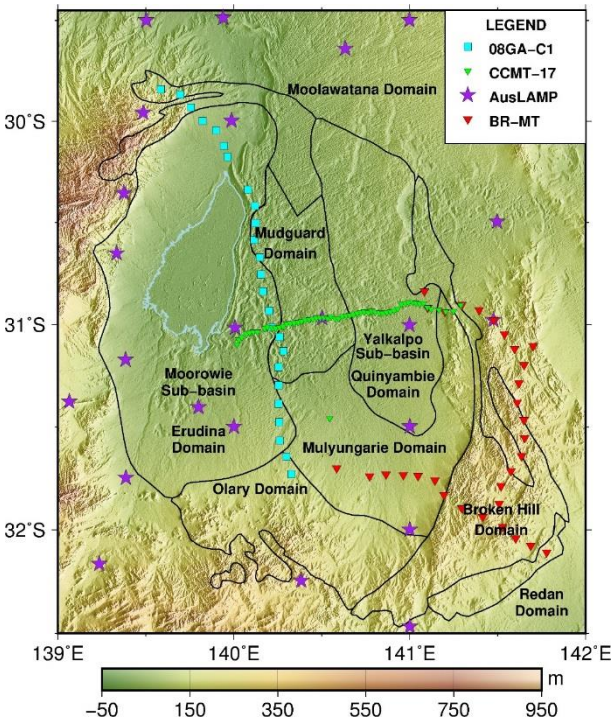

Figure 4 MT stations over topography of the Curnamona Province with geological domains. Yellow triangles showing the broadband MT transect which cuts across strike of the Erudina, Mudguard and Quinyambie Domains. Puple stars show AusLAMP stations, green squares are broadband MT stations along a seismic line 08GA-C1 and orange diamonds show legacy EM stations.

RESULTS

A smooth 2D inversion (Rodi and Mackie 2001) was undertaken for both TE and TM modes in the bandwidth 10^{-3} – 10^{3} s. The resistivity and phase floor errors were set to 5% and 2.5%, respectively, with a final RMS of 1.93. The 2D inversion model reveals a resistive upper crust and three zones of low electrical resistivity (Figure 5). A conductive sedimentary layer (C1 ~1 Ω.m) from the surface to ~200 m, thins to <100 m about 40 km along the profile. Below the sediments to 15 km there is a resistive upper crust (R1, R2 and R3 ~10,000 Ω.m) almost across the whole profile, except for a conductor (C3 ~10 Ω.m) located 80 – 100 km along the profile at a depth of 4 km. The lower crustal anomaly (C4, 1-10 Ω.m) is widespread starting from a depth of 15 km which is probably the brittle-ductile boundary and extending to at least the Moho. Finally, we note a near vertical conductor (C2 ~100 Ω.m) 45 km along the profile that connects the most conductive part of the lower crust C4 to the near surface, where the sedimentary cover is thinnest.

DISCUSSION AND CONCLUSION

A significant feature from the 2D resistivity inversion is C2 that has a footprint from the brittle-ductile boundary near 15 km above the C4 conductor, to the topographic basement high. A possible cause of this footprint is from fluids accumulating at and below the brittle-ductile boundary, until overpressure results in hydro-fracturing of the brittle crust above (Connolly and Podladchikov 2004) resulting in a conductive footprint from the alteration of fossil fluid pathways, usually through zones of weakness, which have previously been observed at mineral deposit locations such as Olympic Dam and the Beverley Deposit (Heinson et al. 2006; Thiel et al. 2016). The mid-crust conductor, C3, is situated at the boundary near a major unnamed fault that is situated on the eastern edge of the 1590 Ma magmatic Benagerie Ridge that may have acted as a pathway for the fluids. It is possible to speculate that the large C3 conductor, of width ~15 km and possible extent > 100 km, might have resulted from a large scale thermal event that weakened the crustal rheology, and when compounded with paleo-stresses led to the eventual formation of the deep sub-basin C1 during the Cambrian.

ACKNOWLEDGEMENTS

We thank the Geological Survey of South Australia for funding for the SA sites and access to their broadband MT instruments, and the Australian Society of Exploration Geophysicists Research Foundation for providing funding for the NSW sites. Other instrumentation was provided by AuScope. Field logistical support was provided by Havilah Resources by accommodating the field crew at the Portia Mine Site in South Australia. Thanks to Goran Boran, Yohannes Didana, Paul Soeffky and Sam Jennings for field and technical support. Figures were produced using GMT and WinGlink.

REFERENECS

Connolly JAD Podladchikov YY (2004) Fluid flow in compressive tectonic settings: Implications for midcrustal seismic reflectors and downward fluid migration. J. Geophys Res 109: 1–12.

Fabris A Gouthas G Fairclough MC (2010) The new 3D sedimentary basin model of the Curnamona Province: geological overview and exploration implications. MESA Journal 58: 16-24.

Griffin WL Begg GC Reilly SYO (2013) Continental-root control on the genesis of magmatic ore deposits. Nature Geoscience 6(11): 905–10.

Groves DI Santosh M (2015) Province-scale commonalities of some world-class gold deposits: Implications for mineral exploration. Geoscience Frontiers 6(3): 389–99.

Heinson GS Direen NG Gill RM (2006) Magnetotelluric evidence for a deep-crustal mineralizing system beneath the Olympic Dam iron oxide copper-gold deposit, southern Australia. Geology (7): 573–6.

McCuaig CT Hronsky JMA (2014) The mineral system concept: The key to exploration targeting. Applied Earth Science 126: 153–75.

Robertson K Heinson G Thiel S (2016) Lithospheric reworking at the Proterozoic–Phanerozoic transition of Australia imaged using AusLAMP Magnetotelluric data. Earth Planet Sci Lett 452: 27–35.

Rodi W Mackie RL (2001) Nonlinear conjugate gradients algorithm for 2-D magnetotelluric inversion. Geophysics 66(1): 174–87.

Selway K (2014) On the causes of electrical conductivity anomalies in tectonically stable lithosphere. Survey Geophysics 35(1): 219–57.

Tassara S González-Jiménez JM Reich M Schilling ME Morata D Begg G Saunders E Griffin WL O'Reilly SY Grégoire M Barra F Corgne A (2017) Plume-subduction interaction forms large auriferous provinces. Nature Communications 8(1): 843.

Thiel S Soeffky P Krieger L Peacock J Heinson G (2016) Conductivity response to intraplate deformation: Evidence for metamorphic devolatilization and crustal-scale fluid focusing. Geophys Res Lett 1–9.

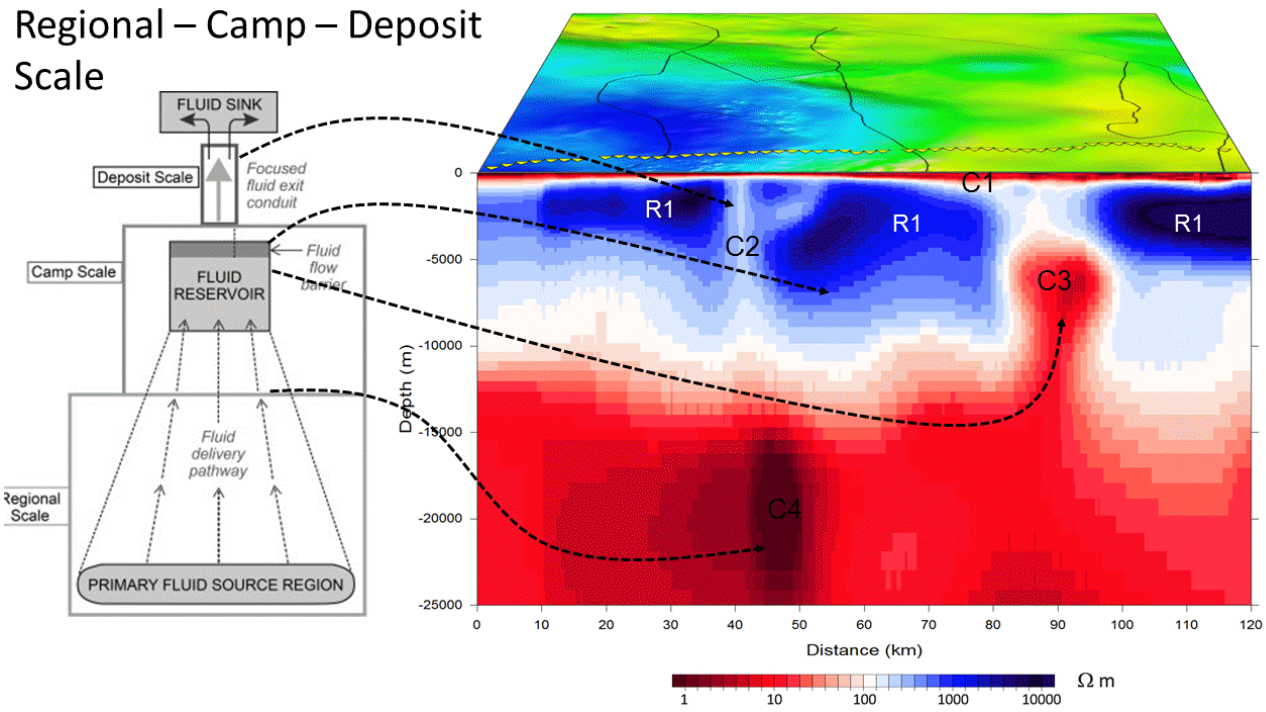

Figure 5 Right hand side shows the 2D inversion along the profile to a depth of 25 km. The left-hand figure is the concept mineral system footprint, and an estimate of how this maps to inverted section

Geo-radar LOZA and it application for sounding high resistive sections in South Africa

Berkut A[1], P. Morozov P[2], Ulyantsev N[3] , Hallbauer-Zadorozhnaya V[4], Stettler E[5]
[1]VNIISMI. Ltd. Moscow, Russia, lozaberk@yandex.ru
[2]Pushkov Institute of Terrestrial Magnetism, Ionosphere and Radio Wave Propagation, Moscow, Russia, moroz5@yandex.ru
[3]Loza Radar Inc., Russia, un@lozaradar.com
[4]Tshwane University of Technology, Pretoria, South Africa, valeriya.hallbauer@gmail.comn,
[5]University of Witwatersrand, Johannesburg, South Africa, stettlere@gmail.com

SUMMARY

New principles of Loza GPR series allows to reach electromagnetic wave penetration to depth up to 100-200 m. New features of the weak echo signals coming from these depths can be interpreted using a time-domain version of coupled Wentzel-Kramers-Brillouin theory. Experiments with geo-radar LOZA in South Africa showed good results for searching for various objects hiding in high resistive surroundings. We delimited a paleoriver, the void in old partially destroyed mine and a kimberlite pipe

Keywords: deep ground penetrated radar, dielectric permeability, modeling, kimberlite pipe

INTRODUCTION

The LOZA is the ground penetrating radar developed and manufactured in Russia. The LOZA can be used for small depths but can also reach larger depths in wet soils to delineate low- contrast geological boundaries: (deep penetrat radar, DPR). Distinctive features of the LOZA are: enhanced pulse power, signal energy concentration in the lower part of the frequency band, large dynamic range of registered echo signals. The DPR allows the study of subsurface media and structures previously not accessible by other types of GPR. The LOZA is a non-invasive instrument and have been successfully used in numerous countries (Russia, Australia, Egypt, USA, UK, Kazakhstan, Chili etc). The LOZA is used for various purposes such as search for hydrogeological objects, paleo-reliefs, kimberlite pipes and fissures, voids in the underlying medium, and geological structures. Some experiments with the DPR were carried out in South Africa in 2018 where traditionally GPR were used only for mine exploration.

The radar LOZA

Main technical characteristics of standard Loza-N DPR are:

- Receiver frequency band is 1-50 MHz;
-. Antennas: resistively loaded half-wavelength dipoles of Wu-King type, central frequencies from 25 MHz (6 meter) to 50 MHz (3 meter long);
- . Transmitter voltage supplied to antenna are 10 and 21 kV;
-. Pulse repetition rate: 150-200 1/s;
- Radar potential (max transmitted over min received signal) is not less than 120 dB.

A sketch of the radar LOZA is shown in Figure 1.

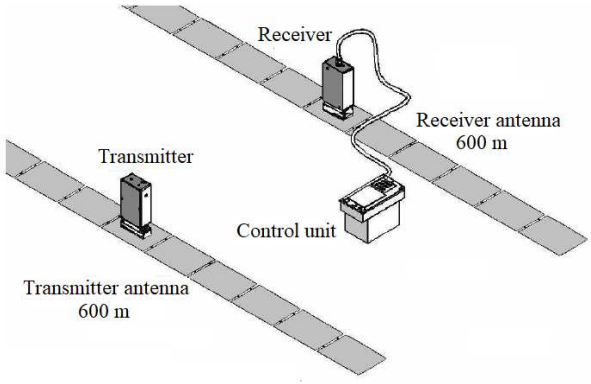

Figure 1. The sketch of the radar LOZA

Transmitter. Peak power reaches its practical limit as allowed by the insulating properties of the surrounding matter. Power pulse is generated by a gradually loaded capacitor, rapidly discharging through a high-voltage hydrogen key. Pulse's duration and shape depend on the antenna parameters. An example of the power pulse is presented in Figure 2.

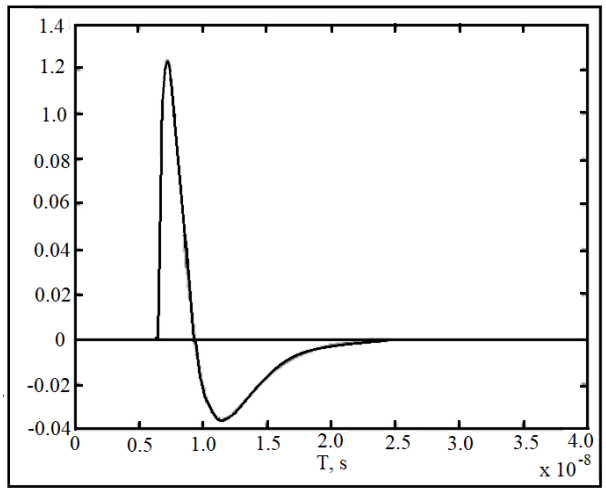

Figure 2. Shape of power pulse.

Antennas. Both transmitter and receiver antennas are non-resonant in order to avoid spurious "ringing". Wu-King resistive loading principle is used, it means that the energy dissipation gradually increase the resistivity between the linear antenna elements. Both antennas are kept apart (distance depending of depth of investigation (Figure 3.)

Figure 3. Field work, antennas keeping 3 m apart.

Frequency band. To reach maximum depth, the pulse spectrum in LOZA-N DPR is shifted to the lower part of the receiver frequency band to 1-50 MHz. The serial LOZA-N SYSTEM contains 50 MHz (3 m long), 25 MHz (6 m), 15 MHz (10 m) and 10 MHz (15 m) resistively-loaded antennas mounted on a heavy- duty nylon band.

Receiver, **signal digitization**. The receiver is a central unit of the LOZA-N. It registers amplitudes using a parallel set of high-rating comparators with sampling frequency: 0.5-1 GHz. By repeating measurements with the input attenuation changing in quasi-logarithmic scale, the LOZA-N processor obtains 256-bit signal representation in 120 dB dynamic.

Physical theory of deep GPR echoes.

Analytical theory of the quasi-1D wave propagation based on a time-domain version of the coupled Wentzel-Kramers-Brillouin (WKB) approximation (Prokopovich et al. 2018) explains weak backward scattering from smoothly stratified subsurface mediums. The initial pulse travels from the earth surface $z = 0$. In particular, the half-space response to the input electromagnetic pulse is given by equation (1):

$$g(s) = -\frac{1}{4}\int_0^{z(s)} \frac{\varepsilon^1(z)}{\varepsilon(z)} f\left[s - 2\int_0^s \sqrt{\varepsilon(\zeta)}d\zeta\right] dz\,, \qquad (1)$$

where $f(s)$ is an initial pulse which travels from the earth surface $(z = 0)$, then, according to the geometrical optics low it reflects from the gradient $\varepsilon^1(z)/\varepsilon(z)$' and returns back covering optical path $p(z) = 2\int_0^z \sqrt{\varepsilon(\zeta)}d\zeta$. Note that ε is relative permittivity (dimensionless). The return signal $g(s)$ is produced by partial reflections of the initial EM pulse $f(s) = dh(s)/ds$ from the gradually varying dielectric permittivity. Equation (1) is a sum of partial reflections due to the permittivity gradients, it can be considered as an integral equation for the unknown function $\varepsilon(z)$. For mathematical modeling the function $\varepsilon(z)$ can be presented as the function:

$$\varepsilon(z) = \frac{\varepsilon_0 + \varepsilon_1}{2} - \frac{\varepsilon_0 - \varepsilon_1}{2} erf\left[\frac{2z - z_0 - z_1}{\sigma(z_1 - z_0)}\right], \qquad (2)$$

The parameters of (2) are shown in Figure 4.

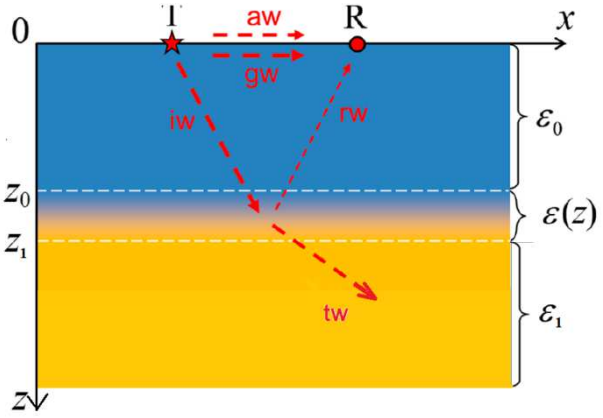

Figure 4. Geometry of the simulated scenario and schematic representation of the radar signal components. **aw** is an air wave, **gw** is a direct (ground) wave, **iw** is the incident wave, impinging on the transition layer, **rw** and **tw** are the waves reflected and transmitted by the transmitted layer respectively.

An example of the function describing relative chargeability is shown in Figure 6a as well as a theoretical signal for this law of chargeability

distribution (Figure 6b). In Figure 6c is presented the real field data and mathematical modeling using equation (1) and decreasing $\varepsilon(z)$as shown in the Figure 5a.

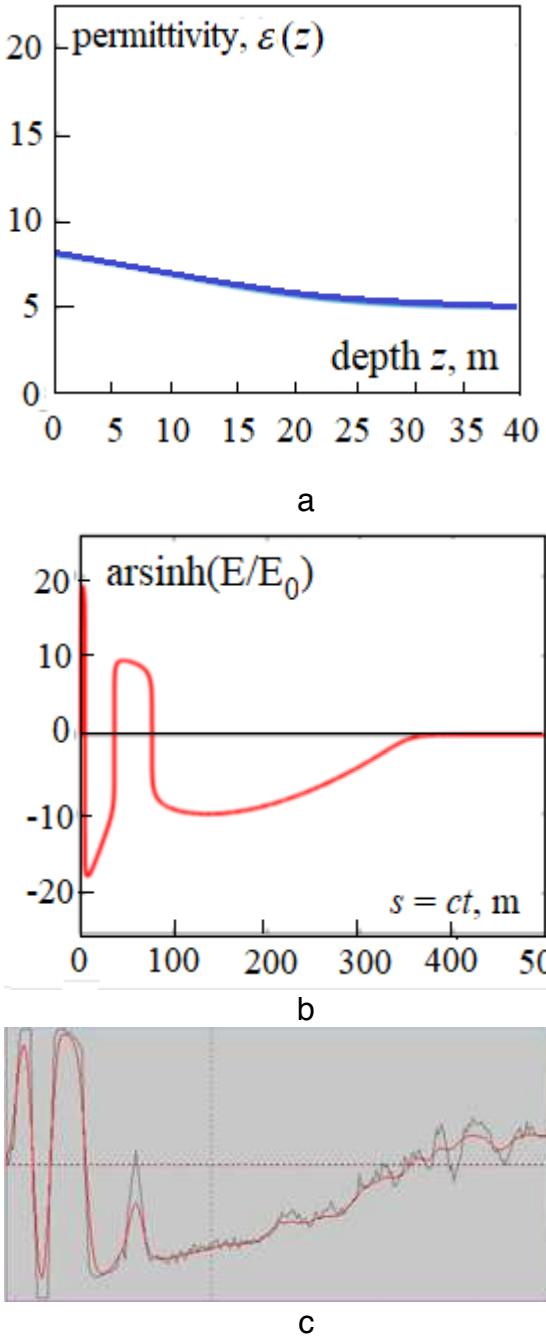

Figure 5. Model of vertical distribution of relative dielectric permeability (a), received signal in quasi-logarithmic scale (c) and mathematical modeling using (1).

RESULTS AND DISCUSSION

Experiments with the deep geo-radar LOZA have been carried out in high resistive settlements in South Africa for different purposes. The LOZA N has been used. The frequency band is 1-50 MHz, transmitter power 10 kW, length of antennas are 3m (50 MHz), distance between the antennas is 3 m, accuracy of the receiver is 100 μV, time interval 512 ns, time step (discretization) 1 ns distance between readings are 40 cm.

1. Paleoriver. Figure 6 demonstrates the radiogram along a profile crossing a paleoriver. The altitudes of the reading were taken into account.

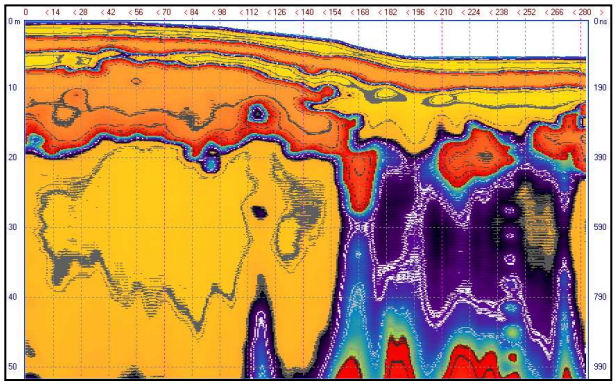

Figure 6. Geo-radar crossing a paleoriver.

The paleoriver can be clearly observed between 0 -154 m (right part of profile, blue and purple colour), the borders of the paleoriver are vertical. The bottom of the paleoriver is located at the depth of about 20 m. An old alluvial diamond mine is located 200-300 m away (Figure 7). It is possible that the observed object is a part of the complicate paleoriver system widely distributed in the North West Province in South Africa.

Figure 7. Plan of the profile located close to the old alluvial mine.

Void. The target is to define a possible void in an old and partially destroyed mine. According to the LOZA N data a void is observed along the profile between stations 40-48 m at the depth 12-13 (Figure 8, black ring). The anomaly has a high contrast compared to surrounding rocks.

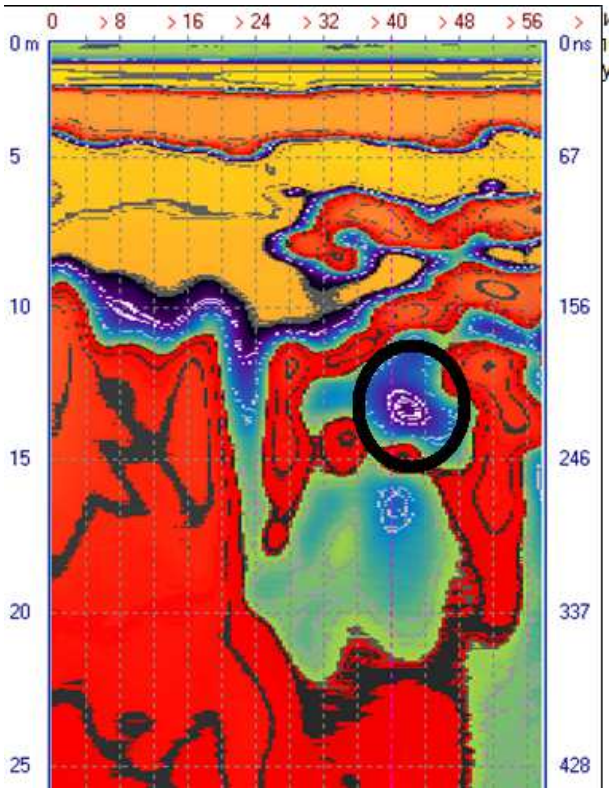

Figure 8. Void is observed at the depth 12-13 m.

Kimberlite pipe. A kimberlite pipe was observed in Lichtenberg area in South Africa. It is known from drilling into the pipe and was found at a depth of 65 m. However, it took only 30 minutes for radar fieldwork before in the screen of the instrument LOZA N the shape of this pipe was discovered.

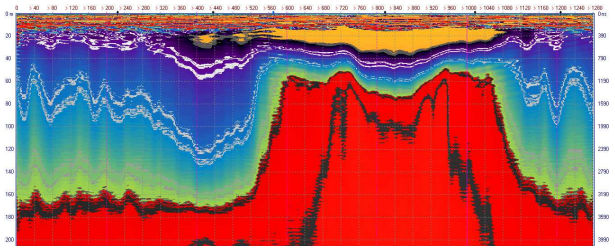

Figure 10. Kimberlite pipe in Australia

References

Bremmer H (1958) Propagation of Electromagnetic Waves, Handbuch der Physik / Encyclopedia of Physics, v. 4/16, pp. 423-639. Springer

Prokopovich I, Popov A, Pajewski L, Marciniak M (2018) Application of coupled-wave Wentzel-Kramers-Brillouin approximation to ground penetrating Radar. Remote Sens. 2018, 10, 1-20; doi:10.3390/rs10010022

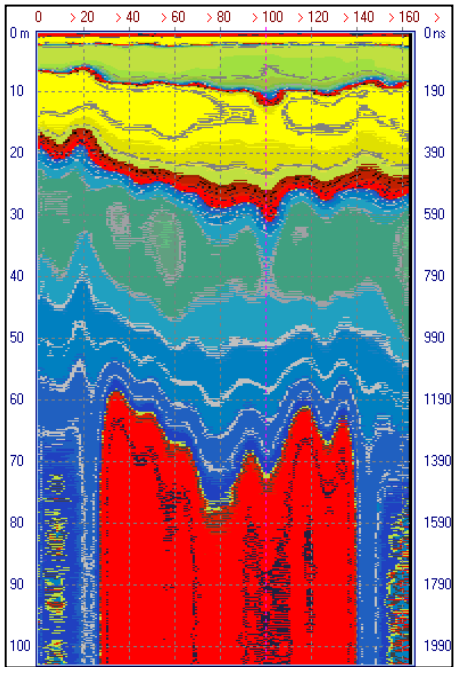

Figure 9. Kimberlite pipe discovered using the LOZA N. Shape of kimberlite pipe is shown by red colour.

Interpretation of the radar data showed an object of high contrast with sub vertical borders. The object is located between 30 and 140 m of profile (Figure 9) . Top surface of this object is covered by 60 m layered sediments. Amplitudes and phases of this object showed the highest values of dielectric permittivity ε and conductivity σ compared to surrounding rocks.

In Figure 10 is shown a kimberlite observed in Australia in 2016 that has the same shape as described above.

CONCLUSIONS

New principles of Loza GPR series allows to reach electromagnetic wave penetration to depth up to 100-200 m. New features of the weak echo signals coming from these depths can be interpreted using a time-domain version of coupled WKB theory. Experiments with geo-radar LOZA in South Africa showed good results for searching for various objects hiding in high resistive surroundings. We delimited a paleoriver, the void in old partially destroyed mine and a kimberlite pipe. We expect that the instrument LOZA N will surely step into the market in any country.

High-resolution shallow TEM sounding technique for the near-surface exploration

I. Shelokhov[1], M. Sharlov[2], I. Bouddo[3], N. Misyurkeeva[4], Yu. Agafonov[5]

[1] Institute of the Earth's Crust of the Siberian Branch of the RAS, sia@ierp.ru
[2] SIGMA-GEO Ltd., Institute of the Earth's Crust of the Siberian Branch of the RAS, sharlov@sigma-geo.ru
[3] SIGMA-GEO Ltd., Institute of the Earth's Crust of the Siberian Branch of the RAS, biv@sigma-geo.ru
[4] Institute of the Earth's Crust of the Siberian Branch of the RAS, mnv@ierp.ru
[5] SIGMA-GEO Ltd., Institute of the Earth's Crust of the Siberian Branch of the RAS, agafonov@sigma-geo.ru

SUMMARY

Transient electromagnetic (TEM) surveys have been used broadly in Russia and worldwide for engineering geology, groundwater prospecting, and other near-surface applications. Shallow TEM results obtained in different climatic and geological conditions prove the efficiency of the method in diverse near-surface applications. Having a penetration range from 10 to >500 m, the method can be used for estimating the depths to aquifers and permafrost, structural mapping, contouring intrusive and extrusive igneous bodies, environment monitoring, etc. The reliability of the predictions based on TEM data has been proven by subsequent drilling.

Keywords: Transient electromagnetic soundings, groundwater exploration, permafrost mapping, FastSnap

INTRODUCTION

Transient electromagnetic (TEM) surveys have been used broadly in Russia and worldwide for engineering geology, groundwater prospecting, and other near-surface applications (Bucharsky et al., 1986; Gomulsky et al., 2010; Plotnikov and Kozhevnikov, 2004; Agafonov et al., 2013, 2016; Ranieri et al., 2005; Shaaban et al., 2016, etc.), as well as for petroleum and mineral exploration (Mandelbaum et al., 1983; Korolkov, 1987; McNeill, 1980). Voltage decay patterns are highly sensitive to the presence of conductors associated with ore bodies, water saturation, clay, etc. Another advantage of the method is that it does not need galvanic grounding and works in any climate and terrain.

The resolution of shallow transient electromagnetic (sTEM) data has improved greatly in two recent decades due to breakthrough in micro-electronics providing advanced facilities for data acquisition and processing (nanosecond sampling rates, high-resolution ADC, etc.).

Extensive sTEM surveys at a density reaching 33 points per km2 have demonstrated high performance in solving diverse problems of geosciences from structural mapping to environment monitoring within a range of depths from 10 to 500 – 600 m.

FASTSNAP DIGITAL TELEMETRIC EQUIPMENT

The FastSnap digital telemetric equipment was designed in Russia in 2005 by Stefanenko S.M., Pospeev A.V., Agafonov Yu.A., and Sharlov M.V. and is currently available in its third modification (Sharlov et al., 2010, 2017). The system comprises light and small portable receiver and transmitter units placed in Pelicase shock-proof and tight plastic cases (Figure 1 A) which can be easily installed in any terrain and even in hardly accessible areas.

Earth's transient responses are recorded by multi-channel telemetric receiver units set next to loops or lines (Figure 1 B), are digitized by ADC and transmitted to PC in a in full wave-form.

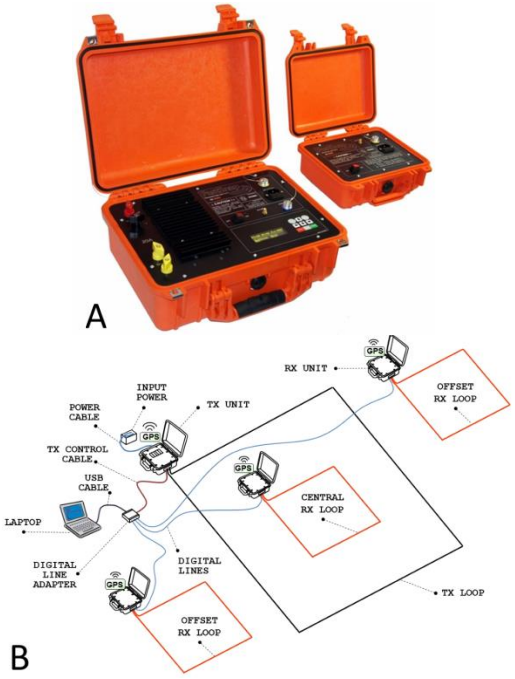

Figure 1. FastSnap equipment. A: Transmitter (current switch) and receiver units (left and right, respectively); B: Three-channel configuration.

CASE STUDY: sTEM FOR MAPPING AQUIFERS

There are up to seven near-surface aquifers at sites within the Angara-Lena step. The resolution of shallow TEM surveys allows mapping them reliably, both in depth and laterally. High-density 2D surveys are advantageous by imaging subtle details of the section which allows creating resistivity cubes as reference for borehole placement in zones of greatest water abundance (Figure 2).

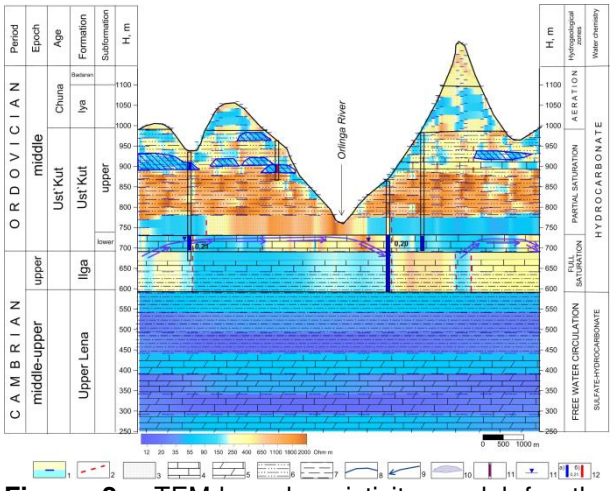

Figure 2. sTEM-based resistivity model for the Angara-Lena step, with elements of fluid dynamic and geological interpretation.
1 – resistivity layers; 2 – faults inferred from sTEM data; 3 – 7 – lithologies: sandstone (3), limestone (4), dolomite (5), siltstone (6), mudstone (7); 8 – groundwater table, lower Ust'-Kut Fm.; 9 – water flow direction; 10 – suspended aquifer lenses in aeration zone; 11 – wells; 12 – hydrocarbonate (a) and sulfate-hydrocarbonate (b) water chemistry (numerals at intervals (a) and (b) show salinity in g/l).

Field surveys, demonstrate high sensitivity of transient responses to aquifers within depths from 10 to 500 m. TEM data can be used to map aquifers even with almost fresh water in different settings.

CASE STUDY: sTEM FOR MAPPING PERMAFROST

Most of oil and gas fields in West Siberia are located within permafrost areas. Therefore, studies of permafrost have important implications for petroleum exploration, as well as for construction of production and transportation infrastructure.

Shallow TEM surveys were successfully applied to image a Paleogene-Quaternary section with permafrost in the Yamal-Nenets district (Shelokhov et al., 2017), within 400 – 450 m depths (Figure 3).

The section comprises several resistivity layers (from top to bottom): high-resistivity (100 to 2000 Ohm·m) frozen Quaternary lacustrine-alluvial, alluvial-marine, and glacial-marine deposits (~180 m thick modern permafrost, with two resistivity sub-layers); 25 – 40 Ohm·m paleopermafrost, free from ice inclusions (frost-bound rocks); 10 – 15 Ohm·m Eocene opoka clay of the Lyulinvor Fm. (unfrozen rocks); regionally continuous 15 to 30 Ohm·m sand of the upper Tibei-Sale Fm., possibly, also paleopermafrost (frost-bound rocks).

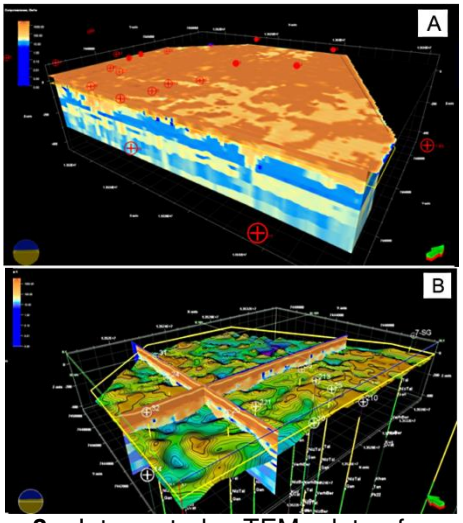

Figure 3. Interpreted sTEM data from West Siberia. A: cube of near-surface resistivity; B: map of modern permafrost base.

Thus, the sTEM surveys in the Yamal-Nenets district (Shelokhov et al., 2017) have revealed:

- Details of the near-surface to depths above 500 m poorly resolvable by seismic methods;
- Two sub-layers in modern permafrost;
- Depth to permafrost base along the base of the Tibei-Sale Fm;
- Heaving patterns, with heaves related to zones of permafrost thickening and inferred vertical gas conduits;
- Possible accumulations of gas hydrate and free gas.

It is important that sTEM can image shallow subsurface within depths from 10 to 500 m that are beyond the resolution of seismic surveys used for oil and gas exploration. Therefore, TEM-based images of permafrost can serve as reference for improving the quality of seismic results.

CASE STUDY: sTEM FOR SEISMIC DATA PROCESSING

The majority of oil and gas fields in Western Siberia are in the area of permafrost distribution. When interpreting seismic survey data in areas where permafrost is developed, it is necessary to take into account its influence on seismic data. Underestimation of this influence on the reflecting

horizons can lead to significant errors in structural model. Calculation of static corrections by conventional methods (by smoothing the variations of the travel time) artificial synclines arise on the section. We propose an approach to the upper part of the section velocity model building from transient electromagnetic soundings data.

The relationship between the resistivity and was first presented by L. Faust in 1953. We analyzed the possibility of applying this empirical equation for reconstructing the acoustic properties of the section according to the shallow TEM data. Velocity models obtained as a result of the performed transformations have high correlation dependence. According to the results of mathematical modeling and field data, it is shown that application of the developed technique will lead to an improvement in the quality of seismic data processing, i.e. will improve the accuracy of oil and gas field's geological models (Figure 4).

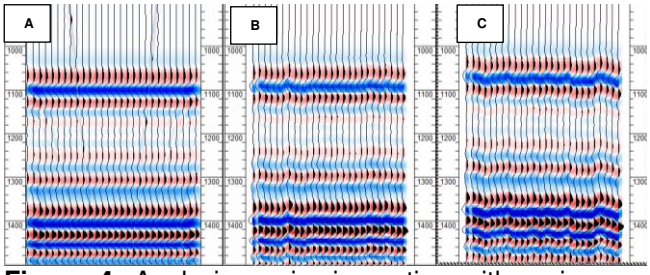

Figure 4. Analyzing seismic section with various processing methods: A – etalon section; B – section with shallow TEM static corrections; C – section with first break static corrections.

CONCLUSIONS

The use of advanced digital telemetric systems such as FastSnap extends the scope of shallow TEM surveys and provides a quantum leap in solutions to geoelectric problems. Highly sensitive high-frequency broadband channels enhance penetration at the account of both shallower and greater depths recording both early-time responses of near-surface as well as weak late-times responses of deep structures. Simultaneous use of multiple channels allows deploying multi-offset arrays of increased performance and information value. With the reliable high-tech instruments, one field team can perform 15 to 20 soundings per day by three-channel systems with 100 × 100 m transmitter loops.

Shallow TEM results obtained in different climatic and geological conditions prove the efficiency of the method in diverse near-surface applications. Having a penetration range from 10 to >500 m, the method can be used for estimating the depths to aquifers and permafrost, structural mapping, contouring intrusive and extrusive igneous bodies, environment monitoring, etc. The reliability of the predictions based on TEM data has been proven by subsequent drilling.

REFERENCES

Agafonov, Yu.A., Gomulsky, V.V., Sharlov, M.V., Tokareva, O.V., Tarasov, I.A., Buddo, I.V., 2013. The use of shallow TEM surveys for near-surface studies in East Siberia, in: Engineering Geophysics-2013, Proc. Conf., Gelendzhik, 22-26 April 2013, pp. 33-38.

Agafonov, Y.A., Aksenovskaya, A., Egorov, I., Kolesnikov, D., Sharlov, M., 2016. High-density shallow TEM surveys for groundwater prospecting in East Siberia. 23rd Electromagnetic Induction in the Earth Workshop, Chiang Mai, Thailand.

Bucharsky, B.V., Goryachev, V.V., Pavlov, A.T., 1986. Shallow modification of TEM surveys. Izv. Vuzov. Geologiya i Razvedka 8, 74 – 79.

Gomulsky, V.V, Markovtseva, O.V, Agafonov, Yu.A, Egorov, I.V., 2010. Use of shallow TEM surveys for detection of secondary oil and gas accumulations, in: Proc. GeoBaikal-2010, Irkutsk.

Korolkov, Yu.S., 1987. Transient Electromagnetic Soundings for Oil and Gas Exploration. Nedra, Moscow, 117 pp. (in Russian)

Mandelbaum, M.M., Rabinovich, B.I., Surkov, V.S., 1983. Geophysical Methods for Oil and Gas Exploration in the Siberian Craton. Nedra, Moscow. (in Russian)

McNeill, J.D., 1980. Application of transient electromagnetic techniques. Geonics Limited, Missisauga, Canada, TN 7, 17 pp.

Plotnikov, A.E., Kozhevnikov, N.O., 2004. TEM surveys for near-surface applications: potentiality assessment. Geofizika, No. 6.

Ranieri, G., Haile, T., Alemayehu, T., 2005. TEM-Fast small-loop soundings to map underground tunnels and galleries connecting the rock-hewn churches of Lalibela, Ethiopia. Geoarchaeology: An International Journal 20 (5), 433–448.

Shaaban, H., El-Qady, G., Al-Sayed, E., Ghazala, H., Taha, A.I., 2016. Shallow groundwater investigation using time-domain electromagnetic (TEM) method at Itay El-Baroud, Nile Delta, Egypt. NRIAG Journal of Astronomy and Geophysics 5, 323–333.

Sharlov, M.V., Agafonov, Yu.A., Stefanenko, S.M., 2010. Advanced telemetric systems SGS-TEM and FastSnap. Efficiency and experience of use. Pribory i Sistemy Razvedochnoi Geofiziki 31 (1), 27 – 31.

Sharlov, M.V., Buddo, I.V., Misyurkeeva, N.V., Shelokhov, I.A., Agafonov, Yu.A., 2017. Experience of efficient near-surface studies by the shallow TEM method using the Fastsnap system. Pribory i Sistemy Razvedochnoi

Geofiziki 38 (2), 8 – 23.

Sharlov, M.V., Buddo, I.V., Misyurkeeva, N.V., Shelokhov, I.A., Agafonov, Yu.A., 2017. Transient electromagnetic surveys for high-resolution near-surface exploration: basics and case studies. First break volume 35.

Shelokhov, I.A., Misyurkeeva, N.V., Buddo, I.V., Agafonov, Yu.A., 2017. Experience in the use of shallow TEM surveys for permafrost studies, in: Engineering Geophysics-2017, Extended Abstracts, 13-th Conf. and Exhibition, Kislovodsk.

Imaging shallow oil and gas deposits using of TDIP, SIP, TDEM/IP and AMT methods

Marek Sada[1], Joanna Figuła[1], Michał Stefaniuk[2], Adam Cygal[1,2]
[1] PBG Geophysical Exploration Co. Ltd., Warsaw, Poland, m.sada@pbg.com.pl, j.figula@pbg.com.pl
[2] AGH University of Science and Technology, Cracow Poland, stefaniu@agh.edu.pl, cygal@agh.edu.pl

The Wankowa oil field is one of the shallowest deposits occurring in the Polish Carpathians. This feature makes it very good to test different geophysical methods, configuration of measurement systems, and finally determine their suitability for hydrocarbon exploration.
The main purpose of the research was:

- development of IP methodology dedicated to specific Carpathian deposits,
- checking the distribution of the polarization parameter obtained using the TDEM method in relation to the polarization parameter obtained using the TDIP method (pole-dipole array).

As part of experimental work, induced polarization measurements in the time domain were made exploiting the IRIS Instruments system. A pole-dipole array with a length of measuring dipole equal 30 meters was used. The cross-section up to a depth of approximately 450 meters obtained as a result of the interpretation was adopted as a reference for other experiments. The other methods that were performed on the Wankowa oil reservoir are TDEM/IP, AMT, TDIP and SIP using an equatorial arrays for different distances between AB and MN dipoles. Measurements for these methods were made exploiting Phoenix Geophysics Ltd. equipment: V8-6R receivers and TXU-30 transmitter for generating electromagnetic wave. The polarization parameter in the TDEM method was calculated using the cole-cole model in the inversion process.

As a result of the interpretation, cross-sections with the distribution of resistivity and the polarization parameter were created from methods independent of each other. The oil reservoir in resistivity imaging (based on the AMT and TDEM methods) is a high-resistivity zone covered from above by an anticline low-resistivity structure that can be associated with a seal (trap) for hydrocarbon accumulation. Within the deposit structures, there are anomalous values of the induced polarization parameter - which is an additional indicator of hydrocarbons. Analyzing the results obtained, it seems that in the Carpathian conditions the use of a complex of methods: TDEM with calculated induced polarization parameter and AMT can significantly improve the accuracy of drilling.

As a result of the research, no clear conclusion was obtained regarding the relation of the IP parameter obtained as a result of the measurement with the classical method and the parameter calculated from the TDEM method. There are similarities in the qualitative image, while the quantitative interpretation requires further research and analysis. The induced polarization method in classical approach has a number of limitations (e.g. depth range). In experimental measurements, high power generators were used, but despite this the signal strength on the MN dipoles located at a large distance from the electrode B (larger depths) was weak. Therefore, quite interesting results obtained from the TDEM method with the polarization parameter on the Wankowa deposit, encourage further research and experiments using this method.

This paper was prepared based on results of investigations carried out in the framework of the project entitled “Experimental, complex and multi-variant interpretation of seismic, magnetotelluric, gravity and borehole data as a tool to improve the effectiveness of structural and reservoir research” – Applied Research Program III (In Polish: Program Badań Stosowanych III

Keywords: Induced polarization, Transient electromagnetic, Audiomagnetotellurics, Oil deposit

Integrated interpretation of airborne and ground geophysical data for graphite exploration in Northern Norway

V. C. Baranwal[1], J. S. Rønning[2,*], H. Gautneb[3], B. E. Larsen[4], F. Ofstad[5] and M. Brönner[6,*]
[1]Geological Survey of Norway (NGU), vikas.baranwal@ngu.no
[2]Geological Survey of Norway (NGU), jan.ronning@ngu.no
[3]Geological Survey of Norway (NGU), havard.gautneb@ngu.no
[4]Geological Survey of Norway (NGU), bjorn.eskil@ngu.no
[5]Geological Survey of Norway (NGU), frode.ofstad@ngu.no
[6]Geological Survey of Norway (NGU), marco.bronner@ngu.no

*Also affiliated with Norwegian University of Science and Technology (NTNU)

SUMMARY

As part of a government funded programme for mineral exploration in Norway (MINN and MINS), NGU acquired new high resolution frequency-domain helicopter electromagnetic (HEM), airborne magnetic and airborne radiometric data during 2011-2015. HEM data was collected at five frequencies (980 and 7000 Hz in co-axial setting and 880, 6600 and 34000 Hz in coplanar setting) as in-phase and quadrature components. The total magnetic field was measured using a cesium vapor magnetometer. We jointly interpret HEM and magnetic data from the Vesterålen area in Northern Norway to revisit known graphite deposits and to explore for new potential areas.

A correlation of low magnetic anomalies and low apparent resistivity obtained from these data is noticed from already known areas with abundant graphite and from new sites with exposed graphite at the surface. Based on this correlation, new potential areas for graphite deposits are identified and refined for further follow up and detail investigation using ground geophysical methods and core drilling to confirm the deposits and whether it is economical.

EM31 and 2D resistivity measurements at new and earlier known locations show that graphite exists in banded formations instead of a continuous formation as indicated by HEM data. More ground and drilling investigations are planned to be done this summer. Rock samples from the area are being analyzed at the NGU laboratory to investigate its carbon content and magnetic properties. Later, all the available ground and drill core information will be used to perform 3D modeling and inversion of the HEM data to investigate depth of the conductive structures.

Keywords: HEM data, frequency domain, airborne magnetic, graphite exploration, integrated interpretation

Integrated structural and lithological interpretation of magnetotelluric sounding data versus detailed 3D seismic survey, example from Lublin Basin, Eastern Poland.

Michal Stefaniuk[1], Marek Sada[2], Joanna Figuła[2], Adam Cygal[1], Krzysztof Dzwinel [3]

[1] AGH University of Science and Technology, stefaniu@agh.edu.pl
[2] PBG Geophysical Exploration Ltd., m.sada@pbg.com.pl
[3] ORLEN Upstream Ltd, Krzysztof.Dzwinel@orlen.pl

SUMMARY

The subject of the paper is advanced interpretation of magnetotelluric sounding data for detailed recognition of geological section. The experimental surveys with use of set of electromagnetic methods including magnetotellurics and audiomagnetotellurics were made along 6.0 kilometer long part of test seismic profile located inside of the area of also experimental unique detailed 3D seismic survey. The general aim of experimental electromagnetic surveys was comparing the results of seismic and electromagnetic data interpretation and analysis of possibility of supporting or substituting seismic survey by independent geophysical data. From the other point of view results of interpretation of excellent, detailed seismic data were used for testing of role of starting model building based on good geological model recognition and role of suitable constrains construction for increasing of resolution of electromagnetic methods in detailed recognition of geological medium.

Magnetotelluric data acquisition was made with use of V8 receivers of Phoenix Geophysics. Sounding sites were located along profile with spacing 100.0 m (continuous profiling). Additionally, 3.0 kilometer extensions of both ends of the profile with spacing of ca. 250 m were made for avoiding of marginal computational effects. Standard remote reference data processing as well as advanced robust data processing were applied to recorded data. 1D Occam inversion was applied for first stage of interpretation and LSQ code was used for analysis of parametric sounding made close to borehole St -1, located in the center of the profile. Well – logging and borehole geological data as well as resistivity pseudo section based on 1D Occam inversion results were used for initial model building. Constrained sounding inversion was used for computing of 2D resistivity cross sections. Comparation of results of magnetotelluric data interpretation with reference geological model based on interpretation of high resolution seismic data allowed to evaluate the range of possible use of magnetotelluric data in recognition of geological structure and lithological differentiation in relation to local (specific for Lublin Basin) geological conditions. Interpretation of magnetotelluric soundings supplied supplementary data especially in relation to deep basement tectonics and some lithological differentiation and weak fault zones(strike – sleep faults?) that are not visible on seismic cross – section.

This paper was prepared based on results of investigations carried out in the framework of the project of acronym “GASLUPSEISM” made in the framework of “Blue Gas I” program financed by *Minister of Science and Higher Education of Poland through National Centre of Research and Development, Polish Oil and Gas Company and Orlen Upstream Ltd . Presentation was prepared in the framework of AGH University of Science and Technology Statutory Research, no:11.11.140.322.*

Keywords: magnetotellurics, constrained inversion, reflection seismic, structural interpretation, lithology .

Integrating resistivity into petroleum exploration on the Barents shelf: a geological perspective

Kim Senger[1]
[1]University Centre in Svalbard, kim.senger@unis.no

SUMMARY

The Norwegian part of the Barents shelf represents a frontier hydrocarbon province covering over 700 000 km^2 with 153 exploration wells drilled offshore to date. In addition, 17 exploration wells were drilled onshore Svalbard from 1963 to 1994. The Barents shelf has been severely uplifted during the Cenozoic, which led to significant impacts on the petroleum system; including source rock maturation, reservoir quality, trap and seal integrity and re-migration of hydrocarbons. Exploration well results nonetheless suggest a working petroleum system, with almost half of the exploration wells encountering hydrocarbons. Many of these, however, were technical discoveries in under-filled traps or with only residual gas remaining. One of the keys to exploration success on the Barents shelf is to make use of controlled source electromagnetic (CSEM) data to provide pre-drill estimates of pay zone resistivity and thus differentiate between low and high hydrocarbon saturation.

In this contribution, I first review the use of CSEM in exploration on the Barents shelf in the past decade focusing on case studies including the very shallow Wisting oil discovery, the sub-commercial Pingvin gas discovery and the recent CSEM-driven Kayak gas discovery. I subsequently present a comprehensive analysis of wireline data from offshore and onshore exploration wells, focusing on the geological controlling parameters on resistivity. Formation resistivity is primarily controlled by the presence and connectivity of electrically conductive fluids, i.e. brine. The matrix is usually insulating in sedimentary basins and resistivity is thus primarily controlled by: 1) porosity, 2) brine conductivity, 3) brine connectivity and 4) brine saturation. I illustrate how resistivity varies both vertically and laterally as a function of porosity reduction, and focus in particular on the resistivity contrast between hydrocarbon-bearing reservoir sandstones and the overlying source rock shales of varying quality and maturation levels.

Keywords: CSEM, MT, petroleum, Arctic, exploration

Joint interpretation of MT and VES data for static shift correction. Case study from eastern part of Polish Outer Carpathians.

Jakub Wazny[1], Michal Stefaniuk[1], Adam Cygal[1], Marek Sada[2] and Michal Cwiklik[1]

[1] AGH University of Science and Technology, jwazny@agh.edu.pl
[2] PBG Geophysical Exploration Ltd., m.sada@pbg.com.pl

SUMMARY

The inversion results of magnetotelluric measurements performed in eastern part of Polish Outer Carpathians are difficult in interpretation due to the presence of static shift phenomenon. Particularly exposed to this galvanic distortion are vertically shifted amplitude curves while phase curves remain unchanged. The phenomenon is caused by the geological situation of measurement environment, characterized by fold and thrusted structure with angles of layers dipping up to 90 degrees. This implies lithological heterogeneity of the subsurface zone and a varied topography of the area. Inversion of magnetotelluric data results in large errors associated with rescaling the resistivity, especially in the deep zone. For this reason it is necessary to use the interpretative methodology to eliminate static shift.

Therefore, in points of magnetotelluric soundings VES measurements were conducted. Asymmetrical array in two orthogonal directions: parallel and perpendicular to the strike of geological structures was used, which corresponded to the TE and TM mode orientation. The advantage of this approach was to obtain VES curves of apparent resistivity being a reference to the curves of both modes of the magnetotelluric method.

One-dimensional joint inversion of MT and VES data was carried out, which was the basis for performing two-dimensional inversion of MT data.

Results of joint interpretation were compared with results of independent inversion of MT data. The methodology allowed to increase the efficiency of interpretation of the studied area and the reliability of the final result obtained.

This paper was prepared based on results of investigations carried out in the framework of the project *"Experimental, complex and multi-variant interpretation of seismic, magnetotelluric, gravity and borehole data as a tool to improve the effectiveness of structural and reservoir research"* – Applied Research Program III, financed by Minister of Science and Higher Education of Poland through National Centre of Research and Development.

Keywords: static shift, magnetotellurics, vertical electric soundings, joint inversion

Magnetotelluric imaging for hydrocarbon exploration in mountainous regions: a case study

R. Streich[1] and A. Abhishek[2]
[1] Shell Global Solutions International B.V., rita.streich@shell.com
[2] Shell India Markets Pvt. Ltd., A.Abhishek@shell.com

SUMMARY

While magnetotelluric (MT) imaging is widely used for imaging the Earth's deep crustal structure, use of MT for hydrocarbon exploration purposes is less common. We have investigated the potential of MT to aid exploration activities in fold-and-thrust belt settings, where it is difficult to acquire seismic data of sufficient quality and coverage to provide accurate subsurface information. The primary targets for our survey are strongly resistive thrust sheets. Sensitivity studies show that, although strong resistors are not a favorable target for MT, we should be able to image resistors of the expected lateral size and depth range. However, it is unlikely that structural details or the base of the resistors will be resolved.

The real MT data set used in this study comprises 72 stations, most of which are located along a central line, with a sparse 3D grid on either side. Usable data were obtained in the range of about 2700 s to 20 kHz, with periods longer than 1000 s present at about half of the receivers. We discarded data with estimated errors higher than 20% of the apparent resistivity magnitude. Data weights were assigned using error estimates from processing, and emphasizing low frequencies to encourage deep model updates despite the relatively sparse and low-quality low-frequency data available. Elevation changes in the area amount to more than 1000 m. To account for the strong topography in forward modeling, while using a finite-volume frequency-domain modeling scheme with non-uniform, but structured grids, 20 m vertical discretization is used in the depth range containing topography. Below the topography and laterally away from the main line, cell sizes grow gradually. Our survey area is located about 30 km from a coast, requiring us to include the sea into the model.

We invert the xy and yx components of apparent resistivity, and start the inversions from a homogeneous half-space with different horizontal and vertical resistivities. By first using high frequencies only, and gradually including lower-frequency data at later stages of the inversion, we resolve small-scale near-surface resistivity variations, and achieve overall better data fit than when including all frequencies at once or starting from low frequencies.

Based on exploration drilling, two distinct resistive bodies are known to exist. The shape of the deeper body is a geological question of special interest. Images of the real data clearly show resistors consistent with previous knowledge. Especially the top of the shallower resistive body is recovered well. A deeper resistive body appears to be imaged as a feature of slightly elevated resistivity in parts of the inversion model, and merged into a single body with the shallower resistor in other parts.

Using synthetic studies to analyze the reliability of our images further, we find that a deep resistive body indeed has sufficient influence on the MT data to be detectable. However, we also see that such a body cannot be resolved in inversion images, even when extending the data set in areal coverage and frequency range, and increasing station density. This is a clear demonstration of the known discrepancy between sensitivity and resolution. Furthermore, we show that the deeper feature of slightly elevated resistivity primarily results from the boundaries of receiver coverage; it disappears in synthetic images if the survey area is extended laterally. We conclude that we cannot interpret this feature, although doing so would be tempting given the a priori knowledge.

The results of this synthetic-aided analysis show the importance of scrutinizing image reliability to prevent premature, biased geological interpretation. While we have to conclude that MT alone cannot resolve separate stacked resistive sheets in the prospect area, we further investigate potential added value from integrating the MT with other available geophysical data.

Keywords: Magnetotelluric, inversion, hydrocarbon exploration, resistor, confidence assessment

Magnetotelluric studies of Subandian fold belt, Bolivia

N. Palshin[1,2], R. E. Giraudo[3], D. Yakovlev[2], R. Zaltsman[2] and S. Korbutiak[2]
[1]Shirshov Institute of oceanology, RAS, palshin@ocean.ru
[2]Nord-West Ltd, mail@nw-geophysics.com
[3]YPFB Corporación, rgiraudo@ypfb.gob.bo

SUMMARY

The two largest MT surveys were carried out in Subandian fold belt, Bolivia. The surveys were aimed at better understanding of a complicated geological structure and petroleum system of the fold and thrust belt in two specific survey areas. Broadband MT data were acquired along 16 profiles in the northern survey area at 1392 sites and along 41 profiles at 2229 sites in the southern survey area. In 30% of sites loop-in-loop TDEM data were acquired for statics shift correction purposes. The distance between profiles was about 4-5 km, while distance between sites comprised300 m in anticlines and 600 m in synclines. 5 component MT data were collected at a period band from 0.0001 to 1000 s using MTU-5A instruments with MTC-150 induction coils. The normal duration of recording at each site was from 16 to 20 hours (overnight recording). Dimensionality analysis showed that impedances are close to 2D: no rotation or transformations of transfer functions were applied. Combined static shift correction procedure, which includes both spatial averaging and TDEM based correction, was developed and successfully applied. Unconstrained and constrained bimodal 2D OCCAM inversion was used for constructing resistivity images along profiles. Practically all MT acquisition profiles coincide with seismic ones, thus geological interpretation was based both on seismic sections and resistivity images using logging data as additional constraints. Good coincidence of resistivity images with seismic sections are clearly seen in synclines, while in anticline's cores the resolution of resistivity images is better that seismic ones. The results of MT joint interpretation along with seismic and logging data give important structural constrains, especially at the core of anticlines. New targets (already delineated with seismic) were outlined and confirmed with MT. Magnetotellurics is an effective technology to delineate resistivity contrasts in areas where seismic faces problems, i.e. the Subandean fold belt.

Keywords: magnetotellurics, joint interpretation, hydrocarbon prospecting, Subandian fold belt

INTRODUCTION

The two largest MT surveys were carried out in Subandian fold belt, Bolivia. The surveys were aimed at better understanding of a complicated geological structure and petroleum system of the fold and thrust belt in two specific survey areas: Subandino Norte (SAN) and Subandino Sur (SAS). Recent advances in MT technology, a considerable increase of quantity and quality of data and joint interpretation of MT data with seismic and logging data allows to increase efficiency of magnetotellurics. Magnetotellurics becomes an efficient technology additional to seismic one especially in fold and trust belts. However, there is still some skepticism about the method, especially related to hydrocarbon exploration. The results recently obtained in the Subandian fold belt can significantly improve the impression about the method among petroleum geologists.

DATA ACQUISITION, PROCESSING AND ANALYSIS

The location of the survey areas is shown in Figure 1. Field work started in March and was completed in November, 2017. Broadband MT data were acquired along 16 profiles in SAN at 1392 sites and along 41 profiles at 2229 sites in SAS. In 30% of sites loop-in-loop TDEM data were acquired for statics shift correction purposes.

Figure 1. The location of survey areas: Subandinao Norte (SAN) and Subandino Sur (SAS).

About 30 field crews were operating simultaneously. 4WD pickup, boats and helicopters were used for personal and instruments transportation. The length of profiles varied from 40 to 60 km and all profiles were oriented across the geological strike.

The distance between profiles was about 4-5 km, while the distance between sites comprised 300 m in anticlines and 600 m in synclines.

5 component MT data were collected at a period band from 0.0001 to 1000 s using MTU-5A instruments with MTC-150 induction coils (33 instrument sets were used). The normal duration of a recording at each site was from 16 to 20 hours (overnight recording). The main challenges were (1) high lightning activity, (2) rainy and hot weather, (3) damage of cables and electrodes by animals. About 20% of sites were re-measured.

A new efficient robust RR data processing approach was applied (Epishkin, 2018), which allowed to get reliable estimates of a complete set of transfer functions (impedance, tipper and horizontal magnetic tensor) at all sites.

Dimensionality analysis based of a phase tensor invariants estimation showed that impedances are close to 2D. For the most of data values of β parameter were less than 5° and the orientation of phase tensor ellipses coincide with the geological strike and profiles orientation (see Figure 2). Thus, impedances in measured coordinates were considered as TE and TM modes: no rotation or transformations were applied.

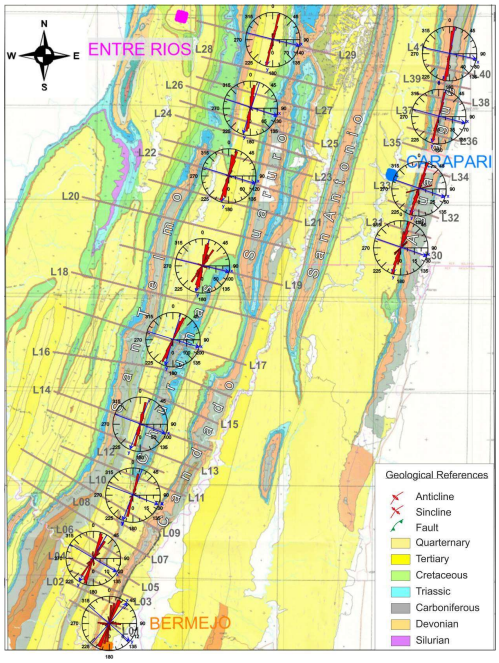

Figure 2. Geological map and orientation of phase tensor ellipses in Subandino Sur.

Combined static shift correction procedure, which includes both spatial averaging and TDEM based correction, was developed and successfully applied. (see Figure 3).

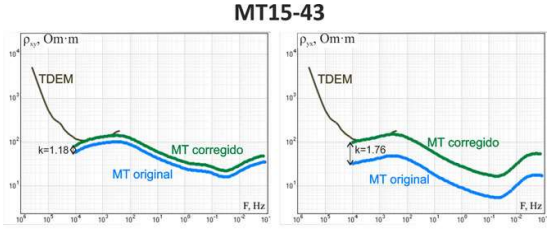

Figure 3. Static shift correction using TDEM data (example for site MT15-43, SAS). TE mode at the left panel and TM one at the right panel.

2D INVERSION AND CONDUCTIVITY STRUCTURE CHARACTERIZATION

According to the technical requirement an unconstrained and constrained bimodal 2D OCCAM inversions were used for constructing resistivity images along profiles. A multistage approach was applied with a uniform halfspace as a starting model in the very beginning. For the specific structure of Subandian fold belt TM mode gives more information about a sedimentary cover, than TE mode, but both modes are required for constructing reliable models. In the final stage high resistive basement at a depth of 8 km (from seismic data interpretation) was introduced as a constraint (see Figure 4).

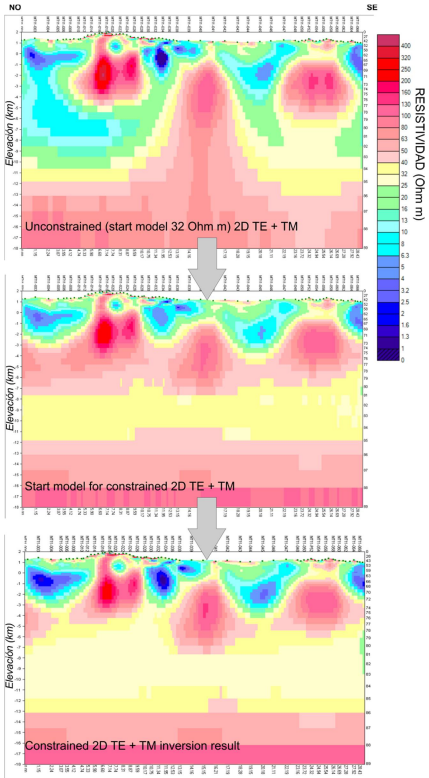

Figure 4. Example of 2D inversion procedure for profile 21, SAN. From top to bottom: unconstrained inversion, constraints and spatial averaging applied (new starting model), constrained inversion.

Available petrophysical and logging data were used for conductivity structure characterization: typical resistivity values for the main geological formations were estimated.

TECTONIC AND GEOLOGICAL BACKGROUND

In the Central Andes, the back-arc thrusting started in late Oligocene and is continuing. The sedimentary section involved in thrusting consists of Cambrian to Oligocene preorogenic strata and Oligocene-Miocene to recent continental synorogenic infill. The back-arc system of the Bolivian orocline consists of seveal tectonic zones and includes a narrow thrust-and-fold belt.

The northern branch of the belt (Subandino Norte) is characterized by large-scale thrust sheets (10–20 km of offset) and broad synclines filled with 6000 m of syntectonic Neogene sedimentary rocks. The survey area on the surface is represented by several elongated ridges and valleys oriented from the northwest to southeast and corresponding to anticlinal and synclinal structures. Despite geological and geophysical studies carried out in the area and several exploratory wells, no commercial hydrocarbon deposits have been discovered, although on the basis of geological and geophysical studies and known oil and gas fields in Madre de Dios basin, the hydrocarbon potential of this basin was estimated as high (Baby et al., 1995; Baby et al., 1997; Zubeita, 2008).

In the southern branch, a regional east-verging thrust divides the southern Bolivian Subandean zone into two fold-and-thrust belts that differ according to their thrust system geometry. The western belt is characterized mainly by fault-propagation folds and fault-bend folds, whereas the eastern belt is characterized by fault-propagation folds and passive roof duplexes. The Silurian-Devonian succession is covered by more than 2000 m of upper Paleozoic and Mesozoic sandstones with no potential detachments; in some places it is also covered by several thousand meters of synorogenic Neogene sedimentary rocks (Baby et al., 1997). Subandino Sur is the main oil and gas producing region in Bolivia. Both survey areas are the “so-called” multi-level decollement thrust-and-fold zones. (see Figure 5)

JOINT INTERPRETATION

Practically all MT acquisition profiles coincide with seismic ones, thus geological interpretation was based both on seismic sections and resistivity images using logging data additional constraints.

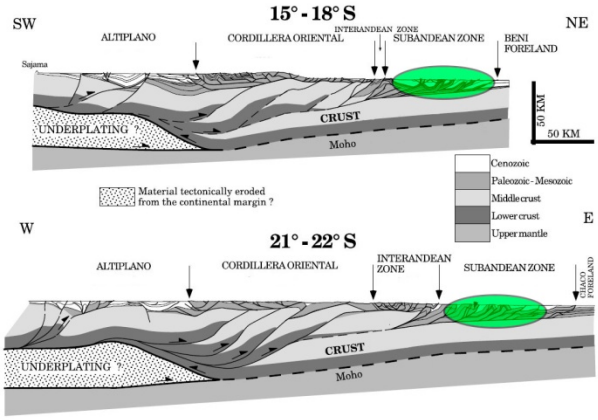

Figure 5. Schematic regional profiles crossing northern (top panel) and southern parts of Andes in Bolivia. Location of survey areas is outlined. Modified from Baby et al., 1997.

Good coincidence of resistivity images with seismic sections are clearly seen in synclines, while in anticline’s nuclei with sub vertical dip of layers (and reflectors) the resolution of resistivity images is better (see Figure 6).

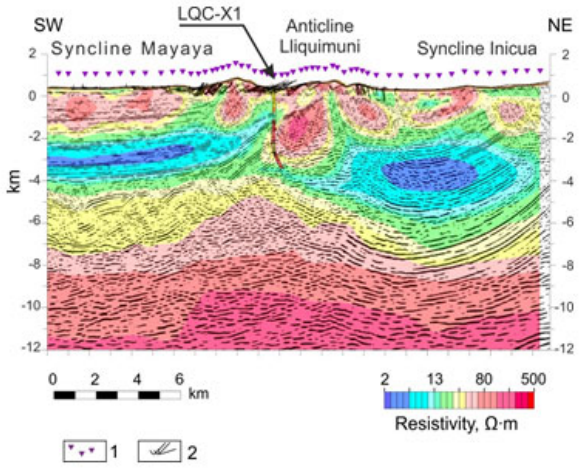

Figure. 6. Resistivity image and seismic section (example for line 17, SAN). 1 – MT sites, 2 – sedimentary layers dip on the surface.

In Subandino Norte survey area a big number of faults parallel to the geological strike were outlined in anticlines. The whole survey area is divided into two parts by a system of oblique faults. A two level resistivity structure was revealed: the upper structural level is characterized by pop-up and palm tree structures, while the lower level is characterized by duplex structures (see Figure 7).
A map of the depth to Devonian formation (main source rocks) was constructed.

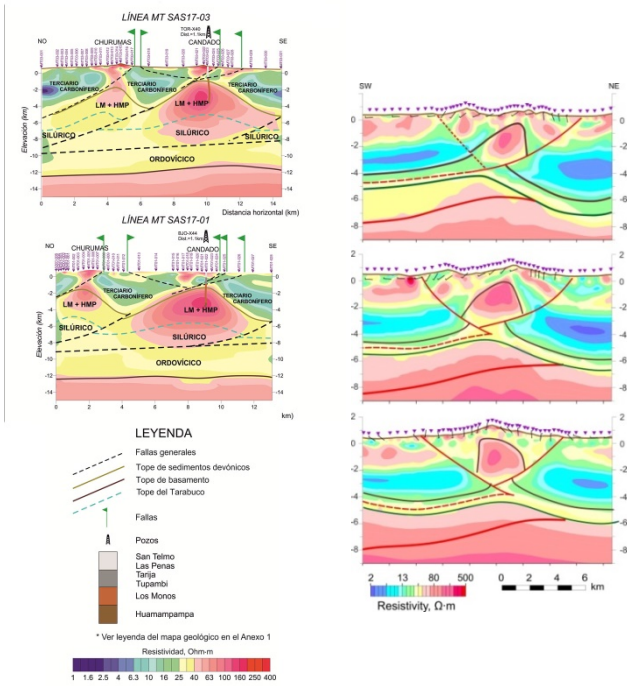

Figure 7. Examples of resistivity images interpretation. SAS – left panel, SAN – right panel

In Subandino Sur survey area a systematic southwest - northwest shift between the uppermost structural level and the underlying Devonian structures was outlined (tectonic discordance) (see Figure 7). Detailed resistivity images of buried Devonian structures with HC prospects were constructed (see Figure 8).

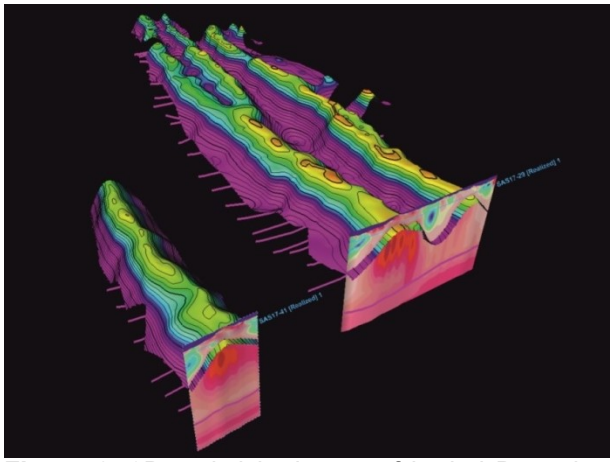

Figure 8. 3D resistivity image of buried Devonian anticlines.

CONCLUSIONS

The results of MT joint interpretation along with seismic and logging data give important structural constrains, especially at the core of anticlines. Several decollements were confirmed. New targets (already delineated with seismic) were outlined and confirmed with MT.

Magnetotellurics is an effective technology to delineate resistivity contrasts in areas where seismic is faced with problems, i.e. in the Subandean fold belt and other similar geological provinces.

ACKNOWLEDGEMENTS

Authors are grateful to Yacimientos Petrolíferos Fiscales Bolivianos (YPFB) for giving permission to present the results of SAN and SAS projects and fruitful discussions during the report preparation. The research was funded by “Nord-West Ltd” and by FASO Russia (theme No. 0149-2018-0005).

REFERENCES

Baby, P., I. Moretti, B. Guillier, R. Lima&i, E. Mendez, J. Oller, and M. Specht (1995), Petroleum system of the northern and central Bolivian sub-Andean zone, in A. J.Tankard, R. Sukrez S., and H. J. Welsink, Petroleum basins of South America: AAPG Memoir 62, p. 445-458.

Baby, P., Rochat, P., Mascle, G. and Hérail, G. (1997), Neogene thrust geometry and crustal balancing in the northern and southern branches of the Bolivian Orocline (central Andes), Geology 25;883-886 doi: 10.1130/0091-7613

Epishkin D (2018), Development of data processing methods for magnetotellurics PhD thesis, Moscow State University, Moscow.

Zubieta, D. (2008), El sistema petrolero paleozoico Subandino Norte nordeste be Bolovia, VII Congreso de Exploración y Desarrollo de Hidrocarburos (Simposio de Sistemas Petroleros de las Cuencas Andinas).

Magnetotelluric study on a diapir in Qom basin, central Iran

B. Oskooi[1,4], M. Moradi[2] and P. Pushkarev[3]
[1]Associate professor, Institute of Geophysics, University of Tehran, boskooi@ut.ac.ir
[2]PhD. Student, Institute of Geophysics, University of Tehran, m.morady@ut.ac.ir
[3]Associate professor at Lomonosov Moscow State University, pavel_pushkarev@list.ru
[4]Guest researcher, Division of Geosciences and Environmental Engineering of the Department of Civil, Environmental and Natural Resources Engineering, Luleå University of Technology, Luleå, Sweden.

SUMMARY

Diapirs are used as liquid or gas storage because salt formations are considered to be extremely impermeable and non-reactive geological structures. Shurab diapirs located at NW of Kashan in Qom basin of central Iran are candidates for gas storage. They belong to a group of diapirs that have pierced to the surface. A previous 2D seismic survey across the diapir No. 4 from Shurab diapirs could not resolve the geology and tectonic structure of the diapir due to the complexity of the formation and sharp variations of the wave velocity in the top part of the diapir. Magnetotelluric (MT) data in a cooperative inversion scheme with geological and seismic information resolve the structure quite well. We used NLCG algorithm and mainly REBOCC to invert TE and TM modes data simultaneously by putting more weight on TE mode data of course. The study shows a clear image of the salt body in agreement with the geological information from resistivity and density logs of boreholes as well as the previous seismic results. MT data result in a better resolution of the flanks and overhangs of the salt compared with the seismic data. From MT data we could also detect the Sen-Sen fault in the Eastern part of the diapir No. 4 which attributes its critical role to push the salt body up to a great extent.

Keywords: Diapir, magnetotelluric, Qom basin, seismic and 2D inversion.

INTRODUCTION

Application of salt diapirs in the liquid or gas storage has been documented since the first investigation in Canada in the early 1940s, during World War II (Bays 1963). Salt formations are extremely strong, impermeable and non-reactive geological structures. The impermeability of the salt arises from tightness of its structure and the absence of open natural joints and fissures.

Moreover, flowing liquid and gas through open artificial fractures is hindered by high plastic deformability of salt rock. Also, salt formation itself is not subject to changes due to environmental changes outside of the formation structure.

The factors that determine whether or not a reservoir or salt cavern storage facility will make a suitable storage facility are both geological and geographical (Baikpour et al. 2016).

A salt structure at the NW of Kashan is investigated for the purpose of gas storage. The structure belongs to a group of diapirs so called Shurab diapirs (SD), that have pierced the ground surface. Dome no. 4 is partly marked by a group of hillocks and was firstly investigated by a 2D seismic survey. Figure 1b and c show the SD and especially the dome No.4.

The weakness of the seismics to provide a clear image of salt structure, gave rise to further exploration on the structure in more detail by the magnetotelluric (MT) method. So we expect that resistivity contrast between the salt body and surrounding sediments makes MT as an applicable tool for mapping geological and tectonic of salt dome No. 4.

In this paper we try to find the correlation between tectonic, geology and geophysical results. So, in the following we introduce geology and tectonics of SD and then show the inversion result of the MT data and discuss on integrated interpretation of the MT data and seismic results.

GEOLOGY AND TECTONIC

The area of investigation is located in the transition zone between the structural units of the central Iran (CI) and the Sanandaj-Sirjan zone (SSZ), which shows similarities and is bordering the Zagros zone (Figure1a).

Extensive volcanic activity occurred during the Eocene. The main tectonic influence resulted from the Arabian plate and Eurasian plate collision in Oligocene-Miocene. It caused subduction below the southern margin of CI. The Early Miocene volcanic arc of CI is related to this seduction (Amirbehboudi et al. 2015). The Qom Basin at the southern edge of CI is considered as a back-arc basin before the collision happened.

Volcanic rocks (Eocene), Lower Red (Oligocene),

Qom (Oligo-Miocene) and Upper Red (Mi-ocene) are the main formations in the area of study (Figure 2).
The tectonic system which is most probably responsible for the main development of the Shurab group of salt diapirs is also a dextral (right -lateral) strike slip fault system. It is forming compressive pop-up or push-up structures, where the salt piercement took place. Whereas this fault system is mainly responsible for the development of the salt diapirs, the basin development is related to a local extension zone, which may be responsible for having initiated the pillow stage of the salt diapirs (Figure 1c).
Additionally a movement along faults or piercing into faulted areas may play an important role. The schematic drawing of strike slip step over situations can directly be applied to the main NW-SE trending strike slip zone (Principal Displacement Zone(PDZ)) in the greater area of the Shurab diapirs (Figure 1d).

METHODS

Simultaneous variations of the natural electromagnetic field in the two horizontal electric $(\mathrm{E_x}, \mathrm{E_y})$ and three magnetic $(\mathrm{H_x}, \mathrm{H_y}, \mathrm{H_z})$ directions are measured as s function of time. After transformation into the frequency domain the impedance tensor, $\mathrm{Z} = \begin{bmatrix} \mathrm{Z_{xx}} & \mathrm{Z_{xy}} \\ \mathrm{Z_{yx}} & \mathrm{Z_{yy}} \end{bmatrix}$ and tipper vector, (A, B) connecting the measured fields in the frequency domain for a given frequency, can be estimated.

$$\begin{bmatrix} \mathrm{E_x} \\ \mathrm{E_y} \\ \mathrm{H_z} \end{bmatrix} = \begin{bmatrix} \mathrm{Z_{xx}} & \mathrm{Z_{xy}} \\ \mathrm{Z_{yx}} & \mathrm{Z_{yy}} \\ \mathrm{A} & \mathrm{B} \end{bmatrix} \begin{bmatrix} \mathrm{H_x} \\ \mathrm{H_y} \end{bmatrix} \quad (1)$$

The estimated impedance data are represented as apparent resistivity ρ_{ai} and phase, φ_i, according to the following relations

$$\rho_{ai} = \frac{1}{\mu_0 \omega} |Z_i|^2 \quad (2)$$

$$\varphi_i = phase(Z_i) \quad (3)$$

Where i=xx,xy,yx,yy and μ_0 the magnetic permeability of free space (Oskooi et al 2014). The apparent resistivity and phase curves can then be inverted to estimate geoelectrical resistivity models via inversion schemes.
There are different inversion algorithms for 2D inversion of MT data. Among all REBOCC algorithm and Mode-EM have potential to add geological information as a model-covariance matrix in the inversion process. Whereas, Non-linear Conjugate Gradient (NLCG) algorithm provides results with more details.
In this paper we use both REBOCC and NLCG algorithms to add geological information and seismic results to the inversion process.
In the inversion process we use both TE and TM modes data with greater weight on TE mode as it has a potential to resolve deep resistive structures (Berdichevsky and Dmitriev 2008).

RESULTS

The results after adding geological and seismic information to the inversion process is shown in Figure 3a. From surface to the depth of 3 Km, Quaternary sediments, Upper Red, Qom and Lower Red formations and salt body are differentiated. Resistivity contrast between salt and Eocene volcanic rocks is not sharp enough to be detected by MT. Resistivity and density logs and geological information from depth of 400 m to 900 m is shown in Figure 3b. Resistivity value in MT section is exceeded to more than 5000 ohmm in salt due to cavities in the upper part of the diapir. Sharp variation in the resistivity and density logs is due to those cavities. The eastern and western parts of the diapir No. 4 is separated by faults. Among them, Sen-Sen fault plays more efficient role to pushing the salt up.
In order to compare geology, seismic and MT results, all information including geology, resistivity and post stack depth migration (PSDM) section are coincided and shown in a 3D view (Figure 4). Seismic section could not resolve diapir structure because the velocity contrast between salt and surrounding sedimentary layers is extremely high. But MT data provides accurate information of salt body especially at the top of the diapir. Also, MT is shown a good agreement between geology, tectonic and seismic results.

CONCLUSIONS

Salt diapirs are used as liquid or gas storage because salt formations are extremely impermeable and non-reactive geological structures. Shurab Diapirs located at the NW of Kashan is condidated as a gas storage. Dome no. 4 is partly marked by a group of hillocks and was firstly investigated by old 2D seismic line. Seismic results were with poor quality ,especially at the top of the diapir no. 4 due to the complex geological structure of the diapr. MT data reslove geological and tectonic of the salt body much better.
In order to add additional information to the inversion we use a cooperative inversion sheme by REBOCC (Siripunvaraporn and Egbert 2000) and NLCG (Rodi and Mackie 2001) algorithms. So, geological information and seismic reflectors in

PSDM section are added as the starting model and a priori model, respectively, in REBOCC. Then, inversion model from the previous stage is used as a starting model in the NLCG algorithm. In this stage, inversion is done with more weight on the TE mode data as it is more sensitive to the deep resistive structures.

Results show good aggrements with the regional tectonic, resistivity and density logs and geological inforation from the well. Schematic diagram of tectonic actvity in study area is compared with MT data and show that Sen-Sen Fault has a critical role in lifting the diapir.

ACKNOWLEDGEMENTS

This work was originally funded by the research council of the University of Tehran. We thank the National Gas Storage Company for supplying the geophysical data which were collected by the Russian North West company. We are also grateful to the Zamin Ab Pey company for supplying the hardwares and softwares as well as logistical support when we prepared and analysed the data. The Nord West group is also acknowledged for the scientific advice.

REFERENCES

Amirbehboudi, C. et al. (2015) UGS Phase 1 Development Plan of the Nasrabad-e-Kashan Salt Structural Model. DGC-Technical Report (Rev.1) submitted in January 2015

Baikpour S, Motiei H and Najafzadeh K (2016) Geological and geophysical study of salt diapirs for hazardous waste disposal. Int. J. Environ. Sci. Technol.
doi: 10.1007/s13762-016-1036-x

Bays CA (1963) Use of salt solution cavities for underground storage. In: Symposium on Salt, Northern Ohio Geological Society, 564

Berdichevsky M N and Dimitriev V I (2008) The interpretation model In: Models and methods of magnetotellurics.Springer, pp 383-452

Oskooi B, Pedersen L B and Koyi H A (2014) A Magnetotelluric signature for the Zagros collision. Geophysical Journal International,196, Issue 3: 1299–1310

Rodi W and Mackie R L (2001) Nonlinear conjugate gradients algorithm for 2D magnetotelluric inversion. Geophysics, 66: 174 – 178

Siripunvaraporn W and Egbert G, (2000) An efficient data-subspace inversion method for 2-D magnetotelluric data, Geophysics, 65: 791-803

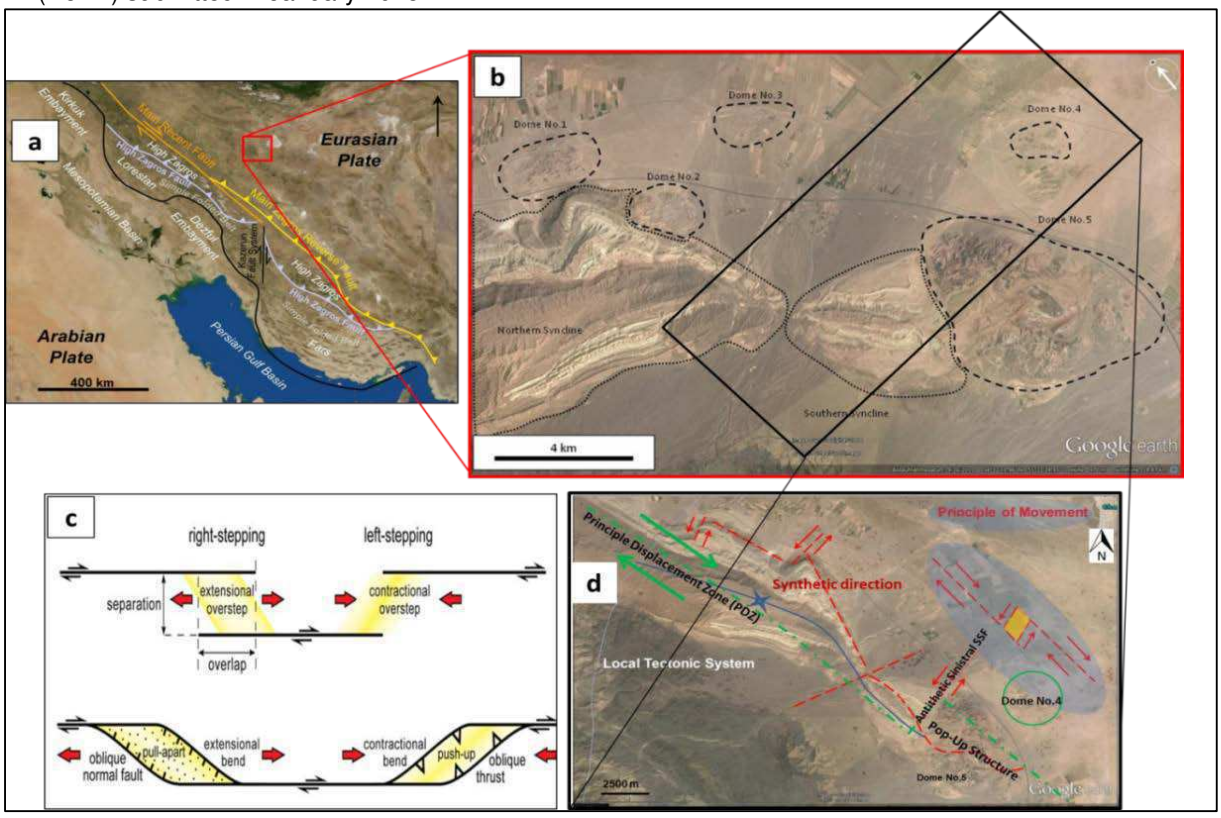

Figure 1. a) Study area on tectonic map of Iran, **b)** Shurab Diapirs No. 1 to 5, **c)** schematic diagram of strike slip faults that is responsible for push-up or pop-pull structures and **d)** map of faults on satellite picture.

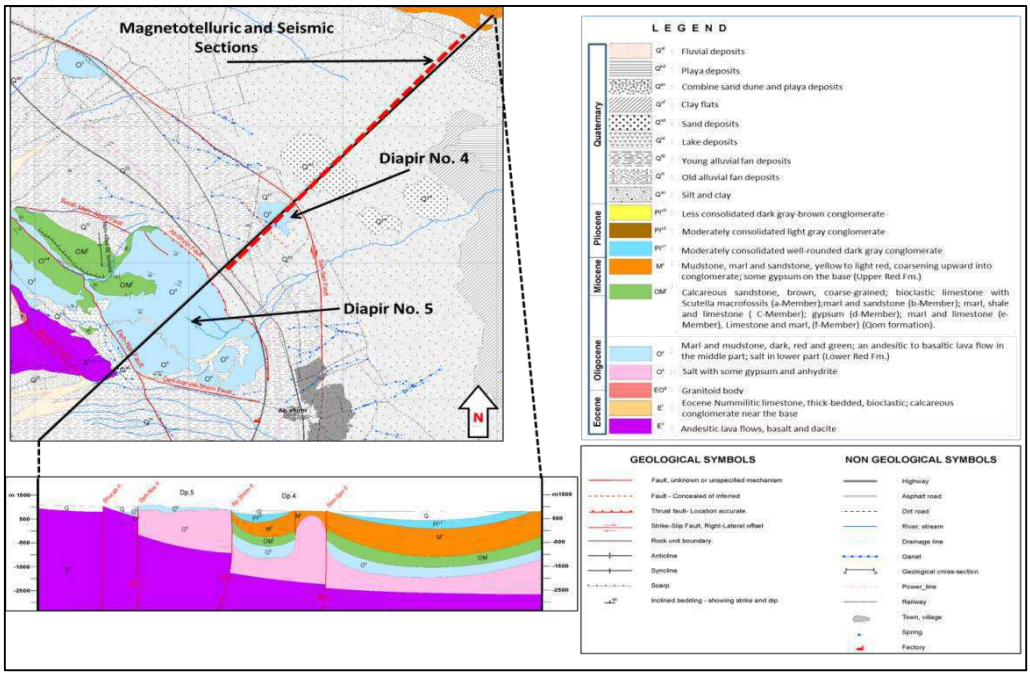

Figure 2. Geology map and section of study area. Location of 2D seismic and MT profile is located with dashed red line.

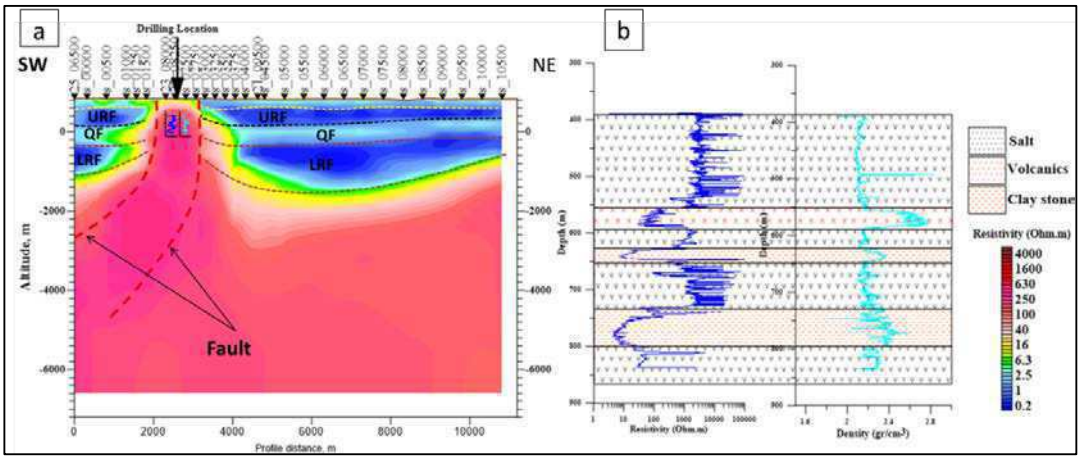

Figure 3. a) 2D inversion result after combination of geological information and seismic results and **b**) resistivity and density log at drilling location from 400 to 900 m with geological information from well.

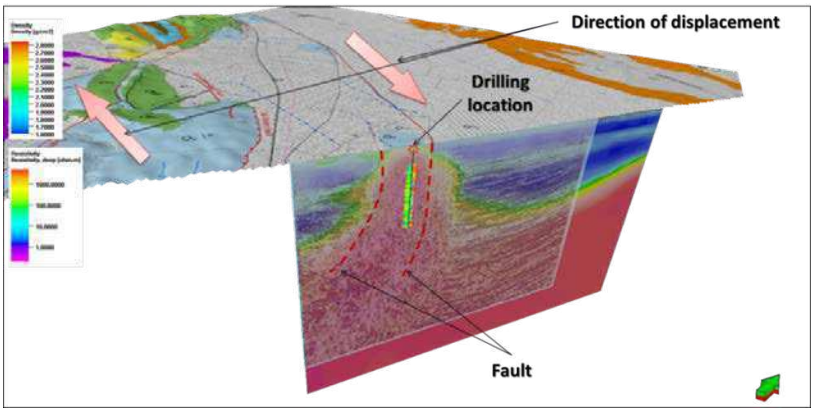

Figure 4. Comparison between tectonic, Geology, seismic and resistivity and density logs across diapir No.4.

Mineral systems mapping using magnetotellurics: Examples from Canada and Australia

A.G. Jones[1,3], S. Thiel[2], K. Robertson[2], M. Dentith[3], G. Heinson[4], J.A. Craven[5]
[1]Complete MT Solutions Inc., Ottawa, Canada, alan.jones@complete-mt-solutions.com
[2]Geological Survey of South Australia, Adelaide, Australia
[3]University of Western Australia, Perth, Australia
[4]University of Adelaide, Adelaide, Australia
[5]Geological Survey of Canada, Ottawa, Canada

SUMMARY

Increasingly the search for world-class deposits is using the mineral system concept as a framework to identify the most prospective terrains within which to explore. An important implication of this concept for geophysics is that, in addition to the well-established approach of seeking responses from targets that comprise the immediate mineralised environment, a whole set of new targets are presented. These include source zones for metals and/or metal-bearing fluids (brines or magmas) and also the conduits through which these fluids passed, both before and after precipitation of the deposit-forming metals. Alternatively, geophysics can map lithospheric structures to identify regions likely to concentrate fluid flow.

Electrical conductivity is highly sensitive to a very minor (<1%) content of interconnected low resistivity minerals, and these mineral system processes will alter the electrical properties of the crust and mantle. Electromagnetic imaging, using the natural-source magnetotelluric (MT) technique, maps the spatial variations in electrical conductivity. Given the inherent scalability of MT, zones can be mapped from the near surface to deep in the lithospheric mantle. Thus, MT offers the greatest tool in the geophysical arsenal for mapping mineral systems at all scales.

We will give examples of the application of MT for mineral systems mapping. In Canada the Yellowknife Fault Zone, mapped during Lithoprobe, lies directly above a crust/upper mantle diffuse region of reduced resistivity, suggesting flow through a generally increased permeability region rather than along defined fault zones. Diamondiferous kimberlites in multiple localities across Canada are the correlated with enhanced conductivity in the mantle. Insights from AusLAMP and subsequent infill surveys across the Gawler Craton shows there exists good correlation between conductive zones interpreted as lithospheric scale conduits and expressions of mineral systems in the upper crust. In Western Australia MT has mapped major faults and terrain boundaries, which were probable foci of fluid flow.

Modelling and monitoring induced electric fields (IEFs) in Ireland and the UK for space weather applications

J. Campanyà[1], P.T. Gallagher[1], S.P. Blake[1], M. Gibbs[2], D. Jackson[2], C. Beggan[3], G.S. Richardson[3], C. Hogg[4]

[1] School of Physics, Trinity College Dublin, Dublin, Ireland, joan.campanya@tcd.ie
[2] Met Office, Exeter, UK
[3] British Geological Survey, Edinburgh, UK
[4]Dublin Institute for Advanced Studies, Dublin, Ireland

SUMMARY

Induced electric fields (IEFs) at the Earth's surface caused by geomagnetic storms are a natural hazard that have the potential to disrupt and damage ground-based infrastructures such as electrical power distribution networks, pipelines, and railways. In this study we evaluated the possibilities for modelling and monitoring IEFs in Ireland and the UK caused by geomagnetic storms.

Magnetic time series from the magnetic observatories and local and inter-station electromagnetic tensor relationships were used to model the IEFs at several locations in Ireland and the UK, including locations where no measurements were performed during the geomagnetic storms. Coherence values between 0.5 and 0.95, and signal-to-noise ratio between 1 dB and 15 dB were observed when modelling IEFs. Within these ranges of values, the accuracy at modelling IEFs was controlled by the influence of local geomagnetic sources, and by the distance of the site of interest to the closest magnetic observatory.

The modelling approach for modelling IEFs was then used to create a database with IEFs including large geomagnetic storms. Magnetic field data measured at permanent magnetic observatories, IEFs measured at Eskdalemuir (ESK), Lerwick (LER), and Hartland (HAD) magnetic observatories since 2012, and modelled IEFs were used to train several machine learning techniques for monitoring IEFs in Ireland and the UK. Differences between measured and both modelled and monitored IEFs were quantified using the correlation coefficient, the performance parameter, and root-mean-square error.

Keywords: Induced Electric Fields, Geomagnetic storms, Space Weather, Machine Learning

Modelling geomagnetically induced electric fields using a 3-D electrical conductivity model and AusLAMP data

L.Wang[1], G. Paskos[1], J. Duan[1], A. Lewis[1], T. Kemp[1], W. Jones[1]

[1]Geoscience Australia, GPO Box 378 Canberra Australia, liejun.wang@ga.gov.au

SUMMARY

Geomagnetically induced currents (GICs) in the Earth surface and interior are caused by geomagnetic storms and other natural field variations. GICs in the Australian region are distorted by conductivity contrasts caused by oceans, geology and enhanced crustal conductivity structures.

This study provided a regional indicator of geomagnetic induction hazards across Australia by modelling the distribution of induced surface electric field using a continental-scale 3-D electrical conductivity model of Australia. The model includes broad electrical structures of the oceans, resistive cratons, sedimentary basins and enhanced conductivity anomalies beneath the continent. The amplitude and orientation of the induced electric field at periods of 360 s and 1800 s are presented and compared to those derived from a simplified ocean-continent electrical conductivity model.

In Australia, the geophysical step of GICs modelling commonly involves calculating induced electric fields based on geomagnetic field data from the closest geomagnetic observatory and then applying the “plane wave” approach on 1-D electrical conductivity models. A 1-D model provides a useful first-order approximation for the effect on surface electric field, but the Australian continent’s internal structure has a complex three-dimensional distribution of electrical resistivity, which affects the electric field and can change the predicted values by up to a factor of 4 in some places when compared to 1-D modeling.

We developed a telluric field prediction system by using the Geoscience Australia geomagnetic observatory network and data from the Australian Lithospheric Architecture Magnetotelluric Project (AusLAMP). The AusLAMP data allows comparison between the observed telluric field and the predicted telluric field using a half-space, local 1-D models or 3-D telluric tensors based on the first available continental-scale 3D electrical conductivity model. Our study, made using MT tensors derived from 3-D modelling of an electrical conductivity model, shows the estimation method based on 1-D assumptions may be valid in central and southeast Australia where electric fields are less distorted, but will lead to inaccurate GIC estimates in Western Australia, some inland areas, and coastal areas. Estimation of the geomagnetically induced electric fields across the Australian continent requires detailed modeling of the 3-D lithospheric conductivity structure using AusLAMP data.

Keywords: Geomagnetic Induction Hazards; Geomagnetically induced fields, 3-D modelling, Australian Continent ; AusLAMP.

Monitoring hydraulic stimulation using telluric sounding

N. Rees[1], G. Heinson[2] and D. Conway[3]
[1]The Australian National University, nigel.rees@anu.edu.au
[2]The University of Adelaide, graham.heinson@adelaide.edu.au
[3]The University of Adelaide, dennis.conway@adelaide.edu.au

SUMMARY

We present our findings from *Rees, N., Heinson, G. and Conway, D., 2018. Monitoring hydraulic stimulation using telluric sounding. Earth, Planets and Space, 70(1), p.7.*

The telluric sounding (TS) method is introduced as a potential tool for monitoring hydraulic fracturing at depth. The advantage of this technique is that it utilises the measurement of electric fields only, which are cheap and easy to measure when compared with magnetotelluric measurements. Additionally, the transfer function between electric fields from two locations is essentially the identity matrix for a 1D Earth no matter what the vertical structure. Therefore, changes in the earth resulting from the introduction of conductive bodies underneath one of these sites can be associated with deviations away from the identity matrix, with static shift appearing as a galvanic multiplier at all periods.

We test the viability of the TS method for monitoring hydraulic stimulation on both a synthetic dataset and a case study of an enhanced geothermal system conducted in Paralana, South Australia. The synthetic data example shows small but consistent changes in the transfer functions associated with hydraulic stimulation, with grids of Mohr circles introduced as a useful diagnostic tool for visualising the extent of fluid movement. The Paralana electric field data were relatively noisy and affected by the dead band making the analysis of transfer functions difficult. However, changes in the order of 5% were observed from 5 s to longer periods. We conclude that deep monitoring using the TS method is marginal at depths in the order of 4 km and that in order to have meaningful interpretations, electric field data need to be of a high quality with low levels of site noise.

Keywords: Telluric sounding – Hydraulic stimulation – Monitoring – Transfer functions

MT study of La Rosa diapir (Betic Range, SE Spain)

Estefanía Górriz [1]; Alex Marcuello*[1]; Juanjo Ledo[1], Pilar Queralt[1], Anna Martí[1], Lluís Rivero[2], Frederic Escosa[1] and Eduard Roca[1]

[1]Geomodels, Dept. of Earth and Ocean Dynamics, University of Barcelona, alex.marcuello@ub.edu
[2]Dept. Mineralogy, Petrology and Applied Geology, University of Barcelona

SUMMARY

In Salt Tectonics, the MT technique appears as an adequate tool to characterize the saline structures. It takes advantage of both the high resistivity contrast between the salt bodies and the host media, and the typical depths of interest up to few km.

The main tectonic structure in the SE of the Iberian Peninsula is the Betic range, and several saline structures are common in the northern flank of the Inner Prebetic Front. These bodies are aligned along a WSW-ENE direction, and in some places, they crop out as diapirs. One of these diapirs is the La Rosa one, which shows an NW-trending elongated shape and is the most productive exploitation in the region, but nowadays its size and origin are not well understood.

In this work, we present the results obtained from an MT survey implemented to study this area. It consisted of 54 sites in the frequency range of 1000-0.1 Hz. The presence of a power line of 400 kV crossing the area of study has been a challenge for the data processing and analysis, and here we include the workflow used. The 3D model has been obtained with the ModEM code and it also contains 32 vintage VES acquired in the surrounding area by early 90's. The model shows an EW trending resistive body below the diapir, but extending beyond the limits observed on the surface. It is interpreted as the salt body related with the diapir. This interpretation is supported by the results of a gravity survey also performed there. It displays a negative gravity anomaly trending EW in the same place that the imagined resistive body, and its associated with a low-density body in the gravity model. The integration of these two 3D models is also presented here.

MT survey in the northern part of Subandian fold belt, Bolivia

N. Palshin[1,2], R. E. Giraudo[3], D. Yakovlev[2], R. Zaltsman[2] and S. Korbutiak[2]
[1]Shirshov Institute of oceanology, RAS, palshin@ocean.ru
[2]Nord-West Ltd, mail@nw-geophysics.com
[3]YPFB Corporación, rgiraudo@ypfb.gob.bo

SUMMARY

MT survey was carried out in the northern part of Subandian fold belt (Subandino Norte), Bolivia. Despite the geological and geophysical studies carried out in the area and several exploratory wells, no commercial hydrocarbon deposits have been discovered, although on the basis of geological and geophysical studies and known oil and gas fields in Madre de Dios basin, the hydrocarbon potential of this basin was estimated as high. The survey was aimed at better understanding of complicated geological structure and petroleum system of the area. Broadband MT data were acquired along 16 profiles at 1392 sites. Dimensionality analysis showed that impedances are close to 2D: no rotation or transformations of transfer functions were applied. Combined static shift correction procedure, which includes both spatial averaging and TDEM based correction, was developed and successfully applied. Unconstrained and constrained bimodal 2D OCCAM inversion was used for constructing resistivity images along profiles. All MT acquisition profiles followed seismic ones, thus geological interpretation was based both on seismic sections and resistivity images using logging data as additional constraints. Good coincidence of resistivity images with seismic sections are clearly seen in synclines, while in anticline's cores the resolution of resistivity images is better that seismic ones. A big number of faults parallel to geological strike were outlined in anticlines, thus the whole survey area is divided into two parts by system of oblique faults. A two level resistivity structure was revealed: the upper structural level is characterized by pop-up and palm tree structures, while the lower level is characterized by duplex structures. A map of the depth to Devonian formations (main source rocks) was constructed.

Keywords: magnetotellurics, 2D inversion, joint interpretation, hydrocarbon prospecting, Subandian fold belt

MT survey in the southern part of Subandian fold belt, Bolivia

N. Palshin[1,2], R. E. Giraudo[3], D. Yakovlev[2], R. Zaltsman[2] and S. Korbutiak[2]
[1]Shirshov Institute of oceanology, RAS, palshin@ocean.ru
[2]Nord-West Ltd, mail@nw-geophysics.com
[3]YPFB Corporación, rgiraudo@ypfb.gob.bo

SUMMARY

MT survey was carried out in the southern part of Subandian fold belt (Subandino Sur), Bolivia. Subandino Sur is a main oil and gas producing region in Bolivia. The survey was aimed at better understanding of complicated geological structure and petroleum system of the fold and thrust belt. Broadband MT data were acquired along 41 profiles at 2229 sites. Dimensionality analysis showed that impedances were close to 2D: no rotation or transformations of transfer functions were applied. Combined static shift correction procedure, which includes both spatial averaging and TDEM based correction, was developed and successfully applied. Practically all MT acquisition profiles coincide with seismic ones, thus geological interpretation was based both on seismic sections and resistivity images using logging data as additional constraints. Good coincidence of resistivity images with seismic sections are clearly seen in synclines, while in anticline's cores the resolution of resistivity images is better that seismic ones. A systematic southwest - northwest shift between the uppermost structural level and underlying Devonian structures was outlined (tectonic discordance). Detailed resistivity images of buried Devonian structures (anticlines) with HC prospects were constructed.

Keywords: magnetotellurics, joint interpretation, hydrocarbon prospecting, Subandian fold belt

Multi-physical characterization of near-coastal cryosphere onshore Spitsbergen, Arctic Norway

P. Betlem[1,2], and K. Senger[2]
[1]Iceland School of Energy, Reykjavik University, peterb@unis.no
[2]Department of Arctic Geology, University Centre in Svalbard, kims@unis.no

SUMMARY

The Arctic archipelago of Svalbard forms the northwestern corner of the Barents shelf. Glaciers cover roughly two-thirds of Svalbard's landmass, with the remaining area strongly affected by continuous permafrost. An active petroleum system is manifested onshore Svalbard by numerous gas seeps and gas accumulations beneath permafrost and favourable source rock intervals. Detailed knowledge about the dynamic state, extent and sealing properties of permafrost is currently lacking. The remote Arctic environment is suitable for efficiently conducting geophysical data acquisition on snow-covered ground with minimal environmental impact. Electromagnetic (EM) data has only been acquired within the past decade to provide constrains on, amongst others, the permafrost thickness and internal permafrost variability (e.g., ice content). Geophysically, permafrost is characterized by both high sonic velocity and resistivity, and relatively low dielectric permittivity. Permafrost in coastal proximity is affected not only by surface temperatures and heat flux, but also by thermal trends associated with large bodies of water. The near-coastal zones are especially important considering that thinning of permafrost towards the shoreline may enable sub-permafrost fluid migration towards the surface. Limited data exist on the occurrence of such migration pathways. We here present an integrated electrical resistivity tomography (ERT) and ground penetrating radar (GPR) study targeting permafrost response to coastal proximity at three distinct study areas onshore Spitsbergen.

Two-dimensional ERT profiles were acquired at Elveneset, Colesbay, and Festningen in August 2017. Roll-a-long Wenner surveying relied on four LUND multiconductor cables in conjunction with an ABEM Terrameter SAS 1000/4000 ERT instrument powered by an external battery. At each site a main profile of ca. 600 m was recorded perpendicular, and supplemented by two sections of 400 m parallel to the shoreline. For enhanced resolution, electrode spacing was halved to 5 m in near-shoreline proximity (<200 m). Both I.P. and resistivity were measured for the entirety of the lines. Pre-processing of the datasets consisted of outlier removal and linear regression analysis. ProfileR inversion code distributed with ZondRes2D, version 5.2, was applied to the processed dataset.

At Elveneset, a highly resistive band (>35 kOhmm), that we interpret as permafrost, from ca. 1 to 15 m deep is observed starting ca. 50 m away from the shoreline. Thickening to more than 25 m occurs ca. 325 m into the profile, with the increased thickness likely a result of elevation changes and coastal distance. At Colesbay, a similar but less intense trend is observed from ca. 150 m. The Colesbay model features a more pronounced active layer, and indicates a significant increase in thickness (50 m) at a distance 500 m away from the coast. Festningen is characterized by the absence of highly resistive bands, but in turn features discontinuous, shallow and deep pockets of high resistivity, possibly linked to local geology. The vertical bedrock layering at Festningen allows us to correlate the near-surface EM acquisition with the resistivity signature of relevant exploration wells onshore Spitsbergen which have penetrated the same stratigraphy.

The ERT interpretation was aided by ca. 50 km of 2D GPR profiles at each site, acquired using a Malå GPR unit with 25 MHz and 50 MHz snake antennas on snow-covered ground in April 2017. The presence of saline aquifers and saline seawater intrusions has likely impacted the data acquisition, but fails to explain the significant differences between the sites. A discontinuous and thinning permafrost state up to almost a kilometer away from the shoreline is an important observation, not least for gaining a better understanding of the onshore release points of Svalbard's active petroleum system. Similar to the seeps in the fjords, gas may be released from the subsurface through these coastal areas of weak seal capacity and enhanced permeability, and directly escapes to the atmosphere.

Keywords: Svalbard, permafrost, EM, ERT, GPR

Northern Australian lithospheric architecture from AusLAMP

J. Duan, A. Kirkby, D. Kyi and W. Jiang
Geoscience Australia, Jingming.Duan@ga.gov.au

SUMMARY

New datasets have been collected under Geoscience Australia's Exploring for the Future program (EFTF) in an under-explored part of northern Australia. The aim is to characterize the geology of this part of the tectonic plate from the surface down to the base of the lithosphere through multidisciplinary data collection and synthesis. The new datasets will provide pre-competitive data and knowledge for attracting exploration and reducing exploration risk.

This presentation will describe new datasets collected between Tennant Creek in the Northern Territory and Mount Isa in Queensland, a survey area of 700 km x 800 km, as part of the Airborne Electromagnetic survey (AusAEM) and the Australian Lithospheric Architecture Magnetotelluric Project (AusLAMP). Data from a total of 180 new AusLAMP sites have been acquired in this region as part of Geoscience Australia's EFTF program.

This presentation will show these new data and associated models from the survey area. Results from the data provide new insights on the lithospheric architecture and mineralisation in the region. The magnetotelluric inversion models show a crust/mantle-scale conductivity anomaly interpreted to be part of the Carpentaria Conductivity Anomaly, which is a major deep electrical conductivity structure across Queensland. The models also show some crustal conductivity anomalies aligning with major crustal boundaries. Those boundaries are considered to be important factors for mineralisation in the region, with some known mineral deposits occurring at the margin of these conductivity anomalies.

Keywords: Magnetotelluric, EFTF, AusLAMP, Architecture, Mineral

On the application of the controlled source radiomagnetotellurics (CSRMT) for near surface exploration

B.Tezkan[1], I. Muttaqien[1], A. Saraev[2]
[1]Institute of Geophysics and Meteorology, University of Cologne, Germany
[2]Institute of Earth Sciences, St. Petersburg State University, Russia

SUMMARY

Conventional radiomagnetotelluric method (RMT) does not need an active transmitter due to the use of the EM-field of the existing radio transmitters near the survey area. Therefore, it is logistically simple and enables spatial measurements on the survey area in a short time. However, the method has a big disadvantage: there exist no radio transmitters below 10 kHz. Therefore, the penetration depth is limited. In addition, there may be no sufficient transmitter if a RMT survey will be conducted in a remote area.
An alternative solution is to build a transmitter to create the electromagnetic field instead of using the field of existing radio transmitters in the vicinity of the survey area (CSRMT method). A rectangular signal with base frequencies between 0.1 kHz and 150 kHz is injected through a grounded electric dipole. Electric and magnetic field components are observed at these frequencies and at their subharmonics, so that apparent resistivities and phases are observed in a broad frequency range between 1 kHz and 1000 kHz. Inline or broadside configuration can be used. A scalar CSRMT survey was carried out on the buried faults north of St. Petersburg to test the applicability of this method to the mapping of near-surface faults. A 700 m electric dipole with base frequencies of 0.5, 11.3, 30 and 105 kHz was used as a transmitter. Smooth apparent resistivity and phase values as a function of frequency from 1 kHz to 1 MHz were observed in the far field zone for the inline configuration at 57 stations by using a station distance of 20 m. The observed apparent resistivity and phase TM-mode data were interpreted using the 2D inversion algorithm, and a good data fitting could be obtained. The resistivity structure beneath the survey area (down to a depth of 80 m) could be derived and the buried faults could be mapped successfully. An excellent correlation of observed RMT and CSRMT transfer functions and 2D conductivity models was achieved.

Overview and preliminary results of magnetotelluric study of the Kasane hotspring region in northwest Botswana.

Calistus D. Ramotoroko[1], Andreas Junge[2] and Elisha Shemang[1]
[1] Department of Earth & Environmental Sciences, Botswana International University of Science & Technology,
[2] Facheinheit Geophysik, Goethe-Universität.

SUMMARY

Kasane is a famous tourist destination in Botswana. Its pleasant climate especially in spring and summer seasons is always worthy for most visitors and residents. Kasane hot spring at the meeting point of four countries – Botswana, Zambia, Namibia and Zimbabwe, with temperature of 43.5 ºC is the only known hot spring which exits in Botswana. It lies at about 145 m south of the Chobe River, northwest Botswana. There are no scientific studies on Kasane hot spring and we do not know of the existence of other hot springs in the area. This research is the first detailed research on hot springs in Botswana and an ongoing effort started early 2018 with the goal of developing a conceptual model for the Kasane geothermal hotspring based on the conductivity distribution at depth. Together with additional geological and geochemical studies, the magnetotelluric results are used to infer a comprehensive understanding about the Kasane geothermal hotspring, particularly about the reservoir and the heat source.
The data is acquired by a mixture of Phoenix and Metronix MT systems at various sample rates for approximately 12 hrs. The acquired MT time-series data are processed using industry standard processing software. After data processing, the modelling is performed with a combination of COMSOL Multiphysics and MATLAB through a LiveLink connection. Also, Egbert's (2012) ModEM code and Mackie's (2012) magnetotelluric inversion code are used for the 3-D inversion of the MT responses. The 3-D modelling results are compared and we evaluate the differences between the two 3-D resistivity models and discuss the implications any differences and similarities have for the definition of the geothermal reservoir and resource.

Keywords: Magnetotelluric, Kasane, northwest Botswana, Hotspring, Geothermal

Pseudo-3D direct current resistivity for underground water surveying

Zhenwei Guo[1,2,3], Chunming Liu[1,2,3*], Jianxin Liu[1,2,3], Hua Zhou[4], Shuaijun Zhao[5,6], Haibing Li[5]
1,Key Laboratory of Metallogenic Prediction of Nonferrous Metals and Geological Environment Moni-toring （Central South University), Ministry of Education, Changsha 410083, China
2,Hunan Key Laboratory of Nonferrous Resources and Geological Hazard Exploration, Changsha 410083, China
3, Bureau of Geology & Mineral Exploration and Development of Hunan 402 Team, Changsha, 410004, China
4,School of Geosciences and Info-physics, Central South University, Changsha, 410083, China
5,Geological Environment Monitoring Station of Hunan Province, Changsha, 410007, China
6,School of environmental studies, China University of Geosciences, Wuhan, 430074, China

*Corresponding Author
guozhenwei@csu.edu.cn; lifuming001@163.com; ljx6666@126.com;

SUMMARY

The direct current (DC) resistivity method has been applied in geophysical exploration for many years. 3D DC resistivity array has also been applied for surveying since long time ago. However, due to the limitation of the topography of the surveying field, 3D array is not the efficient way to acquire the data. The 2D profiles are not effective to interpret the DC resistivity result. In this paper, we present a pseudo-3D DC resistivity array for the data acquisition. Both the synthetic data and real data cases can prove that the pseudo-3D DC resistivity array provide a better resistivity image than 2D array. Compared to the 3D array, it also can reduce the data acquisition time.

Keywords: DC resistivity, pseudo-3D, underground water

INTRODUCTION

The direct current (DC) resistivity method is a useful geophysical technique to describe the various resistivity of the earth. The electrical resistivity varies with the rock or sediment type, porosity and water situation. Traditionally, arrangements called Schlumberger array are using four electrodes for vertical soundings or horizontal profiling.

Resistivity is calculated by using the relationship between resistivity, an electric field, and current density (Ohm's law). The assumption is where the earth is homogeneous and isotropic, so the calculated resistivity is defined as the apparent resistivity (Dobrin, 1988).

Early discussion of DC resistivity method could be found in Sumner (1976), and Sharma (1997). In order to collect the sounding and profiling data, multi-electrode array was provided to measure the data (Dahlin, 1989；2000). The dense array of data can provide more details for the resistivity interpretation.

A towed array data acquisition system has been used where a carriage of electrodes towed by a vehicle (Panissod et al., 1998). The towed array provides a fast data acquisition approach.

2D data acquisition arrays, such as Schlumberger array, pole-pole, pole-dipole and dipole-dipole arrays are using no more than four electrodes to measure the data. 3D data acquisition employs all the electrodes as the transmitters and receivers electrodes.

In this paper, we proposed a pseudo-3D DC resistivity data acquisition system, which provides a 3D resistivity cube. This pseudo-3D data array provides faster and more efficient data acquisition system than 3D data array. Additionally, the pseudo-3D data array provides more detailed information than 2D data array.

Method

The pseudo-3D array uses the transmitter electrodes in a line. As shown in Figure 1, the "Red Cross" is the location of the transmitter electrodes. The "Black Cricle" is the location of the receiver electrodes. From A_{-13} to A_{13}, the distance is 2.6 times of the width of area 6. The infinitely powered electrode is located at position 1. The transmitter equipment is located at position 3.

We assume that the coordinates (-a,-b) and (a,b) are at the corners of area 6. The coordinates of transmitter electrodes (x,y) is given as:

$$(x,y)=\begin{cases}(x,0);when\ |x|\le a\\(a+2^i,0);when\ a<x\le(3a+1),\\(-a-2^i,0);when-(3a+1)\le x<-a\end{cases}\quad(1)$$

where *x, y, a, i* are integers.

The neighbor distance is *c* in horizontal direction(*X*); and *d* in vertical direction (*Y*). When the distance of the transmitter line is 2.6 times of the width of the measurement area 6, the coordinate origin is assumed as the center of measurement area.

The coordinate of the transmitter is given as:

$$(X_c,Y_c)=(x\times c,y\times d)=(x\times c,0)\quad(2)$$

The Pseudo-3D array could measure the data as pole-pole or pole-dipole way.

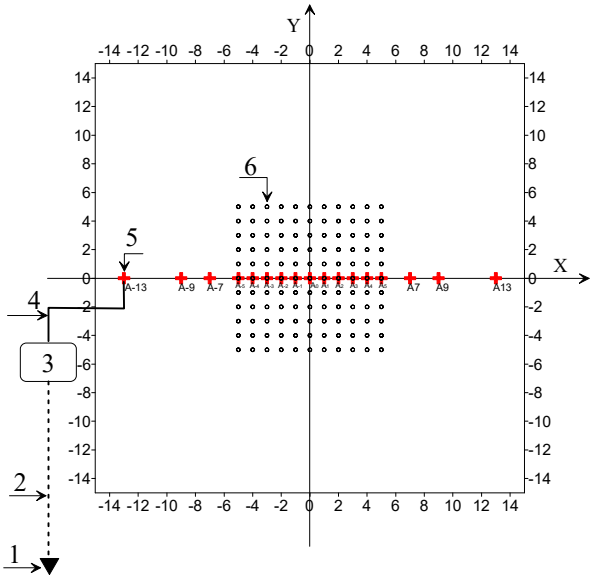

Figure 1: The observation system of pseudo-3D DC resistivity surveying

Numerical modeling and inversion results

In order to compare the 2D array, 3D array and pseudo-3D array data acquisition, we test the method by inverting the synthetic data. The area of the field is 300×300 m^2. The distance between the neighbor electrodes is 20 m. A 10 Ωm resistivity cube is embedded in the 1000 Ωm formation. The side length of the cube is 100 m. It is located at （-50,-50）~（50,50）, and the top of the cube is buried at 20 m.

The inversion results are given in Figure 2, Figure 3, and Figure 4. The Figures 2, 3, and 4 show the results of 2D, 3D and pseudo-3D DC resistivity inversion.

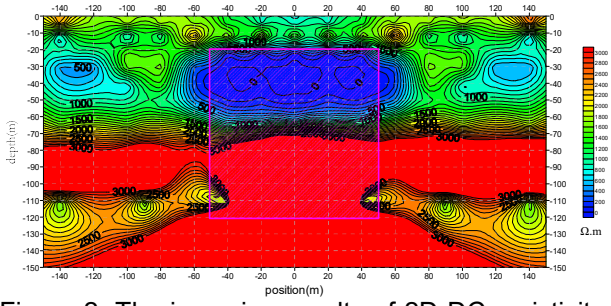

Figure 2: The inversion results of 2D DC resistivity surveying

The pink square is the position of the true model. Figure 2 shows that the high resistivity layer below 70 m as artifacts. The low resistivity anomaly is just half thickness of the real model.

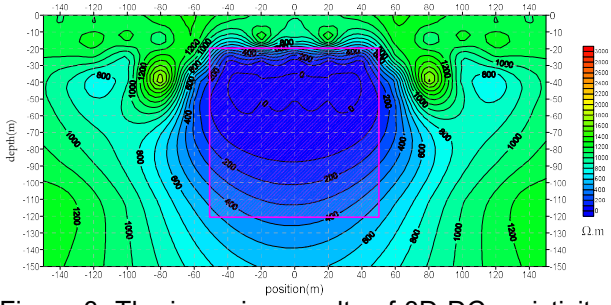

Figure 3: The inversion results of 3D DC resistivity surveying

Figure 3 shows the 3D DC resistivity inversion result. The low resistivity anomaly fits the true model well. The background resistivity is also around 1000 Ωm. This result is better than the 2D case.

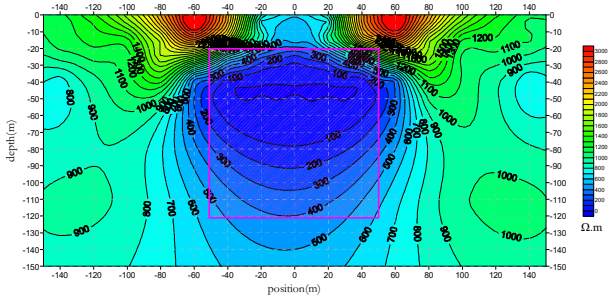

Figure 4: The inversion results of pseudo-3D DC resistivity surveying

Figure 4 shows the inversion results of the pseudo-3D DC resistivity data. The data acquisition is more efficient than the 3D case. The low resistivity anomaly is limited in the pink square. The result fits the true model not bad. However, there are two high resistivity artifacts near surface located at (-60, 0) and (60, 0). This result is also better than the image shown in 2D case.

Real data case

In this section, we are testing the pseudo-3D method on the groundwater exploration case. The field work has been done in Zixing, China.

Figure 5 shows the field of the groundwater exploration. In Figure 5, the three blue profiles are designed to measure the pseudo-3D DC resistivity data. The transmitter electrodes are located at the long profile in the middle. The receiver electrodes are located at the three profiles.

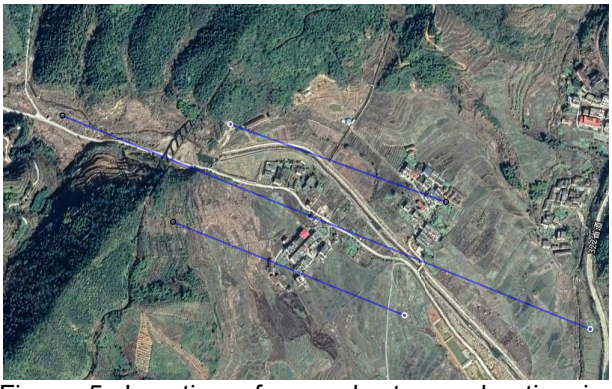

Figure 5. Location of groundwater exploration in Zixing.

Figure 6 shows the 2D DC resistivity inversion results of the groundwater exploration. From the resistivity image, the high resistivity anomaly is interpreted as the granite rocks. The low resistivity anomaly is below the granite rocks. However, the inversion of pseudo-3D DC resistivity shows the opposite conclusion, which is shown in the Figure 7.

Compares the two Figures 6 and 7, we can find that the Figure 7 provide a better resistivity image for the interpretation. The smooth resistivity image gives a low resistivity layer above the granite rocks. At the position of 300, the oblique structure is good for save the groundwater. Because the security reason, we design a drilling well at the position 400.

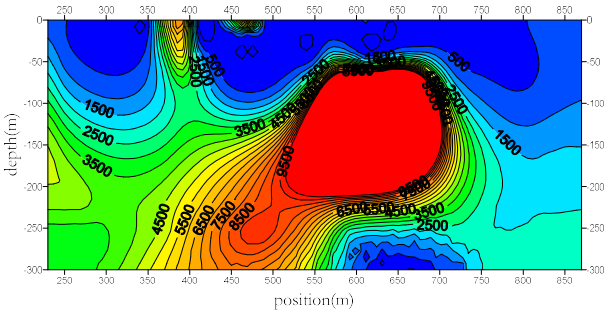

Figure 6. 2D DC resistivity inversion results.

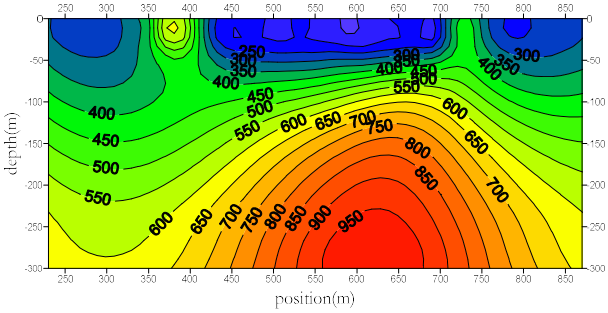

Figure 7. Pseudo-3D DC resistivity inversion results.

From Figure 7, the resistivity image gives a low resistive area between positions 0-400. A fault F1 degree 50 has been found near the 400 position. So the reason of the low resistivity area is caused by the rock fracture zone being filled with the water. The high resistivity between the positions 450-750 is caused by the Silica and Granite zone. Near the surface, the low resistivity layer is due to the sediments of the Quaternary alluvium and the river.

Based the interpretation discussed with the geologist, the decision is to drill a well at the position 400.

Figure 8. The ground water well at the 400 position.

The photo as shown in Figure 8 is given the drilling result. The groundwater is pumped from underground. The well has been drilled through the shallow granite rock layer. The fracture zone found by the drilling could be the reservoir for the underground water.

CONCLUSIONS

In this paper, we present a pseudo-3D DC resistivity array to enhance data acquisition efficiency. This pseudo-3D DC resistivity array can provide a better resistivity image from the inversion than the 2D array. Compared to the 3D array, it reduces the data collection time but provides the similar result. Both the synthetic data and the real

field data show that the pseudo-3D DC resistivity array is an effective and efficient method for geophysical exploration.

ACKNOWLEDGEMENTS

The author has the financial supported by “The International Postdoctoral Exchange Fellowship Program”. Project funded by China Postdoctoral Science Foundation grant number [2017M622607].

REFERENCES

Dahlin, T., (1989). The development of a cable system for vertical electrical sounding and a comparison of the Schlumberger and Offset Wenner methods. Licentiate Thesis LUTVDG/(TVTG-1005)/1-77, Lund University, 77pp.

Dahlin, T.(2000). Short note on electrode charge-up effects in DC resistivity data acquisition using multi-electrode arrays. Geophysical Prospecting, 48(1), 181-187.

Sharma, P. V. (1997). Environmental and engineering geophysics Cambridge University Press Cambridge. United Kingdom.

Sumner, J. S. (1976). Principles of induced polarization for geophysical exploration. Elsevier. Amsterdam, Netherland, 277.

Panissod C., M. Dabas, A. Hesse, A. Jolivet, J. Tabbagh, A. Tabbagh, (1998). Recent developments in shallow depth electrical and electrostatic prospecting using mobile arrays, Geophysics, 63(5), 1542-1550.

Quantitative Geothermal Interpretation of Electrical Resistivity Models of the Rathlin Basin, Northern Ireland

R. Delhaye[1,2], V. Rath[1], A. G. Jones[1,3], M. R. Muller[1,4], D. Reay[5]
[1]Dublin Institute for Advanced Studies (DIAS), 5 Merrion Square, Dublin 2, Ireland
[2]National University of Ireland, Galway, University Road, Galway, Ireland
[3]Complete MT Solutions Inc. (CMTS), Ottawa, Canada
[4]Private Consultant, Cambridge, UK
[5]Geological Survey of Northern Ireland (GSNI), Belfast, UK

SUMMARY

The Rathlin Basin is the deepest sedimentary basin in Northern Ireland – Permian and Triassic reservoir sediments are known to exist to at least 2300 m depth – and presents an interesting low-to medium-enthalpy geothermal resource. Two deep boreholes within the basin provide evidence of elevated temperatures at depth, prompting geophysical exploration of the basin using magnetotellurics (MT) as one component of the IRETHERM project. MT data were acquired on a rectangular grid of 39 sites across a third of the onshore portion of the basin to investigate its lithological characteristics and spatial variation.

One-dimensional resistivity models were obtained at each site, revealing that the sediments of interest lie beneath a mudstone layer of even lower resistivity. As a conseqence of the shielding effect of the overlying mudstone layer, it is both difficult and unreliable to interpret the deeper target sediments based solely upon modelled resistivity. An automatic scheme for interpreting sub-horizontal resistivity layers was developed to facilitate imaging and analyses of the models. Although not a general approach, the boundary identification method functioned well for the 1D MT models within the research area when compared to borehole records, and a conservative reservoir volume of approx. 75 km^3 of combined Permian and Triassic sandstones was estimated to be present beneath the survey.

Based upon new, high-quality temperature data available in the Ballinlea 1 borehole, an approximate estimation of thermal energy as a function of final reservoir temperature has been derived from the interpretable MT resistivity model volume, over a range of final reservoir temperatures from 85 to 25 °C. The resulting best case of a final temperature of 25 °C results in an estimated Indicated Geothermal Reserve (IGR) of $8.2x10^{18}$ J beneath the MT survey area. The resulting estimates suggest that exploitation of the maximum volume of sediments would occur for a final temperature of ~50 °C.

Repeatability and reproducibility of transient electromagnetic measurements with respect to monitoring techniques

M. Bär[1] and K. Spitzer[1]
[1]Technical University Berakademie Freiberg
matthias.baer@geophysik.tu-freiberg.de

SUMMARY

We develop monitoring techniques using transient electromagnetics (TEM). Whenever pore fluids come into play the electric conductivity is a sensitive indicator of structures and processes. Technologies associated with subsurface fluid migration are, e.g., Carbon Capture and Storage (CCS) and Enhanced Oil Recovery. We aim at developing cost-effective monitoring techniques with a TEM surface-to-borehole setup, in this case for CCS. The use of a borehole sensor increases the sensitivity of our method at depth, particularly close to the reservoir.

To identify significant changes in the transient response and relate them to the sequestrated carbon dioxide it is crucial to ensure the reliability and stability of the measurement system. Therefore both reproducibility and repeatability of transient responses have to be thoroughly scrutinized and quantified. This is a challenging task due to the high dynamic bandwidth of transient electromagnetic data. Slight changes in the survey setup or environmental noise can have a significant effect on the induced voltage in the receiver.

We present a statistical evaluation scheme to analyze transient electromagnetic measurements with respect to repeatability and reproducibility during time-lapse monitoring. Since October 2017, we are performing transient electromagnetic measurements on a monthly basis on a test field located in Tharandt (Saxony)/Germany. For each survey, we are using the same layout for the transmitter loop and the receiver points. A series of statistical hypothesis tests (two-sample Kolmogorov-Smirnof test, k-sample Kruskal-Wallis test, Durbin-Watson test) is applied to the complete time series to check the underlying distributions, median values, variances and correlation among the transient responses.

To meet the requirements of the statistical tests we transform the data to a convenient range of values thereby reducing the disadvantageous high dynamic bandwidth. A simple logarithmic transformation is not practical due to sign reversals in the transient response caused by separate loop measurements. Our data transformation is based on the normalization of each gate of the response to its corresponding decade. We show that the evaluation scheme is very sensitive to changes in the transmitter current strength and the transmitter loop area.

Keywords: transient electromagnetics, repeatability, reproducibility, statistics, carbon dioxide

Repeatability of land-based controlled-source electromagnetic measurements in industrialised areas and including vertical electric fields

K. Tietze[1], O. Ritter[1,2], C. Patzer[1,2], P. Veeken[3], and M. Dillen[3]
[1] GFZ German Research Centre for Geosciences, Telegrafenberg, D-14473 Potsdam, Germany.
Contact: ktietze@gfz-potsdam.de
[2] Freie Universität, Department of Earth Sciences, Malteserstr. 74-100, D-12249 Berlin, Germany
[3] Wintershall Holding GmbH, Friedrich-Ebert-Str. 160, D-34119 Kassel, Germany

SUMMARY

Over the last decade, an increasing number of numerical studies have proposed controlled-source electromagnetic (CSEM) techniques for monitoring of fluid flow in reservoirs, e.g. in the framework of hydrocarbon production or CO2 storage scenarios. One of the fundamental prerequisites for any monitoring application in practise is the repeatability of the measurements. Independent of any changes in the subsurface, measurements are affected by temporal variation of EM noise, alteration of equipment and technical limitations. Here, we report on CSEM measurements acquired across a producing oil field on land in three consecutive surveys between 2014 and 2016. As conductivity changes in the reservoir structure are not expected for this time frame, the data sets provide an excellent basis to study the repeatability of such measurements over a time span of 2.5 years. Our results suggest that repeatability of CSEM measurements depends on source-receiver distances, component of the transfer function, source-polarisation, and relocation errors, in particular at sites close to the source, where the geometry and characteristics of the source fields vary rapidly in space. Best repeatability was observed for receiver stations at 2–4 km distance from the source and frequencies < 20 Hz. At these stations, phases and amplitudes of transfer functions usually agreed within ±1° and ±5 % between measurements.
We also measured the vertical electric field (Ez) with a newly developed receiver chain in a 200 m deep observation borehole. Although amplitudes of Ez are about one to two orders of magnitude smaller than amplitudes of horizontal electric fields, recordings of Ez are stable. More importantly, Ez response functions of three measurements between 2015 and 2016 show excellent quality and similar repeatability as horizontal electric fields indicating that conditions at greater depth are more stable than at surface.

Keywords: Controlled-source electromagnetics, monitoring, vertical electric field measurement, hydrocarbon resources

Resistivity image of Baryatinskaya crustal high-conductive anomaly based on the results of areal MT-survey

Victor Kulikov[1,2], Sergey Zaytsev[2], Elena Aleksanova[1], Ivan Varentsov[3], Ilya Lozovsky[3], Nikolay Shustov[2] and Andrey Yakovlev[1,2]

[1] Nord-West Ltd., Moscow, Russia, alex-len@inbox.ru
[2] Moscow State University, Moscow, Russia
[3] Geoelectromagnetic Research Center of IPE RAS, Moscow, Russia

SUMMARY

The results of interpretation of MT data acquired on north-west slope of Voronezh crystalline core-area in 2007 - 2014 are presented. It was a part of the international project, which main issue was survey of Baryatinskaya and Kurskaya crustal high-conductive anomalies. Scientists from Lomonosov Moscow State University, Geoelectromagnetic Research Center of The Schmidt Institute of Physics of the Earth of the RAS, Subbotin Institute of Geophysics of the NAS of Ukraine and Nord-West Ltd. took part in this project.

MT survey of this area started in 1990th when high-conductive anomaly in the crust was found. From 2007 the survey of this anomaly was supported by Russian Foundation for Basic Research (RFBR). Since then the MT data was acquired in 142 sites along 12 lines using two type of equipment: MTU (Phoenix Geophysics) with magnetic coils and LEMI with flux-gate magnetometers. The range of periods for the most of sites is from 300 Hz to 10 000 sec.

The analysis of impedance (Z) and tipper (W) was carried out. It showed, that northern part of area has close to 2D structure and on the south it more likely 3D, because two conductive zones with different direction join there. 2D inversion for MT lines on the northern part of area was carried out in 2012.

In 2017 3D inversion of all MT data (Z and W) was carried out using ModEM software and supercomputer «Lomonosov» (Research Computing Center of Lomonosov Moscow State University). Resistivity image obtained from 3D inversion shows the boundaries of the Baryatinskaya and Kurskaya crustal high-conductive anomalies, their deep resistivity structure and their connection with well-known high-conductive areas of Ukrainian craton. The resistivity images were compared with geological, gravity and magnetic data. Some interesting features connected with the main geological structures were discovered.

Keywords: Magnetotellurics, MT survey, crustal high-conductive anomalies, resistivity image, 3D inversion

Resistivity imaging of an analogue of the transition zone between the sedimentary cover and the basement of deep sedimentary basin for geothermal exploitation

J. Porté[1,2], M. Darnet[2] , J-F Girard[1], N. Coppo[2], J-M Baltassat[2], F. Bretaudeau[2] and P. Wawrzyniak[2]
[1] IPGS (UMR 7516 CNRS / University of Strasbourg), j.porte@brgm.fr, jf.girard@unistra.fr
[2] BRGM (French Geological Survey), m.darnet@brgm.fr, n.coppo@brgm.fr, jm.baltassat@brgm.fr, f.bretaudeau@brgm.fr, p.wawrzyniak@brgm.fr

SUMMARY

The transition zone between the basement and the sedimentary cover is becoming an increasingly attractive target for the development of geothermal energy in deep sedimentary basin as encountered in the Upper Rhine Graben. Several geothermal power plants already exploit this target but the transition zone is however still poorly known with the presence of large permeability heterogeneities. Studies are currently ongoing in order to develop conceptual models on how it is formed and how heat can be exploited. In this study, we evaluate the ability of resistivity imaging by Controlled-Source Electromagnetic (CSEM) method in frequency domain, to identify favorable areas for the development of Enhanced Geothermal System (EGS). We performed a land-CSEM survey on an analogue of the transition zone in a well-known catchment basin at Ringelbach (Vosges mountains in France), to assess the relevance of such data. Gathered data consist in a 3D-grid of 48 reception sites uniformly distributed over the whole basin and using a single transmitter.
We performed 2.5D inversions of a data subset with the parallel adaptive finite-element code MARE2DEM to image the resistivity structure through a profile of interest and compared the result to a former Electrical Resistivity Tomography (ERT) inversion. CSEM inversion extended the shallow ERT image in depth and allowed to obtain a resistivity image of the transition zone. The integration of these results with existing geological and geophysical knowledge allowed identifying and mapping a fault zone as well as the fractured zone at the top of the unaltered granite basement. Results of this study demonstrate the importance of acquiring resistivity data at the target depth before drilling to maximize the success rate of a deep EGS project and point out the interest of pursuing the study with the 3D inversion of the whole set of data.

Keywords: Geothermal energy, Land-CSEM, 2.5-D inversion

Introduction

Following the success of the geothermal pilot site of Soultz-Sous-Forêts (Alsace) for the production of heat and electricity, several new projects are currently in development or are already in production, as the new geothermal power plant of Rittershoffen (Alsace, France). In order to better understand the geothermal target in Alsace, the CANTARE-Alsace project aims to characterize the transition zone between the basement and the sedimentary cover of the deep sedimentary basin of the Rhine Graben. Controlled-Source Electromagnetic (CSEM) investigation was undertaken on a shallow analogue of the transition zone, the catchment basin of Ringelbach (Vosges), to develop resistivity imaging in these contexts. Many information are available on its shallow structure due to the presence of two wells and several geophysical surveys (Well-logging, ERT, NMR) carried out between 1999 and 2007. Available geophysical data are summarized by Baltassat (2017). We expect the CSEM data to extend the maximum depth of investigation of former resistivity images (limited to 50 meters). In this paper, we present the first results of a 3D CSEM survey performed in 2017 and compared these against legacy data.

Study site

Studied since 1975, the catchment basin of Ringelbach is a well-known hydrogeological site, analo-

gous in surface to our target in depth, making it a perfect study site of the transition zone of deep sedimentary basin. According to previous studies, the site is composed of resistive sandstone (1000-3000 $\Omega.m$) superposed over two granitic facies with a NE-SW fault separating the site in two blocks (Figure 1). The first one is identified as a weathered granite being conductive (250-1000 $\Omega.m$), whereas the second one as a fresh granite with a strong resistive signature ($>$3000 $\Omega.m$). Laboratory measurements (Belghoul, 2007) showed that the high conductivity of the Ringelbach weathered granite is related to its increased porosity but also as result of former hydrothermal alteration succeeding the granite burial (Wyns, 2012). The fault zone identified on the geological map and near the center of the P1 profile (Figure 1 and projected ERT result on Figure 2) displays a shallow conductive anomaly around 200 $\Omega.m$. The two 150m deep wells are located on the sedimentary cover over the Heidenkopf (HEI) and the Hurlin (HUR) (Figure 1) and found a thin sandstone layer (70 meters thick in HEI and 30 meters in HUR) lying over a thin layer of granitic sand (around 20 meters thick) and finally over weathered granite. Unaltered granite has neither been seen in the wells nor imaged by the ERT method due to its limited depth of investigation (50m).

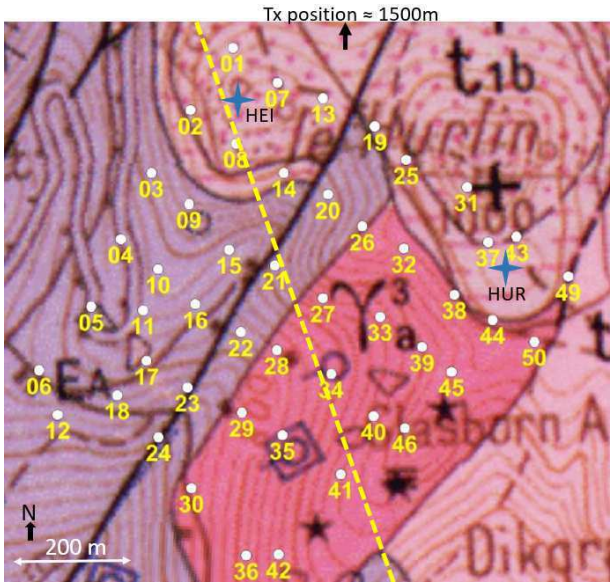

Figure 1: Geological map of the Ringelbach Basin with the reception grid and the P1 profile from former ERT survey (yellow dashed line). Blue crosses show well locations; the Heidenkopf (HEI) and the Hurlin (HUR). The center of the loop (Tx) is located around 1500 meters North from the nearest point of the grid ©IGN 2017

CSEM survey

The 3D Land-CSEM survey was carried out the first week of July 2017, over a 750$\times$800 m^2 area with 48 reception sites gathered over a quasi uniform 3D-grid (Figure 1). Acquisition used Metronix ADU-07 acquisition systems, whereas the source was a Metronix TXM-22 and its control unit TXB-07. The source position was located at 1500 meters North from the Ringelbach basin on the sedimentary cover. The survey design originally planned two orthogonal electric transmitters, but the high resistivity from very dry sandstones at the source location drastically limited the injected current. It restrained our data set to a unique current polarisation by the use of an inductive transmitter. The horizontal loop used was 1184 meters long, covering an area of 93 720 m^2. Twelve frequencies were gathered varying from 0.25 Hz to 8192 Hz using square-wave signals. Audio-Magnetotelluric (AMT) sequences were also recorded in each site but are not presented.

Methods

Data were processed in the frequency domain using BRGM software PROCATS, allowing us to estimate transfer functions for all harmonics of the square wave signal using robust processing (Streich et al (2013) and Smaï and Wawrzyniak (2018)). Quality control was performed sorting data with poor signal to noise ratio and looking manually for the smoothness of the amplitude and phase curves with frequency. Data are highly contaminated by noise below 8 Hz and above 4096Hz. Some harmonics of the fundamental frequencies were kept within this range for the amplitudes of the electric fields but no harmonics were kept for the phases as they were too noisy. In this study, we focus on 2.5D resistivity imaging for calibration purposes and to prepare for future 3D inversions. We selected 9 stations through the grid to form a profile similar to the one of interest P1 (Figure 1) imaged by former ERT surveys (Baltassat, 2017) and providing us a direct way to compare our results. Figure 2 displays ERT inversion result superposed on our CSEM inversion results and shows the main resistivity structures from the Ringelbach basin. On the ERT results, we can observe a thin resistive sedimentary cover lying over a more conductive weathered granite to the North-

West, a fault zone with conductive anomalies in the center of the profile and to the South-East a block of fresh granite with a transition around receiver RX34. Inversions of the CSEM data were performed using the open-source parallel adaptive finite-element 2.5D code MARE2DEM (Key and Ovall, 2011) which use a modified OCCAM inversion approach (Key, 2016) looking for the smoothest model explaining the data. The code uses an unstructured triangular grid allowing to include topography in our model.

Results

First inversions used amplitude and phase data from the electric field oriented to the East as this component is the strongest for a horizontal transmitting loop located to the North. However, data suffer from strong static shift effects affecting our images. It resulted in structures totally incoherent with a priori geological information. Hence, as phase are not affected by static shifts (Zonge and Hughes, 1991), we chose to invert only phase data from the East-West electric field at the fundamental frequencies in the range of 8 Hz to 4096 Hz, resulting in 9 frequencies per site and giving us the best result according to a priori information. Figure 2 shows the result of the CSEM data 2.5D inversion. Shallow structures are in good agreement with the resistivity image obtained previously by ERT on profile P1. Indeed, the resistive block of fresh granite appears clearly in the South of the profile and vanishing at the conductive fault area. Resistivity values are over 2000 $\Omega.m$ for the fresh granite and around 250 and 500 $\Omega.m$ in the fault zone. We can see that the conductive anomaly from the fault area extends in depth compared to ERT result. The sedimentary cover (1000 $\Omega.m$) is less well imaged with a thicker resistive layer than expected (around 200 meters instead of 80 meters according to well data). This is likely to be related to the lack of high frequency data (>4096 Hz) and hence of shallow depth of investigation (<100m). We also identify a conducting layer dipping to the North from the fault area and lying over a resistive body with similar resistivity as fresh granite.

Discussion and perspective

First results of this study gave us a deeper resistivity image of the Ringelbach basin, an analogue of the transition zone between the basement and sedimentary cover of deep sedimentary basin. The choice to keep the inversion using only phase data with limited number of parameters questions the relevance of our result. Nevertheless, synthetic cases were modelled and successfully inverted, supporting the consistency of our first images. Furthermore, our result is in good agreement with former resistivity information. Another point of discussion is the ability to image the conductive layer deeply under the sedimentary cover. Indeed, the limit between sedimentary cover and conductive weathered granite is too deep compared to well data. Transmitter imprint or 3D effects may degrade the resolution of the image to the North of the profile and explain the discrepancy. In future work, we will include AMT data in a joint inversion scheme to refine resistivity image further and confirm our resistivity model. We will also perform a 3D inversion of all the receivers to remove any potential 3D effects.

Conclusion

This work show the benefits of using EM methods to discriminate between resistive fresh granite and conductive weathered granite on a shallow analogue of the transition zone at the top of a granitic basement. Resistivity imaging could therefore be an efficient way to identify weathered granite areas more likely permeable with the presence of pre-existing fractures and hence avoiding unaltered and impermeable granites less favourable for geothermal reservoir development. A remaining challenge is though how to upscale our method to make such measurements underneath a thick sedimentary cover (>3km).

ACKNOWLEDGMENTS

This work was supported by the Agence Nationale pour la Recherche under the grant agreement ANR-15-CE06-0014 (CANTARE-Alsace project) and the different project partners: IPGS-CNRS; BRGM (French Geological Survey); LHYGES-CNRS; ÉS-Géothermie.

REFERENCES

Baltassat JM (2017) Réinterprétation des investigations géophysiques du bassin du Ringelbach avec les données de forages et les mesures en laboratoire. BRGM/RP-66694-FR

Belghoul A (2007) Caractérisation pétrophysique et hydrodynamique du socle cristallin. PhD thesis, Université Montpellier II-Sciences et Techniques du Languedoc

Key K (2016) MARE2DEM: a 2-D inversion code for controlled-source electromagnetic and magnetotelluric data. Geophysical Journal International 207(1):571–588

Key K, Ovall J (2011) A parallel goal-oriented adaptive finite element method for 2.5-D electromagnetic modelling. Geophysical Journal International 186(1):137–154

Smaï, Wawrzyniak (2018) Razorback, an open-source python library for magnetotelluric robust processing. (Submitted)

Streich R, Becken M, Ritter O (2013) Robust processing of noisy land-based controlled-source electromagnetic data. Geophysics 78(5):E237–E247

Wyns R (2012) Etude géologique du cadre structural et des forages du bassin versant de recherche du ringelbach (soultzeren, haut-rhin). Tech. rep., BRGM/RP-56540-FR

Zonge KL, Hughes LJ (1991) Controlled source audio-frequency magnetotellurics. In: Electromagnetic Methods in Applied Geophysics: Volume 2, Application, Parts A and B, pp 713–810

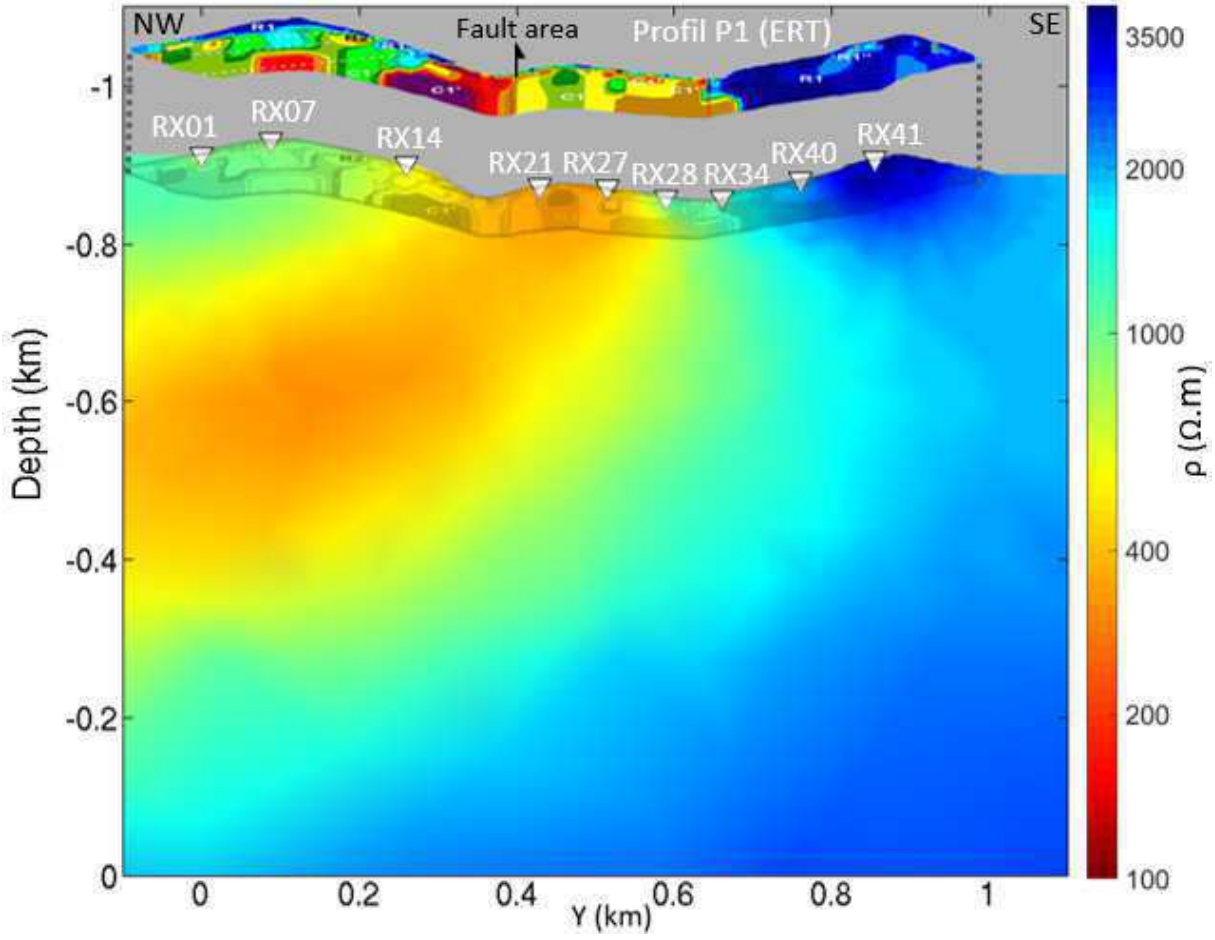

Figure 2: CSEM data 2.5D inversion result over the P1 profile from Baltassat (2017). Former ERT inversion is displayed and its shadow is projected over our result with the fault crossing location represented by an arrow. Source location is around -1.5 km in the y-direction with a 0.4 km shift on the x-axis

The Resistivity Structure of the Meitlar area in the Hengill geothermal field, SW Iceland

Ásdís Benediktsdóttir[1], Knútur Árnason[1]

[1]Iceland Geosurvey, ÍSOR (Iceland)

SUMMARY

The Meitlar area is located in the south-western part of the fissure swarm of the Hengill central volcano, SW-Iceland. This Hengill central volcano, which is also a geothermal field, marks a triple-junction in the tectonic structure of Iceland, connecting the Reykjanes Peninsula, the Western Volcanic Zone and the South Iceland Seismic Zone. The data were collected for and owned by Reykjavík Energy in order to understand the potential of the area for geothermal utilization. We present a 3D model using 114 magnetotelluric (MT) and time domain electromagnetics (TEM) sounding pairs. The TEM soundings were used to correct the MT soundings for static shift prior to the 3D inversion. The WSINV3DMT code was used for the inversion and the off-diagonal elements of the impedance tensor were the input data.

The results reveal the 3D resistivity structure of the area. The low-resistivity layer domes up in two pipe-like structures that have a similar strike as most of the geological features in the area (N30°E). A NW-SE discontinuity is observed across the two pipes. The western pipe is more pronounced than the eastern pipe. It bends in the southern part just like the surface hyaloclastite ridges, forming a more N-S oriented up doming low-resistivity cap. The two up-doming pipes are a possible up-flow zones of high-temperature fluid.

Keywords: Magnetotellurics, Time domain electromagnetics, Iceland, High-temperature geothermal system

Sinkholes 3D geometry by shallow electromagnetics in Yucatan Peninsula, Mexico.

Pérez-Flores, Marco A.[1] and Ochoa-Tinajero, L.E.[2]
[1] Department of Applied Geophysics, CICESE, mperez@cicese.edu.mx
[2] Department of Applied Geophysics,CICESE,
eotinajero@gmail.com

SUMMARY

The Yucatan peninsula is constituted by a calcareous sedimentary sequence which has given origin for a wide formation of sinkholes, underground rivers and caverns because of karst. A regional unconfined aquifer is the principal source of fresh water supply of the region. The conceptual model describes a freshwater lens floating over a saltwater layer because of the marine intrusion where the thickness depends on the coast proximity. With the goal to know the hydrogeological characteristics of the karst system like sinkholes, underground rivers, caverns and the interface of fresh/salt water mixing zone, we applied geophysical technics for their exploration. We applied electromagnetics methods at low induction numbers (EM-LIN or EMDF) on a karstic system where The Chac-Mool sinkhole is located, Quintana Roo, Mexico. The 3D inversion shows a model that allows us to correlate the path of the underground rivers with the resistivity of the subsurface. Two underground rivers cross between them, making a complex 3D conductivity geometry.

Keywords: sinkholes, low induction numbers, karst.

Some examples of application of simultaneous joint inversion of independent geophysical data in a spatial recognition of salt and subsalt structures

Adam Cygal[1], Michal Stefaniuk[1], Jolanta Pilch[1], and Anna Kret [2]

[1] AGH University of Science and Technology, cygal@agh.edu.pl
[2] PBG Geophysical Exploration Ltd., a.kret@pbg.com.pl

SUMMARY

The presentation shows results of integrated interpretation of independent geophysical data sets. Multivariate interpretation was based on results of simultaneous joint inversion of magnetotelluric and gravity data constrained by result of depth migration seismic reflection data. In the first stage the methodology was used for recognition of variability of P-wave velocity in the low-velocity zone, in order to determine the seismic static correction and building deep velocity models for seismic depth migration. Research area was located in the northern part of Polish Lowland, where research problem is focused on variable thickness of Pleistocene and Neogene sediments and thickness of evaporite sediments. Joint inversion of different geophysical data sets, supported by available geological and borehole data, allowed to generate high-resolution geophysical cross-sections. Moreover, such high-quality input material allowed to perform a comprehensive and highly accurate geological interpretation of results of geophysical data processing.

This paper was prepared based on results of investigations carried out in the framework of the project entitled “Experimental, complex and multi-variant interpretation of seismic, magnetotelluric, gravity and borehole data as a tool to improve the effectiveness of structural and reservoir research” – Applied Research Program III (In Polish: Program Badań Stosowanych III).

Keywords: Magnetotellurics, Transient Electromagnetic Method, seismic data processing, simultaneous joint inversion, static correction.

Steel Casing Effects on CSEM Monitoring of Unconventional Reservoir Stimulation

M.Couchman[1], M.E.Everett[1], J.Charbonneau[1], R.Robinson[1]
[1]Dept. Geology and Geophysics, Texas A&M University, mattc1990@tamu.edu

SUMMARY

Real-time monitoring of the efficiency of hydrocarbon extraction from unconventional reservoirs represents a significant challenge to the oil & gas industry. Here we explore the capability of controlled source electromagnetic (CSEM) methods to detect electrically conductive injected fluids associated with hydraulic fracturing. We compute idealized CSEM signatures of conductive fluids injected from a lateral wellbore and determine such effects as the position of the injection site along a lateral wellbore and its conductivity, while also considering cases where fluids spread into given fracture zone volumes for both cases of constant injection and post injection spreading. We also consider separately the effects of the highly conductive steel casing of lateral and vertical wellbores on the CSEM in-line response.

Keywords: CSEM, Unconventional, Finite-Element, Steel-Casing

INTRODUCTION

Real-time monitoring of the efficiency of unconventional hydrocarbon extraction in hydraulic fracturing environments is an increasingly important challenge for the oil and gas industry. Here we seek to create more efficient fracture monitoring techniques based on CSEM imaging of fluid movement away from a lateral wellbore in unconventional settings. This goal is addressed by undertaking fundamental studies of terrestrial CSEM responses in the presence of injected fluids associated with hydraulic fracture stimulation of unconventional reservoirs.

The 3-D finite element algorithm used to compute the CSEM responses is modified from Badea et al. (2001) which solves Maxwell's equations as formulated in terms of Coulomb gauged potentials.

The effect of the highly conductive wellbore must be taken into account. There have been multiple recent approaches for computing the CSEM response of a wellbore or similar highly conducting body (e.g Patzer et al. 2017, Puzyrev et al. 2016). Here we use local refinements of a finite element mesh to allow a small diameter wellbore to be modelled. While the diameter of the wellbore can not be reduced to that of a realistic case, the transverse conductance formulae [1] may be used to determine an appropriate conductivity for a larger, easily-modelled wellbore. Locally refining the mesh around the wellbore proves essential in reducing CSEM response inaccuracies caused by large asymmetric and poorly-shaped tetrahedra in the vicinity of the high conductivity contrast region between wellbore and host sediment.

$$C=\sigma A \qquad [1]$$

We aim to explore the extent to which the conductive fluids associated with hydraulic fracturing can be detected using the terrestrial CSEM method. This study, in particular, shows the effect of varying wellbore, fluid, and host-rock parameters on the in-line electric field amplitude response to a point dipole transmitter with a transmitter moment of 1 A-m, operating at a frequency of 1 Hz.

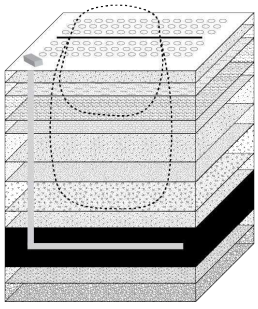

Figure 1: Schematic of an unconventional CSEM field setup with vertical and lateral wellbore (gray). The transmitter shown here is a long grounded electric dipole (black line on surface) with a set of receivers (ellipses). An idealization of primary electric field lines is shown (black-dashed).

DETECTION OF CONDUCTIVE FLUIDS

A 1-D model, including a locally-refined lateral wellbore, (with a conductance matched to a wellbore with a diameter of 20 cm, wall thickness of 2 cm and conductivity of $5x10^6$ S/m) has conductive fluid being forced out of a lateral wellbore

horizontally in both perpendicular directions into specified fracture zones. The fracture zones are both 200 x 193.75 x 6.25 m and have a conductivity of 1.24 S/m. While this is clearly an exaggerated thickness for the fluid filling such a fracture zone, this can be compensated for by using the conductance concept. The computed secondary in-line electric field amplitude shows an almost indistinguishable variation for cases with and without the fluid-filled fracture zones. However, by producing difference plots between the responses of models in which the fluid-filled fracture zones are present and absent, we can much better discern the effect of the conductive fluid. The fluid-filled fracture zone now has a potentially detectable signature (figure 2). While the amplitude of this difference remains relatively small, it does scale with transmitter dipole moment. The detectability will depend on the ambient noise level at a particular oilfield operations site.

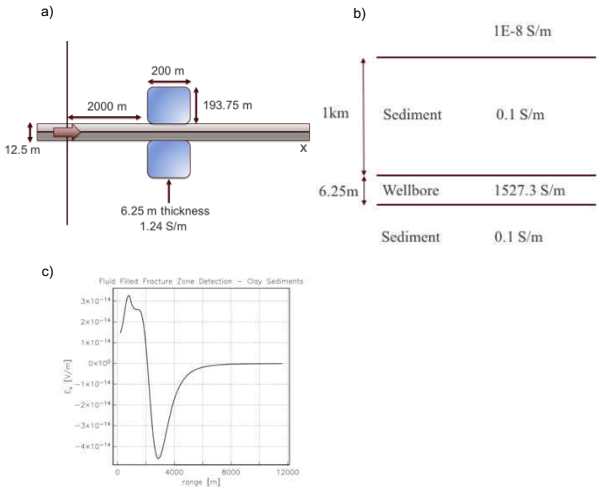

Figure 2: (a) Depth slice at 1 km showing fracture filled fluid zones (blue) on either side of the wellbore (grey). The transmitter is at the origin at the surface (red). (b) Geoelectric model comprising of a 12.5 x 6.25 m wellbore buried beneath 1 km of a conductive sediment such as heavy clays. (c) Difference in secondary in-line electric field amplitude for cases with and without the fluid filled fracture zones for positive offsets.

HOST SEDIMENT CONDUCTIVITY

In the previous sections, the lateral wellbore is buried beneath 1 km of sediment with a conductivity of 0.1 S/m. The latter value is associated with heavy clays, and hence a host conductivity of 0.01 S/m was also tested to more closely represent terrigeneous sediments. The results shown in figure (3c), compared to those of (2c) show an amplitude roughly 2 orders of magnitude larger.

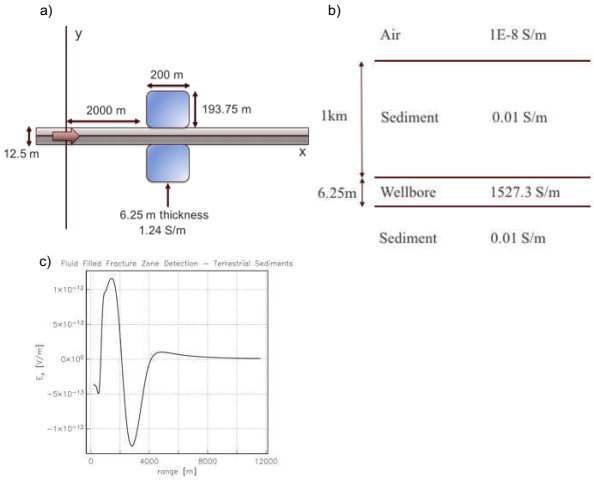

Figure 3: (a) Depth slice at 1 km. (b) Geoelectric model comprising of a 12.5 x 6.25 m wellbore buried beneath 1 km of terrigeneous sediments. (c) Difference in secondary in-line electric field amplitude for cases with and without the fluid filled fracture zones for positive offsets.

FRACTURE ZONE LOCATION

In the next scenarios we tested, the fluid-filled fracture zone remains on both sides of the lateral wellbore but its position is varied along the wellbore. This is done to test the effect on the CSEM response of the lateral position of the fluid-filled fracture zones, for example, these could represent different hydraulic fracturing stages. The geoelectrical model from figure 3 remains otherwise unchanged. From Figure 4 it is evident that the maximum electric field amplitude as a function of location of the fluid zone varies in two ways. First, the peak electric field amplitude due to the fluid-filled fracture zone is higher at smaller receiver offsets. Second, the peak electric field amplitude due to the fluid-filled fracture zone is also found at smaller transmitter-receiver offsets for lower offsets between the transmitter and fluid-filled fracture zones.

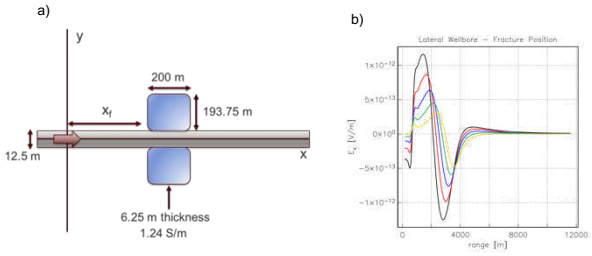

Figure 4: (a) Depth slice at 1 km (b) Difference in secondary in-line electric field amplitude for cases with and without the fluid filled fracture zones for positive offsets for cases where the offset x_f is equal to 2000 (black), 2200 (red), 2400 (blue), 2600 (green) and 2800 m (yellow).

SPREADING OF INJECTED FLUID

Tests for two cases involving an idealized spreading of fluids have been conducted. The first case (figure 5) involves continuous injection wherein the conductivity of the fluid-filled fracture zones on either side of the lateral wellbore remains constant. In this case, the fluid spreads evenly in all directions, leading, as expected, to increased CSEM responses from the fluid-filled fracture zones for larger fluid volumes. It must be noted that this idealized model of fluid transport is for CSEM test-of-concept only and does not have a realistic geomechanical or fluid transport basis.

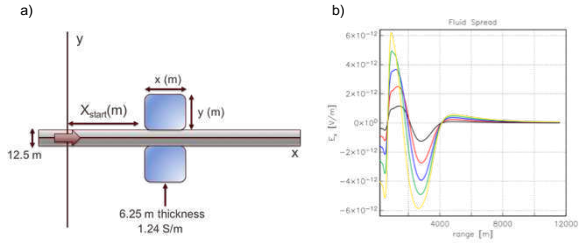

Figure 5: (a) Depth slice at 1 km. (b) Difference in secondary in-line electric field amplitude for cases with and without the fluid filled fracture zones for positive offsets for cases where the volume of the fluid filled fracture zone is equal to $2.4x10^5$ (black), $2.2x10^6$ (red), $6.2x10^6$ (blue), $1.2x10^7$ (green) and $2.0x10^7$ m^3(yellow).

In the second case (figure 6), the fluid injection is stopped, and the fluid dissipates into a fracture zone of variable area. Thus, the conductivity within each fracture zone decreases as the fluid volume increases. We find that the CSEM response due to the fluid does increase for a small increase in the fluid-filled fracture zone volume, before reducing at higher volumes. This is due to a trade-off between larger volume against a reduction in conductivity. From the results, it appears that the fluid-filled fracture zone is more detectable as a smaller, higher conductivity zone rather than a larger, lower conductivity volume.

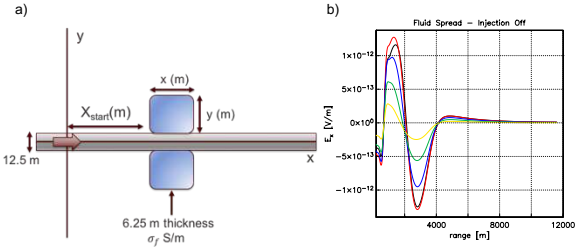

Figure 6: (a) Depth slice at 1 km. (c) Difference in secondary in-line electric field amplitude for cases with and without the fluid filled fracture zones for positive offsets for cases where the volume of the fluid filled fracture zone is equal to $2.4x10^5$ (black), $2.2x10^6$ (red), $6.2x10^6$ (blue), $1.2x10^7$ (green) and $2.0x10^7$ m^3(yellow).

LATERAL WELLBORE EFFECTS

The impact of the lateral wellbore by itself and in particular the effect of its depth and the lateral wellbore toe on the secondary in-line electric field amplitude are important factors to consider. Firstly we investigate a case in which the lateral wellbore depth ranges from 600-1400-m (figure 7). The modeling results show a reduced surface response when the wellbore in located at greater depths, due to the increased vertical distance between the transmitter and the lateral wellbore.

The effect of a finite-length lateral wellbore was then investigated with the toe located at transmitter (TX)-lateral toe (LT) horizontal offsets ranging between 2-12 km (figure 8). The presence of the lateral wellbore toe is shown to enhance responses at large ranges for greater TX-LT offsets, which is likely due to the termination of the lateral wellbore acting as a secondary dipole source within the geoelctrical system.

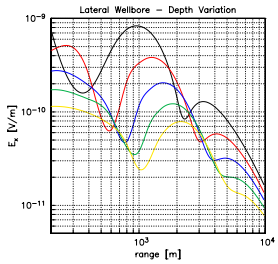

Figure 7: Secondary in-line electric field response of a lateral wellbore buried at depths of 600 (black), 800 (red), 1000 (blue), 1200 (green) and 1400 m (yellow). The wellbore is buried beneath a sediment with a conductivity of 0.01 S/m.

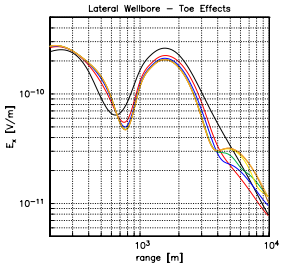

Figure 8: Secondary in-line electric field response of a lateral wellbore buried beneath 1km of sediment with a conductivity of 0.01 S/m. The wellbore has termination points at TX-LT offsets of 2000 (black), 3000 (red), 4000 (blue), 6000 (green), 8000 (yellow), 10000 (brown) and 12000 m (orange).

VERTICAL WELLBORE EFFECTS

Due to limitations imposed by the local refinement algorithm the vertical wellbore is modelled as a rectangular prism with a horizontal cross section of 25 x 25-m and conductivity of 170 S/m. The impact of the depth extent of the vertical wellbore on the secondary in-line electric field amplitude was computed, with wellbore depth-extents ranging from 600-1400 m being investigated. The results showing an increased response for larger vertical wellbore extents. Following this an investigation into the dependence of the transmitter-vertical wellbore (VW) offset were conducted, with TX-VW offsets ranging between 0-5km. The results show that as the TX-VW offset decreases the responses become increasingly larger due to the cross proximity between the highly conductive wellbore and transmitter.

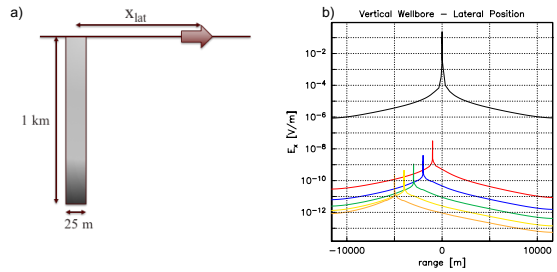

Figure 9: (a) Cross-section showing lateral position of 1km long vertical wellbore (b) Secondary in-line electric field response of a vertical wellbore embedded in sediment with a conductivity of 0.01 S/m. The wellbore has TX-VW offsets of 0 (black), 1 (red), 2 (blue), 3 (green), 4 (yellow) and 5 km (orange).

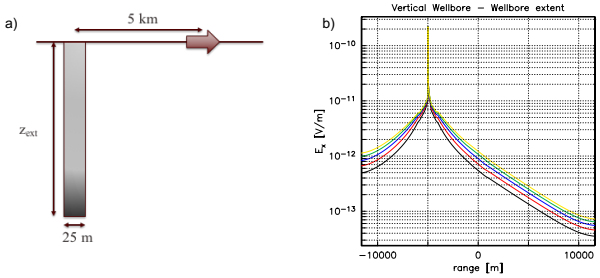

Figure 10: (a) Cross-section a vertical wellbore of length z_{ext} with a TX-VW offset of 5km (b) Secondary in-line electric field response of a vertical wellbore embedded in sediment with a conductivity of 0.01 S/m. The wellbore has extents (z_{ext}) of 600 (black), 800 (red), 1000 (blue), 1200 (green) and 1400 (yellow).

CONCLUSIONS

The CSEM signal from a fully 3D subsurface model wherein conductive fluid is forced into a fracture zone is dependent on several factors including the conductivity contrast between the fluid and the surrounding sediment and the position of the fluid-filled fracture zone with respect to the transmitter.

The signal strength from the model wherein conductive fluid spreads into increasingly larger fracture zones progressively increases with the volume of the fluid filled fracture zone, as a constant injection is applied. However, in the case where the fluid spreads after the injection is terminated, there is a trade-off, as far as the CSEM signature is concerned, between the volume of the fluid-filled fracture zone and the conductivity of the fracture zone.

The steel casing used in hydraulic fracturing projects has a profound effect on the electric field response with secondary responses from steel casing producing potentially large amplitudes depending on where the vertical wellbore is positioned with respect to the the transmitter. The depth and lateral extent of the lateral wellbore also has a large effect. Accurate information regarding the wellbore parameters must be utilized to obtain accurate interpretation of CSEM monitoring data.. In future work, the CSEM response of a composite vertical-lateral wellbore system will be modeled.

REFERENCES

Badea EA, Everett ME, Newman GA, Biro O (2001) Finite-element analysis of controlled-source electromagnetic induction using Coulomb-guaged potentials. Geophysics 66: 786-799

Patzer C, Tietze K, Ritter O (2017) Steel-cased wells in 3-D controlled source EM modelling. Geophysics Journal International 209: 813-826

Puzyrev V, Vilamajo E, Queralt P, Ledo J, Marcuello A (2017) Three-dimensional modelling of the casing effect in onshore controlled-source electromagnetic surveys. Surveys in Geophysics 38: 527-545

SWEMDI: Space Weather Electromagnetic Database for Ireland

J. Campanyà[1], P. Gallagher[1], S. Blake[1], C. Hogg[2], R. Scanlon[3], D. Jackson[4], M.Gibbs[4], D.Reay[5], D. Kiyan[2], J. Fullea[2], V. Rath[2]

[1]School of Physics, Trinity College Dublin, Dublin, Ireland. email contact: joan.campanya@tcd.ie
[2]Dublin Institute for Advanced Studies (DIAS), Dublin, Ireland
[3]Geological Survey of Ireland, Ireland
[4]Met Office, Exeter, UK
[5]Geological Survey of Northern Ireland, UK

SUMMARY

The Space Weather Electromagnetic Database for Ireland (SWEMDI) project funded by the Geological Survey of Ireland (GSI, www.gsi.ie) is currently collecting new long-period electromagnetic (EM) data in Ireland, and developing a digital database with old and new long period magnetotelluric (LMT) data that will contain key information for the understanding and constraining of Ireland's EM properties. The database will include: 1) Raw and clean LMT time series acquired in Ireland, 2) local and inter-station tensor relationships relating the EM fields measured at the same site and EM fields measured at different locations; 3) a 3-D electrical resistivity model of Ireland's lithosphere. SWEMDI database will be publically available in 2019 from GSI and EPOS (www.epos-ip.org). This database will have direct impact to the research so-called space weather hazard that solar activity can cause in ground-based infrastructures, and to the study of thermal and compositional structure of present day Ireland's lithosphere.

Keywords: Database, Space Weather, Electromagnetic, 3-D Magnetotelluric Modelling, Ireland's lithosphere.

Systematically changes in MT signal during deep drilling operations

N. Haaf[1,2], E. Schill[1,2], R. Karlsdottir[3], K. Arnason[3]
[1]Karlsruhe Institute of Technology, nadine.haaf@kit.edu
[2]Institut für Angewandte Geowissenschaften, Technische Universität Darmstadt
[3]ISOR GeoSurvey Reykjavic Iceland

SUMMARY

The Horizon 2020 project "Deployment of deep enhanced geothermal systems for sustainable energy business (DEEPEGS)" aims at demonstrating advanced engineering technologies in geothermal reservoirs under different geological conditions in Iceland and France. The concept of developing a deep EGS well at Reykjanes comprises injection of fluid underneath the conventional geothermal field to support production. Therefore, the 2,500 m deep RN-15 production well was deepened to 4,659m depth in the framework of the Icelandic Deep Drilling Program (IDDP-2) from August 2016 until January 2017. The drilling progress was slowed down due to partial and up to total circulation loss. Below 3,200 m total circulation loss indicates a highly permeable zone and led to total lack of cuttings

The continuous magnetotelluric monitoring of injection of drilling fluid at comparably high flow rates is resented in this study. Magnetotelluric monitoring during fluid injection may reveal information on the directional development of the reservoir and the evolution of preferential hydraulic connectivity.
In September 2016, two continuous running MT stations, GUN and RAH, were installed on the Reykjanes peninsula. RAH and GUN are located about 6 and 1 km away from IDDP2. Both MT stations are equipped with two electric dipoles in N-S and E-W direction, as well as three magnetic sensors oriented in N, E and vertical direction. Magnetotelluric monitoring was carried out between December 2016 and July 2017 with a sampling frequency of 512 Hz. The processing of the first data from the late drilling phase revealed the bad data quality of RAH hence it was stopped in May 2017. Consequently, MT data were processed using single site method.
First results from the late drilling period reveal changes in the resistivity distribution over time. Prominent changes were in particular noticeable about 24-48 hours before seismic events occurred. Further observations of a decrease in resistivity correlates with days of loss of circulation fluids. In general, most of the changes are observable in the YX-component of the transfer functions suggesting a directional dependency. However, for final interpretation, different possible sources of the signal changes will be investigated such as comparison with the variation of the Earth's magnetic field.

Keywords: Magnetotelluric, Monitoring, EGS, DEEPEGS, Iceland

Temporal and spatial variability of space weather driven telluric fields in Northwestern Russia

D. Epishkin[1], V. Pilipenko[2,3], E. Sokolova[2], Ya. Sakharov[4], N. Yagova[2], and V. Selivanov[4]
[1]"Nord-West" Ltd, Moscow, Russia, dmitri_epishkin@mail.ru
[2] Institute of Physics of the Earth, Moscow, Russia
[3] Geophysical Center, Moscow, Russia
[4] Polar Geophysical Institute, Apatity, Russia

Magnetic storms and substorms have a potential to cause serious failures of space and ground technological systems. The investigations of space weather effects at high latitude are of great importance for mitigation possible risks connected with threats to electric power supply infrastructure caused by geomagnetically induced currents (GICs). The potential difference due to telluric fields is responsible for GICs in grounded electric power systems. Monitoring of the geomagnetic field variations are carried out by world-wide array of magnetometers, while regular long-term observations of GICs and telluric electric fields still are not so common and need more consolidated efforts.

We present the first results of the analyses of temporal and spatial variability of telluric electric fields in the Eastern Fennoscandia and their comparison with available GIC measurement in electric power grids. We calculated "synthetic" telluric fields from the IMAGE geomagnetic records via the impedance relationship (plane wave approximation of the external field). The information on impedance tensors is provided by the deep electromagnetic array BEAR performed over the Shield. We also use some magnetotelluric data from sites in the North-western Russia.

The elaborated algorithm of telluric E(t) field synthesis for a geomagnetic field variations H(t) uses standard frequency domain relationship between electric and magnetic fields via the complex impedance tensor Z(f). The Fourier transform is applied for magnetic records in a running time window $W(\tau)$ to produce a set of spectral estimates of H(f) and corresponding spectral estimates of telluric field $E(f)= Z(f)*H(f)$. Inverse Fourier transform performed for each running window results in estimation of $E(\tau+dt(i), i=0,n)$, where dt(i) is a time shift from the beginning of the record. Thus for a specific moment of time we have several electric field estimates, which are averaged to get final synthetic electric field time series E(t). The program was successfully tested on the synthetic magnetic and electric fields of COMDAT project. The preliminary results include:

(a) the analyses of E-field variations (intensity and polarization) at several sites for selected space weather events: magnetic storm, substorm, and Pi3 pulsations.

(b) analyses of induced telluric field dependence on the local geoelecrical structure: comparison of E-field disturbances for several sites with contrasting geoelectric parameters in Eastern Fennoscandian Shield with its complicated deep conductivity pattern: from resistive Archaean domains to conductive Palaeoproterozoic mobile belt (Lake Ladoga conductivity anomaly);

(c) The modelling results have been compared with observations of the system to monitor GIC in electric power lines deployed at Kola Peninsula and Karelia by the Polar Geophysical Institute and Center for Physical and Technical Problems of North's Energetic. The E-fields synthesized from data of IMAGE stations via local impedances have been compared with GIC measurements at nearest sites.

Keywords: synthesis of telluric fields, Eastern Fennoscandian Shield, GIC, space weather

Acknowledgements: We acknowledge the data from IMAGE array, BEAR project, and support by grant № 16-17-00121 from the Russian Science Foundation and grant №16-05-00543 from the Russian Foundation for Basic Research.

Temporal variation in the resistivity structure of Aso volcano, Japan, over the magmatic eruptions from 2014 to 2015, as inferred by CSEM volcano monitoring system, ACTIVE

T. Minami[1], M. Utsugi[2], H. Utada[3], T. Kagiyama[4] and H. Inoue[5]
[1]Earthquake Research Institute, University of Tokyo, tminami@eri.u-tokyo.ac.jp
[2]Aso Volcanological Laboratory, Kyoto University, utsugi@aso.vgs.kyoto-u.ac.jp
[3]Earthquake Research Institute, University of Tokyo, utada@eri.u-tokyo.ac.jp
[4]Aso Volcanological Laboratory, Kyoto University, kagiyama@aso.vgs.kyoto-u.ac.jp
[5]Aso Volcanological Laboratory, Kyoto University, hiroyuki@aso.vgs.kyoto-u.ac.jp

SUMMARY

During the last eruption period of Aso volcano (November 2014 to May 2015), a controlled-source electromagnetic volcano monitoring experiment was conducted, using ACTIVE system (Utada et al., 2007). ACTIVE system installed at the first Nakadake crater of Aso consisted of a transmitter located northwest of the crater with four receiver stations of vertical induction coils before the eruptions and three during and after. Several campaign observations of ACTIVE around the first Nakadake crater succeeded in detecting temporal variations in the resistivity structure over the magmatic eruption period. Response variations started in November 2014 has a peak in February 2015 and slightly returned to the values before the eruptions in August 2015. An unstructured tetrahedral finite-element three-dimensional (3-D) inversion was used to interpret temporal variations in the ACTIVE response, accounting for topographic effects. The 3-D inversions revealed that temporal variations in the ACTIVE response are attributed mainly to a broad increase in resistivity at the peak elevation of 750 m to 850 m, present not only just beneath the crater bottom but also outside the crater. The increase in resistivity can be ascribed to decrease of the amount of conductive groundwater in the upper part of the aquifer located at the elevation lower than 800 m. Below the crater, the increase in resistivity is smaller, potentially suggesting magma filling the conduit below the crater. This study demonstrates that 3-D modelling of ACTIVE responses can be effective in understanding temporal variations of volcanic hydrothermal systems. In the presentation, we also plan to share interpretation of ACTIVE data obtained in August 2017, when Aso had already returned to eruptive quiescence.

Keywords: Aso, CSEM, ACTIVE, volcano, inversion

The Cloncurry magnetotelluric survey

J.M. Simpson[1], J. Duan[2] and L. Wang[2]
[1] Geological Survey of Queensland, Department of Natural Resources, Mines and Energy, Queensland Government, PO Box 15216 City East, Queensland Australia 4002, janelle.simpson@dnrm.qld.gov.au
2 Geoscience Australia, Cnr Jerrabomberra Ave and Hindmarsh Drive, Symonston ACT 2609

SUMMARY

In 2016, the Geological Survey of Queensland partnered with Geoscience Australia to collect a high-resolution magnetotelluric survey in the Eastern Succession of Mount Isa in Queensland, Australia. The survey was designed to support the mineral exploration industry by providing information about variation in crustal resistivity. The survey area also encompasses the Ernest Henry mine, a Cu-Au-Ag-Fe gold mine associated with pervasive hydrothermal alteration.

Data were acquired at 476 sites in an area of approximately 40 km x 60 km to the north of Cloncurry in western Queensland. Data were acquired on a regular 2 km grid and each site was occupied for a minimum record time of 16 hours. Phoenix instruments were used to record two orthogonal electric field and three orthogonal magnetic field at each site. Phoenix MTC-150L coils were used to collect magnetic field data, and electric field data were collected by single conductor wires and non-polarizable electrodes with a dipole length of 100 m. Data were processed with Phoenix SSMT2000 software using remote reference station data to improve data quality.

Two-dimensional and three-dimensional inversion of the dataset was undertaken using WinGLink and ModEM 3D inversion codes. An elongate N-S striking conductor was imaged along the eastern margin of the survey, a feature which coincides with the known location of the Carpentaria Conductivity Anomaly. The western part of the model has a resistivity greater than 1000 Ω·m to a depth of approximately 12 km, below which the resistivity decreases. A prominent conductor also is imaged under the location of the Earnest Henry mine. Sensitivity analysis indicates model features are well constrained to a depth of approximately 20 km.

Keywords: magnetotelluric, conductivity, mineral

The physical-geological model of the LS-epithermal Au-Ag deposit (Chukotka) on the result of AMT data integration

E. Ermolin[1], O. Ingerov[2], A.A. Savichev[3], M. Smirnov[4]
[1]"GM-Servise" Ltd, e.ermolin.gms.@gmail.com,
[2]"Phoenix-Geophysics" Ltd, olexandr_ingerov@yahoo.ca
[3]"Saint-Petersburg Mining University", a_savichev@mail.ru
[4]"Lulea University of Technology", maxim.smirnov@ltu.se

SUMMARY

The main objective of the study is to explore the extension of the epithermal quartz gold-bearing vein. The object is located within the Kimmerides of the Okhotsk-Chukotka volcanic belt (Russia). The vein is 500 meters long and 3 meters wide and covered by 100 meters of volcanic rocks. The complex of geophysical methods including AMT soundings, ground gravity and magnetic surveys were performed. The results show that the main vein appears as a resistive zone having a deep channel. In the gravity field it appears as having increased values of the gradient. The 3D inversion of magnetic data has distinctive increase in magnetization coinciding with the location of the body. The regular alteration of the chemical elements associations is observed from the South to the North: sub-ore (Mo-Cu) → ore (Au-Ag-As) → supraore (Sb-Hg). The physical-geological model of the epithermal quartz gold-bearing vein is suggested. The position of northern extension of the vein is obtained as a result of the integrated data analysis. This position was later confirmed by drilling.

Keywords: Magnetotellurics, LS-Epithermal gold, integrated geophysics data interpretation, alternation zone.

INTRODUCTION

There are a lot of medium and large gold-silver epithermal deposits concentrated in the Far East of Russia. As a rule, the richest ores belong to LS-type, with dominance of quartz-vein ore (Hedenquist et al. 2000). Separate ore veins with the thickness of several meters can have up to 1 km in length and consist of 10 - 15 tons of gold. If these veins are satellites of large already workable deposits, their exploration can be economically justified even in case of their being covered by more than 100 meters of volcanic rocks. The prospecting of these objects (3 m thick vein at 100 m depth) is a challenging exploration target and, at the first glance, none of separate geophysical method can cope with it.

In 2013 the authors were given a target to determine the northern extension of the known vein zone on the large ore cluster within the Okhotsk-Chukotka volcanic belt (Figure 1a). This low-sulfidation epithermal quartz vein with the thickness of 3 m has a high concentration of gold (15-20 ppm). The vein is located inside the intermediate- mafic Late Cretaceous lavas and covered by 100- 130 meters of mafic volcanic rocks with layers of ash tuffs. To determine the position of the displaced northern part of the vein, the AMT measurements was performed. In addition, the induced polarization (IP) and resistivity data were acquired, which could not identify the vein covered by conductive tuff layers. According to AMT results the new vein position has been proposed which was confirmed by drilling in 2014. The AMT results were described detailed in the early work (Ermolin et al. 2014).

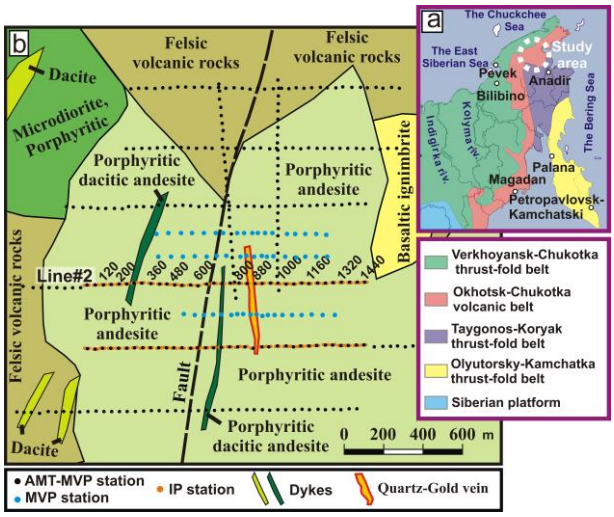

Figure 1a. The position of the investigation region on the tectonic scheme (Tceysler V. M.). **Figure 1b.** The geological scheme of the investigated area.

The target of the current work is to demonstrate the features of geophysical methods (AMT, ground gravity and magnetic survey) by means of which the covered thin vein zone can be determined. The physical-geological model of epithermal gold-bearing quartz vein is positioned by the authors as the main result.

THE GEOLOGICAL MODEL AND SUPPOSED PHYSICAL PROPERTIES

We propose the following geological model of epithermal LS-deposit:

- the source of the fluids as a magmatic rock body of felsic-intermediate composition is necessary (it is usually located on the deposit periphery);
- the presence of the channel for fluids migration is required (deep fault zone);
- impenetrable solid rock block is needed for fluid crystallization in the ore within a thin zone, rather than dissipate in reservoir rocks;
- epithermal veins are accompanied by zone hydrothermal-metasomatic alterations (quartz-adulatory alteration and propylitic lateral zones).

The large fault zones usually correspond to geological block contacts and might be clearly reflected in gravity and magnetic anomaly fields. The zones of the propylitic and quartz-adularia alteration are poor in magnetite relatively to host medium (Sillitoe 2010). Correspondingly, alteration zones are described as the zones of decreasing magnetic susceptibility. It is very likely that the vein and the area of quartz-adularia alterations around it will be both characterized by high resistivity. Therefore, the complex data analysis of AMT-MVP, ground gravity and magnetic survey would be beneficial for detection of the vein.

DATA ANALYSIS

The features of the geophysical response of the vein zone shown in figure 1b divided into two groups: I. - appearance of ore controlling fault; II. – appearance of the ore bodies and the alteration zone around them.

I. Ore controlling fault. The map of magnetotelluric impedance phase at the 300 Hz frequency is shown in figure 2a. The area is divided into two approximately equal parts (East and West) by a sub-meridional fault zone and is well seen on the phase data. The fault is also obvious on the total horizontal gradient of the Bouguer map (gravity data transformation) as the contrast positive anomaly (Figure 2c).

II. Ore bodies and the alteration zone. In figure 2a the central elongated sub-meridional zone of impedance phase of low values attracts special attention. It is located to the east of the fault. The zone consists of three segments, which displace to 120-300 m to the east relative to each other from the south to the north. The central segment is connected with the quartz gold-bearing vein. Its position had been known from before. The position of the northern and the south-western phase anomaly segments corresponds to the position of the veins determined after drilling in 2014 (after AMT work). The local anomalies of horizontal telluric tensor (Figure 2b) also reflect the veins and quartz-adularia alteration position.

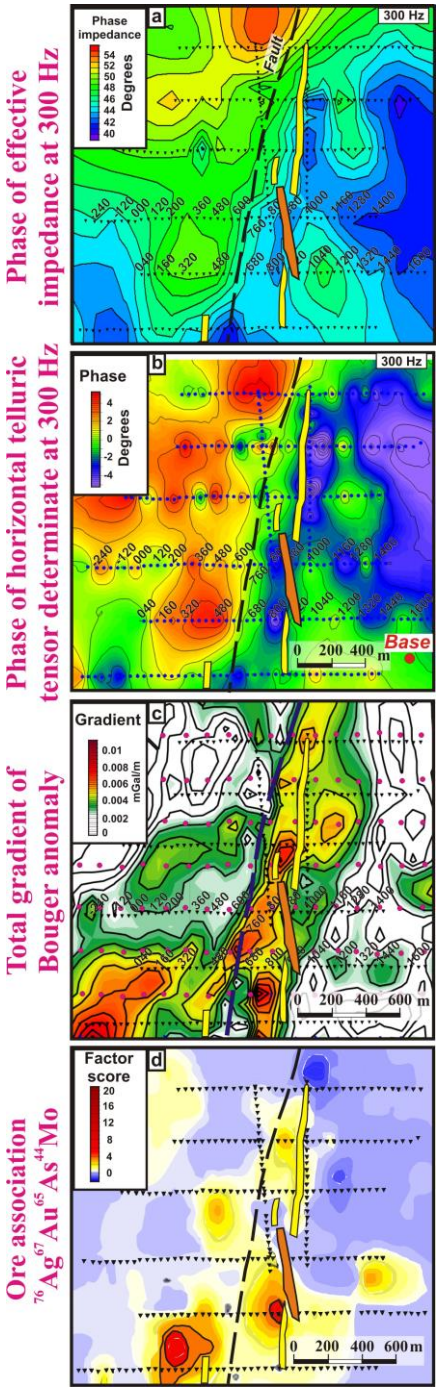

Figure 2. Magnetotelluric phase (a); Phase of horizontal telluric tensor determinant (b); gravity gradient (c), lithogeochemistry analysis results (d).

The analysis of the graphs of parameters and geoelectrical cross-section along line#2 is shown in figure 3. The position of the quartz-adularia mineralization appears on the geoelectrical

cross-section as the high resistivity area (Figure 3-III, blue-purple area within 0760-1000 stations on the altitude from 450 to 200 m). Gold-bearing veins are concentrated inside the area of the peak resistivity values (the purple area). The zone has a deep channel which also appears as the isolator for the depth of at least 1 km. The suits of ash tuffs, which cover the ore zone, appear as low resistivity layers at the altitudes from 600 to 400 m.

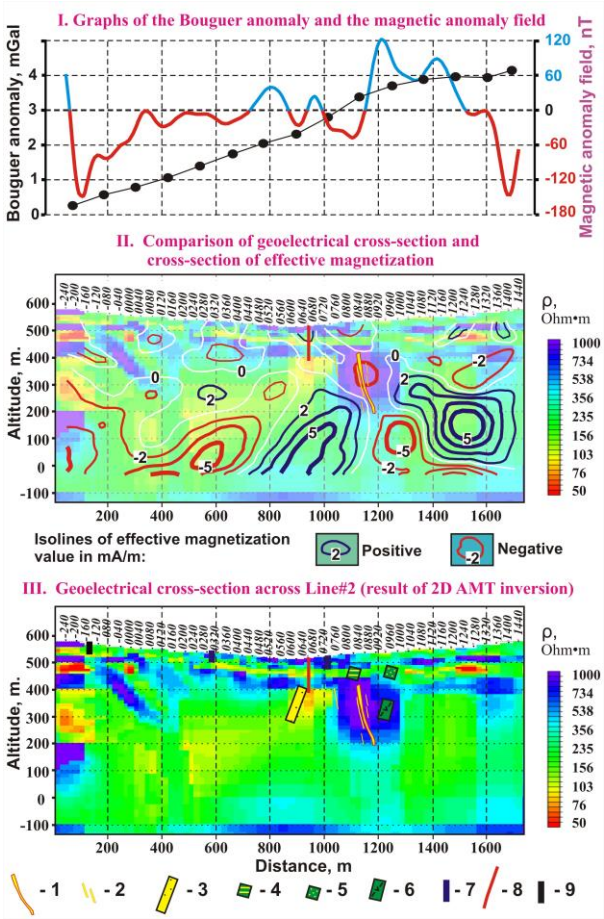

Figure 3. Geophysical data comparison. Legend for 3-III: lithology by drilling data (1-6): 1 – the main gold-bearing vein, 2 – thin gold-bearing veins, 3 – ash tuffs, non-altered, 4, 5 – strongly altered lavas (4) tuffs (5), 6 – porphyritic andesite. Geology mapping data (7-9): the dykes of andesite, 8 – fault, 9 – the rhyolite and andesite contact.

The 3D visualization of the result of 2D inversion (geoelectrical cross-section) is shown in figure 4a. The gold-bearing vein zone is located inside the resistive zone. The zone width increases to the South. In the north veins drop down and shift to the East.

The 3D inversion result is shown in figure 4b. The South part of the vein zone appears in the 3D inversion better than in 2D inversion results. Unfortunately, the part of the vein zone situated deeper than 300 m hardly ever appears on the results of 3D inversion.

Ground magnetic survey. The circum-ore zone of alteration is clearly indicated in the anomalous magnetic field (Figure 3-I, red-blue line). Above the ore zone the apparent bi-polar anomaly is observed. Isolines of effective magnetization (result of the ground magnetic survey inversion) are drawn on the geoelectrical cross-section. The negative values are shown with red lines, while the positive values are shown with blue. The alteration zone appears as the contrast area of negative values of effective magnetization. By analogy with resistivity values, the zone of low values has a deep channel and easterly dip.

Lithogeochemical survey by secondary dispersion halo had been done on the investigated area before 2013 in 20x200 meters step. The re-interpretation of its results was carried out using principal components factor analysis. The distribution of the main ore assemblage Au-Ag-As-Mo is shown in figure 2d. The poly-element anomaly consisting of three segments detects the position of the known veins.

PHYSICAL-GEOLOGICAL MODEL

The integrated analysis of the above discussed data has shown that the ore controlling fault and the known vein zone with the thickness of 3 m covered by 100-meters shield are clearly visible in geophysical fields.

The ore control faults (block boundaries) appear as the zones of:

- increased gradient of the gravity anomaly in Bouguer reduction;
- increased gradient of the magnetotelluric impedance phase.

Quartz-adularia mineralization around vein appears as the zones of:

- increased values of resistivity on the geoelectrical cross-sections. The zone has a deep channel;
- decreased values of the effective magnetization;
- decreased values of the effective phase of magnetotelluric impedance;
- decreased values of the invariant phase of horizontal telluric tensor;

The above mentioned features can be called “geophysical structural-prospecting criteria”. The classical zoning was determined (confirmed) on the basis of geochemical survey: bottom-ore (Mo±Cu) → ore (Au-Ag-As) → upper-ore (Sb-Hg). The described geophysical and geochemical features reflect the physical-geological model of epithermal quartz-vein of LS-deposit.

CONCLUSIONS

As a result of integrated analysis of geophysical and lithogeochemical survey data, the North extension of the known ore vein was predicted in 2013. The prognosis was confirmed by drilling in 2014. The physical geological model of the epithermal quartz-vein gold deposit is suggested. This model can be used by geologists and geophysicists in future prospecting surveys. The following suit of geophysical methods for searching of gold-bearing quartz veins in Chukotka has been suggested by the authors: audiomagnetotelluric sounding (AMT), ground gravity and magnetic surveys. The selected suit of methods is based on measuring naturally occurring fields and makes little environmental impact.

ACKNOWLEDGEMENTS

We acknowledge the support of the Mining Community in Chukotka for access and the opportunity to publish.

REFERENCES

Berdichevsky MN and Dmitriev VI (2008) Models and methods of magnetotellurics. Springer-Verlag, Berlin, Heidelberg

Ermolin E, Ingerov O, Savichev A (2014) Gold exploration in Chukotka region by using audiomagnetotellurics. 22-th EM Induction Workshop Weimar, Germany, 24-30 Aug.

Hedenquist JW, Arribas AR, Gonzalez-Urien E (2000). Exploration for Epithermal Gold Deposits. SEG Reviews, V. 13: 245-277.

Sillitoe RH (2010) Porphyry Copper Systems. Economic Geology.

Ingerov O et al. (2009) Non-grounded Surface Electroprospecting Technique. 70-th EAGE annual Conference. Amsterdam #6149

Rokityansky II (1982) Geoelectromagnetive Investigation of the Earth Crust and Mantle. Spinger-Verlag, Berlin, Heidelberg

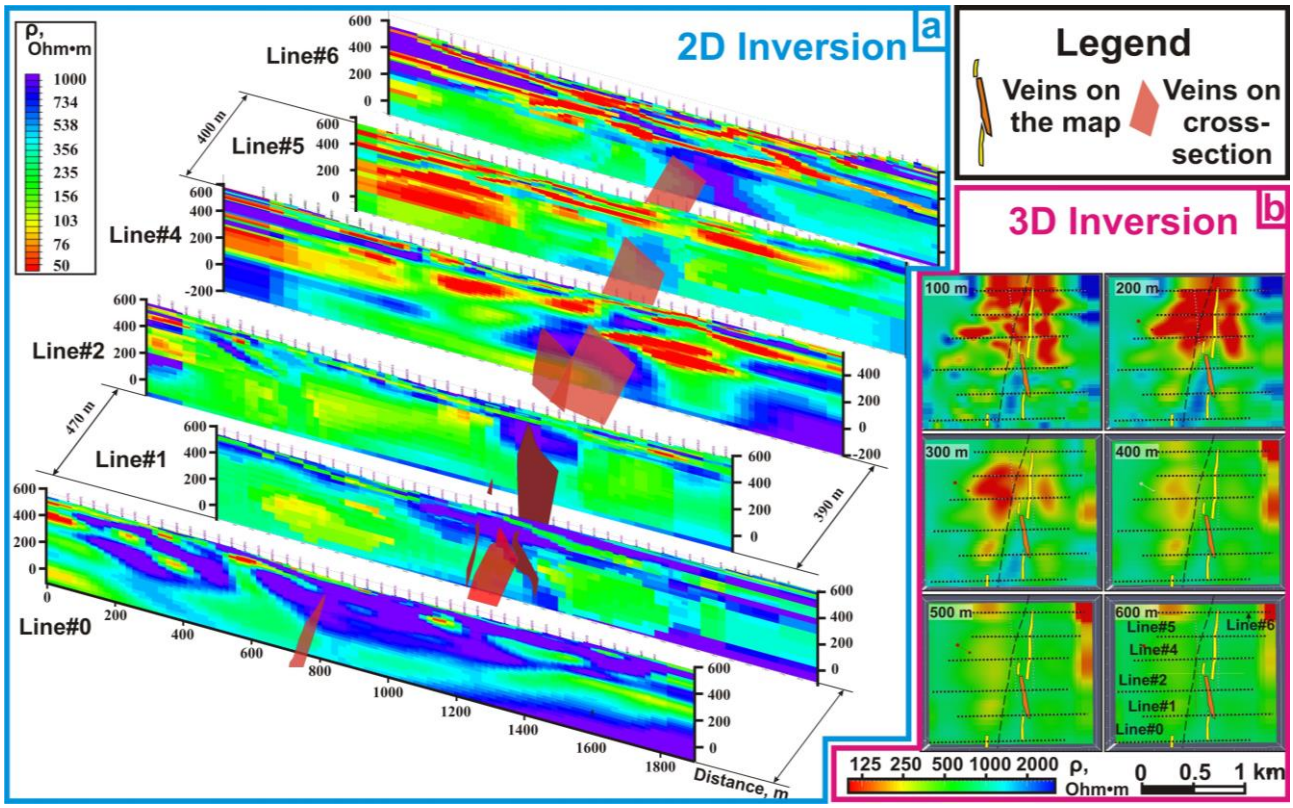

Figure 4. AMT inversion results: a – 3D visualization of the results of 2D inversion of AMT and MVP data (geoelectrical cross-sections). b - 3D inversion result of MT data (slices of 3D model).

The technique and results of joint EM data interpretation: paleovalley exploration case study

Victor Kulikov[1,2], Elena Aleksanova[1], Aleksey Bobachev[2],
Anastasia Solovieva[1], Nikolay Shustov[2]

[1] Nord-West Ltd., Moscow, Russia, alex-len@inbox.ru
[2] Moscow State University, Moscow, Russia

SUMMARY

The technique and results of the joint interpretation of EM data along two lines across paleovalley are presented. The paleovalley is located near Aleksandrovka Geophysical Field Camp in Kaluga region (Russia) and EM data was acquired during summer field courses for students of Moscow State University. EM methods using in this survey were: 1) vertical electrical sounding with induced polarization (VES-IP), 2) time-domain electromagnetic sounding (TDEM) and 3) audio-magnetotelluric sounding (AMT).

Interpretation of apparent resistivity curves obtained for layered geological section, allows defining some parameters, which have a narrow range of equivalence. They are different for direct current methods (VES) and low-frequency induction methods (TDEM, AMT). If the geological section consists of alternation of thin layers with different resistivity, in order to satisfy the observed data of both groups of methods, it is necessary to set, in addition to the resistivity of the layer, its anisotropy or to increase the number of layers. The possibilities and advantages of joint interpretation of apparent resistivity curves for VES and TDEM using special version of IPI 2 Win software are shown.

The results of joint interpretation of EM data showed that the TDEM data determines the position of the roofs of the low-resistivity layers and the VES data determines the thickness and the resistivity of high-resistivity layers. The upper part of the resistivity image obtained from joint interpretation VES and TDEM data was used as the starting model for 2D inversion of AMT data.

Thus, the joint interpretation of the TDEM and VES curves makes the range of possible equivalent resistivity models considerably narrower and allows obtaining new and more reliable information about the resistivity structures than using each of the data of the methods separately. Involving AMT data to the interpretation allows increasing depth of investigation.

Keywords: equivalent models, VES, TDEM, AMT, joint interpretation, paleovalley

Three-dimensional characterization of the geothermal systems in the southern margin of the Gediz Graben (western Turkey) inferred from magnetotelluric data

Ahmet Tugrul Basokur[1], Naser M. Meqbel[2], Özlem Hacioglu[3,4] and Halil I. Arslan[5]
[1]Ankara University, Faculty of Engineering, Department of Geophysical Engineering, Ankara, Turkey, basokur@ankara.edu.tr
[2]Consulting-Geo, Germany, meqbel@consulting-geo.com
[3]Boğaziçi University Kandilli Observatory and Earthquake Research Institute, Istanbul, Turkey, ozlem.cengiz@boun.edu.tr
[4]Karadeniz Technical University, Faculty of Engineering, Department of Geophysical Engineering, Trabzon, Turkey, ozlem.cengiz@ktu.edu.tr
[5]Lemnis Geosciences, Ankara University Technological Development Center, E Blok Nbr:B54 Golbasi, 06830 Ankara, Turkey, halilibrahimarslan@gmail.com

SUMMARY

The western Turkey has abundant number of hot springs resulting from the extensional tectonic regime. The main geothermal fields are developed at the flank of east-west grabens that controlled by normal and detachment faults. Gediz graben is one of the most important area in view of temperature and production rate. Since three-dimensional magnetotelluric interpretation of geothermal systems is a powerful tool for characterization of the deep electrical resistivity structure of geothermal reservoirs with high resolution and accuracy, two magnetotelluric (MT) surveys, namely Salihli hot spring and Girelli field, were performed in the southern flank of Gediz Graben to explore structurally controlled geothermal activities. The MT surveys reveal that the reservoir characteristics of the survey areas differ from each other.

The purpose of the MT survey in Salihli area was to search for additional geothermal sources to enlarge the city heating system. Three-dimensional (3D) inversion of MT data consisting of 74 stations has been performed using ModEM software. The resulting models show that the interface between the sedimentary cover and underlying metamorphic basement has been well delineated due to high resistivity contrast between them. A low resistivity zone associated with the hot spring is situated at shallow part of the resistivity section indicating that the reservoir is probably generated by outflowing along the detachment fault from the base of the graben system and accumulated in the permeable and high porosity sedimentary layers. Towards the west part of the study area, another high conductivity zone is also imaged. This zone can be interpreted as altered rocks of the active geothermal fluid upwelling along the detachment fault or clay sedimentary rocks above the reservoir.

The MT data acquired in Girelli field consists of 27 sites. We have performed various 3D inversions of the collected MT data using the ModEM software. The final resistivity model indicates a good correlation between electrical resistivity distribution and Girelli segment of the detachment fault that controls structural features of the area. The NW-SE directed low resistivity zone interpreted as a fractured hydrothermal system buried at a depth range of 2000-2500 meters and the high resistivity region represents schist-gneiss and Triassic granitic rocks of the metamorphic massif. This contrast indicates the orientation of the north dipping low-angle detachment fault. The hydrothermal area appears to be closely link to conductive zone delineated in three-dimensional model and is spatially coincident with the intersection of the detachment fault and high angle normal faults existing in the study area.

Keywords: Magnetotellurics, Inversion, Geothermal, Western Turkey, Gediz Graben.

Three-dimensional electrical structure of the crust and upper mantle in north-eastern Sweden, using the magnetotellurics method

R. Vadoodi[1], T.M. Rasmussen[1], T. Korja[1] , M.Yu. Smirnov[1] , U. Autio[2] and T.E. Bauer[1]
[1]Luleå University of Technology, Sweden, roshanak.vadoodi@ltu.se
[2]University of Oulu, Finland

Complementary magnetotelluric measurements have been done in northern Sweden in order to investigate in more detail the spatial distribution of a previously mapped NW-SE trending electrical conductor of more than 3000 S in the lower crust. The previously mapped conductive structure was indicated in the Kiruna area and modelled by Cherevatova et al (2015) in a Fennoscandian Shield scale study. The character of this anomaly is unusual when viewed in a global perspective but has interesting similarities to some other electrical conductivity models of tectonic boundaries within the Archaean and the Proterozoic. Four new profiles consisting of 45 broad-band (BMT) magnetotelluric sites were acquired in the period range of 0.001 s to 1000 s in the summers of 2015 and 2017. The geology of the area consists of two distinct units: the Karelian domain (2.4-1.96 Ga) and the Svecofennian domain (1.96-1.78 Ga), whereas the latter can be subdivided into two major phases of crustal growth (1.96-1.87 Ga and 1.80-1.77 Ga). The Karelian rocks towards east along the Swedish-Finish border are mainly composed of metasedimentary and mafic volcanic rocks (Martinsson 1997). Svecofennian rocks are dominated by felsic and mafic volcanic rocks, related intrusive rocks and volcanosedimentary and sedimentary rocks.

Data processing was performed using a robust multi-remote reference technique (Smirnov, 2003). Data quality is generally high due to the absence of nearby infrastructure. Strike and dimensionality analysis was performed before selecting sites for the 2D inversion. Since the phase tensor is independent of the galvanic distortions (Caldwell, 2004), we used this approach to estimate strike direction. At short periods most of the sites exhibit reasonably 2D behaviour with stable strike estimates and skew angle (beta) below 3. However there are obvious 3D effects in the data at longer periods. We have also examined the behaviour of the Q-function misfit for various strike directions. This resulted in identified principal direction of N30W with ambiguity of 90 degrees. Taking into account the previously modelled anomaly is striking NW-SE we have selected a profile direction of N60E for modelling, i.e. roughly perpendicular to its strike. In total 60 stations including 19 from the previous campaigns of the MaSca project (2011-2014) were selected for 2D inversion along four profiles. We performed 2D inversion of the determinant and bimodal TE+TM modes using the REBOOC algorithm (Siripunvaraporn and Egbert., 2000). In most cases we could fit the data. The models compare very well with each other, however there are number of anomalies which are not easily explained due to the fact that they are not coherent between the profiles.

3D inversion using the ModEM program (Egbert et al., 2012) has been performed. At the first stage, we selected 44 sites in the area close to the anomaly. The best fitting model was obtained with normalized data misfit of 1.8 based on an error floor of 5%. The slices from the 3D model were then compared with 2D inversion results. In both type of models, Svecofennian intrusive and supracrustal rocks range from the surface downward to about 20 km in some parts of profiles. The most likely explanation of the deep conductor is that this is associated with graphite in the lower crust. In some part of 3D model, shallow conductors are correlated with metasedimentary supracrustal rocks. The conductors in the middle crust at the north-eastern part of the profiles can be interpreted as the continuation of the Kittilä conductor located in the Central Lapland Greenstone Belt (CLGB). This conductor is related shear zones with abundant hydrothermal alteration and mineralizations and locally graphite-bearing shear zones but more detailed interpretations with geology will be presented in future. The 2D models correspond to 3D inversion results, confirming the main interpretational findings. However, the large area has very sparse coverage of MT sites and therefore additional sites will be measured during the summer 2018 and will be included in the presentation.

Keywords: Magnetotellurics, 2D and 3D inversion, Fennoscandian Shield

Three-dimensional Imaging of Rare-Earth Deposits in the Eastern Mojave Desert, California with Magnetotellurics

J. R. Peacock[1], K. M. Denton[2] and D. A. Ponce[3]
[1]U. S. Geological Survey, jpeacock@usgs.gov
[2]U. S. Geological Survey, kdenton@usgs.gov
[3]U. S. Geological Survey, ponce@usgs.gov

SUMMARY

Rare earth elements (REEs) are crucial to the development of innovative and emergent technologies worldwide. Increasing application and demand of REE commodity trends have prompted necessary exploration efforts of these critical mineral resources. Focused studies and characterization of REE terranes plays a vital role in identifying and understanding the geologic context inherent and unique to REE deposits. Economic REE deposits are uncommon, they are typically derived from magmatic and/or hydrothermal processes that form in alteration zones, often as concealed intrusive structures. Magnetotelluric (MT) methods are ideal exploration tools for studying REE landscapes, because electrical resistivity is sensitive to the more conductive zones of mineralization and alteration that are associated with REE deposits. Once targets are found, full characterization of the deposit is needed, requiring three-dimensional modeling using complimentary geophysical data as constraints, like potential field data and geological information. Two examples are presented using MT data to create a 3-D electrical resistivity model using ModEM, one from Mountain Pass, California, the largest light REE deposit in the contiguous United States, and another from Music Valley, California. These two deposits lie within a known larger northwest trending Proterozoic alteration belt that extends along the southeastern boundary of California, suggesting a potential structural link. At Mountain Pass 60 MT stations were collected in an area of 50 km x 15 km, confined by land access and topography. The geology is complicated, but generally the REE deposit resides in a series of 1.4 Ga carbonitite dikes that appear more conductive than the host 1.7 Ga gneiss. The resistivity model suggests that a conductive body extends west-southwest of the existing open-pit mine to a depth of 1.5 km that maybe associated with intrusion of the REE. A large Mesozoic thrust fault may offset the deposit from its deeper crustal root, making it difficult to interpret intrusion paths from the lower crust to the upper crust. Additional alteration features are apparent to the north of the deposit that could be another potential target. At Music Valley, 60 MT stations were collected over an area of 30 km x 20 km. Multiple alteration events at 1.7 Ga and 1.4 Ga are coeval with REE enrichment. Again, these deposits are demarcated by enhanced conductivity (~ 70 Ohm-m) relative to the host rock, and tectonic activity post deposition has made it difficult to locate deeper crustal structures associated with the deposits. This work is still preliminary and more modeling needs to be done. Enhanced conductivity of these two deposits is related to mineral composition, however at present which mineral phase is controlling conductivity is unclear requiring more investigation using other geophysical data and lab measurements.

Keywords: Magnetotellurics, Rare-Earth elements

Three-dimensional inversion of semi-airborne data collected over an ancient antimony mine in the Saxothuringian zone

M. Cherevatova[1], M. Becken[1], C. Nittinger[1], A. Steuer[2], T. Martin[2], U. Meyer[2], P. Yogeshwar[3], W. Mörbe[3], R. Rochlitz[5], T. Günther[5], M. Schiffler[6], R. Stolz[6], U. Matzander[8], M.Yu. Smirnov[9] and DESMEX WG[1,2,3,4,5,6,7,8]

[1]Institute of Geophysics, University of Münster, Germany, maria.cherevatova@uni-muenster.de
[2]Federal Institute for Geosciences and Natural Resources, Germany
[3]Institute of Geophysics and Meteorology, University of Cologne, Germany
[4]Institute for Mineralogy, Technical University Freiberg, Germany
[5]Leibniz Institute of Applied Geosciences, Germany
[6]Leibniz Institute for Photonic Technologies, Germany
[7]Supracon AG, Germany
[8]Metronix GmbH, Germany
[9]Luleå University of Technology, Sweden

We present a new semi-airborne frequency-domain electromagnetic (EM) system being developed and successfully tested within the DESMEX project (Deep Electromagnetic Sounding for Mineral Exploration). The semi-airborne approach relies on the fact that part of the system is positioned on the ground and the rest is airborne. This allows us to take advantages of both ground and airborne techniques. In particular, a high-moment transmitter can be installed on the ground, therefore stronger EM field can be injected and induced in the sub-surface. Moreover, galvanic coupling is possible. The airborne receivers allow easier, significantly faster, denser and more uniform spatial coverage of the study area. In our implementation, transmitters and electric field receivers are installed on the ground. The magnetic field sensors, such as commercially available fluxgate, total field magnetometers, as well as newly developed induction coils and Superconducting Quantum Interference Devices (SQUID) are installed on a helicopter-towed bird. A typical transmitter that we consider, represent a 1-2km long grounded electric dipole, with a time-varying current of 15-27A injected at base frequencies of 7.5Hz and 10.4Hz, depending on the transmitter used. Such high-moment sources allow to achieve a penetration depth of about 1km and cover an area of 3km x 6km (with dense line spacing) in one flight (~ 2hrs).

Here, we focus on the results of two semi-airborne experiments (2016, 2017) performed in a selected area with ancient antimony mining, located in the Saxothuringian zone (eastern Germany). During these campaigns, the system performance was tested, and the most optimal survey design was determined. In particular, it is beneficial to perform repeated/overlapping flights for different transmitter positions. As a result, the most uniform and dense data coverage can be obtained (without data gaps around source position). Additionally, some regions are better covered providing two or more transfer functions (TF) from different sources.

The flight data processing requires two main steps: motion noise correction (due to vibrations and pendulum-like behavior of the bird) and the TF estimation: $\mathbf{B}(f) = \mathbf{T}(f)\,\mathbf{I}(f)$. In general, the fluxgate data are superior in the frequency range from 1Hz to 300Hz, whilst induction coil data are more reliable at higher frequencies from 100Hz to 3kHz. The 3D semi-airborne inversion models (from different flight areas) are obtained for vertical component TF in the frequency range from 10Hz to 1500Hz. The data are fitted within the error bars, with rather random distribution of the data misfit across sites and frequencies.

The 3D inversion models represent several conductive anomalies, down to a depth of 1km. The study area is remarkable for its deposits of the antimony mineralization. Antimony is presumably genetically associated with the formation of the black shales, which are sub-divided into the upper, phosphorite-bearing and lower alum shales. Therefore, enhanced conductivity in the study area can be explained by the presence of the alum shales. The location of the conductive anomalies matches well the surface geology, representing outcrops of the alum shales to the surface. The resulting model is comparable with other geophysical results, such as 2D electrical tomography model, 1D helicopter-borne EM models and 1D long-offset time-domain models. In order to verify the newly developed semi-airborne technique, these geophysical surveys were conducted by the DESMEX WG prior or at the early stages of the DESMEX project and can be used for verification.

Keywords: semi-airborne electromagnetics, CSEM, 3D inversion, mineral exploration

Three-dimensional modeling of magnetotelluric data in El Tatio - La Torta Geothermal system, North Chile

Ariel Figueroa[1 3], Daniel Diaz[2 3]
[1]Departamento Geofísica, Universidad de Chile, ariel.figueroac@ug.uchile.cl
[2]Departamento Geofísica, Universidad de Chile, ddiaz@dgf.uchile.cl
[3]Centro de Excelencia en Geotermia de Los Andes, Plaza Ercilla 803, Santiago, Chile

SUMMARY

During 2017, 19 magnetotellurics stations in the El Tatio-La Torta geothermal system were measured (Figure 1). Although there are several studies in this zone, the geothermal system characterization is not clear. Therefore, this work pretends to help to perform a three-dimensional modeling of magnetotelluric data through ModEM algorithm. The last inversion results in Figure 2, where there are differents structures associated with La Torta dome (R1), Copacoya dome (R2), Laguna Colorada caldera complex (C1), San Pedro formation (C2) and shallows conductors interpreted as hidrothermal alteration.

Keywords: Geothermal system, Magnetotellurics

INTRODUCTION

Chile is in a convergent margin where, as a consequence of the subduction of the Nazca plate under the South American, the volcanic arc of the Andes has been developed. It hosts more than 200 potentially active volcanoes and at least 12 giant caldera systems (Siebert et al, 2011) These volcanoes have magma at the crustal scale that could serve as sources of heat for the development of local geothermal systems that have the potential to generate clean and sustainable energy (Lahsen, 1986).

El Tatio Geyser field, which has over 100 erupting springs, is the largest geyser field in the southern hemisphere. It is located within the Andes Mountain of northern Chile at 4200 meter above mean sea level (Glennon and Pfaff, 2003). It is in the Altiplano-Puna Volcanic Complex (APVC), which through seismic evidence (Chmielowski et al, 1999), it is proposed to host a regional magma body. The volcanic history on El Tatio, according to Lucchi et al (2009), began in the Miocene and, during inactivity periods begins to act erosives and structurals processes, in addition to the deposit of ignimbrites from external sources.

The exploration in this zone began in 1921 and there has been several surveys (Lahsen and Trujillo, 1976; Cusicanqui et al, 1975; Cumming et al, 2002; Lucchi et al, 2009) in differents periods. Nonetheless, it is not clear the characterization of El Tatio-La Torta geothermal system. Moreover, the computational performance has advanced and today it is possible to perform a 3D inversion through MT data. This work does characterization through depth electrical conductivity structures.

METHODOLOGY

During March and October 2017, 19 magnetotelluric (MT) stations in El Tatio - La Torta geothermal system were installed, they are approximately 1 km apart. Between El Tatio and La Torta wasn't possible install stations due to the inaccessibility part (Figure 1).

The MT method measures natural time-varying electromagnetic waves on the surface to probe the subsurface electrical conductivity (σ , the inverse of resistivity $\rho = 1/\sigma$) (Chave and Jones, 2012). We process the MT data through robust method Egbert and Booker (1986) and we also determinated the strike using algorithm Smith (1995) and phase ten-

sor Caldwell et al (2004) to realize dimensional analysis.

Finally, we modeled MT data with ModEM algorithm (Kelbert et al, 2014) that it is based on Non-Linear Conjugate Gradients (NLCG) and parallelized using MPI, allowing to work with the computational capacity of vatious multi-core PCs, in this case, we worked with Leftraru cluster from Center for Mathematical Modeling (CMM) at Universidad de Chile.

To do the inversion, we applied 3D-Grid program to data mask to smothed curves and delete poor data quality. Also, we performed the grids testing differents cells sizes in x-y-z direction to reduce RMS. We used full impedance, tipper and topography. The preferred model was model with a covariance 0.2, cell number 78-43-144 in x-y-z directions, the tipper error floor 2 %, the impedance error floor 3% for Z_{xy}-Z_{yx}, and 5 % for Z_{xx}-Z_{yy}, using data error 20 % for Z_{xx} -Z_{yy}, and 5 % for Z_{xy}-Z_{yx}. In the last model got, after 149 iterations, an RMS of 2.89.

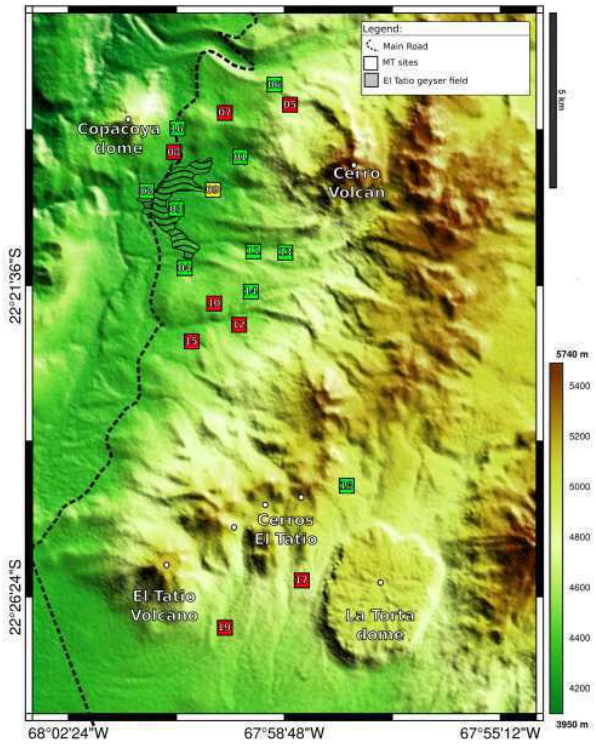

Figure 1: Study zone and location sites. In red stations measured without tipper, in yellow station with problems due to wire cut of N-S dipole and in green stations without problems.

RESULTS AND DISCUSSION

Several sensitivity tests were done, replacing the condutors with original background resistivity (100 Ωm) and run forward model. The results for these tests increased the RMS.

The last model is shown in Figure 2 with two fit curves for stations T04 and T10. Due to wells correlations (Lahsen and Trujillo, 1976), the shallows conductors in El Tatio geyser field are interpreted as hidrothermal alteration, possibly clays. Moreover, the principal aquifer is in Puripicar ignimbrite with a resistivity betwen 40-75 Ωm due to different levels of fracturing and irregular permeability.

The resistor R1, which is under of La Torta dome, it is a rhyolite dome and the last volcanic event in the zone. According to Cumming et al (2002), it is the up-flow zone of the geothermal system and we had similar results with differents scales, possibly due to the method used, where they derived from 2D smooth inversions supplemented by a 3D smooth inversion. The high resistivities would be due to porosity, which tends to decrease with depth and this reduces the effect of bore fluid conditions, thus reinforcing the resistivity increase, countering to some extent the effect of higher salinity that is commonly inferred to lie in deeper parts of most systems (Ussher et al, 2000). Moreveover, this has been seen in others geothermal systems as Darajat, Indonesia (Rejeki et al, 2010) and Glass Mountain, California (Cumming and Mackie, 2010), where the hotter parts of geothermal systems are characterised by higher resistivity. The resistor R2, is associated with Copacoya dome, which is a dacitic dome, that serves as a geologic barrier, don't permiting that fluids pass to the west, rising to the surface through geothermal manifestations.

The conductor C1, is asocciated with Laguna Colorada that is a caldera complex and produced the Laguna Colorada ignimbrite 1.98 Ma (Salisbury et al, 2011) and results of Comeau et al (2015) show a conductor in this zone too. Moreover, Fernandez-Turiel et al (2005) said that it is where likely that the water become heated. The conductor C2, is in thermal inversion zone (according to wells data Lahsen and Trujillo (1976)) and could be due to San Pedro Formation, that is the basament of the zone and is compost of red gypsum clays secuences, red and gray sandstones, gray conglomerates and mantles of salt and gypsum (Marinovic and Lahsen, 1984) and it is possibly altered.

CONCLUSIONS

The current computational performance allows better results in MT data inversions. This work could be improved by including more MT stations to better delimit some structures, but it have a good correlation with previous studies (Lahsen and Trujillo, 1976; Cusicanqui et al, 1975; Cumming et al, 2002; Lucchi et al, 2009). It was shown in Figure 2:

- Shallows conductors due to hidrothermal alteration.
- R1 is under of La Torta dome, and likely the hotter part of geothermal system.
- R2 associated with Copacoya dome that act as a geologic barrier to fluids.
- C1 associeted with Laguna Colorada caldera complex.
- C2 associated possibly with San Pedro Formation.

ACKNOWLEDGMENTS

This work was financially supported by Centro de Excelencia en Geotermia de Los Andes (CEGA), Proyecto FONDAP 15090013.

REFERENCES

Caldwell TG, Bibby HM, Brown C (2004) The magnetotelluric phase tensor. Geophysical Journal International 158(2):457–469

Chave AD, Jones AG (2012) The magnetotelluric method: Theory and practice. Cambridge University Press

Chmielowski J, Zandt G, Haberland C (1999) The central andean altiplano-puna magma body. Geophysical Research Letters 26(6):783–786

Comeau MJ, Unsworth MJ, Ticona F, Sunagua M (2015) Magnetotelluric images of magma distribution beneath volcán uturuncu, bolivia: Implications for magma dynamics. Geology 43(3):243–246

Cumming W, Mackie R (2010) Resistivity imaging of geothermal resources using 1d, 2d and 3d mt inversion and tdem static shift correction illustrated by a glass mountain case history. In: Proceedings world geothermal congress

Cumming W, Vieytes H, Ramírez C, Sussman D (2002) Exploration of the la torta geothermal pospect, northern chile. TRANSACTIONS-GEOTHERMAL RESOURCES COUNCIL pp 3–8

Cusicanqui H, Mahon W, Ellis A (1975) The geochemistry of the el tatio geothermal field, northern chile. In: Second United Nations Symposium on the Development and Utilization of Geothermal Resources, pp 703–711

Egbert GD, Booker JR (1986) Robust estimation of geomagnetic transfer functions. Geophysical Journal International 87(1):173–194

Fernandez-Turiel J, Garcia-Valles M, Gimeno-Torrente D, Saavedra-Alonso J, Martinez-Manent S (2005) The hot spring and geyser sinters of el tatio, northern chile. Sedimentary Geology 180(3):125–147

Glennon JA, Pfaff RM (2003) The extraordinary thermal activity of el tatio geyser field, antofagasta region, chile. GOSA Trans 8:31–78

Kelbert A, Meqbel N, Egbert GD, Tandon K (2014) Modem: A modular system for inversion of electromagnetic geophysical data. Computers & Geosciences 66:40–53

Lahsen A (1986) Origen y potencial de energía geotérmica en los andes de chile. Geología y Recursos Minerales de Chile, Univ de Concepción, Chile 423

Lahsen A, Trujillo P (1976) El campo geotermico de el tatio, chile. proyecto geotermico corfo-onu. Tech. rep., Internal Report

Lucchi F, Tranne CA, Rossi PL, Gallardo C, De Astis G, Pini GA (2009) Volcanic and tectonic history of the el tatio area (central andes, northern chile): explanatory notes to the 1: 50,000 scale geological map. Geoacta, Spec Publ 2:1–29

Marinovic N, Lahsen A (1984) Hoja calama, region de antofagasta. carta geologica de chile no. 58, 1: 250,000. Servicos Nacional Minero Geologico

Rejeki S, Rohrs D, Nordquist G, Fitriyanto A (2010) Geologic conceptual model update of the darajat geothermal field, indonesia. In: Proceedings World Geothermal Congress, vol 2010, pp 25–29

Salisbury MJ, Jicha BR, de Silva SL, Singer BS, Jiménez NC, Ort MH (2011) 40ar/39ar chronostratigraphy of altiplano-puna volcanic complex ignimbrites reveals the development of a major magmatic province. Bulletin 123(5-6):821–840

Siebert L, Simkin T, Kimberly P (2011) Volcanoes of the World. Univ of California Press

Smith JT (1995) Understanding telluric distortion matrices. Geophysical Journal International 122(1):219–226

Ussher G, Harvey C, Johnstone R, Anderson E (2000) Understanding the resistivities observed in geothermal systems. In: proceedings world geothermal congress, pp 1915–1920

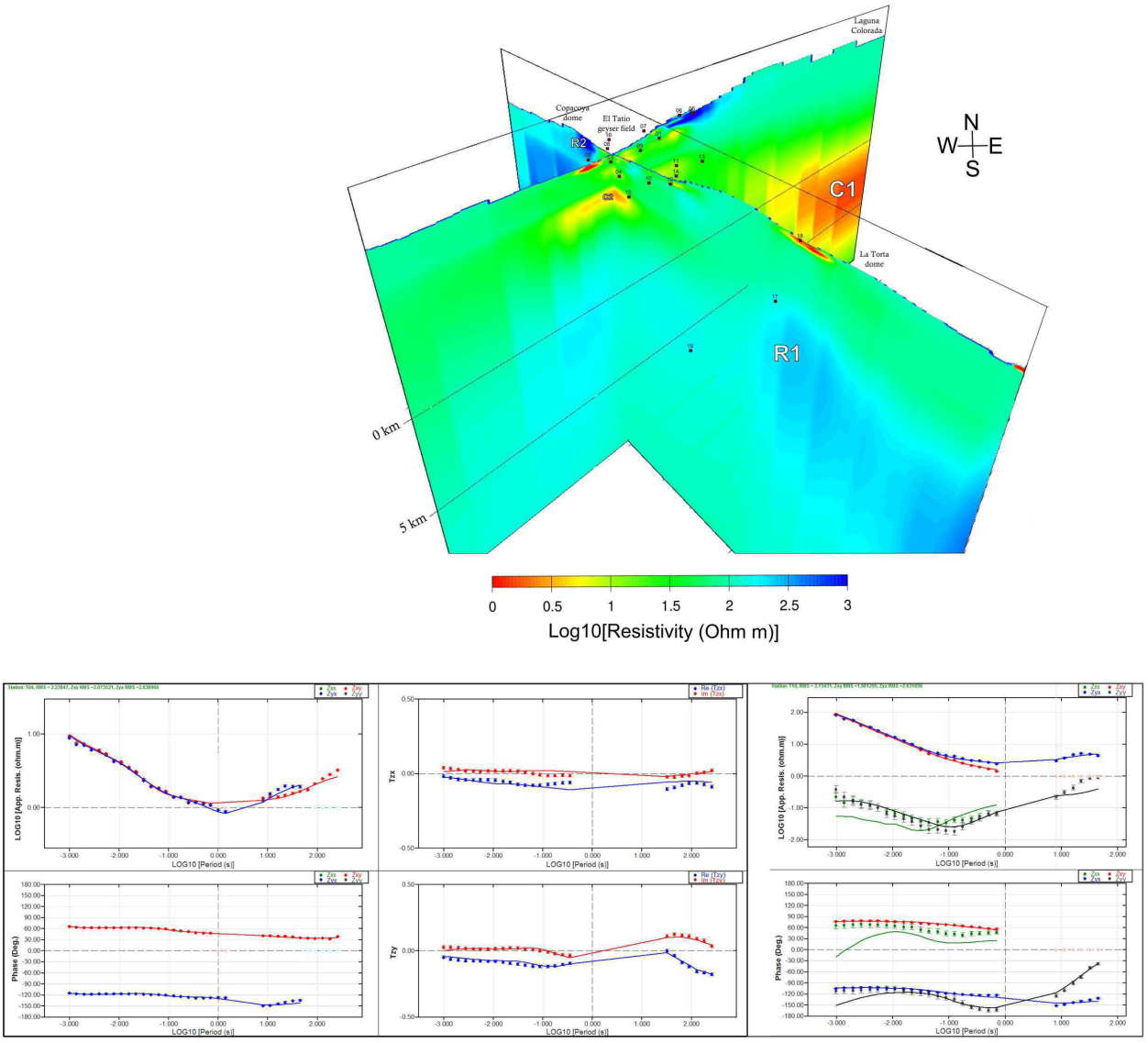

Figure 2: Upper: Electrical resisitivity image from the last model inversion and main conductors and resistors structures. Botton: Examples of two fit stations T04 and T10.

Time-lapse CSEM: lifting the repeatability curse

Daniil V. Shantsev[1], Amir Babakhani[2], Leiv J. Gelius[2], Elias A. Nerland[1]
[1] EMGS, I&I Technology Center, Oslo, Norway, {dshantsev,enerland}@emgs.com
[2] Geoscience Dept, University of Oslo, Norway {babakhani76@gmail.com,l.j.gelius@geo.uio.no}

SUMMARY

Repeatability of acquisition parameters for the base and monitor surveys is an important consideration for time-lapse studies of hydrocarbon reservoirs using marine controlled-source electromagnetics (CSEM). Variations in parameters such as source and receivers positions, conductivity of seawater, source current etc. lead to differences in the recorded EM fields that can mask the 4D EM response. In the existing literature, the repeatability requirements are addressed mainly in the data domain. It means that differences in EM fields caused by non-repeatability in parameters are required to be smaller than differences in EM fields due to production-induced changes in the reservoir resistivity. That requirement looks logical, but can be misleading if the 4D effects are analysed in the model domain rather than in the data domain. Indeed, instead of comparing the two measured CSEM datasets, one can invert them and compare the resulting resistivity models. We demonstrate that the model-domain approach significantly expands the feasibility range of 4D CSEM.

Our analysis focuses on two examples. The first one is a simple “canonical” 2.5D model considered in the time-lapse study by the Scripps Marine EM Lab [Orange et al. 2009]. The second one is a realistic 3D model of the Snøhvit gas field in the Barents Sea. The advantage of choosing the Snøhvit field is that it has been produced for several years and that CSEM data covering the field is available. In both cases the repeatability issues are first addressed by the standard sensitivity analysis assuming a variation in receiver positions and in seawater conductivity between the base and monitor surveys. This standard analysis concluded that 4D CSEM was not feasible. Then we carried out synthetic inversions of the base and monitoring datasets for both examples. Comparing the inverted resistivity models we were able to detect production-induced changes in the reservoirs. Performing the analysis of 4D effects in the model domain rather than in the data domain allows relaxing the repeatability requirements by approximately one order of magnitude.

Though the acquisition parameters vary from survey to survey, it is assumed that their values can be accurately measured and e.g. the inversion software uses the correct receiver positions despite these positions differ between the base and monitor surveys. We have also utilized the fact that the production-induced changes in resistivity are restricted only to the volume of hydrocarbon reservoir, while the background resistivity remains intact. Strict constrains on the background have therefore been applied when running inversions. Random noise in EM data, including the multiplicative noise due to small measurement errors in positions and orientation of sources and receivers, was also included in the analysis. Our results suggest that the random noise is generally a bigger problem for detecting subtle 4D effects, than non-repeatability of survey parameters.

REFERENCES

Orange A, Key K, and Constable S (2009) The feasibility of reservoir monitoring using time-lapse marine CSEM. Geophysics. 74: F21-F29

Keywords: CSEM, time-lapse, 4D, repeatability, inversion

Time-lapse inversion of one-dimensional magnetotelluric data

D. Conway[1], G. Heinson[2], N. Rees[3] and J. Rugari[4]
[1]The University of Adelaide, dennis.conway@adelaide.edu.au
[2]The University of Adelaide, graham.heinson@adelaide.edu.au
[3]The Australian National University, nigel.rees@anu.edu.au
[4]The University of Adelaide, joseph.rugari@adelaide.edu.au

SUMMARY

We present our findings from Conway, D., Heinson, G., Rees, N., & Rugari, J. (2018). Time-lapse inversion of one-dimensional magnetotelluric data. *Earth, Planets and Space*, *70*(1), 27.

We present a new tool for modelling time-lapse magnetotelluric (MT) data, an emerging technique for monitoring changes in subsurface electrical resistivity. Time-lapse MT data have been acquired in various settings, including sites of hydraulic fracturing, dewatering and sequestration. It has been shown in other geophysical techniques that the most effective way to model time-lapse data is with simultaneous inversion, which uses information from all time-steps to produce models with higher accuracy and fewer artefacts. We introduce this method to model time-lapse 1D MT data. As with a standard MT inversion, our routine penalises spatial roughness at each time-step, however we also introduce temporal regularisation. The inversion is simple to apply, requiring only the ratio between regularisation parameters and the desired level of misfit from the user. The algorithm is tested on both synthetic data, and a case study. We find that in the synthetic example our inversion successfully retrieves the main characteristics of the test model and introduces minimal artefacts, even in the presence of significant noise. We also test the effect of changing the ratio of regularisation parameters. In the case study, we produce an easily interpretable model that compares favourably with previous inversions of the synthetic data. We conclude that time-lapse modelling of 1D MT data can be a valuable tool for imaging subsurface change.

Keywords: Magnetotellurics – Time-lapse – Monitoring – Inversion

Time-lapse magnetotelluric monitoring at the Theistareykir geothermal plant (Iceland)

N. Portier[1], P. Sailhac[1,2], S. Warden[1,3] K. Árnason[4] and K. Erbas[5]
[1]Institut de Physique du Globe de Strasbourg UMR 7516 Université de Strasbourg, 5 rue Descartes 67084 Strasbourg, France, nolwenn.portier2@etu.unistra.fr
[2]GEOPS UMR 8148 Bât. 504-509 rue du Belvédère 91405 Orsay cedex, France
[3]Hyperion Geophysical Services, 7, rue de Châtenois, Strasbourg, France
[4]Iceland GeoSurvey (ÍSOR), Grensásvegur 9, 108 Reykjavík, Iceland
[5]Helmholtz Centre Potsdam GFZ German Research Centre for Geosciences, Telegrafenberg, 14473 Potsdam, Germany

SUMMARY

Theistareykir is located 25 km southeast of Husavik on the path of the mid-atlantic ridge in the northern part of Iceland. A geothermal plant project was initiated here in 1999 and consequently, geothermal operations began in November 2017 to reach a total capacity of 90MWe. The power plant counts 18 production wells 2 to 2.5km deep; all extracted fluids are re-injected at a single location thanks to 300-500m deep reinjection wells. The produced temperature varies between 280 and 330°C.

In this work, we attempt to monitor geothermal production using Magnetotellurics (MT). MT is a passive induction electromagnetic method sensitive to resistivity variations in the subsurface. MT has been widely used in geothermal exploration, allowing to detect resistivity anomalies such as fault zones and caprocks. Comparing repeated MT surveys before and after the beginning of geothermal operations may also provide insight about fluid circulation.

Hence, to image resistivity variations caused by geothermal production in Theistareykir, we performed a time-lapse magnetotelluric experiment. Nine stations were measured during summers 2017 and 2018, respectively before and after the beginning of production. Each measurement lasted between 48 to 96 hours. We used sampling rates of 512Hz, 8,192Hz and 65,536Hz. Data were filtered for power line noise using notch filters and then processed using the Bounded Influence Remote Reference Processing (BIRRP) program which uses robust regression with a Bounded Influence estimator. We present here our first results, comparing them to those acquired during previous MT campaigns at Theistareykir. Besides, we also performed a continuous monitoring experiment using instruments from the Geophysical Instrument Pool of Potsdam (GIPP) settled in summer 2017. These new continuous MT measurements and related questions of time resolution will be shown at Helsingør for comparison but are not detailed in this abstract to maintain clarity and conciseness.

Keywords: Magnetotelluric, Time-lapse, Monitoring, Theistareykir, Geothermal

INTRODUCTION

The Magnetotelluric method (MT) is an electromagnetic geophysical exploration technique sensitive to conductivity variation in the subsurface. Peacock et al. (2012, 2013) introduced the concept of time-lapse MT to monitor the Enhanced Geothermal System (EGS) of Paralana in South Australia. They studied the impact of hydraulic stimulation performed in July, 2011 by comparing repeated MT surveys before and after the EGS fluid injection. They observed a coherent change above measurement error in the MT response, suggesting that transient variations in subsurface conductivity generated from fluid injection may be measured using EM methods. Didana et al. (2016) also used magnetotellurics monitoring to study the Habanero ESG project in South Australia. Their pre and post injection data analysis show possible conductive fractures in agreement with observed micro-seismic events. More recently, Abdelfettah et al. (2018) published another study using time-lapse and continuous MT data to monitor the Rittershoffen geothermal plant in France. We performed a similar MT experiment at the Theistareykir geothermal plant in Iceland. We repeated MT measurements at nine stations before and after the beginning of production starting in November 2017. In addition, we deployed a semi-permanent station allowing to perform continuous measurements. In this abstract, we present the 2017 field campaign to give an idea of our measurements and initial electrical state prior to the start of production.

THEISTAREYKIR

Geological setting

The North American tectonic plate asthenosphere flows under the Eurasian plate and interacts with a deep-sealed mantle plume. This process results in a high volcanic activity leading to the creation of Iceland. Theistareykir is located on the path of the mid-atlantic ridge in the northern part of the country (see Fig. 1). Its bedrock is constituted by both sub glacial eruption products (hyaloclastites, typically formed of pillow basalts, breccias and tuffs) and recent basaltic lava flows (younger than 10,000 years).

Geothermal plant

Surface exploration in Theistareykir started in the 1970s and the first exploration drilling was performed in 2002. The construction of the plant started in April 2015. A first phase began in November 2017 to produce 45 MWe. The second phase started in April 2018 to reach a total production of 90 MWe. The power plant counts 18 production wells 2 to 2.5 km deep which extract a hot geothermal fluid. Produced temperatures are ranging between 280 and 330°C. Then, the condensate steam is injected in the subsurface using wells 300/500 m deep.

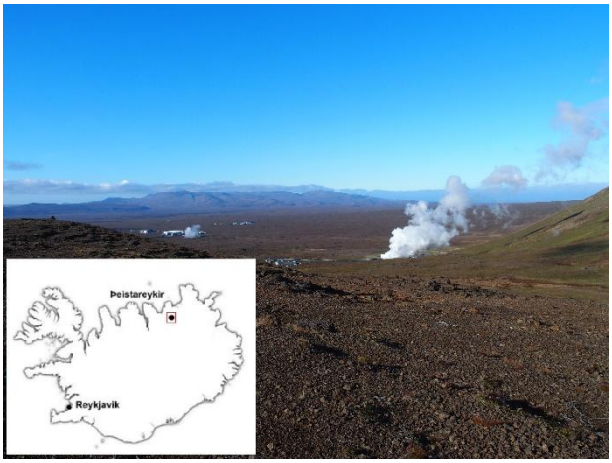

Figure 1. Photo and map of Theistareykir geothermal plant in the northern part of Iceland.

MAGNETOTELLURICS

Magnetotellurics is a passive electromagnetic method allowing to investigate the conductivity variation with depth. The depth scale ranges from a few tens of meters for audiomagnetotellurics (AMT) to tens of kilometers. This technique measures simultaneously the electric E [V/m] and magnetic B [A/m] fields. They are linked by the magnetotelluric impedance Z. The apparent resistivity ρ and phase Φ can be calculated using the impedance in spectral domain (see eq. 1 and 2).

$$\rho(\omega) = \frac{|Z|}{\mu\omega} \quad (1)$$

$$\Phi(\omega) = \arctan\left(\frac{Im(Z)}{Re(Z)}\right) \quad (2)$$

where μ is the magnetic susceptibility [H/m] and ω is the angular frequency [rad/s].

EXPERIMENT

Several MT campaigns were conducted in the Theistareykir area. ISOR (Karlsdóttir et al., 2012) performed 101 MT and 38 TEM soundings from 2009 to 2012. In MT, the five components (Ex, Ey, Hx, Hy and Hz) were recorded during 16 to 22 hours using instruments from Phoenix Ltd. (MTU type). The 3D modeling highlights a low resistivity cap underlying a high resistivity core. These different properties would reflect rock alteration linked to the temperature. The study of high-temperature geothermal areas by Kahwa (2012), based on the analysis of MT and Time Domain EM (TDEM) data, confirmed these results. This work completes the one done by Suriyaarachchi (2012). We chose to apply time-lapse MT to monitor the beginning of geothermal fluid extraction.

We measured nine MT stations before the beginning of the production. Continuous measurements were also performed one station in the vicinity of the production area. The locations of these stations allowed to cover the geothermal area (see Fig. 2) and often coincide with those of MT stations occupied during previous studies.

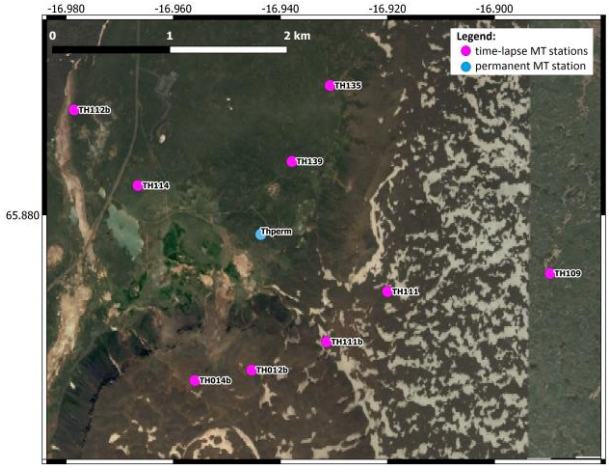

Figure 2. Map of the 10 MT stations. The semi-permanent station is depicted in blue. The time-lapse stations appear in pink (notice that TH109 is located outside the geothermal energy exploitation area).

Since the extraction has begun in November 2017, repeated measurements in 2018 would help

characterize possible preferential paths of the geothermal fluid and the evolution of the geothermal reservoir. MT time-lapse measurements were performed using METRONIX ADU-07 stations. We deployed 50 m long dipoles with impolarizable porous pots to measure the E field; the H field was measured using MFS-06 probes for its horizontal components and CM13 probes for its vertical component. We used sampling rates of 512 Hz, 8,192 Hz and 65,536 Hz. We present here only the first result for the 512 Hz acquisition. Measurements lasted between 48 h and 96 h (see Fig. 3).

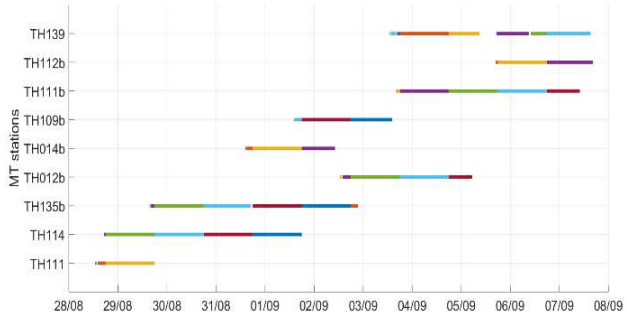

Figure 3. Chronogram of 512 Hz time-lapse MT measurements.

2017 RESULTS

Data were first filtered for power line noise using notch filters. Then, they were processed using the Bounded Influence Remote Reference Processing (BIRRP) program developed by Chave et al. (2004). As shown in Fig.3, each station has at least one other simultaneous records at another station; we use it as a remote reference at frequencies higher or equal to 4Hz (at lower frequencies, processing will be done using another remote station located at Krafla). We present here two stations acquired during summer 2017 before the beginning of production.

The first station, TH109, is located in the Eastern part of the survey area (see Fig. 2), outside the geothermal energy exploitation area. It is on top of a ~12,000 years old lava flow. A relatively high apparent resistivity, *i.e.* greater than 100Ω.m, was measured at low periods. The apparent resistivity reaches a minimum of 10-30Ω.m between 0.3 and 0.5s before increasing up to several tens of Ω.m at greater periods.
This apparent resistivity plot is very close to the one obtained by ISOR (Karlsdóttir et al., 2012) at site thr109, located about 400m West of TH109 (see Fig. 4).
Also, this behaviour is consistent with the WE_3 resistivity profile described in the report of Kahwa (2012), actually passing through thr109. This profile was obtained by inverting TDEM measurements: the high resistivity layer, seen down to depths of 400m in this Eastern area of the profile, is interpreted as an unaltered rock formation as the one identified in Árnason et al. (1987) for the Nesjavellir field located in SW Iceland. The low resistivity cap found beneath it is attributed to the smectite-zeolite zone at temperature range of 100-220°C. Below this unit of low resistivity, at higher temperature, resistive chlorite replaces smectite and zeolite disappears: a high resistive unit can be found, interpreted as the chlorite-epidote zone.

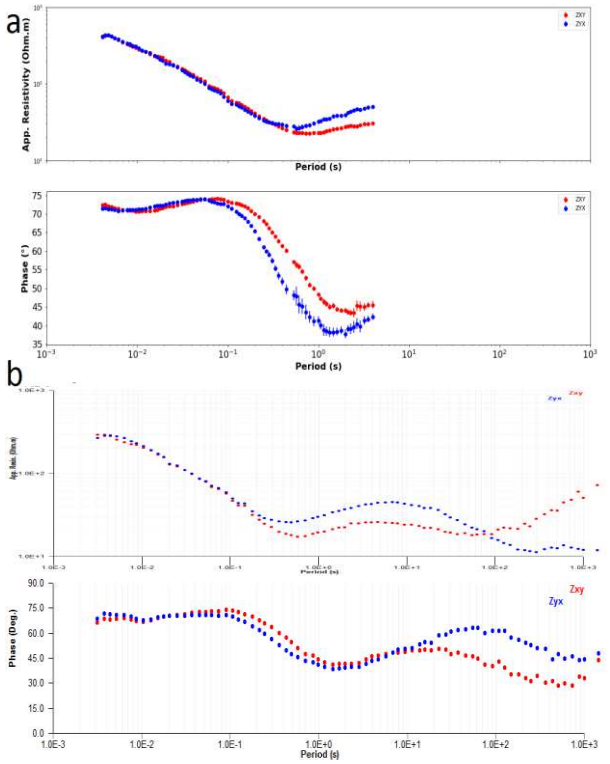

Figure 4. Apparent resistivity and phase plots of TH109 (a) and thr109 (b), acquired by ISOR. The two stations are not collocated.

The second sounding curves shown here are from TH114 (see Fig. 2), a station located in a mud flat near Theistareykir, about 600m North of thr102, acquired by ISOR (Karlsdóttir et al., 2012) near the WE_3 profile. This station is characterized by a low resistivity area (*i.e.* smaller than 10Ω.m) at low periods, followed by an increase in resistivity around 10^{-1}s up to about a 100Ω.m at 2s for the xy polarization.
Again, the observed behaviour is consistent with results obtained by ISOR (see Fig.5) and with the WE_3 profile, as Kahwa explains that the low resistivity cap (the smectite-zeolite alteration zone) reaches the surface near Theistareykir. Besides, there is a static shift at TH114 that was not observed at thr102, these sites are not collocated so we consider that this is probably caused by a small anomalous conductive body near TH114 station.

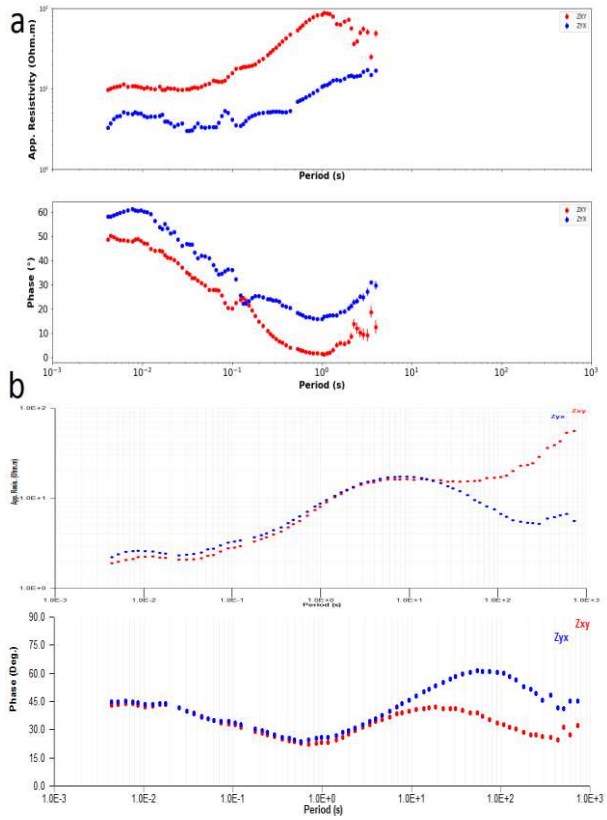

Figure 5. Apparent resistivity and phase plots of TH114 (a) and thr102 (b), acquired by ISOR. The two stations are not collocated.

CONLUSION

We performed a MT monitoring experiment at the Theistareykir geothermal plant. Repeated measurements before and after the beginning of production in November 2017 may provide insight about fluid circulation. Hence, 9 MT stations were measured in summer 2017. In addition, a semi-permanent station is also recording the resistivity variation over time. Our first results reflect the initial state prior to the beginning of the exploitation and are coherent with the observation done by ISOR (Karlsdóttir et al., 2012) and Kahwa (2012),according to which a low resistivity zone covers a high resistive unit. These units are respectively interpreted as smectite-zeolite zone and chlorite-epidote zone. West of the geothermal area, unaltered rock formation covers the smectite-zeolite zone. Further work will be done using all time-lapse and continuous records to track changes during the 2017-2018 period.

ACKNOWLEDGEMENT

We thank the Landsvirkjun (The National Power Company of Iceland), ISOR (Iceland Geosurvey) and GFZ German Research Centre for Geosciences) for the useful information and their support. We also would like to thank Hreinn Hjartarson and Steinn Agust Steinsson for their warm welcome in Theistareykir and Krafla. This work has been carried out under the framework of the LABEX ANR-11-LABX-0050 _G-EAU-THERMIE-PROFONDE and benefits from a funding from the state managed by the French National Research Agency as part of the Investments for the future program.

REFERENCES

Abdelfettah Y, Sailhac P, Larnier H, Matthey PD, Schill E (2018) Continuous and time-lapse magnetotelluric monitoring of low volume injection at Rittershoffen geothermal project, northern Alsace-France. Geothermics 71: 1-11 doi: 10.1016/j.geothermics.2017.08.004

Árnason K, Flóvenz Ó, Georgsson L.S., Hersir, G.P. (1987) Resistivity structure of high temperature geothermal systems in Iceland. International Union of Geodesy and Geophysics (IUGG) XIX General Assembly, Vancouver Canada, Abstracts V, 477

Chave AD, Thomson DJ (2004) Bounded influence magnetotelluric response function estimation. Geophysical Journal International 157: 988-1006 doi: 10.1111/j.1365-246X.2004.02203.x

Didana YL, Heinson G, Thiel S, Krieger L (2016) Magnetotelluric monitoring of permeability enhancement at enhanced geothermal system project. Geothermics 66: 23-38 doi: 10.1016/j.geothermics.2016.11.005

Kahwa E (2012) Geophysical exploration of high-temperature geothermal areas using resistivity methods-case study: Theistareykir area, NE-Iceland. Report 14 in: Geothermal training in Iceland 2012. UNU-GTP, Iceland, 235-263.

Karlsdóttir R, Vilhjálmsson AM, Árnason K, AT Beyene (2012) Theistareykir Geothermal Area, Northern Iceland 3D- Inversion of MT and TEM Data, ISOR-2012/046 Project 7000/12.

Peacock JR, Thiel S, Reid P, Heinson G (2012) Magnetotelluric monitoring of a fluid injection: Example from an enhanced geothermal system. Geophys. Res. Lett. 39: L18403 doi:10.1029/2012GL053080

Peacock JR, Thiel S, Heinson G, Reid P (2013) Time-lapse magnetotelluric monitoring of an enhanced geothermal system. Geophysics 78: B121-B130 doi:10.1190/GEO2012-0275.1

Suriyaarachchi NB (2012) Joint 1D inversion of MT and TEM resistivity data from the Theistareykir high-temperature geothermal area, NE-Iceland and comparison with alteration and temperature logs from boreholes. Report 32 in: Geothermal training in Iceland 2012. UNU-GTP, Iceland, 793-822.

Time Domain Electromagnetic Soundings in the Aqeb and Basalt Wellfields in Jordan

Gerhard Kapinos, Gerhard.Kapinos@bgr.de
[1]Nidal Jahed, gprtdem@yahoo.com
[2]Nidal Atteyat, nedal.atteyat@memr.gov.jo
[3]Armin Margane, armin.margane@gmail.com

SUMMARY

In spring 2018, 42 Time Domain Electromagnetic (TEM) soundings were carried out along 3 profiles in the Aqeb and Basalt wellfields in Northern Jordan to investigate deep aquifers, update groundwater contour maps and to adapt the groundwater exploitation management in response to the influx of 600,000 Syrian refugees.
While the Aqeb Wellfield is overused since several decades supplying water to the North-West of Jordan, which results in fast dropping groundwater levels, the Basalt Wellfield is proposed as a new wellfield and a water conservation area. The geological structures in the area are derived from wells and are not well understood. No geophysical investigations have been carried out so far. The TEM study is a very first geophysical groundwater survey with the aim to provide better knowledge of the geological conditions and to map the aquifer structures, sizes and saturation.
The target of the investigation are Upper Creataceous limestone sequences at depths between 400 and 800m known as the A7/B2 aquifer overlain by a thick basalt layers, being itself a good aquifer.
The data were recorded with a Zonge System and a with a loop size of 200 x 200 m and transients up to 90 ms were obtained.
For the interpretation of the data common 1D inversion techniques were applied initially and available wells data are used to constraint the inversion. The first models show a thin conductive mudflat layer followed by a basaltic resistive layer and a more conductive layer indicating water saturated structures.
However, to image the base of the A7/B2 aquifer and structures at depths larger than 800m, a magnetotelluric investigation is planned, aiming at joint modeling of both MT and TEM data sets.

What lurks below: plumbing the depths of the hydrothermal system at Yellowstone

P. A. Bedrosian[1], C. Finn[1], K. Dickey[2], W. S. Holbrook[2], E. Auken[3] and J. Pedersen[3]
[1]U.S. Geological Survey, pbedrosian@usgs.gov
[2]Virginia Polytechnic Institute
[3]Aarhus University

SUMMARY

Yellowstone National Park's hydrothermal systems are well mapped at the surface, yet the groundwater flow systems, and the structural controls on them are almost completely unknown. There are more than 10,000 thermal features within the park, the largest concentration on Earth, including geysers, hot springs, mud pots, and fumaroles. These features are driven by the interaction between the deep-crustal magmatic system and the shallow hydrologic system. A few of the most iconic features, such as Old Faithful, have been the subject of focused geophysical studies, but the vast majority remain unexplored with respect to the pathways for the fluids and heat that drive them and the structures that control their location.

To comprehensively investigate these systems, over 4,200 line-kilometers of magnetic and airborne electromagnetic (AEM) data were flown in late 2016 over a significant portion of the caldera including a majority of the known thermal areas. Data were collected in high-resolution blocks over the Upper, Middle, and Lower Geyser Basin corridor, as well over Norris Basin and the northern part of Yellowstone Lake. Additional widely-spaced regional lines provide coverage throughout the remainder of the caldera. Both deterministic and stochastic inversions have been carried out on the complete data set, with average depth-of-investigation between 300 m and 500 m, dependent primarily on subsurface resistivity.

The models image extremely low resistivity, coincident with magnetic lows, beneath the northern part of Yellowstone Lake, in close correspondence with mapped vents, fractures and hydrothermal explosion craters. Throughout the park, such coincident lows in resistivity and magnetic field are typical of regions of mapped surface alteration, yet are also imaged at depth in areas without mapped surface alteration. Shallow drill holes exist in several of the thermal areas; lithologic data and thermal profiles within them suggest that alteration mineralogy is the primary control on resistivity, and that temperature, porosity, and fluid salinity are second-order contributors. Sub-vertical resistivity boundaries beneath many thermal areas are interpreted to reflect faults and fractures, potential conduits for deep thermal fluids. Thin, sub-horizontal conductors are further imaged extending away from thermal areas, can be correlated with boundaries between individual lava flows, and are interpreted to reflect the lateral flow of meteoric fluids, in some cases connecting multiple thermal areas. Finally, at the edge of the thermal areas, a characteristic outward-dipping interface between altered and unaltered volcanic flows is consistent with the geometry of a classical hydrothermal circulation cell.

Keywords: Yellowstone, hydrothermal, airborne electromagnetics, alteration

Imaging and monitoring the Reykjanes supercritical geothermal reservoir in Iceland with time-lapse CSEM and MT measurements

M. DARNET[1], N. COPPO[2], P. WAWRZYNIAK[3], S. NIELSSON[4], G.O. FRIDLEIFSSON[5], E. SCHILL[6]

[1]BRGM, m.darnet@brgm.fr
[2]BRGM, n.coppo@brgm.fr
[3]BRGM, p.wawrzyniak@brgm.fr
[4]ISOR, Steinthor.Nielsson@isor.is
[5]HS-ORKA, gof@hsorka.is
[6]KIT, eva.schill@kit.edu

SUMMARY

MT is traditionally used for geothermal reservoir characterization and a few recent studies have demonstrated its potential for monitoring reservoir development. One of the main challenges is though the presence of anthropogenic noise and/or variability of the Earth magnetic field that can obfuscate the EM signals of interest. We have investigated the benefits of adding CSEM data to tackle this challenges with actual time-lapse CSEM/MT surveys acquired in 2016 and 2017 over the Reykjanes geothermal field in Iceland before and after the stimulation of the supercritical RN 15/IDDP2 well.

Our study shows that the resistivity model derived from the joint inversion of CSEM and MT data fits best with the resistivity logs from the RN15 well in terms of geometry and actual resistivity. Stand-alone CSEM and MT inversions only partially recover the resistivity structure of the field, mainly due to the insufficient illumination of subsurface because of high levels of noise.

For the monitoring of the stimulation, time-lapse MT data turned out to be too noisy to be of any use. On the other hand, CSEM data showed high degree of repeatability. It showed that the main parameter controlling the CSEM survey repeatability is the ratio of the CSEM signal to external noise (S/N) of the baseline and monitor surveys. Since the S/N ratio of CSEM surveys is mainly dependent on the transmitter design, it offers the possibility to optimize the survey to maximize the chance of detecting time-lapse signals of interest. We have however not identified any deep (5km) EM signals related to the thermal stimulation of the reservoir in supercritical conditions, most likely due to the limited sensitivity of our CSEM equipment and setup for monitoring resistivity changes at such great depths.

This study was part of the DEEPEGS project, which received funding from the European Union HORIZON 2020 research and innovation program under grant agreement No 690771.

Keywords: Controlled-Source Electro-Magnetics, Magneto-Tellurics, Geothermal, Monitoring, Imaging